Characterization of the Molecular Mechanism of the Tissue-Specific and Developmentally Regulated Alternative Splicing of *SCN9A* Exon 5

Thesis

Characterization of the molecular mechanism of the tissue-specific and developmentally regulated alternative splicing of *SCN9A* exon 5

Chiara Chiavelli

A Thesis Submitted in Fulfillment of the Requirements of the
Open University, (UK)
for the Degree of Doctor of Philosophy

Life Sciences

International Centre for Genetic Engineering and Biotechnology
ICGEB Trieste, Italy

Director of Studies: Prof. Francisco E. Baralle, M.D. Ph.D.

Supervisors: Prof. Charles ffrench-Constant, Ph.D.
Marco Baralle, Ph.D.

April 2015

DATE OF SUBMISSION : 19 FEBRUARY 2015
DATE OF AWARD : 9 MAY 2015

To my parents

"We are here for this - to make mistakes and to correct ourselves,
to stand the blows and to hand them out.
We must never feel disarmed: nature is immense and complex,
but it is not impermeable to the intelligence;
we must circle around it, pierce and probe it, look for the opening or make it."

The Period Table, Primo Levi

Table of contents

List of figures and tables

Figures

1. Introduction

3. Results

Abbreviations

2'MOE-PS: 2'-O-methoxyethyl phosphorothioates

2'OMe-PS: 2'-O-methyl phosphorothioates

alfa-TM: α tropomyosin

AO: antisense oligonucleotide

ATP: adenosine triphosphate

BFNIS: benign familial neonatal-infantile seizures

BP: branch point

BrS: Brugada syndrome

CCD: cardiac conduction disease

CELF: CUG-BP1 and ETR3-like factors

CFTR: cystic fibrosis transmembrane conductance regulator

CIP: congenital insensitivity to pain

CNS: central nervous system

cTNT: cardiac troponin T

CUG-BP1: CUG-binding protein 1

DCM: dilated cardiomyopathy

DMD: Duchenne muscular dystrophy

DRG: dorsal root ganglia

Dscam: Drosophila melanogaster down syndrome cell adhesion molecule

eNOS: endothelial nitric oxide synthase

ESE: exonic splicing enhancer

ESS: exonic splicing silencer

ETR3: embryonically lethal abnormal vision-type RNA binding protein 3

FGFR2: fibroblast growth factor receptor 2

GEFS+: generalized epilepsy with febrile seizures plus

hnRNP: heterogeneous nuclear ribonucleoprotein

HYPP: hyperkalemic periodic paralysis

IEM: inherited erythromelalgia

ISE: intronic splicing enhancer

ISS: intronic splicing silencer

JNK2: c-Jun N-terminal kinase 2

LNA: locked nucleic acid

LQT-3: long QT syndrome type 3

ME: mutually exclusive

mRNA: messenger ribonucleic acid

NMD: nonsense-mediated decay

NMDA R1: N-methyl-D-aspartate receptor 1

nPTB: neuronal polypyrimidine binding protein

nt: nucleotide

PAM: potassium-aggravated myotonia

PEPD: paroxysmal extreme pain disorder

PMC: paramyotonia congenita

PMO: phosphorodiamidate morpholino

PNA: peptide nucleic acid

PolII: RNA polymerase II

PPT: polypyrimidine tract

Pre-mRNA: precursor messenger ribonucleic acid

PSD-95: postsynaptic density protein 95

PTB: polypyrimidine binding protein

RBM: RNA binding domain

RNA: ribonucleic acid

RRM: RNA recognition motif

SFN: small-fibre neuropathy

SIDS: sudden infant death syndrome

SMA: spinal muscular atrophy

SMEI: severe myoclonic epilepsy of infancy

SMN2: survival motor neuron 2

SNAP25: synaptosomal-associated protein 25

snRNA: small nuclear ribonucleic acid

snRNP: small nuclear ribonucleoprotein

SRSF: serine/arginine-rich splicing factor

TIA1: T-cell restricted intracellular antigen 1

TTX: tetrodotoxin

U2AF: U2 snRNP auxiliary factors

VGSC: voltage gated sodium channel

Abstract

The voltage-gated sodium channel $Na_v1.7$, encoded by *SCN9A* gene, is expressed in dorsal root ganglia (DRG) and in sympathetic ganglia and it is considered to be one of the major player in the regulation of pain perception. The linkage to several human pain disorders confirms its pivotal role in pain pathway. The gene contains an exon 5 pair, 5N and 5A, that are mutually exclusive spliced. These exons encode part of the voltage sensor of the channel; although the alternative splice variants differ by only two amino acids, they differentially affect the amplitude of the currents generated and the excitability of nociceptive neurons.

In this study I mapped some of the splicing regulatory elements that determine *SCN9A* exon 5 developmentally regulated mutually exclusive splicing. In the first stages of development, characterized by a major inclusion of the neonatal form, ETR3 plays an essential role acting on both sides, favouring 5N and inhibiting 5A inclusion. For the switching towards a major inclusion of exon 5A some elements have been identified. Fox1 helps the recognition of the weak 5A 5' splice site, interacting with four *cis*-acting elements downstream of exon 5A. Furthermore an exonic splicing enhancer (ESE), bound by SRSF1 and SRSF6, improves the usage of 5A weak 3' splice site. At the same time 5N inclusion is inhibited by the presence of two silencers, one exonic recognized by PTB and one intronic close to 5N 5' splice site.

The duplication of this exon is well conserved in six out of nine voltage-gated sodium channel (VGSC) genes and some elements mapped for *SCN9A* gene display a great homology in other family members. The investigation of possible common factors reveals

some interesting results: for example the ESE in the adult form is present in at least other three VGSCs.

1. Introduction

1.1. Overview of pre-mRNA splicing.

In eukaryotic cells the primary RNA transcript (pre-mRNA), synthesized in the nucleus by RNA polymerase II (Pol II), undergoes several modifications before being transported into the cytoplasm, where translation takes place. These processing events occur both co- and post-transcriptionally and include for example the 5' end capping, the cleavage and the polyadenylation at the 3' end (Kornblihtt et al., 2004; Moore and Proudfoot, 2009). Furthermore, since the primary transcripts contain multiple non-coding intervening sequences (introns), which separate the coding sequences (exons), a central step of the mRNA maturation is the splicing reaction (Gilbert, 1978).

Introns must be precisely removed by the spliceosomal machinery in the nucleus before the mRNA can be transported to the cytoplasm. The major spliceosome, that excides the vast majority of introns, is characterized by the presence of U1, U2, U4/U6 and U5 small nuclear RNAs and at least 170 protein factors. In a subset of eukaryotes, some introns are spliced by a less frequent type of spliceosome, called minor spliceosome, formed by U11/U12 and U4atac/U6atac snRNPs. These members display comparable functions in respect to the components of the major one (Burge et al., 1998; Jurica and Moore, 2003).

Spliceosome complex assembly is directed by consensus sequences that mark the intron-exon boundaries: the 5' splice site, the branch point, the polypyrimidine tract and the 3' splice site (Fig. 1.1A). The 5' splice site (*donor site*) is a degenerate 9-nucleotide motif (C/A)AG/GURAGU (where R is A or G) at the exon-intron junction comprising the region from -3 to +6. The GU dinucleotide (in bold in Fig. 1.1A) is universally conserved, in fact a

mutation of one of these two residues completely abolishes the splicing reaction (Montell and Berk, 1984). This *cis*-acting element is initially recognized by the U1 snRNA 5' (Fig. 1.1B). The 3' splice site is characterized by three elements: the polypyrimidine tract (PPT), a region with an high percentage of pyrimidines, the branch point (BP), that contains the adenosine important for the first *trans*-esterification step of the splicing reaction and generally located within 18-40 nt of the 3' splice site (Reed and Maniatis, 1988), and the 3' splice site, *acceptor site* (YAG, where Y is C or U). The degenerate BP sequence (YNYURAY) interacts with U2 snRNP, while the U2 snRNP auxiliary factors (U2AF) bind the PPT and the 3' splice site (Fig. 1.1B). The more conform to the consensus sequence is the 5' splice site and the longer is the PPT, the more efficient is the splice site definition (Ast, 2004).

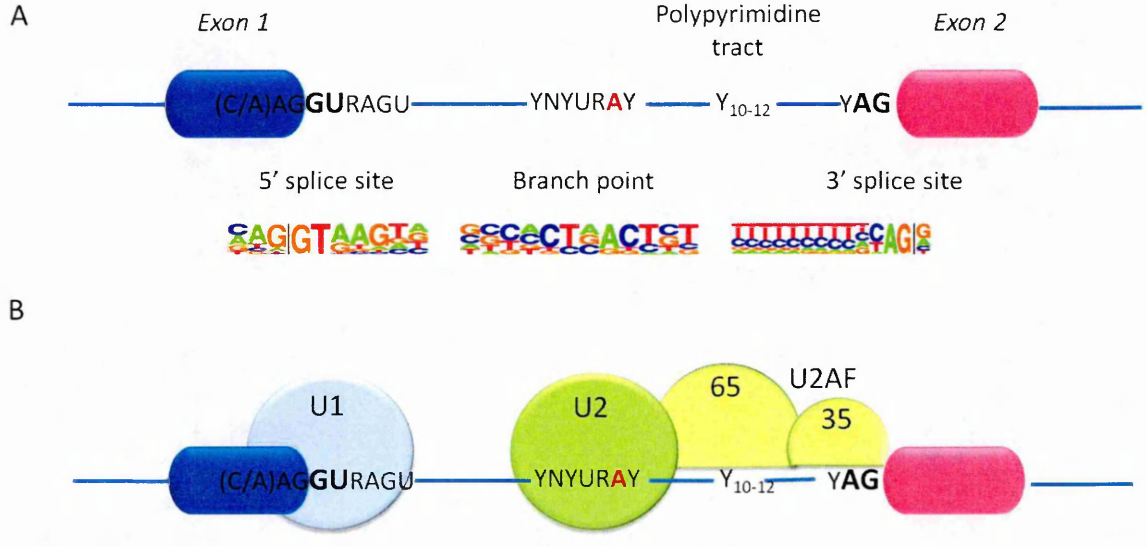

Figure 1.1. (A) Schematic representation of exon-intron boundaries and consensus sequences for 5' and 3' splice sites and branch point. Polypyrimidine tract means region rich in pyrimidines. The A in red is the branch point. (B) Schematic representation of the direct interactions between U1 snRNP with the 5' splice site, the U2 auxiliary factors, U2AF65 and U2AF35, with the polypyrimidine tract and the 3' splice site, respectively, and U2 snRNP with the branch point sequence.

The spliceosomal assembly begins with the ATP-independent interaction of U1 snRNP with the 5' splice site by base-pairing of U1 snRNA with the consensus sequence of the 5' end. This earliest complex (E complex) is characterized also by the binding of SF1/mBBP protein and U2AF to the branch point and to the polypyrimidine tract and 3' splice site, respectively (Konarska, 1998; Wahl et al., 2009). Subsequently, U2 snRNP displaces SF1/mBBP and binds the branch point sequence in an ATP-dependent manner, leading to the formation of A complex. After that the pre-assembled U4/U6.U5 tri-snRNP is recruited, forming the inactive B complex. Several rearrangements activate the B complex into the B* complex, which catalyses the first *trans*-esterification reaction, forming the C complex. After the second catalytic step the spliceosome disassembles (Fig. 1.2) (Will and Luhrmann, 2011).

Intron removal occurs through two consecutive *trans*-esterification reactions catalysed by the spliceosome; in the first step the adenosine 2'-hydroxyl group of the branch point attacks the phosphodiester bond at the 5' splice site, forming a free 5' exon and a lariat intermediate. The second *trans*-esterification, in which the 3' splice site is attacked by the 3'-hydroxyl group of the 5' exon, results in intron excision and exon ligation, producing the mRNA (Brow, 2002).

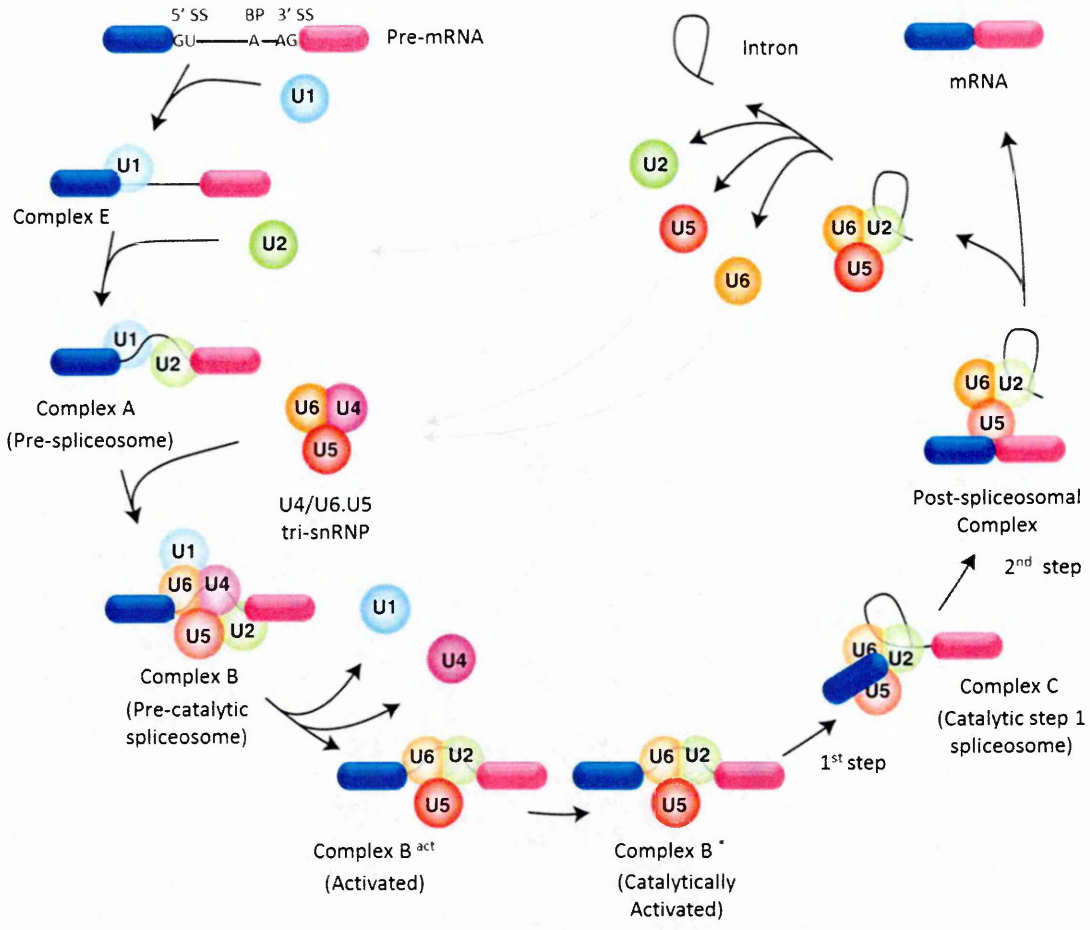

Figure 1.2. Spliceosome assembly. In the earliest E spliceosomal complex, the U1 snRNP is recruited to the 5'ss. In a subsequent step, the U2 snRNP stably associates with the branch point, forming the A complex. The U4/U6.U5 tri-snRNP is then recruited, generating the precatalytic B complex. Major rearrangements in RNA–RNA and RNA–protein interactions, leading to the destabilization of the U1 and U4 snRNPs, give rise to the activated spliceosome (the B-act complex). Subsequent catalytic activation generates the B catalytically activated complex, which catalyses the first of the two steps of splicing. This yields the C complex, that in turn catalyses the second step (adapted from (Will and Luhrmann, 2011)).

This canonical cross-intron model has been studied principally using *in vitro* analysis (Query et al., 1996), but when intron length exceeds 200 nucleotides, as in the case of the vast majority of mammalian introns, it seems that splicing machinery complexes more likely form across the exons.

In this model, called exon definition model, U1 snRNP base pairs with the 5' splice site downstream of an exon and promotes the interaction of U2AF with the polypyrimidine tract/3' splice site upstream of it, leading to the binding of U2 snRNP to the branch point; once assembled, the splicing factors can pair across the long introns, forming the active spliceosomal complex (Berget, 1995; Fox-Walsh et al., 2005).

Since in higher eukaryotes splice sites are degenerated, other auxiliary sequences play an important role in the definition of exons; these elements can be classified by their location and activity as exonic splicing enhancers (ESE) and silencers (ESS), intronic splicing enhancers (ISE) and silencers (ISS) (Fig. 1.3) (McManus and Graveley, 2011).

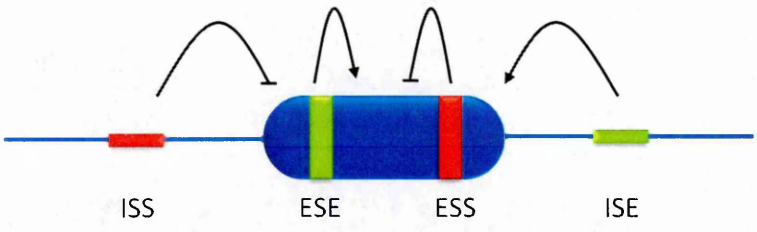

Figure 1.3. An overview of the possible *cis*-acting elements: exonic splicing enhancers (ESE) and silencers (ESS), intronic splicing enhancers (ISE) and silencers (ISS).

Many studies have shown that exon recognition can also be affected by other factors. Among these, of great interest is the Pol II elongation rate, in fact variations in the splicing pattern can be obtained using polymerases that transcribe at different speeds (de la Mata et al., 2003). Moreover, also RNA secondary structure can influence splicing: for example short hairpins or long interactions can modulate exon selection by altering the function of some regulatory elements and proteins (Buratti and Baralle, 2004).

1.2. Alternative splicing.

Pre-mRNA splicing can occur constitutively or alternative. In the first case the exon is always included in the mature mRNA, while in the second one multiple mRNAs can be obtained from the same pre-mRNA by differential joining of 5' and 3' splice sites. Alternative splicing is one of the main protagonists in regulation of tissue-specific gene expression, by generating different protein isoforms that can function in diverse cellular processes (Maniatis and Tasic, 2002).

An estimation of the frequency of alternative splicing in human genes has increased over the years from 5% to more than 95%, partially explaining the discrepancy between the 24.000 estimated protein coding genes and about 100.000 different synthesized proteins (Keren et al., 2010).

Alternative splicing is prevalent only in multicellular eukaryotes and, in particular, it is highly extensive in mammalian nervous system in which it acts as an important spatial and temporal control that influences the synaptic function and the development of neuronal circuits (Grabowski, 2011). Neuron specific alternative splicing involves, for example, the *SRC tyrosine kinase* and *SNAP25* pre-mRNAs. *SRC* is characterized by the presence of a neuronal specific cassette exon (N1), which is repressed in non-neuronal cells by the polypyrimidine binding protein (PTB); during neuronal differentiation, PTB is replaced by neural PTB (nPTB), which is less repressive than the other isoform, leading to the inclusion of N1 exon (Chan and Black, 1997; Boutz et al., 2007). On the other hand, SNAP25 (synaptosomal-associated protein 25) has an important role in vesicle stabilization and neurotransmitter release and the alternative splicing of exon 5 creates two mRNAs, encoding different functional protein isoforms. In particular the SNAP-25a is more present in embryonic mouse brain, while SNAP25b becomes the most abundant

isoform in adult brain, supporting the important period of synaptogenesis (Sorensen et al., 2003).

Several different types of alternative splicing patterns exist (Fig. 1.4) through which exons can be included or skipped, extended or shortened, and introns can be removed or retained. Transcription, for example, can initiate at different promoters, forming alternative 5'-terminal exons joining to a common 3' exon, and also alternative polyadenylation sites can be used. When more than one splice site is present within an exon, the exon length can vary due to the use of alternative 5' and 3' splice sites. These two types of AS patterns are the most abundant only after the cassette exon: in this case one exon can be included or excluded. Other two less common events are intron retention and mutually exclusive splicing, which consists in a paired cassette exons where one exon or the other is present in the mature mRNA, but not both (Matlin et al., 2005).

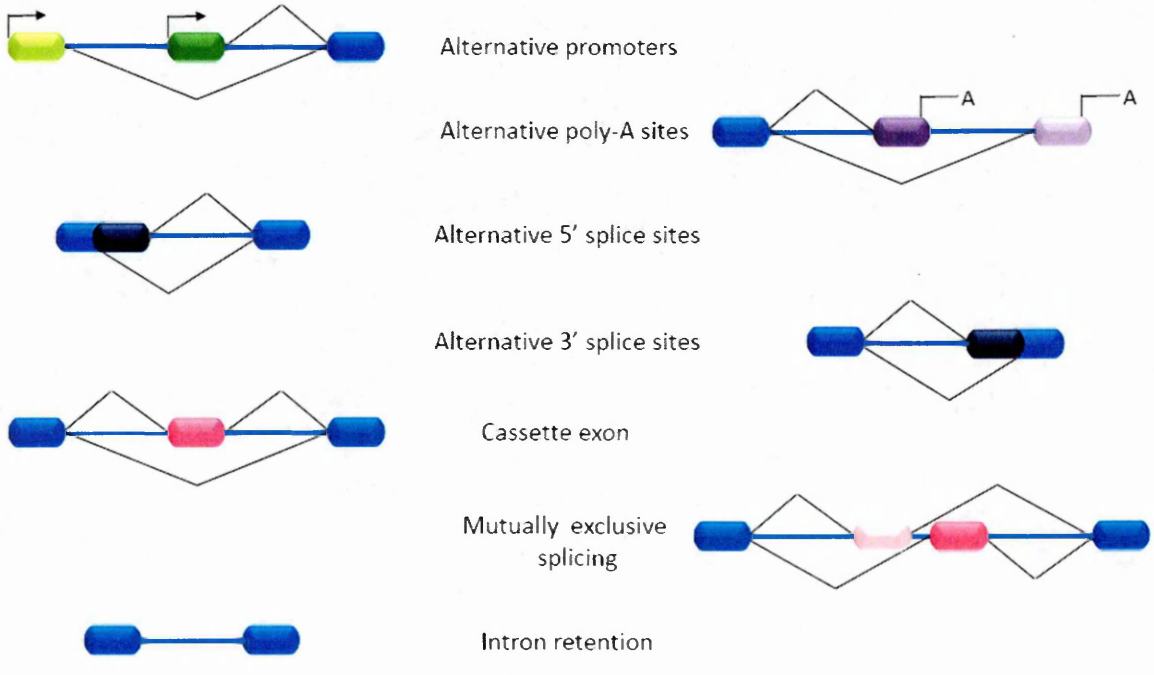

Figure 1.4. Typical types of alternative splicing are inclusion or skipping of one or more exons (cassette exons), mutual exclusion of two or more exons, retained introns and shortening or lengthening of an exon by alternative 5' and 3' splice site. Different promoters and different polyadenylation sites may specify alternative 5' and 3' terminal exons, respectively.

1.2.1. Mutually exclusive splicing: "when two is a crowd".

Mutually exclusive (ME) splicing is a highly regulated mechanism, in which only one exon of a cluster of internal exons can be included in the final mRNA (Smith, 2005). This form of splicing modulates protein functionality, for example by changing biochemical and physical properties of the protein via the inclusion of the alternative exon. The most extreme and fascinating example of ME splicing, as a way of increasing protein diversity, is the *Drosophila melanogaster Down Syndrome Cell Adhesion Molecule (Dscam)* gene, that is involved in the development of neuronal circuits (Zipursky et al., 2006). It contains 115 exons, 95 of which undergo alternative splicing, generating potentially 38,016 distinct mRNAs; these 95 exons are organized in four clusters and the exons within each cluster cannot be spliced to each other in a mutually exclusive manner (Schmucker et al., 2000).

This type of alternative splicing is very common in the regulation of neuronal activity and development. One example is the N-type voltage gated calcium channels, that control neurotransmitter release at the synapse. The intracellular domain of this channel can be modified thanks to ME exons 37a and 37b: in nociceptors the mRNA containing exon 37a is the most abundant species, that is responsible for the large N-type currents of these particular neurons (Castiglioni et al., 2006).

Many studies have been performed to understand the mechanisms that direct this fine-tuned selection and several models have been identified. The first one is steric interference between splice sites, which occurs when the branch point of the downstream exon is too close to the upstream 5' splice site. In fact, if the distance is less than 50 nucleotides, U1 and U2 snRNPs cannot bind in a productive manner and the paired exons cannot be spliced together. One example is *α-tropomyosin* ME exon 2 and exon 3 (Fig. 1.5A) (Smith and Nadal-Ginard, 1989). The second model, proposed for exons 6a and 6b of the human *c-Jun N-terminal kinase 2* gene (*JNK2*), is spliceosomal

incompatibility, regards the major and minor spliceosomes. The major spliceosome recognises the signals GU/AG and removes the vast majority of the introns. However, a small percentage of introns are spliced by the minor spliceosome, which consists of U11, U12, U4atac, U6atac and U5 snRNPs, that uses different splicing signals, AU/AC (Patel and Steitz, 2003). Introns containing 5' and 3' splice sites for the two different spliceosomes can not be spliced together (Sharp and Burge, 1997). For example in the case of exon 6a and 6b of *JNK2* gene, the intron among the two ME exons presents a U12-type 5' splice site and a U2-type 3' splice site (Fig. 1.5B). Spliceosomal incompatibility prevents them from being included both in the final mRNA and also the skipping of the ME exons (Letunic et al., 2002) .

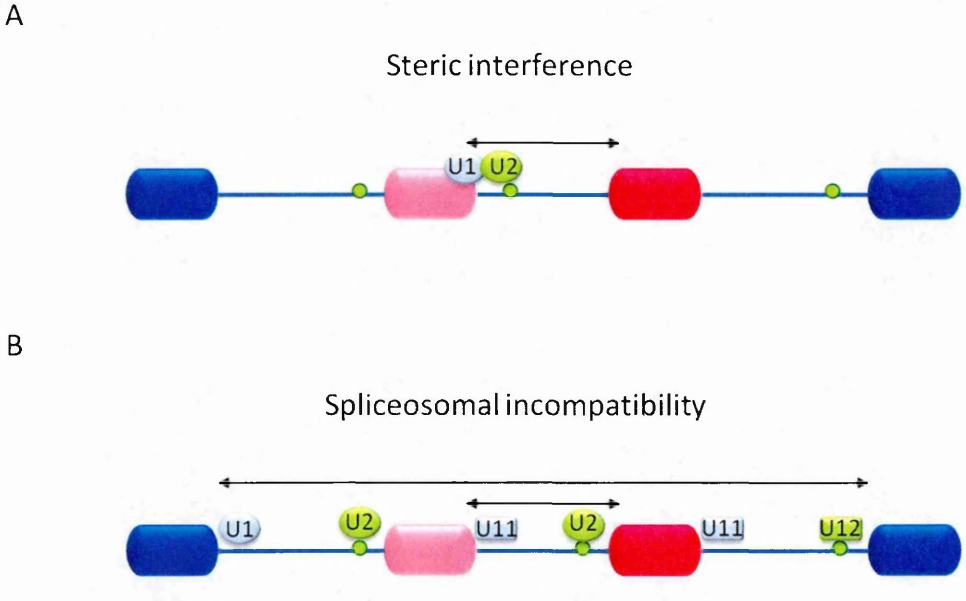

Figure 1.5. (A) Steric interference occurs when the branch point (green dot) of the downstream ME exon is too close to the upstream 5' splice site. Mutually exclusive exons are shown in light and dark pink, constitutive exons in blue. (B) A model of spliceosomal incompatibility. The splice sites used by the "U1/U2" and "U11/U12" snRNP containing spliceosomes that have distinct consensus sequences and are incompatible.

A third form of ME splicing control lies in the fact that in in some cases the choice of only one exon among a ME exons pair is directed by tissue specific *trans*-acting factors, as seen for *α-actinin*. This gene contains an exon pair, SM and NM exons. Exon SM is included only in smooth muscle while the exon NM is included only in non-muscle tissues. The SM inclusion is favoured by the presence of CUG-BP1 (CUG-binding protein 1) and ETR3 (embryonically lethal abnormal vision-type RNA binding protein 3) proteins, that at the same time inhibit NM inclusion. SM exon is also inhibited by PTB, but this negative effect is counteracted by CUG-BP1, that directly antagonizes the binding of the PTB. In this case the mutually exclusive splicing pattern is directed by the combinatorial control of these proteins (Gromak et al., 2003).

Other mutually exclusive events are strictly regulated both by tissue specific factors and by the nonsense-mediated decay (NMD) pathway. This happens when the ME exons are not multiple of three nucleotides. One example is the alternative splicing of exon IIIb and IIIc of the *fibroblast growth factor receptor 2* (*FGFR2*) gene. The transcripts including both the ME exons are produced but, due to a frameshift, a premature stop codon is introduced in exon IIIc activating the NMD pathway to degrade the mRNA (Jones et al., 2001).

The first direct evidence of the relevance of RNA secondary structure in ME splicing derived from the studies on *Dscam* gene. In 2005 Graveley and his group identified in the introns of *Dscam* exon 6 cluster two classes of conserved sequences: a sequence downstream of exon 5, called the docking site, and complementary elements upstream of each exon 6, called the selector sequences (Graveley, 2005). They described that one selector element can bind one docking stretch at a time: this RNA base-pairing competition drives the mutually exclusive selection of only one ME exon 6 (May et al., 2011).

1.3. Splicing regulatory elements and *trans*-acting factors.

Genome sequencing analyses have showed that the majority of splice sites do not precisely conform to the consensus sequence: for example less than 5% of 5' splice sites match perfectly the 9 nucleotide consensus stretch and more than 25% are characterized by three or more mismatches (Zhang et al., 2003). Since there are many cryptic splice sites that should be avoided and the 5' and 3' splice sites are so degenerate, other signals and interactions are necessary to enhance their correct use (Maniatis and Tasic, 2002). The need for these auxiliary signals is even more significant if we consider that the size of a human exon is comprised among 50-250 bps, much shorter respect to the intronic thousands residues: this means that the spliceosomal machinery has to identify small exons within vast intronic sequences (exon definition model), so the auxiliary splicing elements are very important in this early stage of spliceosomal assembly (Berget, 1995; Chen and Manley, 2009). These *cis*-acting elements, as mentioned in section 1.1, are classified according to their effect and position as exonic splicing enhancers and silencers, intronic splicing enhancers and silencers. They do not only play an important role in the recognition of exons *per se* in constitutive splicing, but also in alternative splicing, which is characterized by the presence of competing splice sites (Black, 2003).

1.3.1. Exonic and intronic splicing enhancers and their *trans*-acting factors.

In 1987 it was observed that an exonic sequence in EDA exon of the *fibronectin* gene was involved in the definition of alternative splicing, representing the first evidence for additional *cis*-acting elements (Mardon et al., 1987). Although at the beginning splicing enhancers were originally described as important players only in alternative splicing events, it is known that they also play an essential role in constitutive splicing facilitating the recognition of the splice sites (Schaal and Maniatis, 1999). One of the most well

characterized exonic splicing enhancer (ESE), consisting of six copies of a 13-nucleotide consensus sequence, is involved in inclusion of female specific exon 4 in the *doublesex* gene in *Drosophila*. Exon 4 is not included in males due to its weak 3' splice site. In females the binding of the SR protein Rbp1 and the SR-like protein Tra2 to the ESE, directed by Tra, a female specific protein, leads to exon 4 inclusion (Tian and Maniatis, 1994; Lynch and Maniatis, 1995).

The vast majority of exonic enhancer elements (ESEs) contains purine-rich sequences, which are binding sites for serine/arginine-rich (SR) proteins. These proteins are involved in several steps of spliceosome assembly and act as both essential splicing factors and regulatory factors. SR proteins have a common structural organization, characterized by the presence of one or two RNA recognition motifs (RRM) at the N-terminal and the arginine/serine (RS) domain of at least 50 amino acids with an RS content higher than 40% at the C-terminal: according to this definition, 12 SR proteins have been described in human (Table 1.1) (Tacke and Manley, 1999; Manley and Krainer, 2010).

These *trans*-acting factors are not equally present in all eukaryotes, for example there is no evidence of SR proteins in *S. Cerevisiae*, while *S. Pombe* has only two (Ram and Ast, 2007). In addition to the canonical SR proteins, there are also several SR-related proteins, these include for example Tra2, SRm160/300 and U1-70K (Table 1.2).

Protein name	Gene name	Key domains	Reported function
ASF/SF2	*SRSF1*	RRMx2, RS	Constitutive and alternative splicing activator
SC35	*SRSF2*	RRM, RS	Constitutive and alternative splicing activator
SRp20	*SRSF3*	RRM, RS	Constitutive and alternative splicing activator
SRp75	*SRSF4*	RRMx2, RS	Constitutive and alternative splicing activator
SRp40	*SRSF5*	RRMx2, RS	Constitutive and alternative splicing activator
SRp55	*SRSF6*	RRMx2, RS	Constitutive and alternative splicing activator
9G8	*SRSF7*	RRM, RS, zinc finger	Constitutive and alternative splicing regulator
SRp46	*SRSF8*	RRM, RS	Constitutive and alternative splicing regulator
SRp30c	*SRSF9*	RRMx2, RS	Constitutive and alternative splicing regulator
SRp38	*SRSF10*	RRM, RS	Splicing repressor
SRp54	*SRSF11*	RRM, RS	Alternative splicing repressor
SRp35	*SRSF12*	RRM, RS	Alternative splicing repressor

Table 1.1. Classical SR proteins.

Protein name	Gene name	Key domains	Reported function
hTra2α	*TRA2A*	RRM, RS×2	Splicing activator
RNPS1	*RNPS1*	RRM, RS	Constitutive and alternative splicing regulator
U2AF35	*U2AF1*	RRM, RS, C3H1-type zinc finger×2	Constitutive splicing factor
U2AF65	*U2AF2*	RRM×3, RS	Constitutive splicing factor
U1-70K	*SNRP70*	RRM, RS	Constitutive splicing factor
SRm160	*SRRM1*	RS, PWI	Constitutive and alternative splicing co-activator
XE7	*SFRS17A*	RRM, RS	Alternative splicing regulator

Table 1.2. Examples of SR-related proteins.

SR proteins are predominantly located in the nucleus, in particular structures called speckles, that seem to act as sites of storage of these phosphoproteins together with other important splicing factors (Jimenez-Garcia and Spector, 1993; Caceres et al., 1998). However, these factors are not confined into the nucleus, where they are involved in the splicing regulation, but they shuttle between the nucleus and the cytoplasm at different dynamic rate: ASF/SF2, SRp20, 9G8 and SRp38 at higher rate respect to SRp75 and SRp55 (Caceres et al., 1998; Sapra et al., 2009). Due to this shuttling, SR proteins can regulate several steps of mRNA metabolism, from the synthesis to the degradation, and also play a role in the translation (Twyffels et al., 2011). Moreover the expression of these *trans*-acting factors varies in a tissue-specific manner, conditioning the splicing pattern within different cell lines (Hanamura et al., 1998). Complementation assays with cytoplasmic S100 splicing-deficient extract, lacking the SR proteins, showed that these members are interchangeable in exerting their activity (Zahler et al., 1992). However some differences in their ability to promote splicing have been shown *in vivo*, for example in mouse models: the SR null-mice for ASF/SF2 or SC35 display an early embryonic phenotype, indicating that the members of this family are not completely redundant (Moroy and Heyd, 2007).

Models based on protein-protein interactions have been proposed to explain the mechanisms through which SR proteins facilitate splice sites recognition. Due to their RS domains and depending on their phosphorylation state ASF/SF2 and SC35 can interact with each other, with U1-70K SR related proteins and with U2AF35, suggesting that they facilitate splicing by forming interactions across exons and introns (Fu, 1995; Graveley, 2000). An alternative model for enhancer activity is based on bridging interactions between ESEs and spliceosomal components, through factors such as SRm160 and SRm300. These co-activators, which contain RS domains but lack RRM domains, can

generate multiprotein complex with snRNPs and SR proteins bound to the ESE sequence (Blencowe, 2000). In some cases the binding of the SR proteins can prevent or displace the recruitment of negative regulatory factors to silencers, such as hnRNP A1 (Zhu et al., 2001).

As previously mentioned splicing enhancers can also be found in introns (ISEs), although the number of positive intronic elements described in literature is very low respect to exonic ones. One example is the inclusion of exon 3 of the *apolipoprotein A-II* gene, that is favoured by an ISE within the downstream intronic region and bound by SRp40 and SRp55 (Mercado et al., 2005). Some other 5' splice sites are activated by a U-rich sequence, located immediately downstream: two examples are *Fas* exon 6 and *K-SAM* alternative exon of the fibroblast growth factor receptor 2. In both cases an U-rich ISE sequence is bound by T-cell restricted intracellular antigen 1 (TIA 1) to facilitate the recruitment of U1 snRNP at the adjacent 5' splice site (Del Gatto-Konczak et al., 2000; Izquierdo et al., 2005). Another example of transcript regulated by ISE is the *endothelial nitric oxide synthase* (*eNOS*): in this case the binding of the heterogeneous nuclear ribonucleoprotein L (hnRNP L) at a CA-repeat ISE determines the activation of a weak 5' splice site (Hui et al., 2003). Also RbFox family members are known to exert a positive effect by binding intronic motifs downstream of the target exon, but the mechanism of action of these proteins will be described in detail in section 1.3.3.1.

1.3.2. Exonic and intronic splicing silencers and their *trans*-acting factors.

In contrast to the positive action of exon inclusion of the splicing enhancer elements, there are also other *cis*-acting elements that regulate in a negative manner splice site choice or block spliceosomal activity. In particular the exonic splicing silencers (ESSs) are bound by heterogeneous nuclear ribonucleoproteins (hnRNPs), which are a set of

primarily nuclear proteins that bind pre-mRNA without forming stable association with other RNA-protein complexes. Twenty major proteins have been discovered and designated from A1 to U and a role in splicing regulation has been described for all of them, except to date for hnRNP U (Table 1.3) (Dreyfuss et al., 1993).

Protein name	Key domains	Reported function
A1	RBDx2, RGG	Splicing, export, telomere biogenesis
A2/B1	RBDx2, RGG	Splicing, localization
C1/C2	RBD	Splicing, stability
D	RBDx2, RGG	Splicing, stability, recombination
E1/E2/E3/E4	KHx3	Splicing, stability, translation
F	RBDx3	Splicing
G	RBD, RGG	Splicing
H/H'	RBDx3	Splicing, polyadenylation
I	RBDx4	Splicing, localization, polyadenylation
K/J	KHx3, RGG	Splicing, transcription, stability, translation
L	RBDx4	Splicing, export, stability, riboswitch
M	RBDx4	Splicing
P2	RBD	Splicing, avid binding to poly(A)
Q1NSAP	RBDx3, RGG	Splicing, translation
R1/R2	RBD	Splicing, stability
U	RGG	Nuclear retention

Table 1.3. Major hnRNP proteins (Adapted from (Dreyfuss et al., 2002; Han et al., 2010)).

The vast majority of the hnRNP proteins interact with the pre-mRNA through one or more RNA binding motifs (RBM), with some exceptions such as hnRNP K/J and hnRNP E1/E4, which use a KH domain (Dreyfuss et al., 1988; Burd and Dreyfuss, 1994; Chaudhury et al., 2010).

Most hnRNPs also contain an RGG box (a cluster of Arg-Gly-Gly tripeptides) that could be in combination with other RNA binding domains (RBD) or unique, as in hnRNP U (Kiledjian

and Dreyfuss, 1992). Moreover, hnRNPs may contain other unstructured auxiliary domains such as glycine-rich or proline-rich domains, that are important in the localization of the proteins: for example one glycine-rich nuclear import/export domain (M9) is located at the C-terminal of hnRNP A1 (Weighardt et al., 1995).

Regarding the localization of these *trans*-acting factors, although many of them are nuclear at the steady state, they can shuttle from the nucleus to the cytoplasm (Pinol-Roma and Dreyfuss, 1992), playing an essential role in nucleo-cytoplasmic transport of mRNA (Lee et al., 1996), in mRNA localization (Carson et al., 2001) and translation (Habelhah et al., 2001) and in mRNA stability (Xu et al., 2001). Within the nucleus hnRNPs take part in various processes such as transcriptional regulation (Miau et al., 1998), RNA splicing (Chan and Black, 1997; Chou et al., 1999; Mourelatos et al., 2001), telomere maintenance (Ford et al., 2002) and 3'-end processing (Kessler et al., 1997).

The mechanisms through which exonic and intronic silencers interfere with splicing are known only for a number of cases and they include inhibition of splice site recognition by sterically blocking the recruitment of snRNPs or positive regulatory factors, by masking of the splice sites through multimerization along the RNA and by looping out of an alternative exon by protein-protein interactions (Chen and Manley, 2009).

In the case of alternative splicing control by steric interference many studies have identified the repressive role of hnRNP A1 affecting the recruitment of snRNPs, for example in the regulation of the removal of the second *tat* intron in HIV transcript. In this case hnRNP A1 binds to an intronic splicing silencer (ISS), that overlaps the branch point, leading to a physical block of the association of U2 snRNP (Tange et al., 2001). Another example is the mutually exclusive splicing of exons 2 and 3 of *α-tropomyosin* (*alfa-TM*) transcript: in this case hnRNP H and hnRNP F directly compete with SRSF7 by sterically interfering the binding of the SR protein to the ESE (Crawford and Patton, 2006). Also

some tissue specific *trans*-acting factors can block the recruitment of important splicing factors: for example both the RbFox proteins and ETR3 can prevent the binding to the branch point of SF1 and U2 snRNP, respectively. All these factors and their mechanisms will be discussed in sections 1.3.3.1 and 1.3.3.3.

The inhibitory effect sometimes is not the result of a simple bind and block effect. In some cases multimerization of the *trans*-acting factor along the RNA occurs to prevent the splice site usage. Examples of this mechanism has been observed with hnRNP A1 and the polypyrimidine tract binding protein (PTB) (Blanchette and Chabot, 1999; Wagner and Garcia-Blanco, 2001; Zhu et al., 2001).

A further mechanism of action of silencers occurs through the formation of protein-protein interactions that loop out the alternative exon. For example hnRNP A1 has been shown to bind to silencers in *survival of motor neuron 2* (*SMN2*) exon 7 and intron 7 and the interaction between them in these two separate positions results in the looping out of the exon, suppressing *SMN2* exon 7 inclusion (Kashima et al., 2007).

One of the most studied repressor, that can exert its negative role using all the different mechanisms previously described, is hnRNP I (PTB). This *trans*-acting factor will be described more in detail in section 1.3.3.2.

1.3.3. Tissue-specific *trans*-acting factors.

A comparative analysis of 15 different human tissue and cell line transcriptomes revealed that more than 50% of the alternative splicing events are regulated in a diverse way between tissues, leading to a tissue-specific expression of alternative splicing isoforms (Wang et al., 2008). One level of control of regulation lies in the presence of tissue-specific and developmentally regulated expression of some *trans*-acting factors, such as

PTB/nPTB, NOVA proteins, RbFox proteins and many others. In the next paragraphs some of these tissue-specific factors have been described more in detail.

1.3.3.1. RbFox protein family.

Trans-acting factors can be expressed in a temporal or tissue-specific manner to modulate precisely a defined set of transcripts. Among them RNA binding Fox (RbFox) family plays an important role in tissue-specific alternative splicing regulation (Fukumura et al., 2007). In mammals the RbFox1 family consists of three members: RbFox1 (Fox1 or Ataxin2 binding protein 1, A2BP1), RbFox2 (Fox2 or RNA binding motif 9, RBM9) and RbFox3 (Fox3, hexaribonucleotide binding protein 3, HRNBP3 or NeuN). RbFox1 is expressed in neurons, in skeletal muscle and in heart, while RbFox3 is restricted to neurons (Jin et al., 2003; McKee et al., 2005; Kim et al., 2009). RbFox2 is detected in brain, heart, ovary and also in embryo, hematopoietic and stem cells (Yeo et al., 2007; Gehman et al., 2012; Huang et al., 2012).

These protein isoforms share a single highly conserved RRM domain that is located in the middle of the protein: an intact RRM domain is required to ensure the activity as a splicing regulator (Damianov and Black, 2010). Furthermore, the deletion of the C-terminal abolishes the nuclear localization and also the activity as a splicing regulator (Lee et al., 2006; Kuroyanagi, 2009).

This group of proteins specifically recognizes (U)GCAUG stretches, which are phylogenetically and spatially conserved especially in the flanking introns of brain regulated exons (Jin et al., 2003; Minovitsky et al., 2005; Ponthier et al., 2006). The high affinity and specificity in the recognition of these *cis*-acting elements by the RbFox protein family is mediated through the RRM, thanks to the typical $\beta_1\alpha_1\beta_2\beta_3\alpha_2\beta_4$ fold: the last UGU nucleotides are recognized by the four stranded β-sheets, while the first UGCA

nucleotides are bound by two loops independently from the β-sheet binding interface (Auweter et al., 2006).

RbFox proteins have been described to act both as enhancers or silencers depending on their position respect to the target exon: upstream binding sites are repressive, whereas downstream RbFox sites generally act as enhancers (Fig. 1.6)(Underwood et al., 2005).

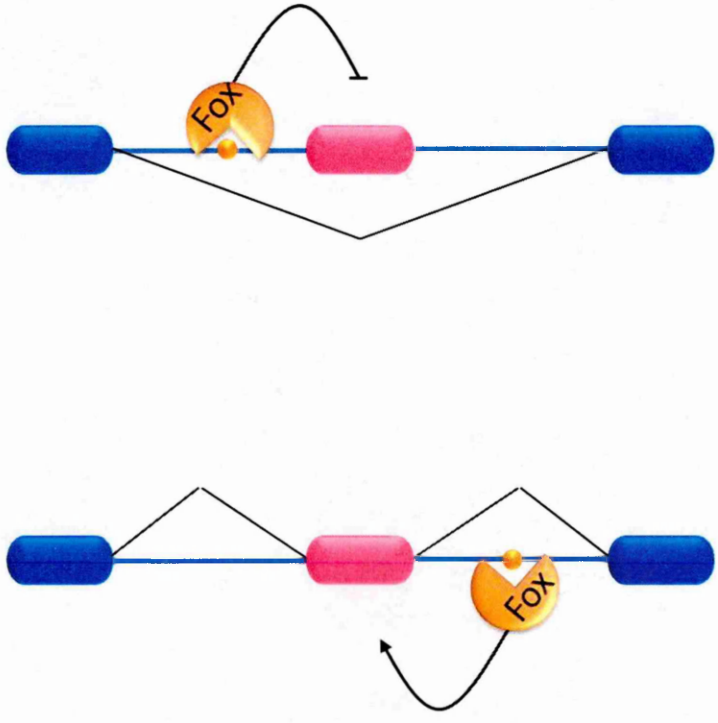

Figure 1.6. RbFox proteins repress exon inclusion by binding to (U)GCAUG element (the orange dot) in the upstream intronic flanking region, while they enhance exon inclusion by binding to the (U)GCAUG element in the downstream intronic flanking region.

Examples of splicing regulation by RbFox1 family members are protein *4.1 R*, *calcitonin/CGRP* and *SCN8A* gene. In the first one RbFox2 promotes exon 16 inclusion binding to a downstream intronic element: this interaction improves the usage of the weak 5' splice site by facilitating U1 snRNP recruitment (Ponthier et al., 2006; Huang et al., 2012). Regarding the repression of exon 4 in *calcitonin/CGRP* transcript it has been demonstrated that RbFox1 and RbFox2 interact with an upstream intronic element, preventing SF1 binding to the branch point and repressing the E complex formation; the proteins also bind an UGCAUG in exon 4, interfering with Tra2β and SRSF6 enhancer

action and blocking spliceosomal E complex formation (Zhou and Lou, 2008). *SCN8A* transcript contains a pair of exons 18 that are mutually exclusively spliced; potential Fox binding sites are present downstream of exon 18A. Using a minigene system the mechanism of regulation of ME exons 18N and 18A has been investigated: in this case RbFox members enhance the inclusion of 18A (Zubovic et al., 2012). These results have been confirmed by *in vivo* studies using $Rbfox1^{+/-}Rbfox2^{-/-}$ mice: the cerebellum of these mutant mice is characterized by the presence of an altered splicing of both the two pairs of ME exons, in particular with the decrease inclusion of exon 18A from 80% to 40% (Gehman et al., 2012; Zubovic et al., 2012).

1.3.3.2. Polypyrimidine tract-binding protein.

One of the best characterized splicing repressor is hnRNP I, also known as polypyrimidine tract-binding protein (PTB). PTB is predominantly found in the nucleus where it exerts its role in splicing regulation, but it can shuttle from the nucleus to the cytoplasm being involved in many other steps of the RNA process such as transport, mRNA stabilization and translation (Romanelli et al., 2013). This protein is expressed in many but not all tissues. In fact in mammals there are two PTB paralogs that are characterized by a tissue-specific expression: the nPTB (PTBP2) and ROD1 (PTBP3). The former is predominantly expressed in adult brain, testis and muscle, while ROD1 is found in haematopoietic cells (Yamamoto et al., 1999; Polydorides et al., 2000; Spellman et al., 2007). PTB and nPTB expression is mutually exclusive, with PTB restricted in non-neuronal cells and nPTB in post-mitotic neurons. Of great importance in the regulation of alternative splicing during neuronal development seems to be the post-transcriptionally switch from the PTB to nPTB (Boutz et al., 2007). Although PTB and nPTB display a 74% of homology in the peptidic sequence, the effects on splicing regulation sometimes are different, with nPTB

exerting a weaker repressive effect respect to PTB, as shown for *c-src* exon N1 and *$Ca_V1.2$ calcium channel* exon 8 (Markovtsov et al., 2000; Tang et al., 2011). There are also some exceptions as *postsynaptic density protein 95* (*PSD-95*) exon 18, in which the two proteins show the same effect (Zheng et al., 2012).

PTB structure consists of four RNA recognition motifs (RRM) and the nuclear localization signals within the N-terminal region (Oberstrass et al., 2005). The optimal *cis*-acting elements recognized by PTB are UCUUC and CUCUCU motifs in pyrimidine-rich contexts (Perez et al., 1997). PTB binding sites are often located in the polypyrimidine tract of the regulated exons, but there are also binding sites in other positions. Many models have been proposed to explain PTB splicing repression. One mechanism proposed is that PTB competes with the splicing factor U2AF65 for binding the polypyrimidine tract (Lin and Patton, 1995). Since most of the PTB regulated exons show the presence of many PTB binding sites both in intronic and/or exonic regions, other mechanisms of action involving the multimeric binding of PTB are also described (Wagner and Garcia-Blanco, 2001; Spellman and Smith, 2006) such as the propagation model. In this case PTB can oligomerize along the pre-mRNA by masking an exon. In other circumstances when PTB binding sites are upstream and downstream of the target exon, PTB-PTB interactions can induce the looping out of the target exon (Wagner and Garcia-Blanco, 2001).

Overall, although I have described a few general models of PTB repression, the reality is that many more exist. It appears that mechanisms are different depending on the exon context and also they appear to be more complex interfering with intron or exon definition. Two examples largely studied in literature are *c-src N1* exon and *Fas* exon 6 (Keppetipola et al., 2012).

The *c-src* N1 exon is included in neurons, while it is repressed in non-neuronal cells by high levels of PTB (Chou et al., 2000). The cell-specific splicing and the PTB repression

were studied taking advantage of an *in vitro* splicing system using two different extracts from neuronal cells (WERI-1) and non-neuronal cells (HeLa) (Black, 1992). To understand the mechanism of inhibition exerted by PTB, Sharma et al. analysed spliceosome assembly on N1 exon in the presence of both extracts. Firstly, they demonstrated that the binding of U1 snRNP to exon N1 5' splice site is not affected by PTB bound to silencer elements flanking the exon. Instead, the binding of PTB to the pre-mRNA prevents the interaction between U1 snRNP and U2AF, inhibiting the formation of the E complex (Sharma et al., 2005).

If in the case of *c-src* N1 exon PTB inhibits intron definition, it counteracts exon definition in splicing of *Fas* exon, that is directed by the antagonistic action of TIA-1 protein and PTB. TIA-1 favours exon 6 inclusion by binding to an ISE downstream of the target exon, promoting U1 snRNP recruitment to the 5' splice site, that in turn stimulates U2AF65 binding to the 3' splice site. *In vitro* analysis shows that, also in this case, PTB does not interfere with the binding of U1 snRNP, but it inhibits the activation of U2AF65 (Izquierdo et al., 2005).

Although the most well-studied role of PTB is as a splicing repressor, it has been published also that it can enhance the inclusion of some exons. One of the first examples described was *CT/CGRP* exon 4, in which PTB binds to an enhancer pyrimidine tract that is part of a pseudoexon, blocking the recognition of the pseudoexon and favouring inclusion of exon 4. Moreover, exon 4 is the terminal exon so PTB could also affect the polyadenylation process (Lou et al., 1999). Recently, using a high-density Affymetrix microarray, the alternative splicing events affected by PTB/nPTB knockdown have been analysed. This analysis has shown that despite the majority of events are upregulated, confirming the important role of PTB as splicing repressor, a number of them are downregulated,

suggesting a positive role of this factor that has to be investigated more in detail (Llorian et al., 2010).

1.3.3.3. CELF family proteins.

The CELF (CUG-BP1 and ETR-3-like factors) family of RNA-binding proteins are found both in the cytoplasm and in the nucleus, where they regulate many processes such as alternative splicing, regulation of the polyadenylation and mRNA stability (Ladd, 2013).

In humans the family is composed of six members, that can be divided in two subgroups: CELF1-2 and CELF3-6. The former subfamily is characterized by a broad expression, including brain, heart, skeletal muscle and developing embryo. The latter family shows a more specific expression: CELF3 and CELF5 are especially expressed in nervous system, while CELF6 in testis, kidney and nervous system. The expression of CELF4 has not yet been precisely defined (Ladd et al., 2001; Ladd et al., 2004).

The structure, common for all the six proteins, consists of three RNA recognition motifs. Among the RRM2 and the RRM3 there is a divergent domain, that seems to have a role in directing RNA interactions, probably due to protein-protein interactions or ensuring a particular conformational state (Dasgupta and Ladd, 2012).

The binding preferences for these proteins are partially characterized: CELF1 (CUG-BP1) binds regions enriched in UGU, CELF2 (ETR3) prefers UG repeats and UGUU motifs, while the binding sites for the other CELF proteins are not well-characterized (Faustino and Cooper, 2005; Marquis et al., 2006). Alternative splicing is one of the processes influenced by this class of RNA binding proteins, that can act both as a splicing enhancers or silencers. Two examples of exons regulated by these proteins are *cardiac troponin T* (*cTNT*) exon 5 and *N-methyl-D-aspartate receptor 1* (*NMDA R1*) exon 5 (Dasgupta and Ladd, 2012).

The *cTNT* exon 5 is included in embryonic cardiac muscle and in skeletal muscle, but it is skipped in adult cardiac muscle, altering in this way the contractile features of the myofibrils. Exon 5 inclusion is favoured by two muscle-specific splicing enhancers, present in the intronic region downstream of exon 5, that are recognized by CELF1 and CELF2 (Ladd et al., 2005). In particular the mechanism of action of CELF2 has been studied: this factor activates complex A formation, promoting the binding of U2 snRNP to the branch point and increasing *cTNT* exon 5 inclusion (Goo and Cooper, 2009).

The gene encoding *NMDA R1* receptor contains two alternative spliced exons, exon 5, encoding the cassette N1, and exon 21, encoding the cassette C1, that are regulated in a neuron specific manner altering the receptor properties at the synapses. It has been shown that CELF2 inhibits N1 inclusion, while it enhances C1 inclusion (Zhang et al., 2002). The inhibitory role of CELF2 on the cassette N1 has been studied more in detail. The factor recognizes specific binding sites surrounding the branch point and the negative role implies a direct antagonism of U2 snRNP recruitment at the branch point (Dembowski and Grabowski, 2009).

Several studies highlight the opposite effect exerted by CELF proteins and PTB such as in case of *β-tropomyosin*, *α-actinin* and *cTNT* (Charlet et al., 2002; Gromak et al., 2003; Sureau et al., 2011). The *β-tropomyosin* gene contains a pair of mutually exclusive exons 6A and 6B that are regulated during myogenic differentiation. In fact exon 6A is predominantly included in non-muscle cells and in myoblasts, whereas the isoform containing exon 6B is found in striated muscle and myotubes. In this case it has been demonstrated that PTB inhibits 6B inclusion in myoblasts through the interaction with the branch point and the polypyrimidine tract. During muscle differentiation the level of PTB decreases, lowering also its inhibitory effect, while the level of CELF1 increases, exerting

its positive role. So far the mechanism appears to be regulated by changes in *trans*-acting factor level rather than a direct antagonism (Sureau et al., 2011).

1.4. Voltage-gated sodium channels.

In nerve, muscles and heart the transmission of electrical impulse is mediated by the gating of membrane associated ion channels. Among them the voltage-gated sodium channels (VGSCs) play a critical role in the rising of the rapid depolarisation during the initial phase of action potential. This type of sodium channels respond to voltage differences on the two sides of the membrane where they are inserted, allowing a sodium influx and causing the depolarization of the cells. In particular this depolarization event in neurons leads to the propagation of the action potential, whereas in cardiac and skeletal muscle the action potential is important to induce a contraction (Catterall, 1992).

In mammals the voltage-gated sodium channel isoforms identified are divided in three groups: the Na_v 1.x channels, that are largely characterized also in exogenous systems; the Na_v 2.x group, that shares about 50% of homology to type 1; and a third group called Na_v 3.x (Goldin, 1999).

Regarding the most studied Na_v 1.x group, nine different isoforms have been identified in mammals: nine distinct genes (*SCN1A-5A, SCN8A-11A*) encode the Na_v 1.1 -1.9 channels (Goldin et al., 2000; Catterall et al., 2005). Mammalian sodium channels, in addition to differences in cellular and tissue expression, also change the expression pattern during development, consistent with a distinct role of each of these in mammalian physiology. In the central nervous system adult neurons show a combination of Na_v 1.1, Na_v 1.2 and Na_v 1.6 (Trimmer and Rhodes, 2004), while in adult DRG sensory neurons there are predominantly Na_v 1.7, Na_v 1.8 and Na_v 1.9 sodium channels (Black et al., 1996). Na_v 1.3 is present in immature neurons and only at low levels in adult neurons. Na_v 1.4 is

prevalently expressed in skeletal muscle (Trimmer et al., 1989); Na_v 1.5 is predominantly expressed in cardiac muscle (Rogart et al., 1989), although it has also been detected in dorsal root ganglia neurons (Renganathan et al., 2002).

The voltage-gated sodium channels are composed of one α subunit of 260 KDa, which forms the core of the channel and regulates the voltage dependent gating and ion permeation, and it is typically associated with auxiliary β subunits (Fig. 1.7). Four different β subunits have been found till now and it was proposed that they may contribute in the stabilization of the α subunit in the membrane and/or in the localization of the α subunit to specific membrane domains (Isom, 2001).

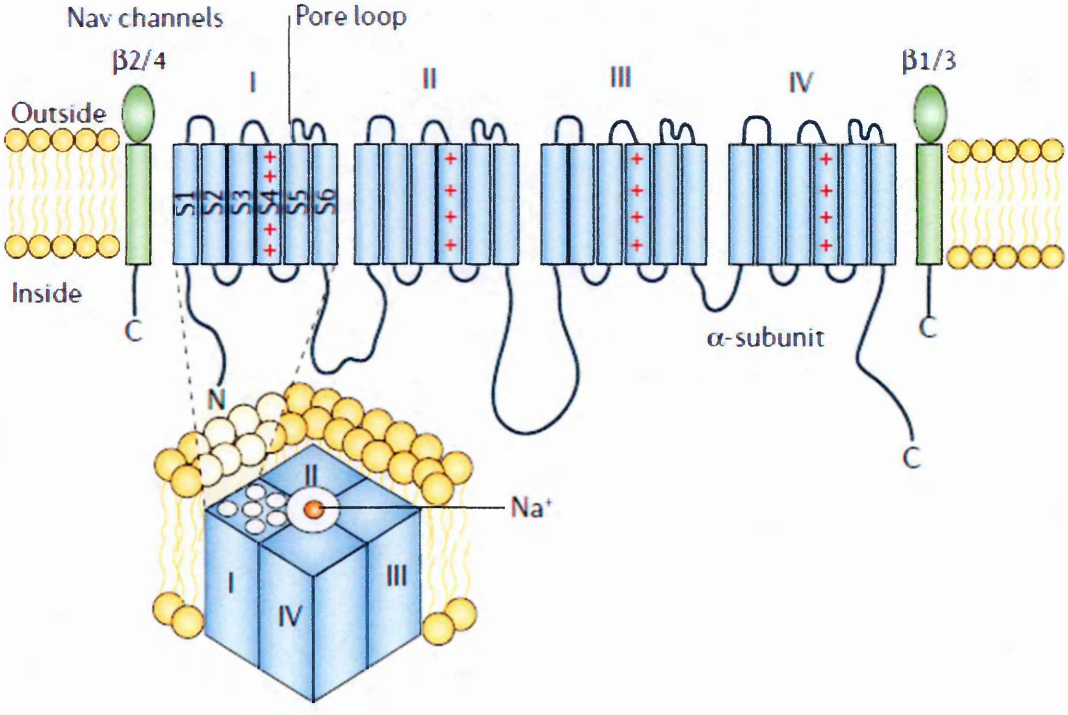

Figure 1.7. Schematic representation of the voltage-gated sodium channel α and β subunits. The α subunit is characterized by four domains each one formed by six transmembrane elements. The positively charged S4 segments constitute the voltage sensor of the channel. In the lower part a 3D model of the voltage-gated channel α subunit is shown.

The α subunit consists of four homologous domains (DI-DIV), each one characterized by six transmembrane α-helix segments (S1-S6) that are connected by intracellular peptide linkers (Plummer and Meisler, 1999; Goldin et al., 2000). In response to the membrane potential the channels can switch between resting (closed), activated (open) and inactivated (closed) state. S4 segments of each domain act as the voltage sensor, due to a positive amino acid at every third position; all S5 and S6 segments and the P-loop between them form the pore (Stuhmer et al., 1989; Yang and Horn, 1995; Catterall, 2000b; Catterall, 2000a). After membrane depolarization the positively charged residues contained in all S4 move towards the extracellular side; this movement induces a conformational change in the pore, opening the channel (Yang and Horn, 1995). The voltage-gated sodium channels allow only sodium entry thanks to a selectivity filter formed by four residues, one per P-loop. The filter, called also DEKA ring from the name of the residues (aspartic acid, glutamate, lysine and alanine), repulses negatively charged ions and the lysine residue plays a role in the specific selection of Na^+ among other positively charged ions. In fact, substituting this residue elicits potassium and calcium entry (Heinemann et al., 1992; Favre et al., 1996; Koopmann et al., 2006).

The voltage-gated sodium channels display different biophysical features, such as the activation and inactivation kinetics, and also different pharmacological properties, for example Na_v 1.1 - Na_v 1.4, Na_v 1.6 and Na_v 1.7 are sensitive to the tetrodotoxin (TTX) block, while Na_v 1.5, Na_v 1.8 and Na_v 1.9 are considered TTX-resistant, because they respond only to high concentrations of the drug (Diss et al., 2004).

To further increase the plasticity in the expression of the sodium channels there are other levels of regulation: the transcription can be modulated by several stimuli, such as growth factors and hormones (Tabb et al., 1994; Black et al., 1997). Many alternative splicing events affect the transcripts, resulting in the generation of multiple channels isoforms.

Moreover, several levels of post-translational modifications may influence the activity of this protein family, such as glycosylation and phosphorylation (Bennett et al., 1997; Cantrell and Catterall, 2001).

1.4.1. Central nervous system sodium channels.

The most important isoforms present in the central nervous system (CNS) are Na_v 1.1, Na_v 1.2, Na_v 1.3 and Na_v 1.6. While Na_v 1.1 and Na_v 1.6 are also found in the peripheral nervous system, Na_v 1.2 and Na_v 1.3 are highly expressed only in CNS. All the isoforms have been amplified both in neurons and in glia cells. They are characterized by specific subcellular localization and a different expression during development. For example, Na_v 1.1 and Na_v 1.3 are found predominantly in the neuronal soma, where they control neuronal excitability. The Na_v 1.2 is distributed along unmyelinated axons, where it contributes to the action potential conduction. Several studies showed that after the myelination process this channel isoform is substituted by Na_v 1.6 channels in the nodes of Ranvier (Smith, 2007).

Mutations on *SCN1A* gene, encoding Na_v 1.1 channel, have been identified in patients affected by inherited forms of epilepsy, such as severe myoclonic epilepsy of infancy (SMEI) and generalized epilepsy with febrile seizures plus (GEFS+) (Escayg et al., 2000; Nabbout et al., 2003). The Na_v 1.1 channel plays an important role in the GABAergic inhibitory neurons; mutations on the *SCN1A* gene impair the neuronal firing, creating an imbalance between the excitatory and inhibitory impulses in the brain, leading to epilepsy and seizures (Catterall et al., 2010). Mutations in the *SCN2A* gene, encoding Na_v 1.2 channel, are linked to several epilepsies: the major part of *SCN2A* mutations have been found in patients affected by benign familial neonatal-infantile seizures (BFNIS).

Furthermore, mutations in this gene have been linked to SMEI and Dravet syndrome (Shi et al., 2012).

Regarding *SCN3A* gene, that encodes the Na_v 1.3 channel, there was only one mutation described associated to epilepsy (Holland et al., 2008). However, recently, new mutations have being identified that change the activity of the channel increasing neuronal excitability and inducing focal epilepsy in children (Vanoye et al., 2014).

For *SCN8A* gene, that encodes the Na_v 1.6 channel, one mutation, generating a truncated protein, has been found in humans leading to dystonia, ataxia and tremor (Trudeau et al., 2006). Recently new mutations have been described in patients affected by epileptic encephalopathy and intellectual disability (O'Brien and Meisler, 2013).

1.4.2. Skeletal muscle and heart sodium channels.

Na_v 1.4 and Na_v 1.5 muscle channels are characterized by different tissue expression: the first one is predominantly found in skeletal muscle, while the second one is highly expressed in heart.

Mutations on *SCN4A* gene, encoding Na_v 1.4, change the activity of the channel and, since one of the key step in muscle contraction is the flow of positively charged ions into the muscle cell, they determine the insurgence of several human neuromuscular diseases, such as hyperkalemic periodic paralysis (HYPP), potassium-aggravated myotonias (PAM) and paramyotonia congenita (PMC) (Koopmann et al., 2006).

The Na_v 1.5, located on the membrane of cardiomyocytes and in Purkinje fibres, plays an important role in the upstroke of the cardiac action potential, ensuring the excitability and the velocity of impulse propagation (Tan, 2006). Mutations affecting *SCN5A* gene cause different arrhythmia syndromes confirming the essential role of Na_v 1.5 in regulating normal cardiac activity. Some examples of diseases linked to *SCN5A* mutations

are long QT syndrome type 3 (LQT-3), Brugada syndrome (BrS), sudden infant death syndrome (SIDS) and dilated cardiomyopathy (DCM) (Amin et al., 2010).

1.4.3. Peripheral nervous system sodium channels.

Three channels are predominantly expressed in the peripheral nervous system: Na_v 1.7 in sensory, sympathetic and myenteric neurons, Na_v 1.8 in sensory neurons and Na_v 1.9 in sensory and myenteric neurons. The expression of Na_v 1.8 is limited to small diameter sensory neurons in dorsal root ganglia and in trigeminal ganglia, where it exerts an essential role in the action potential upstroke. Although the involvement of this channel in inflammatory and cold pain process is described in literature in rat and knockout mice (Dib-Hajj et al., 2010), few mutations causing pain diseases have been described. These mutations result in small-fibre neuropathy and increased neuronal excitability (Faber et al., 2012).

Mutations in the *SCN11A* gene, encoding Na_v 1.9 channels, have been found in patients affected by familial episodic pain syndrome type III and also in this case the mutations determine an increase in neuron excitability (Bennett and Woods, 2014).

Na_v 1.7 channel will be described more in detail in the next section.

1.4.4. Na_v 1.7 channel: painless and painful channelopathies.

Nociception is the process through which thermal, mechanical or chemical stimuli are detected by a group of peripheral nerve fibres, called nociceptors. Their cell bodies are located in the dorsal root ganglia for the body and in trigeminal ganglion for the face (Julius and Basbaum, 2001).

The nociceptors, in response to stimuli, lead to the onset of an action potential, whose genesis and propagation are dependent on voltage-gated sodium channels, that, for this

reason, play an essential role in the regulation of neuronal excitability (Dib-Hajj et al., 2010).

The voltage-gated sodium channel Na_v 1.7, expressed in nociceptive and in sympathetic ganglion neurons, is considered to be the major player in the regulation of perception of peripheral pain due to its gating properties. Furthermore, the study of mutations associated to pain-diseases and behavioural tests performed in nociceptors-specific knockout mice have also emphasised this fact (Rush et al., 2007; Lampert et al., 2010).

Regarding its gating properties this channel produces a fast-activating and inactivating current, but it is slow to recover from fast-inactivation, compared to other channels; it is able to generate a substantial inward current in response to small slow depolarizations, acting as a threshold channel (Cummins et al., 1998; Herzog et al., 2003).

Using animal models the involvement of this channel in inflammatory pain has been demonstrated. Indeed after inflammation induction using carrageenan, an increase in Na_v 1.7 transcripts and proteins has being observed. Furthermore, its deletion only in nociceptive neurons blocked the insurgence of the inflammatory pain (Black et al., 2004; Nassar et al., 2004). The global *SCN9A* knockout in mice is lethal shortly after birth. However, this could be due to the loss of feeding. This channel is in fact also present in olfactory sensory neurons and it was observed that patients lacking the production of Na_v 1.7 were anosmic, confirming the role of this channel in the sense of smell (Nassar et al., 2004; Weiss et al., 2011).

Another important demonstration of the role of Na_v 1.7 in human pain perception came from the discovery that mutations in *SCN9A* gene cause several human pain disorders: inherited erythromelalgia (IEM) (also called primary erythromelalgia, PE), paroxysmal extreme pain disorder (PEPD), small-fibre neuropathy (SFN) and congenital insensitivity to pain (CIP) (Lampert et al., 2010) (Fig. 1.8).

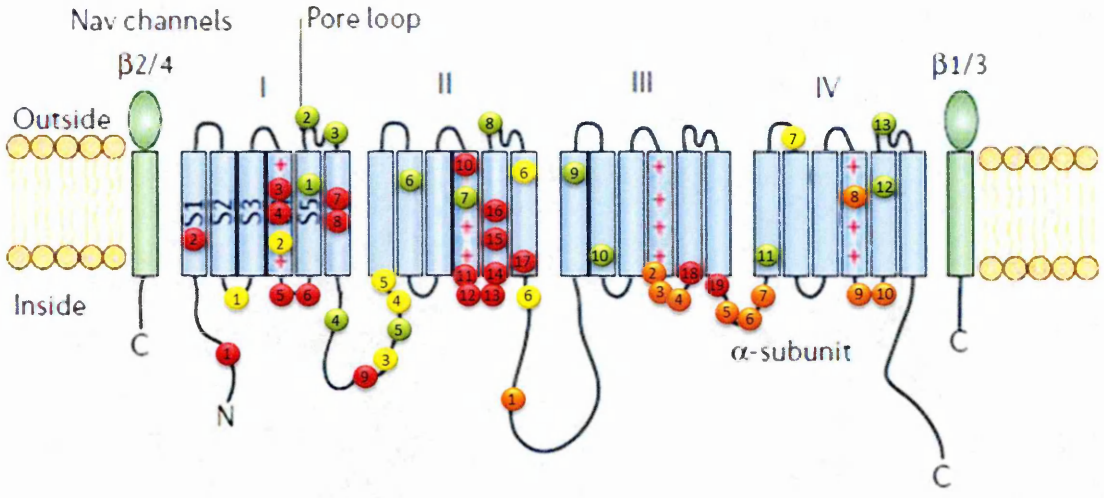

Figure 1.8. Schematic representation of the Na_v 1.7 voltage-gated sodium channel showing the location of known mutations causing CIP (green circles), IEM (red circles), PEPD (orange circles) and SFN (yellow circles)(Adapted from (Lampert et al., 2010; Dib-Hajj et al., 2013)).

IEM is an autosomal dominant disorder that leads to intermittent burning, pain and redness in feet and hands in response to warm stimuli. Interestingly, in some patients, after the early onset in childhood, the severity of the associated pain increases with the age (Drenth and Michiels, 1992; Dabby, 2012). Similar clinical symptoms are described in patients affected by SFN, such as the burning pain in the distal extremities, but SFN can be distinguished by IEM due to particular features such as the general lack of aggravation by warmth or the relief induced by cold (Hoeijmakers et al., 2012). Another pain disorder associated with gain of function mutations in *SCN9A* gene is PEPD. It is a rare autosomal dominant inherited disorder, characterized by flushing and pain in anorectal region and around eyes (Fertleman et al., 2006). CIP is associated with loss of function mutations: in this case patients are unable to feel pain from birth, although the other sensory activities remain intact (Cox et al., 2006; Cox et al., 2010).

1.4.5. Alternative splicing in sodium channel transcripts.

The expression of voltage-gated sodium channels is regulated at different levels such as transcription from multiple promoters, several levels of post-translational glycosylation and alternative splicing of transcripts (Diss et al., 2004; Drews et al., 2005; Koopmann et al., 2006).

Several sodium channel transcripts undergo alternative splicing, for example *SCN1A* with extended exon 11, *SCN3A* with different variants of exon 12, *SCN5A* can be alternative spliced in exon 18, *SCN9A* undergoes alternative splicing resulting in an extended exon 11, and *SCN11A* can result in an alternative spliced isoform lacking exon 16. Furthermore, exon 5 and exon 18 in several sodium channels show developmentally regulated splicing. An overview of some of the different types of alternative splicing in these channels can be found in table 1.4 (Schaller et al., 1992; Makielski et al., 2003; Raymond et al., 2004; Thimmapaya et al., 2005).

Gene name	Splice variants	Comments
SCN1A	Variant 1 Variant 2	Variant 1 contains extended exon 11
SCN2A	Neonatal isoform Adult isoform	Exon 5N Exon 5A
SCN3A	Neonatal isoform Adult isoform Splice variant	Exon 5N Exon 5A This variant contains extended exon 12
SCN5A	Variant 1 Variant 2	Variant 1 contains one extra amino acid in exon 18
SCN8A	Neonatal isoform Adult isoform Neonatal isoform Adult isoform Splice variant	Exon 5N Exon 5A Exon 18N Exon 18A This variant contains extended exon 12
SCN9A	Neonatal isoform Adult isoform	Exon 5N Exon 5A
SCN11A	Splice variant	Δ exon 16

Table 1.4. Examples of different splice variants of voltage-gated sodium channels (Adapted from (Koopmann et al., 2006)).

1.4.5.1. Exon 5 mutually exclusive splicing.

One interesting example of mutually exclusive splicing undergone by several members of the family is that of exon 5. This exon is duplicated in six out of nine VGSCs (Na_v 1.1, Na_v 1.2, Na_v 1.3, Na_v 1.5, Na_v 1.6 and Na_v 1.7) (exon 6 in the case of Na_v 1.5, *SCN5A* gene). These two exons undergo tissue-specific and developmentally-regulated mutually exclusive splicing generating two different structurally and functionally protein isoforms (Lu and Brown, 1998; Heron et al., 2002; Raymond et al., 2004; Gazina et al., 2010). They encode a region of the transmembrane helix S3 and all S4 in domain I, that is part of the voltage sensor of the channel, and they are distinguished by the absence (neonatal or 5'-exon) or the presence (adult or 3'-exon) of an aspartate residue. The conservation of this feature across the family (Tab. 1.5) and species suggests an important role of this alternative splicing event which highlights the interest of studying the functional significance of this exon duplication in the different VGSCs (Diss et al., 2004; Drews et al., 2005; Koopmann et al., 2006).

Gene Channel	*ME Exons*	*Aminoacidic alignment*	*Primary tissues*
SCN1A Na_v 1.1	5N 5A	ITFAFVTEFVNLGNFSALRTFRVLRALKTISVIPGLKTI ITFAYVTEFVDLGNVSALRTFRVLRALKTISVIPGLKTI **** ***** *** **********************	Central nervous system
SCN2A Na_v 1.2	5N 5A	ITFAYVTEFVNLGNVSALRTFRVLRALKTISVIPGLKTI ITFAYVTEFVDLGNVSALRTFRVLRALKTISVIPGLKTI ********** **********************************	Central nervous system
SCN3A Na_v 1.3	5N 5A	IVMAYVTEFVSLGNVSALRTFRVLRALKTISVIPGLKTI IVMAYVTEFVDLGNVSALRTFRVLRALKTISVIPGLKTI ********** **********************************	Central nervous system
SCN5A Na_v 1.5	6a 6	IIMAYVSENIKLGNLSALRTFRVLRALKTISVIPGLKTI IIMAYTTEFVDLGNVSALRTFRVLRALKTISVISGLKTI ***** * *** ****************** *****	Heart muscle Skeletal muscle
SCN8A Na_v 1.6	5N 5A	IMMAYITEFVNLGNVSALRTFRVLRALKTISVIPGLKTI IMMAYVTEFVDLGNVSALRTFRVLRALKTISVIPGLKTI ***** **** **********************************	Central nervous system
SCN9A Na_v 1.7	5N 5A	IMMAYITEFVNLGNVSALRTFRVLRALKTISVIPGLKTI IMMAYVTEFVDLGNVSALRTFRVLRALKTISVIPGLKTI ***** **** **********************************	Peripheral nervous system

Table 1.5. Voltage-gated sodium channels containing exon 5/6 duplication.

The principle subject of my thesis is to characterize the mechanism behind the mutually exclusive splicing of *SCN9A* exon 5N (neonatal) and exon 5A (adult). These two exons are 92 bp in length and they encode part of segment S3 and all the segment S4 of domain I. During development there is an increase in 5A inclusion in dorsal root ganglia, starting from a 35% at the neonatal stage, reaching approximately a 50% in adulthood (Raymond et al., 2004; Choi et al., 2010). Recently it has been hypothesized that changes in Na_v 1.7 electrophysiology due to the different inclusion of exon 5N or 5A determine differences in the location of perceived pain and the age-onset (Chatelier et al., 2008; Choi et al., 2010). The 5A isoform contains a polar, negatively charged residue (aspartic acid) compared to the 5N isoform that retains a polar, non-charged asparagine: this substitution leads to an addition of a negative charge in the electrostatic field (Jarecki et al., 2009). Analyses of the electrophysiological differences between the two isoforms have shown that channels with exon 5A are slower to inactivate at negative potentials than the channels with 5N, leading to a delay in inactivation. This favours larger inward current amplitudes that might increase cell excitability and therefore increase pain sensitivity (Chatelier et al., 2008). Moreover, in at least two cases of gain of function mutations, that lead to inherited erythromelalgia and paroxysmal extreme pain disorder, it has been demonstrated that the 5A variant alters the biophysical properties of the channel in an additive manner besides the effect of the mutation itself, with a possible impact on the disease phenotype, providing a basis for the delayed onset of the symptoms (Jarecki et al., 2009; Choi et al., 2010).

The elucidation of the molecular mechanism behind the alternative splicing of exon 5 in *SCN9A* may unravel in a common mechanism for the splicing of these duplicated exons also in the other channels. Indeed, the alternative exons 5 are conserved in six out of nine members of the family. In the case of the Na_v 1.1 the biophysical features of the two

alternative splice isoforms are known to be markedly different regarding the inactivation kinetics: the 5N variant recovers from inactivation more rapidly than the 5A form, suggesting an important role in the regulation of neuronal excitability (Fletcher et al., 2011). In humans the polymorphism present in the *SCN1A* IVS5N +5 G→A strongly reduces exon 5N inclusion (the AA genotype only produces 0.7 % of neonatal mRNA transcripts in the temporal cortex, compared to 41% for the GG genotype). The decrease in 5N inclusion confers a 3-fold higher risk of febrile seizures in childhood. Furthermore, the treatment of the patients with the AA phenotype is more difficult because the isoform that includes the 5A exon is less sensitive to antiepileptic drugs and it has been associated with an altered dosage in several studies, highlighting the therapeutic potential of mutually exclusive splicing control (Heinzen et al., 2007; Thompson et al., 2011; Sterjev et al., 2012).

In the case of Na_v 1.2 channel, that is widely expressed in human brain, mutations in *SCN2A* gene have been linked to some epilepsy syndromes. Since the inclusion of exon 5A compared to the neonatal one makes neurons more excitable, this can presumably affect seizure susceptibility. Xu et al. analysed the impact of one missense mutation (L1563V), that leads to benign familial neonatal-infantile seizures (BFNIS), in both neonatal and adult backgrounds; the introduction of the mutation showed stronger changes in the electrophysiology of the channel in presence of exon 5N, providing an indication of the role of this developmentally regulated splicing event in the seizure susceptibility regulation (Xu et al., 2007).

In the *SCN5A* gene the alternatively spliced exon 6 (6a and 6) corresponds to the same region in the voltage sensor encoded by exon 5N and 5A, respectively. This gene codes for the Na_v 1.5, the predominant channel in heart, that is essential for action potential initiation in atrial and ventricular cardiomyocytes including cardiomyocytes of the specific

conduction system. Mutations in *SCN5A* gene can cause different cardiac disorders such as long QT syndrome type 3 (LQT3), Brugada syndrome (BrS) and cardiac conduction disease (CCD) (Amin et al., 2010). The differences between the two isoforms containing either exon 6a or 6 result in differences in the electrophysiological parameters of the channel with the neonatal form allowing an additional Na^+ entry which may be important for pH regulation, activity of enzymes and Ca^{2+} homeostasis (Onkal et al., 2008; Schroeter et al., 2010). Furthermore, the amino acidic change resulting from the inclusion of either the alternative exons may affect the channel's response to extracellular chemical factors, such as some drugs as shown for the Na_v 1.1 (Onkal et al., 2008; Fletcher et al., 2011). Pathophysiological implications of this alternative splicing event have also been described. In a case of foetal LQT syndrome, the identified mutations cause much more profound sodium channel dysfunction in the background of neonatal variant, providing a possible explanation for the severe presentation of intrauterine LQT syndrome (Murphy et al., 2012). Furthermore, alternative splicing of exon 6 has also been implicated in Brugada syndrome (Wahbi et al., 2013). In fact, in a patient affected by myotonic dystrophy type 1 with severe arrhythmias, abnormal splicing of *SCN5A* exon 6, characterized by the increase of the neonatal form in the human adult myocardial tissue, was observed indicating that this may also be an important player in conduction system disease, arrhythmias and Brugada pattern.

1.5. Splicing-modulating antisense approaches.

The aim of this project is to map the splicing regulatory elements that determine the developmentally regulated mutually exclusive splicing of *SCN9A* exons 5. The rationale behind this is that knowing the molecular mechanism could facilitate the development of a strategy for the inclusion-exclusion of one or the other, providing a more specific

therapeutic pathway for pain control. Moreover, since the duplication of exon 5 (or 6) is well conserved in other five genes of the same family, it is reasonable that this mechanism could be, at least in part, common in all of them. Considering the fact this ME event also affects the functionality of other channels (section 1.4.5.1), it would be possible to modulate the exon choice in the channels involved in cardiac function or in the central nervous transmission.

During the years a great interest has arisen in the generation of splicing-modulating antisense approaches as powerful therapeutic tools to reprogram splicing or knockdown gene expression. Antisense approaches include antisense oligonucleotides (AOs) or vectors expressing antisense RNA directly inside the cell. The first work reporting the use of an antisense molecule dates back to 1978. Zamecnik and Stephenson were able to inhibit viral replication *in vitro* by targeting a sequence of viral RNA using a short complementary oligodeoxynucleotide. These first single stranded oligonucleotides were characterized by short length and through base pairing with the target mRNA they induced the knockdown of gene expression due to ribonuclease H that degrades RNAs involved in RNA/DNA heteroduplexes (Zamecnik and Stephenson, 1978). In the following years a great effort was spent to improve the efficacy of these oligonucleotides especially through chemical modifications. One of the first chemical improvement consisted in the introduction a phosphorothioate linkage among the nucleotides: this modification protects the antisense molecule from the nucleases, maintaining the sensitivity to the degradation by RNase H (Kole et al., 2012). Taking advantage of other chemical modifications, such as the addition of 2'-O-modifications introduced in the phosphorothioates to induce RNase H resistance, it was possible to develop new molecules that could act through different mechanisms, without disrupting the transcripts, for example, via the modulation of pre-mRNA splicing by steric block or

inhibition of ribosome recruitment to avoid the translation (Crooke, 1999; Dias and Stein, 2002).

Due to their role as splicing modulators, over the past few years there has been a growing interest in modified antisense oligonucleotides as a new therapeutic approach to modulate diseases-associated mutations that alter the splicing pattern. These antisense molecules can affect splicing by blocking the usage of cryptic 5' and 3' splice sites, by inducing exon skipping to eliminate a mutated exon or to restore the open reading frame containing a mutation, or by promoting exon inclusion or skipping to change the protein isoform encoded (Wood et al., 2007). The first application of an antisense molecule to restore the correct splicing pattern was shown by Dominski and Kole (Dominski and Kole, 1993). They were able to inhibit the *β-globin* pre-mRNA aberrant splicing induced by mutations in the first and second intron using 2'-O-methyl phosphorothioates. The same approach has been used to correct many other mutations on the *β-globin* gene that create cryptic 5' and 3' splice sites and also in the case of the *cystic fibrosis transmembrane conductance regulator* (*CFTR*) gene (Friedman et al., 1999; Lacerra et al., 2000).

In the case of the Duchenne muscular dystrophy (DMD) the antisense oligonucleotides have been largely investigated to induce exon skipping in order to restore the open reading frame. In fact the vast majority of the mutations are contained in the non-essential rod domain and they are out-of-frame mutations, blocking the production of dystrophin. However, as shown in the case of in frame deletions that lead to the insurgence of the less severe Becker muscular dystrophy, a protein lacking only a portion of the rod domain is still partially functional (Douglas and Wood, 2013). The antisense oligonucleotides represent a very promising therapeutic approach to induce the

production of a truncated, but still active, dystrophin by inducing exon skipping of the mutated exon and restoring the correct reading frame (Fairclough et al., 2013).

Another mechanism of action of the AOs is the induction of exon inclusion. This mechanism has been exploited for splicing correction in spinal muscular atrophy (SMA). SMA is caused by homozygous or compound heterozygous mutations affecting the *SMN1* gene. Interestingly in humans there is an almost identical second copy of *SMN* gene, called *SMN2*. This paralogus gene contains a synonymous change in exon 7 that causes the disruption of an ESE, weakening the definition of the 3' splice site and promoting exon skipping (Lefebvre et al., 1995; Monani et al., 1999; Cartegni and Krainer, 2002). The truncated proteins encoded by this transcript are very unstable and rapidly degraded (Lorson and Androphy, 2000). In general the total amount of full-length protein derives 90% from *SMN1* and the remaining 10% from *SMN2*. In patients, the 10% of transcripts derived from *SMN2* gene are not sufficient to compensate for the loss of SMN protein caused by mutations on *SMN1* gene (Gennarelli et al., 1995; Lefebvre et al., 1997). To increase the amount of exon 7 inclusion in the *SMN2* mRNA, restoring levels of SMN protein, several antisense approaches have been developed. For example the AOs have been used to antagonize the binding of inhibitory factors to an ISS; also bifunctional oligonucleotides, characterized by an AO with a tail for the recruitment of an SR protein, have been used to increase exon 7 inclusion (Skordis et al., 2003; Hua et al., 2007; Hua et al., 2010).

To date, modified antisense oligonucleotides used to regulate splicing pattern include 2'-O-methyl phosphorothioates (2'OMe-PS), 2'-O-methoxyethyl phosphorothioates (2'MOE-PS), phosphorodiamidate morpholino (PMO), peptide nucleic acid (PNA) and locked nucleic acid (LNA) (Muntoni and Wood, 2011). The PMOs, respect to the other antisense molecules, combine important properties that make them a powerful tool for splicing

modulation. They are RNase H resistant and they show high stability and water solubility and respect to the phosphorothioates they display a higher affinity for the RNA. Moreover, the lack of a charge on the backbone strongly diminishes the insurgence of "off-target effects". The delivery of these non-ionic compounds is improved by conjugation with cell penetrating peptides or addition of a guanidinium group, to form *in vivo* morpholino, extending the usage of the antisense strategy also in adult animals (Summerton, 2007; Moulton and Jiang, 2009).

One of the major limitation of all these antisense oligonucleotides is the maintenance of persistent effects to avoid the problem of repeated dosing. Modified derivatives of U7 small nuclear RNA (snRNA) containing the antisense of the target sequence represent an alternative antisense strategy to confer high stability to the antisense RNA and to obtain long-term modulatory splicing effect. This approach allows also a nuclear accumulation of the antisense, a required feature for splicing modulators. This system has been used for several diseases such as SMA, thalassemia and Duchenne muscular dystrophy (Gorman et al., 1998)(Asparuhova 2004). Since U7 snRNA cassette is characterized by a small size, it can be easily introduced in gene therapy vectors such as lentiviral or adeno-associated viral vectors, as tried both in mice and in canine model of DMD (Goyenvalle et al., 2004; Vulin et al., 2012). U7 antisense derivatives can also be bifunctional by targeting a region through the antisense sequence and by recruiting for example SR proteins through the introduction of their binding sequence (Marquis et al., 2007).

2. Aim of the project

The aim of this project is to characterize the mechanism that directs the mutually exclusive splicing of *SCN9A* exon 5, that encodes part of the voltage sensor of the voltage-gated sodium channel Na_v 1.7. Understanding this splicing process represents a relevant achievement, since this exon duplication seems to exert an important role in defining the exact gain of the channel, confirmed also by the conservation in other members of the family, and since the Na_v 1.7 is strongly involved in pain signalling pathway.

The data obtained from *SCN9A* pre-mRNA splicing analysis revealed that this mechanism is primarily regulated by a combinatorial control of different *trans*-acting factors, some of them tissue-specific and developmentally regulated, as Fox1, PTB and ETR3, and others characterized by a broader expression, such as SR proteins and hnRNP proteins. According to the model, in the first stages of development, characterized by an high percentage of neonatal splice variant, ETR3 on one hand facilitates 5N inclusion and on the other hand it inhibits 5A inclusion. During development the increase of the adult form is directed by several factors: Fox1, acting on the binding sites downstream of exon 5A, and two SR proteins (SRSF1 and SRSF6), binding an ESE in exon 5A. At the same time the inclusion of the neonatal form is inhibited by two *cis*-acting element on exonic an one intronic.

Moreover, some of these regulatory elements seem to be common also for the regulation of exon 5 (or exon 6) mutually exclusive splicing of other voltage-gated sodium channels containing this exon duplication.

3. Results

3.1. Creation of a minigene to study *SCN9A* exon 5N and exon 5A mutually exclusive splicing.

To investigate the molecular mechanism behind the tissue-specific and developmentally regulated mutually exclusive splicing observed for *SCN9A* exon 5N and exon 5A in dorsal root ganglia (DRGs), the entire genomic region from exon 4 to exon 6, encompassing both the two mutually exclusive exons 5N and 5A, was cloned into pcDNA3 vector, creating the minigene construct 9A wt (Fig. 3.1A).

The minigene system is a powerful tool for the study of the regulatory elements that direct an alternative splicing event. The first studies using this approach were interested in the identification of exonic splicing enhancers: in the late eighties for example a sequence in exon EDIIIA of the *fibronectin* gene was described as being important for the alternative splicing regulation thanks to a transient transfection in HeLa cells of alpha globin/fibronectin minigene hybrid (Mardon et al., 1987). A minigene is characterized by the presence of a genomic fragment from the gene of interest comprising the alternative spliced exons surrounded by their flanking intronic regions; in the majority of the cases 300 nucleotides upstream and downstream should be enough and contain the most important regulatory elements (Cooper, 2005).

The minigenes can be transfected in different cell lines, the most common used are for example HeLa, COS and Hek293 cells, that are characterized by a high level of transfection efficiency. RNA is then extracted from the transfected cells and after retro-transcription the splicing pattern is commonly analysed by PCR, since this type of procedure is direct

and offers great sensitivity. Interestingly this minigene system offers many possibilities such as the site-direct mutagenesis, to evaluate, for example, the effect on the splicing pattern of disease-causing mutations, and also these minigenes can be co-transfected with putative *trans*-acting factors to analyse the impact of these proteins in the splicing outcome (Stoss et al., 1999).

It is important to be aware of the limitations this approach has, so the data obtained from the minigene splicing assay must be interpreted carefully. For example, it has been shown that the flanking exons and the intronic regions can influence the rate of inclusion of an exon in a relevant way but sometimes it is not possible to include all the sequences into a minigene due to the large size, affecting the splicing pattern. Moreover, a *cis*-acting element identified as an important regulatory element through the minigene can behave differently in the full length pre-mRNA context.

Although some caveats, this system represents a useful approach to investigate exon 5 *SCN9A* ME splicing, since it has been largely exploited during the years to describe the mechanism behind many alternative splicing events and to discover how some disease-causing mutations affect the splicing outcome (Cooper, 2005; Dasgupta and Ladd, 2012).

After transient transfection of 9A wt minigene in HeLa cells, I analysed the splicing pattern through RT-PCR using a forward primer specific for the vector and a reverse one on exon 6. Three PCR products were detected with the lower band on the agarose gel corresponding to a cDNA product lacking both ME exons 5N and 5A, the middle and major band corresponding to a cDNA product including either exon 5N or 5A, since the size of the two exons is identical, and the upper band representing double inclusion of 5N and 5A (Fig. 3.1B).

To identify which one of the two exons was included in the mRNA transcript an *NdeI* digestion was performed. *NdeI* only digests the amplicon containing exon 5A as this

restriction site is created by the joining of exons 4 and 5A. After *NdeI* digestion two lower bands appear, that are derived from the amplicon product containing only 5A (Fig. 3.1C). The minigene, aside the double inclusion and the double skipping which represent an artefact of the system used, recapitulates the proportion of splicing of these exons found in neonatal DRGs. In fact, in DRGs from neonatal rat (P2-P4) the level of exon 5N inclusion is about 65% and of exon 5A inclusion is 35% (Raymond et al., 2004; Choi et al., 2010). To further confirm the data already published in literature, the endogenous splicing pattern was analysed from RNA extracted by embryonic rat DRGs after two weeks of differentiation in culture (Fig. 3.1D).

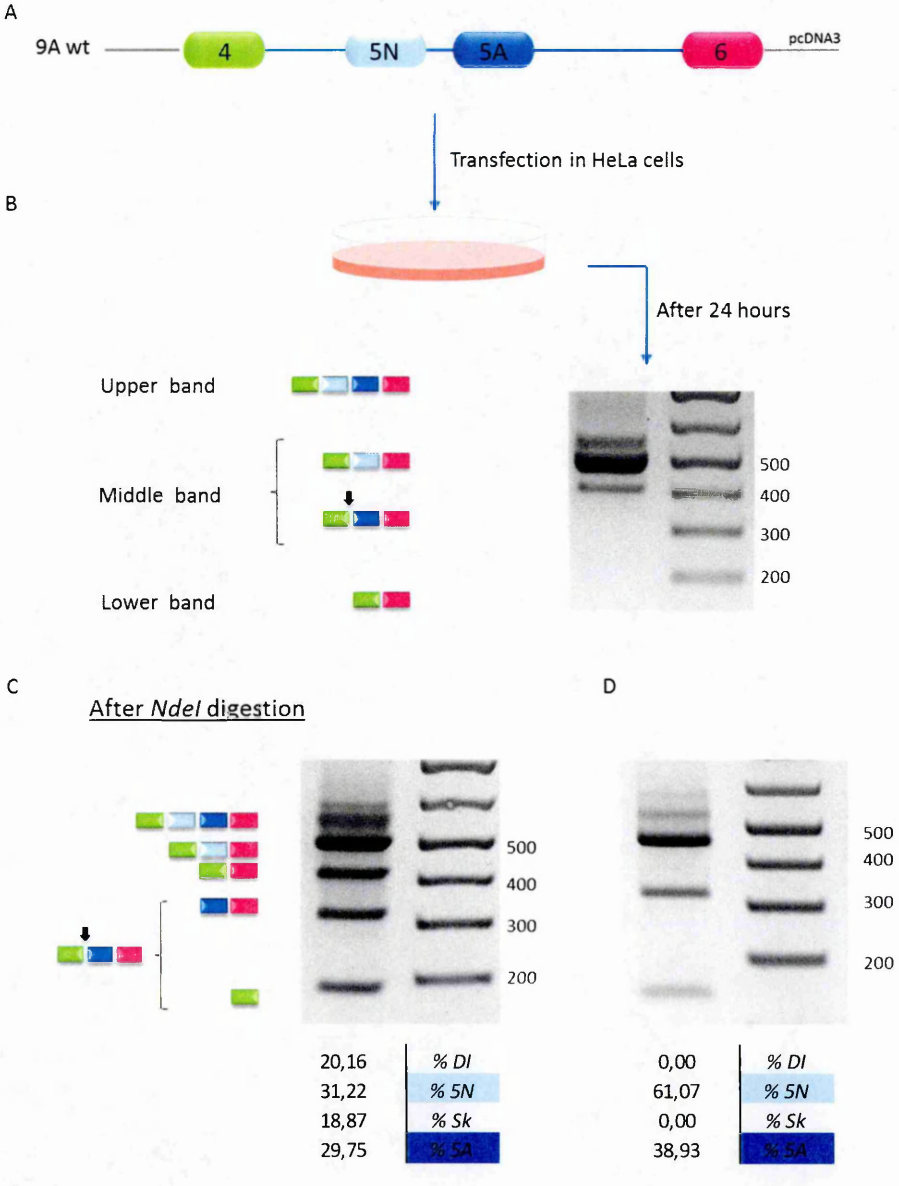

Figure 3.1. (A) Schematic representation of pcDNA3 minigene containing SCN9A exons 4 (green) and 6 (pink), encompassing both the exons 5N (light blue) and 5A (dark blue). (B) Schematic representation of the bands on the agarose gel, on the left. The black arrow shows the unique *NdeI* restriction site. Agarose gel electrophoresis showing RT-PCR products after the transfection in HeLa cells of 9A wt minigene, on the right. Three products are seen on agarose gel electrophoresis with the lowest band representing a cDNA product lacking exons 5N and 5A, the middle and major band representing a cDNA product including exon 5N and the upper band representing a cDNA product including exon 5N and 5A. (C) Agarose gel electrophoresis showing *NdeI* digested RT-PCR products. Since the cDNA products containing either 5N or 5A are of identical size, to discriminate which exon was included the RT-PCR product had been digested with *NdeI* restriction enzyme, specific for only the spliced isoform containing exon 5A. The digested products of the fragment containing exon 5A are the two lower bands. Each product was quantified as a percentage of the total of double inclusion (DI), 5N inclusion, double skipping (Sk) and 5A inclusion. (D) Agarose gel electrophoresis showing the endogenous splicing pattern of *SCN9A* (ex5A-*NdeI*) in DRGs. The upper band represents the neonatal form. The two lower bands derived from the digestion of the PCR product containing only adult exon. Each product was quantified as a percentage of the total of double inclusion (DI), 5N inclusion, double skipping (Sk) and 5A inclusion.

3.2. The mutually exclusive pattern of *SCN9A* exon 5N and 5A is not driven by spliceosomal incompatibility and steric hindrance.

Mutually exclusive exons encode interchangeable peptidic fragments leading to differences in protein activity. To ensure the presence of only one of the ME exons in the mature transcript the process must be strictly regulated. Several mechanisms have been already described in section 1.2.1 that may be responsible for this type of alternative splicing event: spliceosomal incompatibility, steric hindrance between the splice sites, tissue-specific regulation by some *trans*-acting factors and RNA secondary structure (Smith and Nadal-Ginard, 1989; Jones et al., 2001; Letunic et al., 2002; Gromak et al., 2003; Graveley, 2005; Hemani and Soller, 2012).

In some cases, for example, as for the human *JNK1* exons 6 and 7, the mutually exclusive splicing pattern is determined by an incompatibility of the splicing signals. The splice sites for major or minor spliceosome can not be spliced together allowing the inclusion of only one of the two ME exons (Letunic et al., 2002). Simple examination of the splice sites of exon 5N and 5A shows that these are characterized by GU/AG signals, recognized by the

major spliceosome, thus excluding this possibility that this mechanism is behind the mutually exclusive splicing observed (Fig. 3.2).

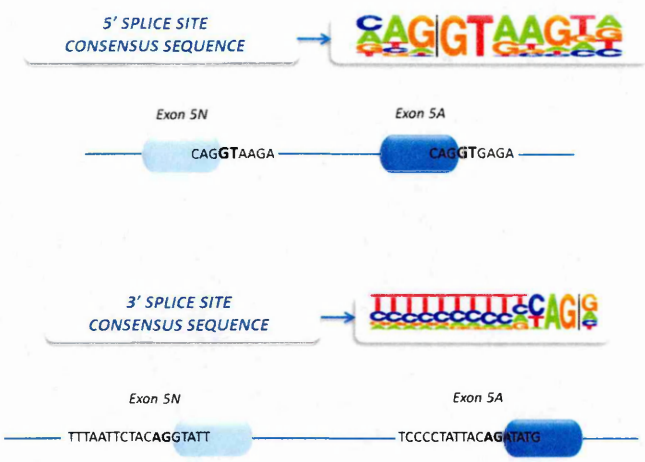

Figure 3.2. Schematic representation of 5' and 3' splice consensus sequences for the major spliceosome and splice site sequences of both the mutually exclusive splicing exons 5N and 5A.

Another mechanism proposed to explain a mutually exclusive choice among exon pair is steric hindrance: if the distance between the 5' splice site and the branch point is shorter than 50 nucleotides, the spliceosome assembly does not occur, preventing the inclusion of both the ME exons, as described for example for exons 2 and 3 of *α-tropomyosin* gene (Smith and Nadal-Ginard, 1989).

Since *SCN9A* exons 5N and 5A are separated by a quite small intron, 115 bp long, I investigated if also in this case the distance between the splicing signals could play a relevant role in the splicing outcome. Taking into consideration the general sequence of the branch point (YNYURAY) and utilising ESE finder prediction program (http://rulai.cshl.edu/cgi-bin/tools/ESE3/esefinder.cgi) I hypothesised the branch point to be TCGTCAC, with A residue in position -28 within intron 5 as the conserved one (Fig 3.3A). This was subsequently confirmed by introducing a point mutation in the adenosine (A→T) (Fig. 3.3A). Indeed, after transient transfection of the minigene 9AmutBP, containing the mutated branch point, RT-PCR and *NdeI* digestion, I observed that the fragments containing exon 5A were completely absent, confirming the A residue in

position -28 as the conserved adenosine of the branch point (Fig. 3.3B); moreover no other branch point was recognized and used to promote 5A inclusion.

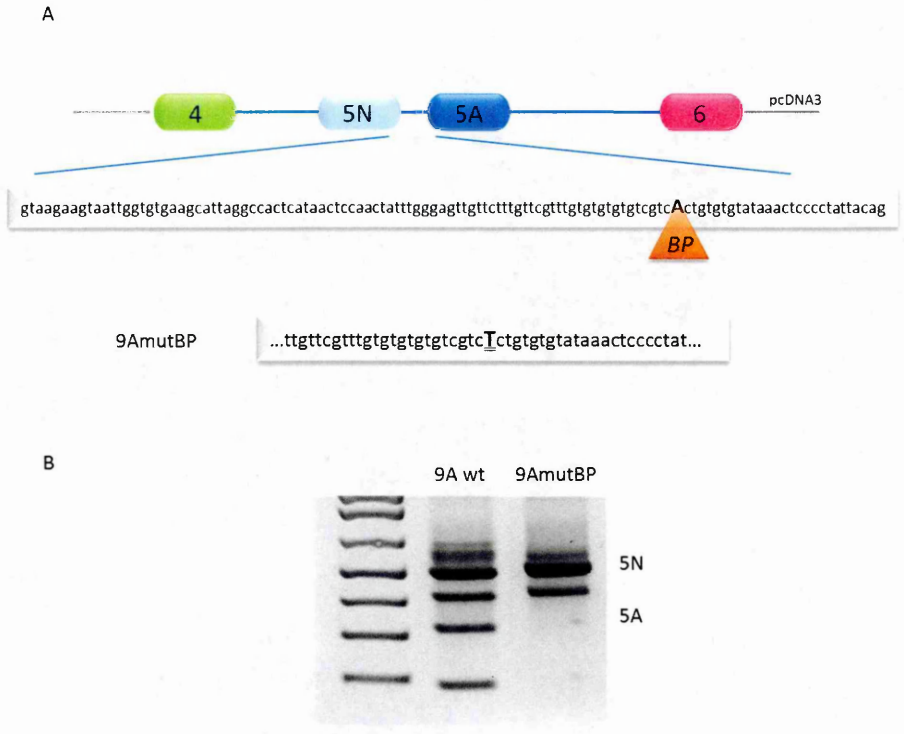

Figure 3.3. (A) Schematic representation of the minigene containing the putative branch point mutated (9AmutBP). The mutated residue is underlined. (B) Agarose gel electrophoresis showing *NdeI* digested RT-PCR products after the transfection in HeLa cells with the upper band representing a cDNA product including exon 5N and 5A, the second band representing 5N inclusion, the third one the skipping and the two lower bands derived from the digestion of the PCR product containing only 5A exon.

Having identified the branch point and in order to investigate if steric hindrance was involved in the mutually exclusive splicing, I created a minigene in which a spacer upstream of the branch point was inserted, to increase the distance between the 5'ss of exon 5N and intron 5 branch site. In particular I chose a 303 bp fragment amplified from intron 31 of *NF1* gene. This fragment analysed with SpliceAid 2 prediction program (http://193.206.120.249/splicing_tissue.html) was shown to be poor in hypothetical enhancer or silencer elements respect to other intronic region analysed (Fig. 3.4A).

Analysing the splicing pattern derived from the transfection of the minigene containing the spacer in intron 5 (9AintNF1), after RT-PCR and *NdeI* digestion I did not detect an

increase in double inclusion of both ME exons, as would be expected if the mutually exclusive outcome was simply driven by steric interference among the 5'ss and the branch point. Intriguingly the 5N inclusion was drastically reduced, suggesting that some important *cis*-acting elements had been moved too far from the target exon 5N to exert their effects (Fig. 3.4B).

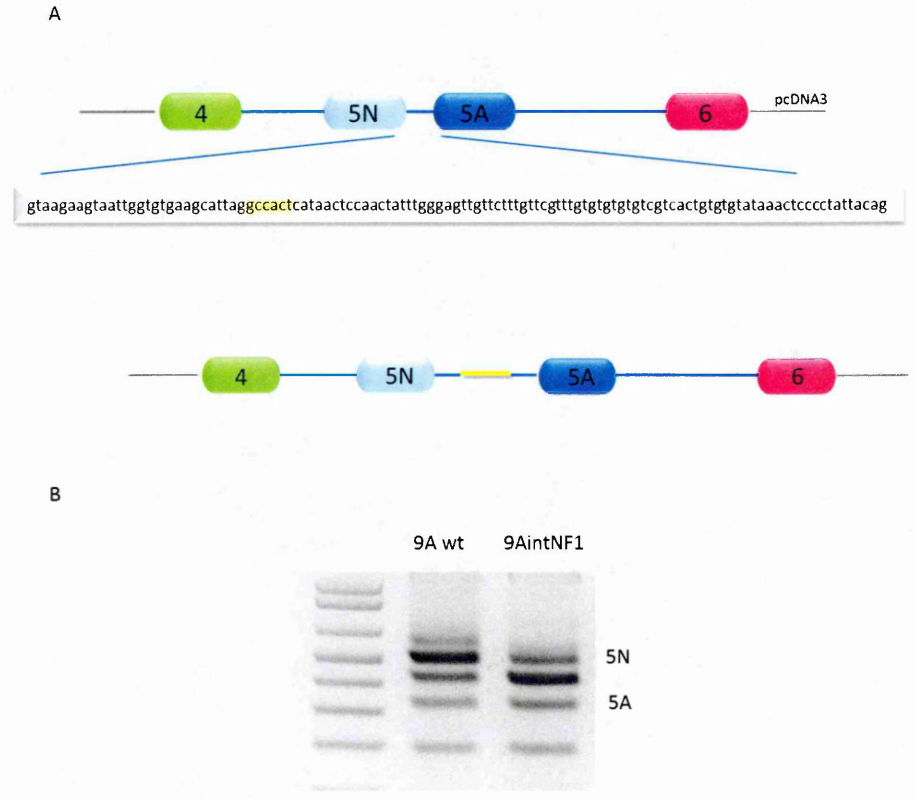

Figure 3.4. (A) In the upper part, schematic representation of 9A wt minigene with the complete intronic sequence, in yellow *AgeI* restriction site, used for the insertion of the spacer. In the lower part, schematic representation of 9AintNF1 minigene with the insertion of the intronic spacer (yellow box). (B) Agarose gel electrophoresis showing *NdeI* digested RT-PCR products after the transfection in HeLa cells with the upper band representing a cDNA product including exon 5N and 5A, the second band representing 5N inclusion, the third one the skipping and the two lower bands derived from the digestion of the PCR product containing only 5A exon.

3.3. Mutually exclusive splicing regulation by *trans*-acting factors.

Many mutually exclusive events have been described to be directed by tissue-specific and developmentally regulated *trans*-acting factors. One example is *α-actinin* exon SM and exon NM. The SM exon is expressed in smooth muscle and the NM exon in non-muscle tissue. The antagonistic regulation by two CELF proteins and PTB defines the mutually exclusive selection of one of the two exons, as described in section 1.2.1 (Gromak et al., 2003).

From the results obtained in section 3.2 intronic *cis*-acting elements necessary for the inclusion of exon 5N appeared to be present in intron 5 suggesting the regulation of the mutually exclusive splicing of *SCN9A* exon 5 is directed by a combinatorial control of *trans*-acting factors.

3.3.1. Analysis of the intronic regions surrounding the mutually exclusive exons 5N and 5A.

To investigate the influence on the splicing outcome of the other intronic regions surrounding exons 5N and 5A and how exon inclusion was influenced by the position of the exons, I created a new minigene where exon 5N was placed in the position of exon 5A and *vice versa* (9A Exswap) (Fig. 3.5A). Interestingly analysis of the splicing pattern showed that when exon 5A, which was previously partially included, was placed in the intronic context of exon 5N, it was fully included whereas exon 5N, that was previously included to approximately 65%, when placed in the intronic context of 5A was fully skipped (Fig. 3.5B).

In order to see if the splicing outcome was drive by exons influencing each other I also examined the splicing profile of the two ME exons independently, deleting each one, obtaining respectively 9AExsw Del ex 5A and 9AExsw Del ex 5N. Transient transfection,

RT-PCR analysis and *NdeI* digestion of these two minigenes did not result in any differences compared to when the two ME exons were present in the minigene 9A Exswap (Fig. 3.5B).

Together with the results obtained in section 3.2, these experiments suggest that *cis*-acting elements in the intronic sequences might play a significant role in the inclusion or exclusion of the ME exons 5N and 5A.

Figure 3.5. (A) Schematic representation of the minigenes containing the mutually exclusive exons swapped and the single deletions of the ME exons (9AExswap, 9AExsw Del ex 5A, 9AExsw Del ex 5N). (B) Agarose gel electrophoresis showing *NdeI* digested RT-PCR products after the transfection in HeLa cells with the upper band representing a cDNA product including exon 5N and 5A, the second band representing 5N inclusion, the third one the skipping and the two lower bands derived from the digestion of the PCR product containing only 5A exon.

3.3.1.1. TG repeats surrounding the branch point affect the inclusion of both the ME exons.

The insertion of a spacer upstream of the branch point led to a decrease in exon 5N, probably due to an increased distance between intronic splicing regulatory elements and the target exon 5N (section 3.2).

To further investigate this phenomena and the putative role of *cis*-acting elements within intron 5, the sequence of the intron was carefully analysed highlighting that the branch point was surrounded by several TG repetitions, 5 upstream and 3 downstream. The alignment of the intron 5 of other species revealed that this TG-enrichment in that region is evolutionary conserved, suggesting the importance of this element in the regulation of this mutually exclusive event (Tab. 3.1).

```
Mouse          GTAAGAAGTGATTGGTGTGGAGCTTTAGACTGCTC--AACTCCAGCTGTTTGGGAGT---
Dog            GTAAGGAGTGATTGGTGTGAAGCATTAGGCCACTCATAACTCCAACTATTTGGGAGTTGT
Human          GTAAGAAGTAATTGGTGTGAAGCATTAGGCCACTCATAACTCCAACTATTTGGGAGTTGT
Rabbit         GTAAGAAGTAATTGGTGTGAAGCATTAGGCCACTCATAACTCCAACTGTTTGGGAGTTGC
               ***** *** ********* *** **** *  ***  ******* ** *********

Mouse          --TTTCTTTGTCTGTGTGTGTGTTGTCACTGTGTCTGTGTATAAACT-CCCCTATTGCAG
Dog            TCTTTGTTTGTGTGTGTGTGTGTTGTCACTGTGT-TGTGTGTGAACT--CCCTATTACAG
Human          TCTTTGTTCGTTTGTGTGTGTGTCGTCACTG----TGTGTATAAACT-CCCCTATTACAG
Rabbit         TCTTTGTTTGTTTGTGTGTGTGTTGTCACCGTGTTTGTGTATAAACTCCCCCTATTACAG
                 *** ** ** *********** ***** *    ***** * ****  ******* ***
```

Table 3.1. Alignment of *SCN9A* intron 5 of four different species: mouse, dog, human, rabbit.

To assess the role of these two $(TG)_n$ stretches two different approaches were utilised. Using the minigene 9AintNF1, in which by inserting the spacer I had distanced the $(TG)_n$ repeats (section 3.2), I recreated the $(TG)_n$ upstream of the insert in order that this element was again close to exon 5N (Fig. 3.6A). After transfection, RT-PCR and *NdeI* digestion I observed that replacing this $(TG)_n$ stretch at a distance similar to the wild type

scenario respect to exon 5N, rescued its inclusion as in the wild type situation (Fig. 3.6B). This result confirmed the role of these TG repeats in favouring 5N inclusion.

Considering the branch point is positioned in the middle of the $(TG)_n$ stretches I also investigated a possible role of this regulatory element on 5A inclusion.

Starting from the minigene 9AintNF1TGup I mutated only the TG repeats downstream of the spacer, creating the minigene 9AintNF1TGup downmut (Fig. 3.6A). After transfection, RT-PCR and *NdeI* digestion I observed exon 5A inclusion was inhibited, whereas 5N inclusion was not affected. An explanation for this observation is most likely that the effect of the $(TG)_n$ on exon 5N was still occurring due to the TGs inserted upstream of *NF1* intron (Fig. 3.6B).

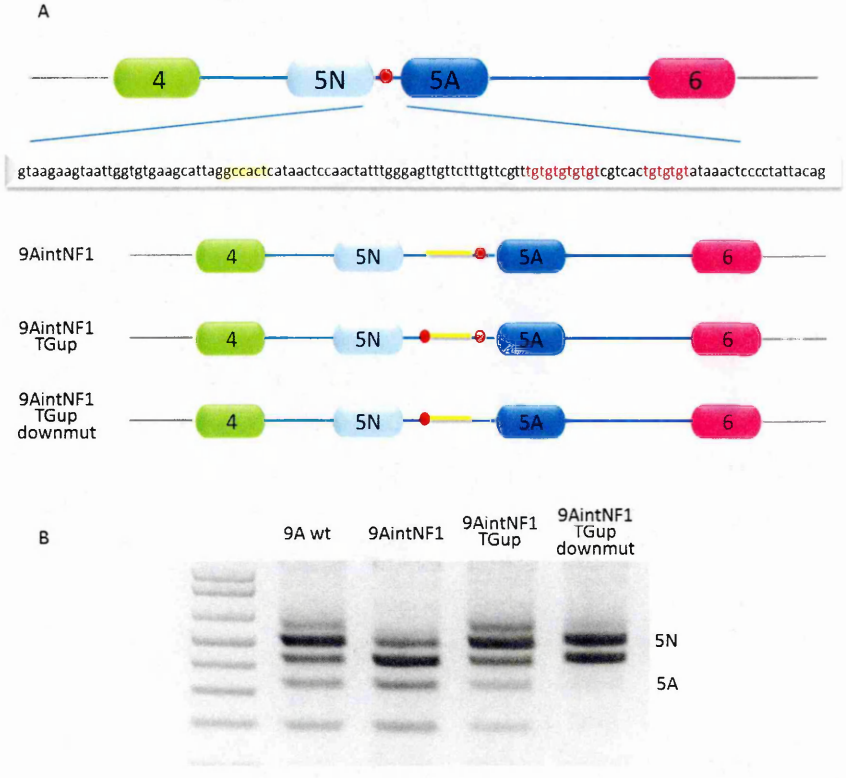

Figure 3.6. (A) Schematic representation of 9A wt minigene with the complete intronic sequence, in yellow *AgeI* restriction site and in red the TG repeats. The last three schemes represent respectively 9AintNF1 minigene, with the insertion of the intronic spacer (yellow part), 9AintNF1TGup minigene, containing the TG repeats (red dot) also upstream of the spacer, 9AintNF1Tgup downmut minigene, characterized by mutated TG repeats downstream the intronic spacer. (B) Agarose gel electrophoresis showing *NdeI* digested RT-PCR products after the transfection in HeLa cells with the upper band representing a cDNA product including exon 5N and 5A, the second band representing 5N inclusion, the third one the skipping and the two lower bands derived from the digestion of the PCR product containing only 5A exon.

To further confirm the presence of this regulatory element and this double effect on both ME exons, using the 9A wt minigene as backbone, I mutated the TG repetitions surrounding the branch point (Fig. 3.7A). The disruption of the TG stretches dramatically impaired the splicing pattern leading to almost double skipping, stressing the importance of this region (Fig. 3.7B).

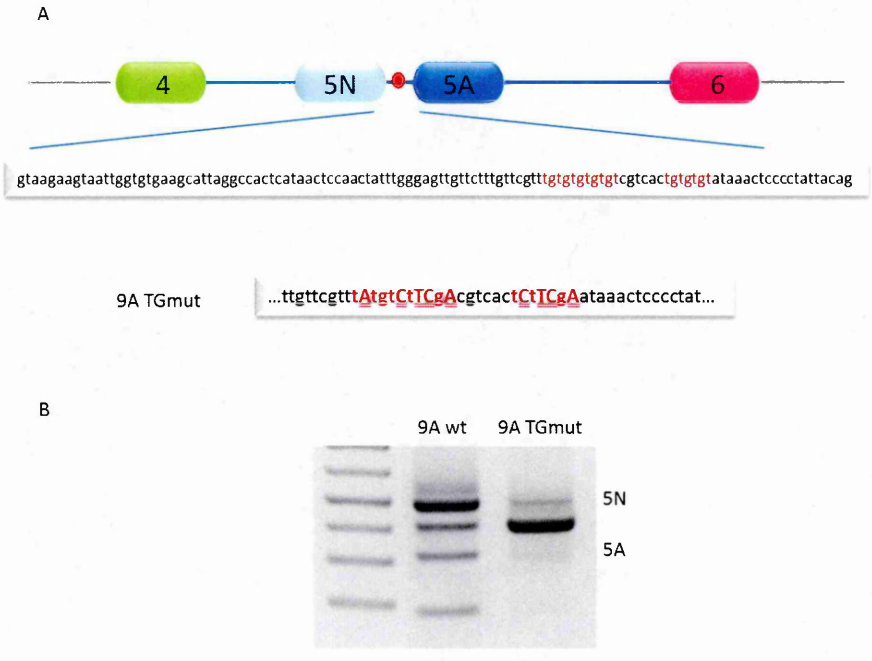

Figure 3.7. (A) Schematic representation of the minigene containing the TG repeats mutated (9A TGmut). In red the region of the TG repeats. The mutated residues are underlined. (B) Agarose gel electrophoresis showing *NdeI* digested RT-PCR products after the transfection in HeLa cells with the upper band representing a cDNA product including exon 5N and 5A, the second band representing 5N inclusion, the third one the skipping and the two lower bands derived from the digestion of the PCR product containing only 5A exon.

3.3.1.1.1. ETR3 and TDP-43 can bind the TGs surrounding the branch point.

In literature at least two proteins have been described to bind TG repetitions, ETR3, one of the six members of CELF (CUG-BP1- and ETR-3-like factor) protein family and TDP-43, a heterogeneous nuclear ribonucleoprotein (Buratti and Baralle, 2001; Faustino and Cooper, 2005). It has been shown that ETR3 can act enhancing inclusion of some alternative exons, as in the case of *cardiac troponin T* exon 5, but also silencing others, antagonizing for example the binding of U2 snRNP to the branch point in *NMDA R1* receptor transcript (Dembowski and Grabowski, 2009; Ladd, 2013). TDP-43 can also act both as splicing activator or repressor, for example favouring exon 3 inclusion in the case of *SKAR* pre-mRNA or by promoting *CFTR* exon 9 skipping thanks to interactions with other hnRNPs such as hnRNP A1 and hnRNP A2/B1 (Buratti and Baralle, 2001; Buratti et al., 2005; Fiesel et al., 2012). Both these proteins thus represent possible candidates as *trans*-acting factors binding the $(TG)_n$ repeats.

To look for a direct interaction between this region and these two RNA binding proteins I performed a pull down analysis using synthetic RNA encompassing both the TG stretches, covalently linked to adipic acid beads (Fig. 3.8A). This RNA was incubated with three different nuclear extracts (NE): one commercial from HeLa cells and two made in house from Hek293 cells and from HEK293 cells where TDP-43 has been depleted. I chose to use these different NEs for two reasons. Firstly from the literature ETR3 seemed to be poorly expressed in HeLa cells, almost undetectable by western blot analysis, Hek293 on the other hand is known to express ETR3 (Dujardin et al., 2010). Secondly, since it was known from previous studies performed in the lab that the affinity of TDP-43 for the TG repeats was very high, I also decided to prepare a NE from Hek293 in which TDP-43 was depleted, to be sure that it did not prevent ETR3 recruitment. After incubation with nuclear extracts RNA-associated proteins were collected, then visualized through western blot.

The results from the pull down demonstrated that both ETR3 and TDP-43 were able to bind this *cis*-acting element. Even in HeLa cells where the signal for ETR3 is not detected in the input, after pull down a slight band could be seen. Interestingly looking at the two samples incubated with the two Hek293 nuclear extracts, ETR3 binding was more pronounced in presence of a low level of TDP-43 (Fig. 3.8B).

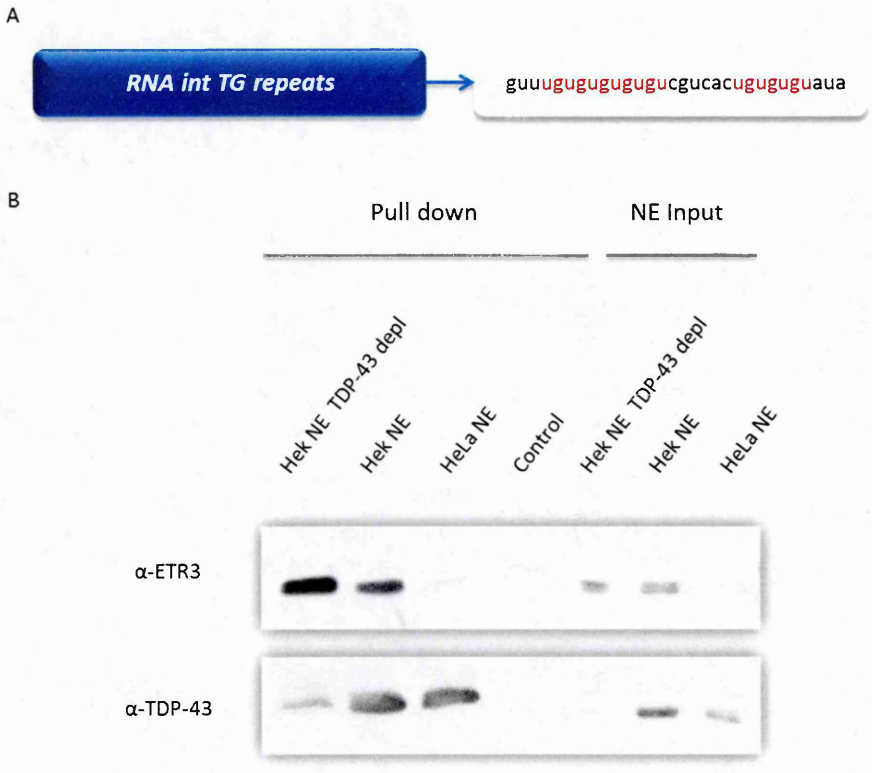

Figure 3.8. (A) Sequence of the synthetic RNA (RNA int TG repeats) used for the pull down assay. In red the TG repetitions. (B) Western blot for ETR3 and TDP-43 of the pull down assay performed using the RNA int TG repeats incubated with three different nuclear extracts: Hek NE with the depletion of TDP-43, Hek NE and HeLa NE.

3.3.1.1.2. Comparison of the effects of ETR3 and TDP-43 on *SCN9A* exon 5 splicing.

In the previous section it was observed that both ETR3 and TDP-43 could directly interact with the TGs surrounding the branch point. I therefore tested the effect of the overexpression of these proteins on the splicing pattern of *SCN9A* wt exon 5. I co-transfected the 9A wt minigene with overexpression plasmids for ETR3 or TDP-43. Considering the fact that in HeLa cells ETR3 is poorly expressed, before overexpressing the two proteins, I performed knockdown of TDP-43, in order to start from a very low level of both of them (Fig. 3.9C). After the silencing of TDP-43, I co-transfected increasing amounts of ETR3 or siRNA-resistant TDP-43 overexpression plasmid, from 50 ng to 700 ng (Fig. 3.9B). TDP-43 seemed not to affect the splicing pattern in a relevant way, whereas ETR3 clearly exerted a strong effect in enhancing the neonatal form and in inhibiting 5A inclusion (Fig. 3.9A).

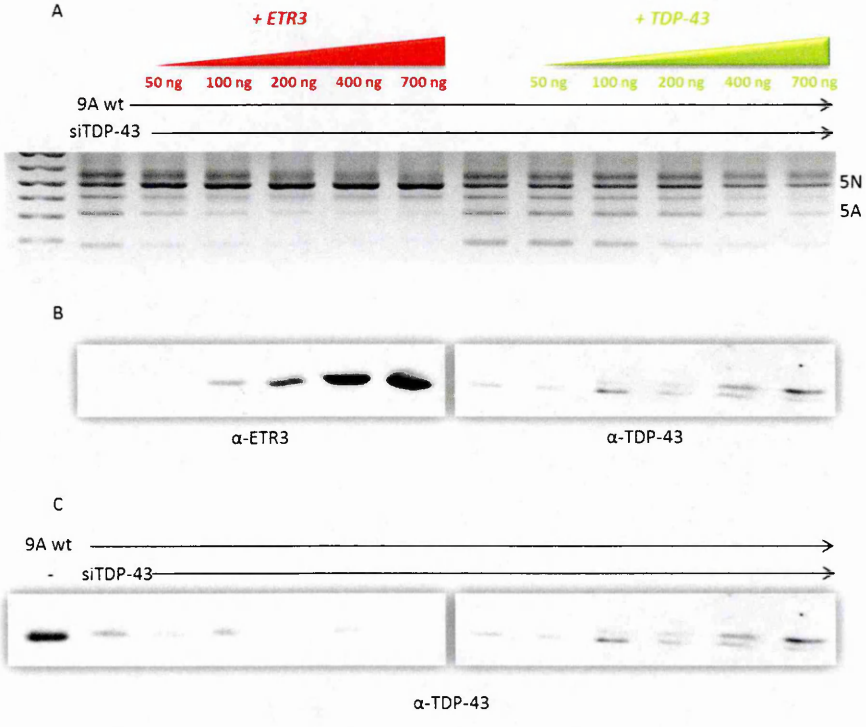

Figure 3.9. (A) Agarose gel electrophoresis showing *NdeI* digested RT-PCR products after the co-transfection of 9A wt minigene with increasing concentrations of ETR3 or TDP-43 overexpression plasmids in HeLa cells with the upper band representing a cDNA product including exon 5N and

5A, the second band representing 5N inclusion, the third one the skipping and the two lower bands derived from the digestion of the PCR product containing only 5A exon. Increasing amount of the two overexpression plasmids were transfected to evaluate the dose-effect relationship. (B) Western blot to check for ETR3 and TDP-43 expressions. (C) Western blot for TDP-43 to control the efficiency of TDP-43 silencing.

To continue the investigation of the role of these two RNA binding proteins I silenced the expression of both ETR3 and TDP43 either singly or in combination. As the level of ETR3 were difficult to detect through western blot, in order to see if this protein was silenced I used Thermo Scientific SuperSignal West Femto Maximum Sensitivity Substrate, that enables detection of low femtogram of proteins (Fig. 3.10B). ETR3 knockdown in HeLa cells led to a decrease in 5N inclusion with an increase of the adult isoform; silencing TDP-43 also resulted in a lower amount of the neonatal product, but in this case I observed mostly an increase in skipping (Fig. 3.10A).

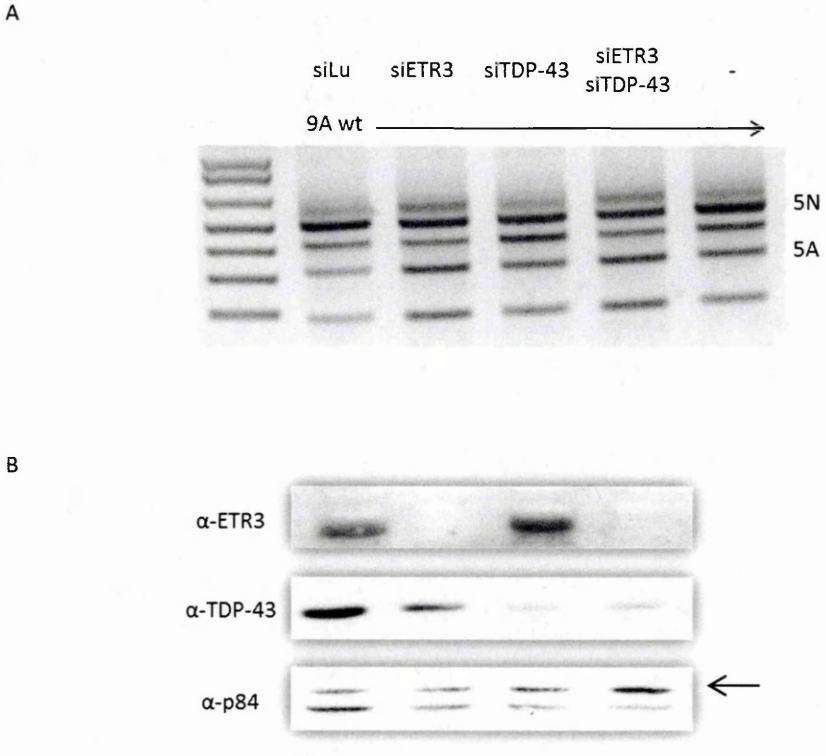

Figure 3.10. (A) Agarose gel electrophoresis showing *NdeI* digested RT-PCR products after transfection analysing the effect of ETR3 and/or TDP-43 knockdown experiments in HeLa cells with the upper band representing a cDNA product including exon 5N and 5A, the second band representing 5N inclusion, the third one the skipping and the two lower bands derived from the digestion of the PCR product containing only 5A exon. (B) Western blot analysis of siRNA experiments, depleting ETR3 and /or TDP-43. The specific band of p84 is marked with an arrow.

3.3.1.1.3. ETR3 promotes 5N inclusion and 5A exclusion.

ETR3 regulates many alternative splicing events acting both as an enhancer or a silencer. For example on one hand it can function as an enhancer promoting the binding of U2 snRNP to the upstream intron of *cardiac troponin T* (*cTNT*) exon 5 (Charlet et al., 2002; Ladd, 2013). On the other hand it inhibits *NMDA R1* exon N1 by binding TG repeats surrounding the branch point, preventing U2 snRNP recruitment (Dembowski and Grabowski, 2009).

To better understand the role of this *trans*-acting factor in *SCN9A* splicing modulation I took advantage of all minigenes outlined in section 3.3.1.1. These minigenes carry the TG repeats at different distances from the two alternative exons (Fig. 3.11A). I co-transfected each one with ETR3 overexpression plasmid. As seen before (Fig. 3.9), after RT-PCR and *NdeI* digestion I observed that the overexpression of ETR3 in presence of the 9A wt minigene dramatically switched the pattern, favouring almost total inclusion of exon 5N. On the contrary ETR3 did not exert any positive effect on 5N when ETR3 overexpression plasmid was co-transfected with 9AintNF1, presumably due to the new position of the TG repeats located too far from the target exon (Fig. 3.11B). To test this hypothesis I also overexpressed the protein with the minigene in which I inserted the *cis*-acting element upstream of the spacer (9AintNF1 TGup). In this case the same stronger effect of 5N enhancement was detected (Fig. 3.11B). This data confirmed a position dependent activity of ETR3 on promoting 5N inclusion.

Interestingly all the co-transfection experiments using 9A wt, 9AintNF1 and 9AintNF1 TGup minigenes showed a clearly significative decrease in 5A inclusion, suggesting ETR3 as a negative regulator of exon 5A inclusion(Fig. 3.11B).

ETR3 overexpression in the presence of the minigene containing mutated TG repeats downstream of the spacer (9AintNF1 TGup downmut) led to an increase in double

inclusion of both ME exons, confirming the negative role of this protein (Fig. 3.11B). Considering that the branch site was located in the middle of the TG repetitions, I hypothesise that ETR3 inhibits exon 5A inclusion by masking the branch point, as in the case of *NMDA R1* transcript (Dembowski and Grabowski, 2009).

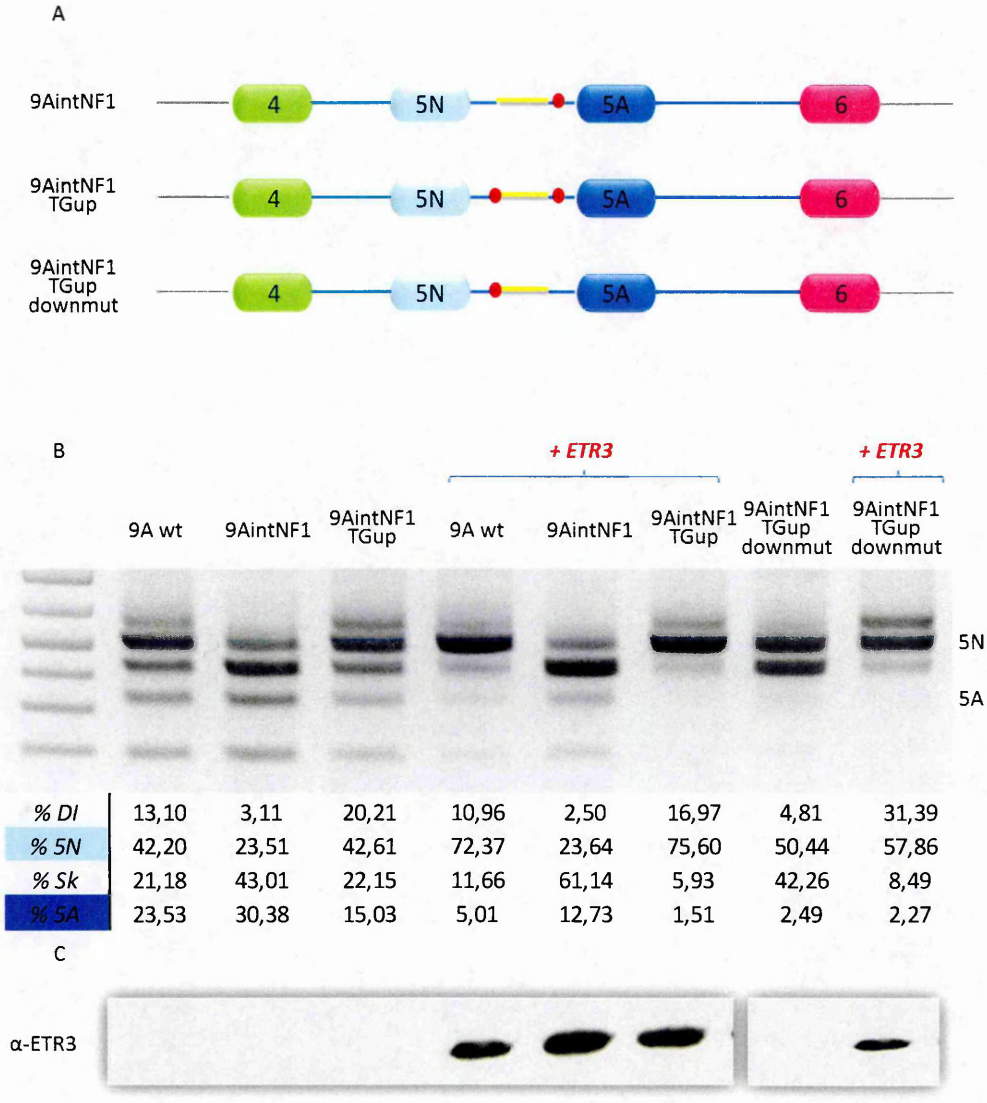

Figure 3.11. (A) Schematic representation of respectively 9AintNF1 minigene, with the insertion of the intronic spacer (yellow part), 9AintNF1TGup minigene, containing the TG repeats (red dot) also upstream of the spacer, 9AintNF1Tgup downmut minigene, characterized by mutated TG repeats downstream the intronic spacer. (B) Agarose gel electrophoresis showing *NdeI* digested RT-PCR products after the co-transfection of the three minigenes with ETR3 overexpression plasmid in HeLa cells with the upper band representing a cDNA product including exon 5N and 5A, the second band representing 5N inclusion, the third one the skipping and the two lower bands derived from the digestion of the PCR product containing only 5A exon. Each product was quantified as a percentage of the total of double inclusion (DI), 5N inclusion, double skipping (Sk) and 5A inclusion. (C) Western blot against ETR3 to monitor the level of the overexpressed protein.

I also performed ETR3 overexpression experiments with the minigene in which the TGs are mutated (9A TGmut) (Fig. 3.12A). The experiment showed an increase in 5N but ETR3 overexpression did not lead to a complete 5N inclusion (Fig. 3.12B; 3.13). This result suggested that this protein might exert its positive effect on exon 5N also binding other *cis*-acting regulatory elements present in the minigene.

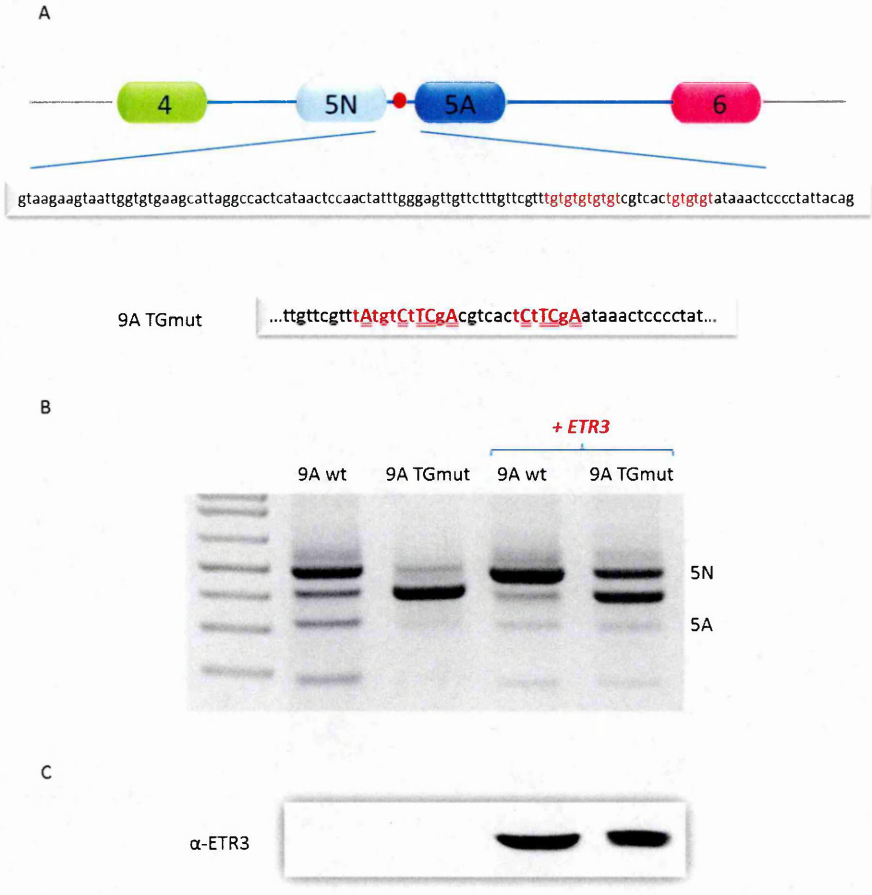

Figure 3.12. (A) Schematic representation of the minigene containing the TG repeats mutated (9A TGmut). (B) Agarose gel electrophoresis showing *NdeI* digested RT-PCR products after the co-transfection of 9A TGmut with ETR3 overexpression plasmid in HeLa cells with the upper band representing a cDNA product including exon 5N and 5A, the second band representing 5N inclusion, the third one the skipping and the two lower bands derived from the digestion of the PCR product containing only 5A exon. (C) Western blot against ETR3 to monitor the level of the overexpressed protein.

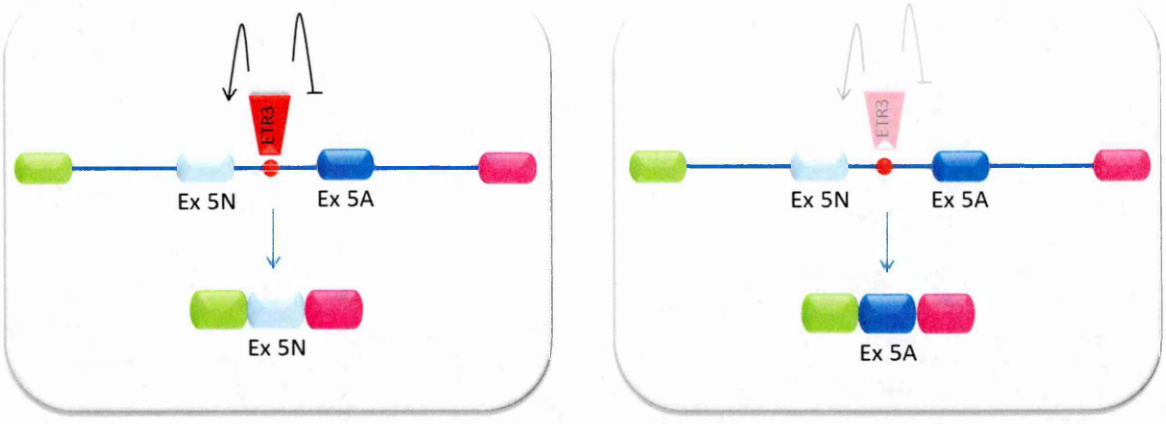

Figure 3.13. Building up the model for the mechanism of *SCN9A* exon 5 mutually exclusive splicing. ETR3 promotes exon 5N inclusion and inhibits exon 5A inclusion by binding a TG-rich region within intron 5 (in red).

3.3.1.2. Intron 5 is necessary to maintain the mutually exclusive pattern.

The data so far collected highlighted the importance of *cis*-acting elements present in intron 5, essential for the definition of the mutually exclusive splicing.

To further support this hypothesis I decided to substitute intron 5 with another intron of the same size from the *α-globin* gene, without changing the first six nucleotides of the 5' splice site of exon 5N (Fig. 3.14A). After transfection of the minigene 9AingGlo 5'ss(+6), RT-PCR and *NdeI* digestion, I observed that, in the presence of a different intron, the splicing pattern lost completely the mutually exclusive feature as I could mainly detect a double inclusion of the two ME exons (Fig. 3.14B).

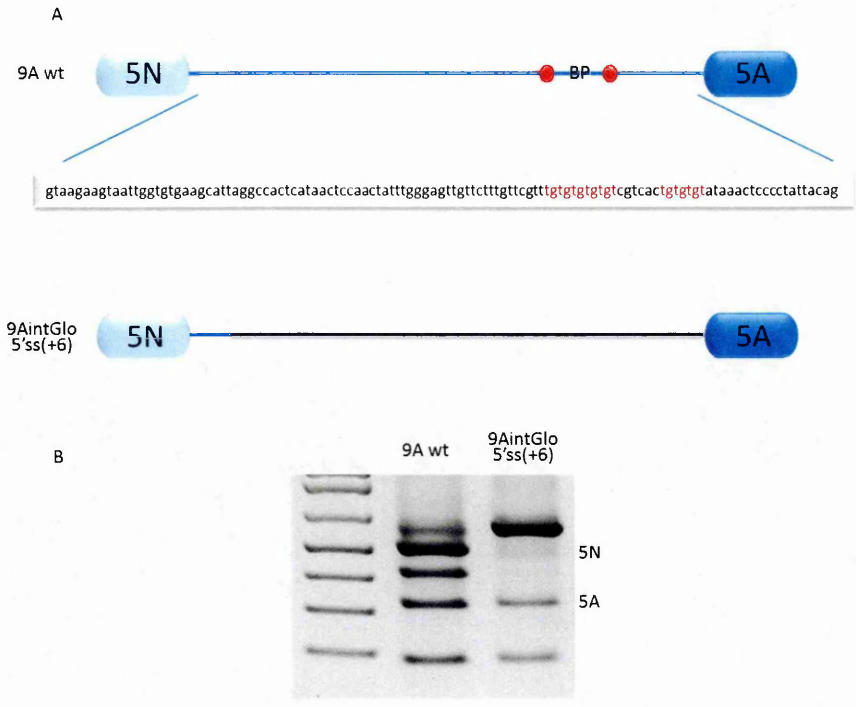

Figure 3.14. (A) Schematic representation of the minigene characterized by the substitution of intron 5 with an *α-globin* intron (in grey)(9AintGlo 5'ss(+6)). (B) Agarose gel electrophoresis showing *NdeI* digested RT-PCR products after the transfection in HeLa cells with the upper band representing a cDNA product including exon 5N and 5A, the second band representing 5N inclusion, the third one the skipping and the two lower bands derived from the digestion of the PCR product containing only 5A exon.

3.3.1.2.1. An intronic splicing silencer close to 5N 5' splice site inhibits exon 5N inclusion.

The strong increase in double inclusion after the substitution of the intron 5 could be justified by the creation of a strong 3' splice site of exon 5A, indeed *in silico* prediction placed a score of 13.67 opposed to the wild type splice site that had a score of 7.97 (MAXENT) (http://genes.mit.edu/burgelab/maxent/Xmaxentscanscoreseq_acc.html), and/or by different *cis*-acting elements contained within the intronic region aside the *cis*-acting element characterised in section 3.3.1.1. To identify further putative *cis*-acting elements located in intron 5, I used the minigene carrying the *α-globin* intron and I reintroduced cassettes of the wild type intronic region in the place of the heterologous intron, creating four different minigenes: 9AintGlo5'ss(+12), 9AintGlo5'ss(+20),

9AintGlo5'ss(+47) and 9AintGlo5'ss(+72) (Fig. 3.15A). These were then transfected in HeLa cells and the splicing profile analysed by RT-PCR. After *NdeI* digestion, I detected an increase in 5A inclusion, that reached almost 100% inclusion of exon 5A after addition of the wild type intron till position +20. The other two minigenes 9AintGlo5'ss(+47) and 9AintGlo5'ss(+72), did not show any evident changes in splicing with respect to the 9AintGlo5'ss(+20) (Fig. 3.15B). The drastic change from the double inclusion towards almost only 5A inclusion observed transfecting the 9AintGlo5'ss(+6) and 9AintGlo5'ss(+20) could be explained by the presence of an intronic splicing silencer (ISS) in the region from +6 and +20 that inhibits 5N inclusion.

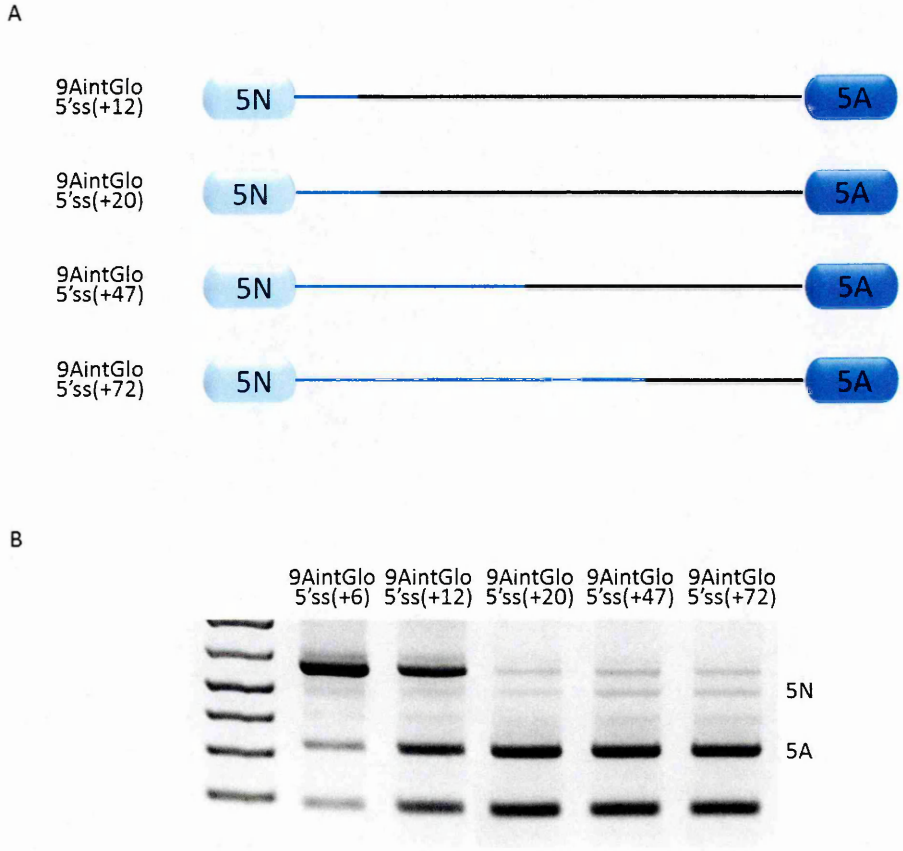

Figure 3.15. (A) Schematic representation of the minigenes characterized by the introduction of different cassettes of the wild type intron 5 (9AintGlo 5'ss(+12), 9AintGlo 5'ss(+20), 9AintGlo 5'ss(+47), 9AintGlo 5'ss(+72)). (B) Agarose gel electrophoresis showing *NdeI* digested RT-PCR products after the transfection in HeLa cells with the upper band representing a cDNA product including exon 5N and 5A, the second band representing 5N inclusion, the third one the skipping and the two lower bands derived from the digestion of the PCR product containing only 5A exon.

This hypothesis was further investigated by deleting the region containing the putative silencer element +6 - +20 from the 9A wt minigene (Fig. 3.16A). After transfection, RT-PCR and *NdeI* digestion, I observed a strong increase in 5N inclusion (Fig. 3.16B). This result confirmed the presence of an intronic splicing silencer (ISS) close to the 5' splice site of exon 5N.

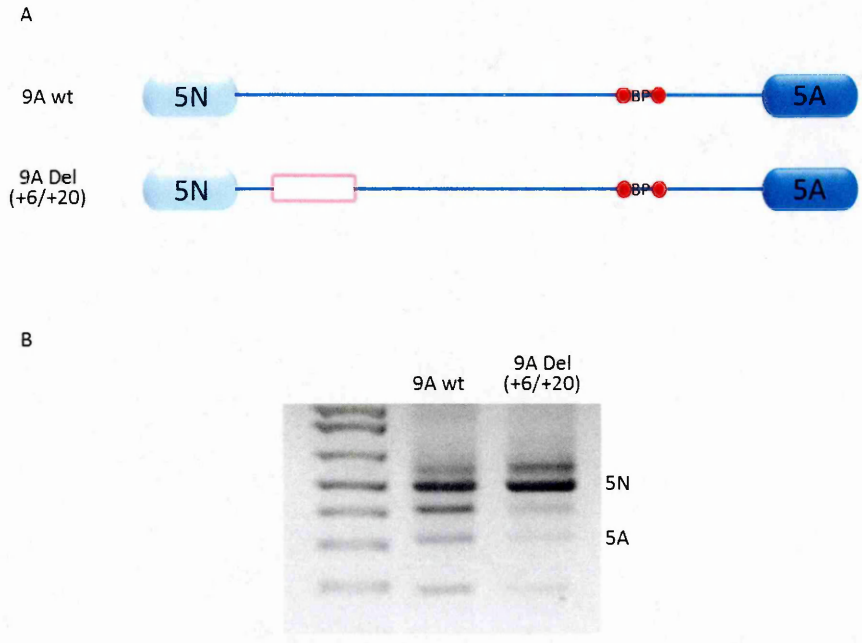

Figure 3.16. (A) Schematic representation of the 9A wt and the 9A Del(+6/+20) minigenes. (B) Agarose gel electrophoresis showing *NdeI* digested RT-PCR products after the transfection in HeLa cells with the upper band representing a cDNA product including exon 5N and 5A, the second band representing 5N inclusion, the third one the skipping and the two lower bands derived from the digestion of the PCR product containing only 5A exon.

3.3.1.2.1.1. Analysis of the *trans*-acting factors binding the intronic splicing silencer.

The negative splicing element mapped in the above section was in close vicinity to exon 5N 5' splice site and could play a role in the developmental switching by partially inhibiting 5' splice site usage.

To identify the proteins that could interact with this ISS, I performed a pull down analysis. I used a synthetic RNA spanning the sequence downstream of exon 5N from +3 to +23. I

decided to slightly expand the sequence to ensure the recognition by *trans*-acting factors that might need a broader region to bind the regulatory element (Fig. 3.17A).

The RNA was incubated with two different nuclear extracts, the commercial HeLa NE and the Hek293 NE made in house.

Western blot analysis of the pull down showed that hnRNP H was strongly binding this element in both NEs. Other proteins also bound this region but to a varying extents. For example, hnRNP A1 binding was pronounced using Hek293 NE but with HeLa NE the signal was detected only after a long exposure. As observed in section 3.3.1.1.1, ETR3 and TPD-43 were also observed to bind and there was a competition among these two factors. In fact using Hek293 NE, the presence of ETR3 strongly reduced TDP-43 binding, compared to what was detected using HeLa NE, which is characterized by very low level of ETR3. Among the proteins detected there was also TRA2β, an SR-like protein. The amount of the protein bound to the *cis*-acting element was higher with incubation of the RNA with Hek293 NE (Fig. 3.17B).

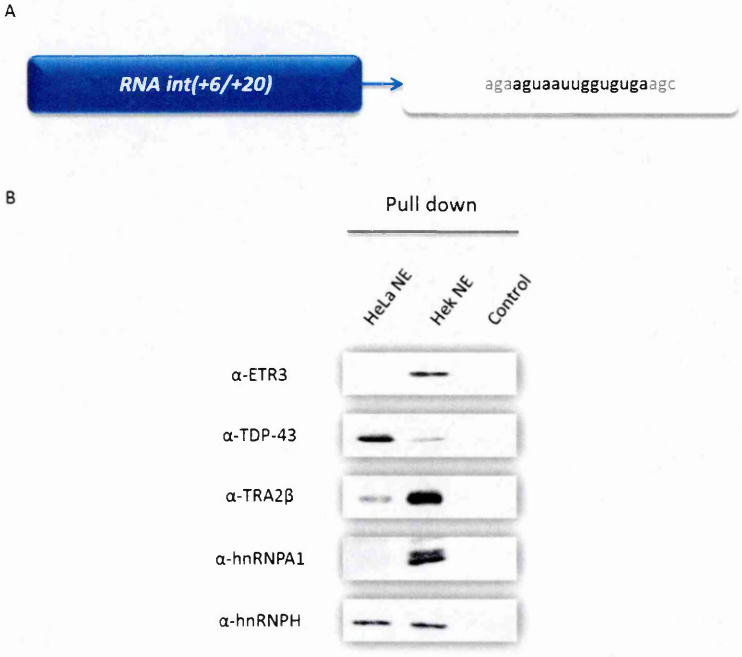

Figure 3.17. (A) Sequence of the synthetic RNA (RNA int(+6/+20)) spanning the region of intron 5 from +3 to +23, used for the pull down assay. (B) Western blot of the pull down assay performed using the RNA int (+6/+20) incubated with two different nuclear extracts: Hek NE and HeLa NE. The control is derived from the beads without RNA, incubated with the nuclear extract.

3.3.1.2.1.2. Assessing the role of hnRNP A1 and hnRNP H.

HnRNP A1 and hnRNP H represented good candidates in exerting the inhibitory effect on 5N inclusion. Both these hnRNPs are known to be splicing repressors and it has been already published that they can alter 5' splice site selection in different ways: inhibiting U1 snRNP binding or antagonizing the recruitment of positive regulatory elements, such as SR proteins (Yang et al., 1994; Buratti and Baralle, 2004).

In order to further investigate this possibility I co-transfected the 9A wt minigene with hnRNP A1 or hnRNP H overexpression plasmids. After RT-PCR and *NdeI* digestion I observed that the overexpression of either protein affected the splicing pattern. A decrease in 5N together with an increase in the skipping was observed with hnRNP A1 overexpression. This decrease in 5N inclusion is in accordance to the result shown in figure 3.16, in which the deletion of this region led to an increase in 5N. A decrease in skipping was detected after hnRNP H overexpression, together with an increase in 5A product. The data obtained is in contrast with the one observed with the deletion of the region, since the level of 5N inclusion did not change in a relevant way (Fig. 3.18A).

Knocking down of both *trans*-acting factors was also performed (Fig. 3.18C). However, in this case the splicing pattern seemed to be unaffected (Fig. 3.18B). This result might be explained by the presence of a residual amount of protein and/or by a certain redundancy of hnRNPs interacting with the ISS.

Further experiments are required to better define the *trans*-acting factor/s exerting a negative effect by binding this intronic region.

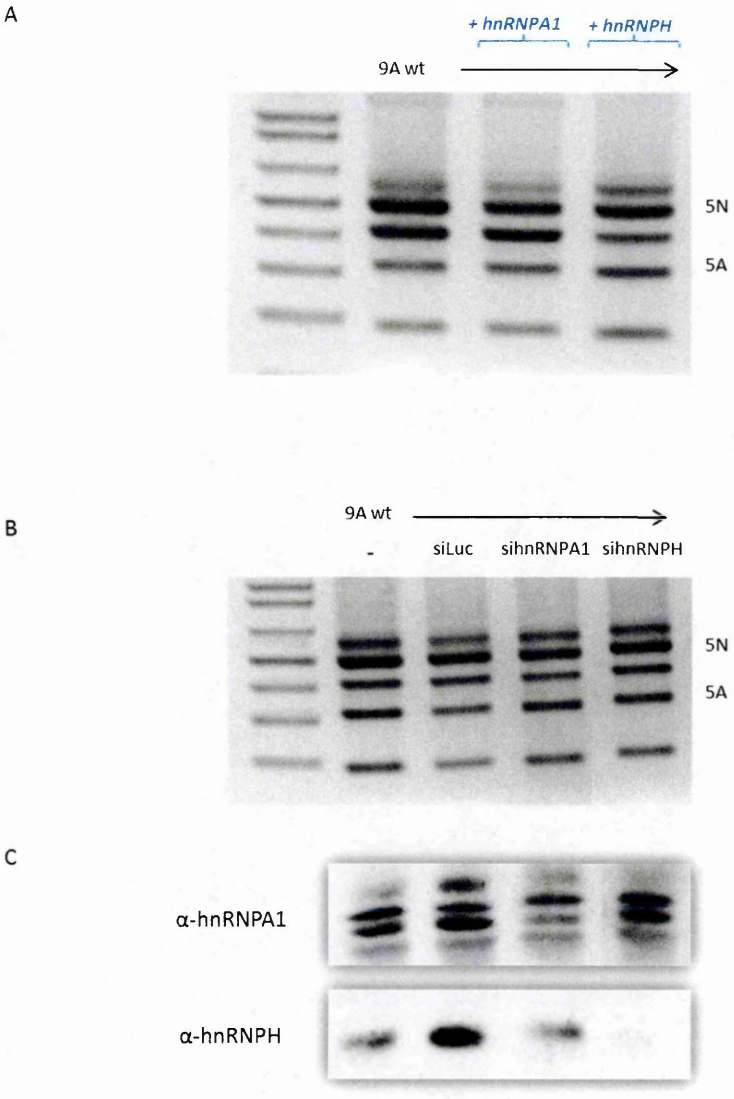

Figure 3.18. (A) Agarose gel electrophoresis showing *NdeI* digested RT-PCR products after transfection analysing the effect of hnRNP A1 and hnRNP H overexpression. (B) Agarose gel electrophoresis showing *NdeI* digested RT-PCR products after transfection analysing the effect of hnRNP A1 and hnRNP H knockdown experiments in HeLa cells with the upper band representing a cDNA product including exon 5N and 5A, the second band representing 5N inclusion, the third one the skipping and the two lower bands derived from the digestion of the PCR product containing only 5A exon. (C) Western blot analysis of siRNA experiments, depleting hnRNP A1 and hnRNP H.

3.3.1.2.2. Identification of positive intronic regulatory elements flanking the intronic silencer.

The pull down analysis of the region +3 to +23 identified three other splicing regulatory factors aside hnRNP A1 and hnRNP H: ETR3, TDP-43 and TRA2β. I had already analysed the effect of overexpressing and silencing ETR3 and TDP-43. Regarding ETR3, the overexpression experiments showed it exerted a strong effect in enhancing 5N inclusion, whereas TDP-43 did not affect 5N inclusion (section 3.3.1.1.2). A stretch rich in TG repeats was contained in the intronic sequence from +6 to +20. Assuming that this could be the region recognized by these proteins I mutated these TG repetitions, creating a new minigene, 9A(TG)5'ssmut (Fig. 3.19A). Interestingly after transfection, RT-PCR and *NdeI* digestion I observed that the absence of this stretch led to a decrease in 5N inclusion (Fig. 3.19B). In order to evaluate if ETR3 exerted a role binding this region, I co-transfect both the 9A wt and the 9A(TG)5'ssmut with the overexpression plasmid for ETR3. After RT-PCR and *NdeI* digestion, ETR3 almost completely induced 5N inclusion when co-transfected with the 9A wt minigene. In contrast with the result seen with the 9A(TG)5'ssmut minigene, the skipping product was detected in this case, suggesting a positive role of ETR3 in 5N definition also by acting on this region (Fig. 3.19B).

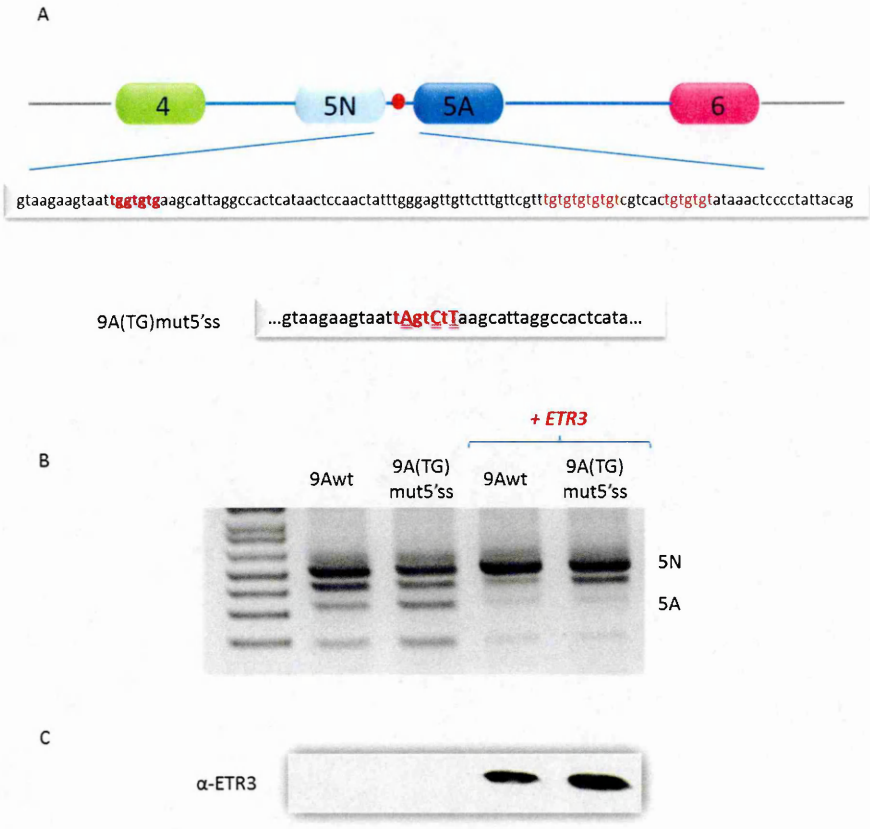

Figure 3.19. (A) Schematic representation of the minigene containing the TG repeats mutated at the 5 'ss of exon 5N (9A(TG)mut5'ss). (B) Agarose gel electrophoresis showing *NdeI* digested RT-PCR products after the co-transfection of 9A(TG)mut5'ss with ETR3 overexpression plasmid in HeLa cells with the upper band representing a cDNA product including exon 5N and 5A, the second band representing 5N inclusion, the third one the skipping and the two lower bands derived from the digestion of the PCR product containing only 5A exon. (C) Western blot against ETR3 to monitor the level of the overexpressed protein.

From the literature it is known that TRA2β, an SR-like protein, acts in general as a enhancer, favouring exon inclusion via (A)GAA motifs; however it is reported that it could also induce exon skipping using different mechanisms that can require direct interactions with the RNA or it can exert an inhibitory effect through contact with other proteins, without any direct interaction with the RNA (Tacke et al., 1998; Grellscheid et al., 2011). In order to investigate the role of this *trans*-acting factor I performed both overexpression and silencing experiments. When I transfected the wild type minigene in presence of the TRA2β overexpression plasmid, after RT-PCR and *NdeI* digestion I detected an increase in

5N inclusion and also a slight increase in double inclusion (Fig. 3.20A). The knocking down of TRA2β did not induce evident changes in the splicing outcome (Fig. 3.20B).

To recapitulate, the deletion of the region from +6 to +20 was indicative of a silencer element that strongly inhibited 5N inclusion. Preliminary experiments have shown that hnRNP A1 and hnRNP H were able to bind this ISS but the negative effect can not be ascribed only to these two factors. This negative regulatory element seemed to be surrounded by other two positive regions, bound by ETR3 and TRA2β. The competition among all the *trans*-acting factors could determine differences in splicing pattern. However, further experiments are required to specifically understand the contribution of each one.

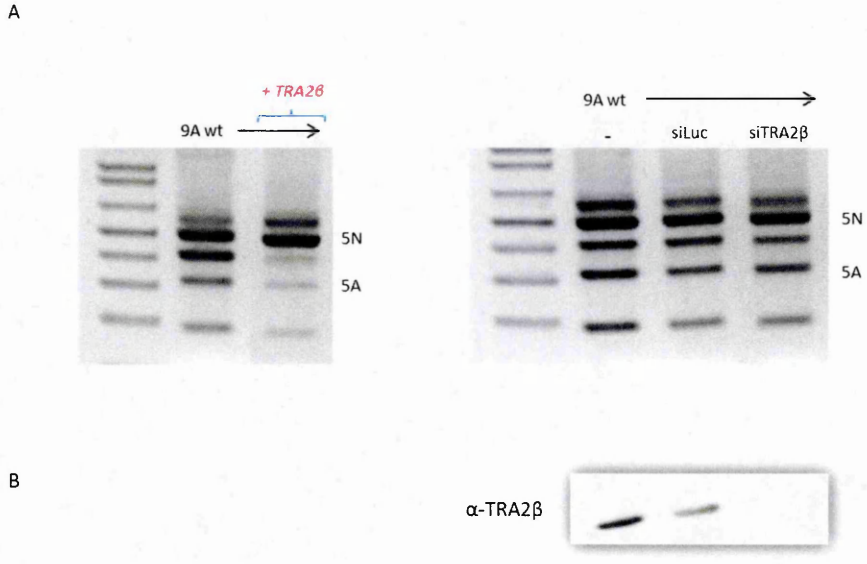

Figure 3.20. (A) Agarose gel electrophoresis showing *NdeI* digested RT-PCR products after transfection analysing the effect of TRA2β overexpression. (B) Agarose gel electrophoresis showing *NdeI* digested RT-PCR products after transfection analysing the effect of TRA2β knockdown experiments in HeLa cells with the upper band representing a cDNA product including exon 5N and 5A, the second band representing 5N inclusion, the third one the skipping and the two lower bands derived from the digestion of the PCR product containing only 5A exon. (C) Western blot analysis of siRNA experiments, depleting hnRNP A1 and hnRNP H.

3.3.1.2.3. Identification of a new *cis*-acting element upstream of the TGs surrounding the branch point.

The substitution of intron 5 completely disrupted the mutually exclusive splicing pattern (section 3.3.1.2). None of the elements identified so far could account for this switch, I therefore continued to investigate the region close to the 3' splice site of exon 5A, proceeding as in section 3.3.1.2.1 by substituting fragments of *α-globin* intron with wild type intronic sequences starting from two different minigenes, 9AintGlo5'ss(+6) and 9AintGlo5'ss(+20), since they showed a completely different splicing pattern (Fig. 3.15B).

In the first part of the analysis I took advantage of the minigene 9AintGlo5'ss(+6): the splicing pattern given by this minigene was characterized by a high percentage of double inclusion (Fig. 3.15B). I initially reintroduced the wild type fragment that covered the region from -15 to -1 at the 3' splice site of exon 5A, creating the minigene 9AintGlo5'ss(+6)3'ss(-15) (Fig. 3.21A). Transfection, RT-PCR and *NdeI* digestion, highlighted the fact that the reintroduction of this part of the 5A wild type acceptor site reduced the inclusion of the adult form, leading to an increase of the product containing only 5N (Fig. 3.21C). This result confirmed that 5A acceptor site was weaker than that created with the intronic portion of *α-globin* one, as previously hypothesised with the *in silico* prediction (section 3.3.1.2.1).

Subsequently I inserted two longer regions from the wild type intron 5. One containing the branch point and the TG repeats downstream of it, and the other from position -43 to -1, encompassing both TGs stretches and the branch point (Fig. 3.21A). The splicing pattern obtained after transfection, RT-PCR and *NdeI* digestion of the 9AintGlo5'ss(+6)3'ss(-32) showed an increase of skipping of both the ME exons. This maybe due to the introduction of the wild type branch point, probably less efficient than the *globin* one. The result obtained using the minigene 9AintGlo5'ss(+6)3'ss(-43) showed

a lower level of skipping respect to the 9AintGlo5'ss(+6)3'ss(-32) (Fig. 3.21C). The difference among the two minigenes was that 9AintGlo5'ss(+6)3'ss(-43) contained both the TGs stretches surrounding the branch point. As shown in section 3.3.1.1.3 the TGs close to the branch point are important for the definition of the ME exons, so it could be that the decrease in skipping was due to the introduction of the entire region.

Despite the intronic cassettes so far inserted, in the minigene 9AintGlo5'ss(+6)3'ss(-43), a large amount of double inclusion was detected, indicating that regulatory elements were still missing from the sequence. Introducing the cassette from -70 to -1, the splicing outcome became more similar to the wild type one, with a strong reduction of double inclusion (Fig. 3.21C) compared to 9AintGlo5'ss(+6)3'ss(-43). A similar approach was also used starting from a different background in which only 5A was included in the final mRNA, using the minigene 9AintGlo5'ss(+20) (Fig. 3.15B). After the insertion of the first fragment I obtained the 9AintGlo5'ss(+20)3'ss(-15) minigene (Fig. 3.21B). Transfection, RT-PCR and *NdeI* digestion showed a completely different splicing pattern, characterized by almost total skipping of both the ME exons, with a slight increase in 5N inclusion (Fig. 3.21C). After transfection of the minigene 9AintGlo5'ss(+20)3'ss(-32), containing the wild type sequence till position -32, RT-PCR and *NdeI* digestion, I detected a decrease in the product containing only 5N, that was not observed transfecting the minigene 9AintGlo5'ss(+20)3'ss(-43), containing the wild type intronic region with both the TGs stretches and the branch point (Fig. 3.21B, 21C). However, the main cDNA product derived from the three constructs remained the skipping of both the ME exons, that could be explained on one hand by an inhibitory effect on 5N inclusion by the previously mapped intronic silencer, and on the other hand by the worsening of 5A 3' splice site strength as shown in section 3.3.1.2.1 (Fig. 3.21B, 21C).

After transfection of the minigene 9AintGlo5'ss(+20)3'ss(-70), that encompassed the whole region from -70 to -1, RT-PCR and *NdeI* digestion showed a splicing pattern that resembled the wild type one, highlighting an important role of this intronic sequence and the fact that it contains several splicing regulatory elements. (Fig. 3.21B, 21C).

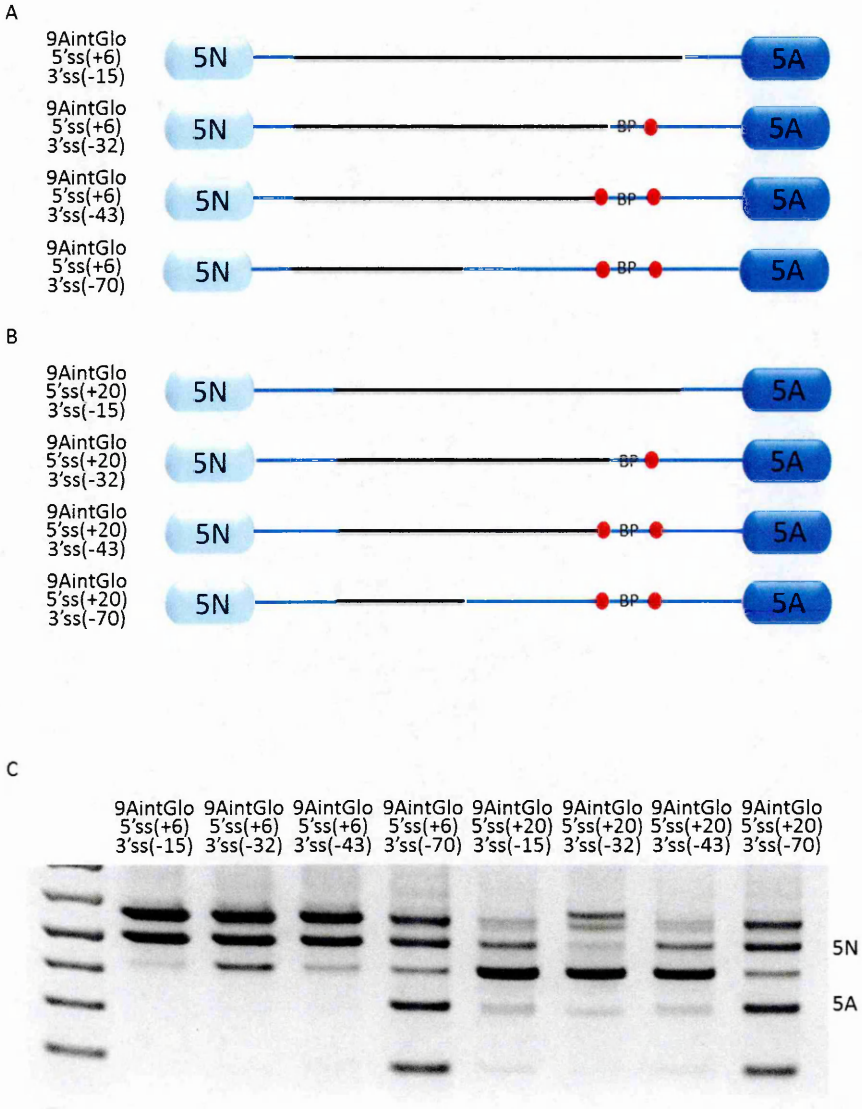

Figure 3.21. (A) Schematic representation of the minigenes characterized by the introduction of different cassettes of the wild type intron 5 (9AintGlo5'ss(+6)3'ss(-15), 9AintGlo5'ss(+6)3'ss(-32), 9AintGlo5'ss(+6)3'ss(-43), 9AintGlo5'ss(+6)3'ss(-70), 9AintGlo5'ss(+20)3'ss(-15), 9AintGlo5'ss(+20)3'ss(-32), 9AintGlo5'ss(+20)3'ss(-43), 9AintGlo5'ss(+20)3'ss(-70)). (B) Agarose gel electrophoresis showing *NdeI* digested RT-PCR products after the transfection in HeLa cells with the upper band representing a cDNA product including exon 5N and 5A, the second band representing 5N inclusion, the third one the skipping and the two lower bands derived from the digestion of the PCR product containing only 5A exon.

To further confirm the data obtained I deleted the elements so far mapped from the wild type minigene 9A wt. I initially performed one big deletion from position -70 to -43 (Fig. 3.22A); after transfection of the minigene 9A Del(-70/-43), RT-PCR and *NdeI* digestion the main product was skipping of both the ME exons emphasising the role of this region and the *cis*-acting elements contained (Fig. 3.22B). Subsequently and in order to perform a finer analysis I created other three minigenes, with small overlapping deletions covering the entire sequence from -70 to -43: 9A Del(-70/-54), 9A Del(-60/-48) and 9A Del(-55/-43) (Fig. 3.22A). Looking at the data obtained after transfection, RT-PCR and *NdeI* digestion of these three minigenes, the region from -60 to -43 appeared to be the most pertinent for the definition of the splicing pattern (Fig. 3.22B).

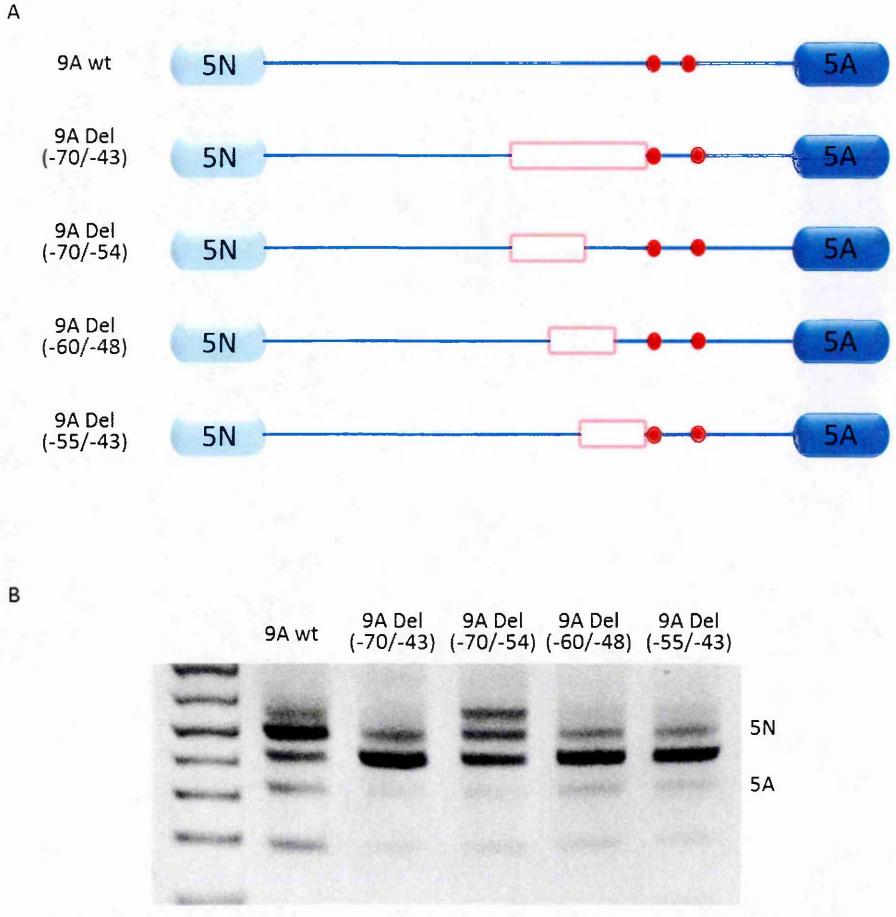

Figure 3.22. (A) Schematic representation of 9A wt, 9A Del(-70/-43), 9A Del(-70/-54), 9A Del(-60/-48) and 9A Del(-55/-43) minigenes. (B) Agarose gel electrophoresis showing *NdeI* digested RT-PCR products after the transfection in HeLa cells with the upper band representing a cDNA product including exon 5N and 5A, the second band representing 5N inclusion, the third one the skipping and the two lower bands derived from the digestion of the PCR product containing only 5A exon.

3.3.1.2.3.1. ETR3 binds a broader region upstream of the branch point enhancing 5N inclusion.

To identify the *trans*-acting factors binding the region from -60 to -43 I performed a pull down analysis using two different nuclear extracts, one from HeLa cells and one from Hek293. I used a synthetic RNA spanning the region from -60 to -43 with the addition of other three residues upstream and downstream to allow the binding of all the factors (Fig. 3.23A).

I checked the binding of several proteins, for example hnRNP A1, hnRNP H, Tra2β did not interact with the RNA, whereas three proteins were able to bind this element: ETR3, TDP-43 and PTB (Fig. 3.23B). Regarding PTB I will discuss its role in the next section, that will be entirely dedicated to this factor. The other two proteins and their role in the mutually exclusive splicing of exon 5 has been sustainably investigated in the previous sections and especially ETR3 has been shown to be important in the definition of the splicing outcome.

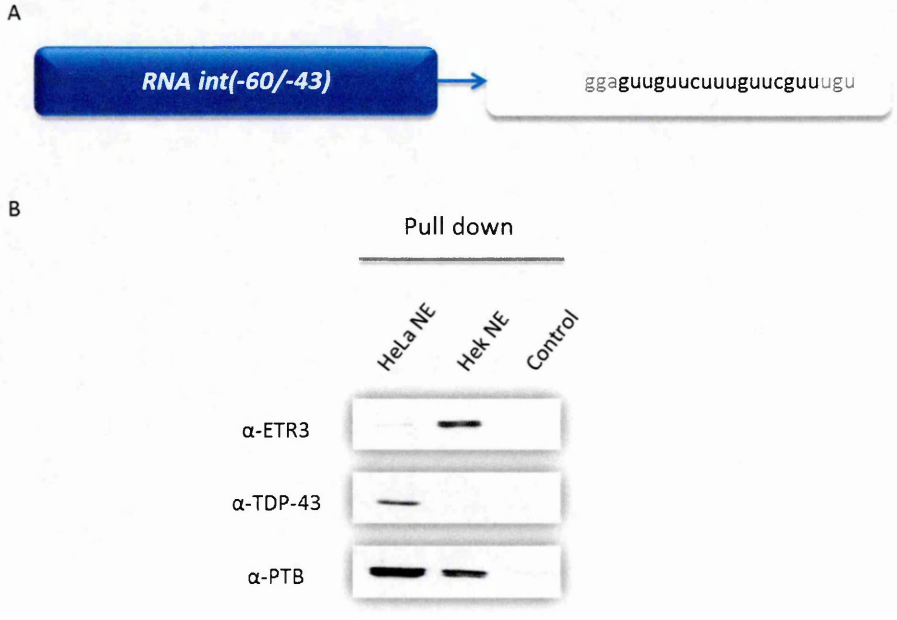

Figure 3.23. (A) Sequence of the synthetic RNA (RNA int(-60/-43)) spanning the region of intron 5 from -63 to -40, used for the pull down assay. (B) Western blot of the pull down assay performed using the RNA int (-60/-43) incubated with two different nuclear extracts: Hek NE and HeLa NE. The control is derived from the beads without RNA, incubated with the nuclear extract.

I took advantage of the previous minigene containing the spacer in intron 5 (9AintNF1), creating a new minigene 9AintNF1insertup in which I inserted the region of interest -60/-43 upstream of the spacer (Fig. 3.24A). After transfection of the 9AintNF1insertup, RT-PCR and *NdeI* digestion I detected a strong decrease in 5N inclusion, a splicing pattern similar to that one observed with the 9AintNF1 minigene. The co-transfection of 9AintNF1insertup with ETR3 overexpression plasmid showed a rescue in 5N inclusion, confirming the positive effect on 5N inclusion exerted by ETR3 binding to this *cis*-acting element (Fig. 3.24B). Although I could detect an increase of 5N (Fig. 3.24B), this was not so strong as the effect seen when I moved the TG repeats stretches upstream of the spacer (minigene 9AintNF1 TGup) (Fig. 3.11B).

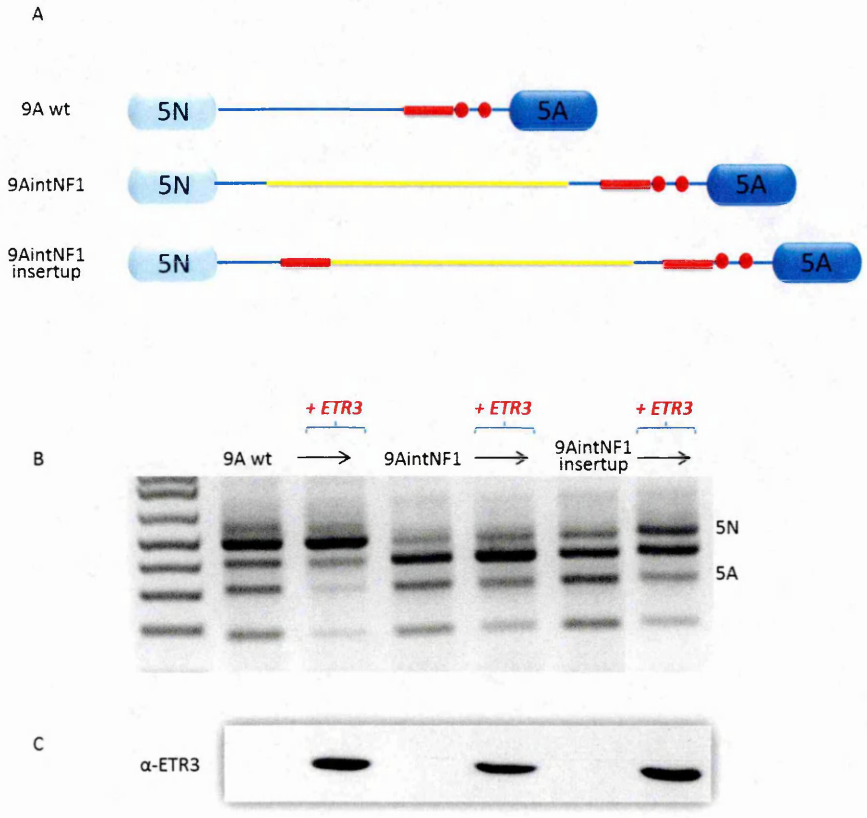

Figure 3.24. (A) Schematic representation of respectively 9A wt, 9AintNF1 and 9AintNF1insertup minigenes. The yellow box represents the NF1 intronic spacer, the two red dots are the TG stretches surrounding the branch point and the red box represents the sequence under investigation from -60 to -43. (B) Agarose gel electrophoresis showing *NdeI* digested RT-PCR products after the co-transfection of the three minigenes with ETR3 overexpression plasmid in

HeLa cells with the upper band representing a cDNA product including exon 5N and 5A, the second band representing 5N inclusion, the third one the skipping and the two lower bands derived from the digestion of the PCR product containing only 5A exon. (C) Western blot against ETR3 to monitor the level of the overexpressed protein.

The position of this new mapped element is exactly upstream of the TGs surrounding the branch point, suggesting that ETR3 binding is not limited just at that region but it acts as a positive regulator of 5N definition binding a broader region (Fig. 3.25).

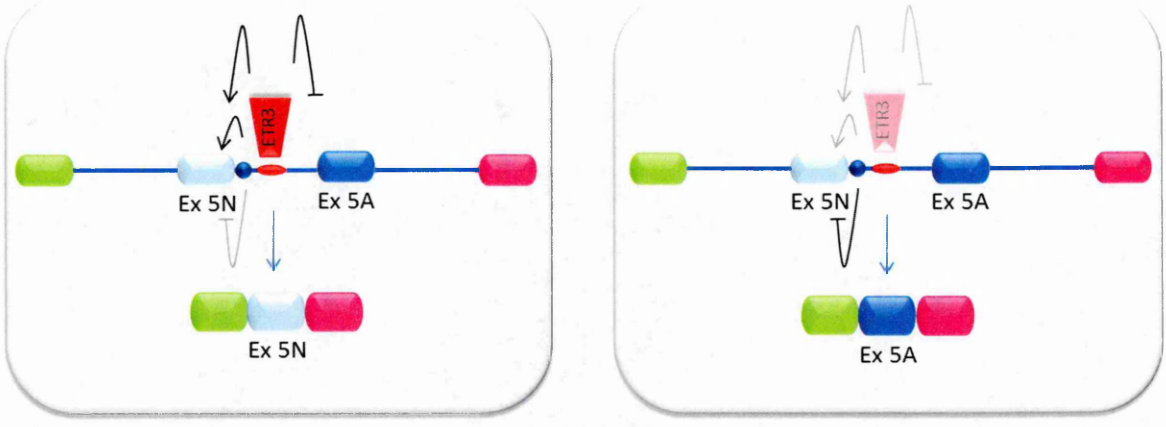

Figure 3.25. Building up the model for the mechanism of *SCN9A* exon 5 mutually exclusive splicing. The region of intron 5 comprised between +6 and +20 represents a composite regulatory element of splicing containing three regulatory elements: two of them favouring 5N inclusion (bound by ETR3 and TRA2β) and one exerting a negative effect (in blue). ETR3 promotes exon 5N inclusion and inhibits exon 5A inclusion by binding a broader TG-rich region within intron 5 (in red).

3.3.1.3. Investigation of the role of the other intronic regions in inclusion of exons 5N or 5A.

The previous results showed in section 3.3.1 highlighted the importance of the intronic sequences surrounding the two exons: the switching of the positions of the exons on one side altered the 5' and the 3' splice site sequence, affecting consequently their strength (section 1.1), on the other hand exon definition was influenced by different intronic *cis*-acting elements.

It is well know that alternative exons are generally characterized by weaker splice sites than constitutively ones and *cis*-acting elements become fundamental for the definition of the splicing outcome (Ast, 2004). Analysis of the donor sequences of the two ME exons highlighted that they differ in just one residue in position +3 (Fig. 3.26A). In particular the 5' splice site of exon 5N, carrying an A residue, is more conform to the consensus sequence (C/A)AG/GURAGU (where R is A or G) than the 5A one, that carries a G residue. Using the 9A wt minigene as a backbone, I investigated the role played by the strength of the donor splice sites by creating minigenes in which the 5A 5'ss was changed to that of 5N and *vice versa,* generating the minigenes 9A ex5A 5'ss mut and 9A ex5N 5'ss mut respectively (Fig. 3.26A).

Transfection of the minigene 9A ex5A 5'ss mut, followed by RT-PCR and *NdeI* digestion displayed a better definition of exon 5A; whereas the minigene carrying the mutation of 5N 5'ss to make it identical to that of 5A led to a decrease in 5N inclusion, increasing the amount of skipping, without affecting the adult form (Fig. 3.26B). These results confirmed the hypothesis that 5A donor splice site is weaker than 5N one. In the minigene with the swapped exons (9A Exswap) the enhancement of 5A inclusion could be at least in part due to the acquisition of a stronger 5' splice site (Fig. 3.5).

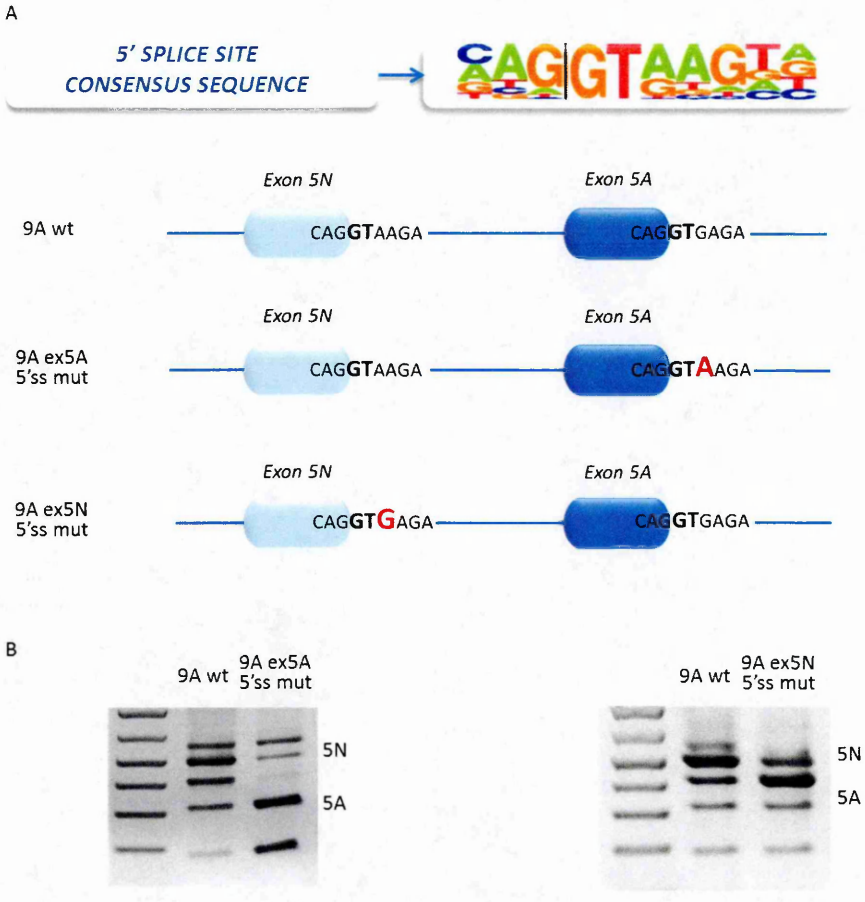

Figure 3.26. (A) In the upper part the 5' splice site consensus sequence is reported. In the lower part schematic representation of 9A wt, 9A ex5A 5'ssmut and 9A ex5N 5'ssmut minigenes. (B) Agarose gel electrophoresis showing *NdeI* digested RT-PCR products after the transfection in HeLa cells with the upper band representing a cDNA product including exon 5N and 5A, the second band representing 5N inclusion, the third one the skipping and the two lower bands derived from the digestion of the PCR product containing only 5A exon.

3.3.1.3.1. Fox1 binds intronic *cis*-acting regulatory elements improving 5A inclusion.

During development, a better definition of the adult exon could be driven by *cis*-acting elements, that can improve the usage of the weak 5'splice site.

Temporal and tissue-specific regulation occurs through *trans*-acting factors that recognize *cis*-acting elements (Kalsotra and Cooper, 2011). Two examples of specific splicing regulators in the nervous system are Nova and RbFox proteins, for which preferred binding sequences are YCAY and (U)GCAUG elements, respectively. Both these elements, due to their sites and temporal expression patterns represented possible *trans*-acting factors that may aid in the inclusion the exon 5A. In fact, clusters of YCAY, recognized by Nova proteins, are involved in the regulation of alternative exons of genes implicated in the synaptic functions (Ule et al., 2005). RbFox family members role in neuronal development has been largely investigated, revealing that they are essential players in the proper cerebellar development and its mature functionality. They affect neuronal excitation and they also exert a key role in promoting differentiation of neuronal progenitors regulating specific alternative splicing events (Fogel et al., 2012; Gehman et al., 2012).

Four (U)GCAUG motifs were present in the intronic sequence downstream of exon 5A. In order to analyse their putative role in the regulation of this mutually exclusive splicing pattern and considering that RbFox proteins are present in a low amount in HeLa cells, I co-transfected the 9A wt construct with an overexpression plasmid for RbFox1 (Fox1), a neuronal-specific isoform (Underwood et al., 2005)(Underwood 2005). After RT-PCR and *NdeI* digestion, the overexpression of Fox1 strongly improved the inclusion of exon 5A and decreased the skipping product (Fig. 3.27B). This mode of action of Fox1 is in accordance with the general mechanism described in literature and the protein acts as an

enhancer by binding Fox binding sites (FBS) located downstream of the target exon (Jin et al., 2003). In order to identify which binding sites were important for the increase in exon 5A inclusion, all FBS were disrupted either singly or in combination by introducing a point mutation in the motif, from (T)GCATG to (T)GCGTG (Fig. 3.27A). As expected, the splicing pattern of the mutant minigenes did not display strong differences respect to the wild type, due to the absence of endogenous Fox1 in HeLa cells. Co-transfecting Fox1 overexpression plasmid with 9A FBS 1m and 9A FBS 1.2m constructs showed that the disruption of only these two sites was not sufficient to block the effect on 5A inclusion. The results obtained by the co-transfection with 9A FBS 2.3m and 9A FBS 1.2.3.m gradually displayed a decrease in the positive effect exerted by Fox1 followed by an increase of the skipping product. However to completely abolish the positive effect and restore the wild type level of skipping, all FBS had to be mutated (Fig. 3.27B). These results confirm that Fox1 aids 5A inclusion through the binding to these motifs and indicate that even a single Fox binding site is sufficient for the enhancement effect on exon 5A inclusion by this *trans*-acting factor (Fig. 3.28).

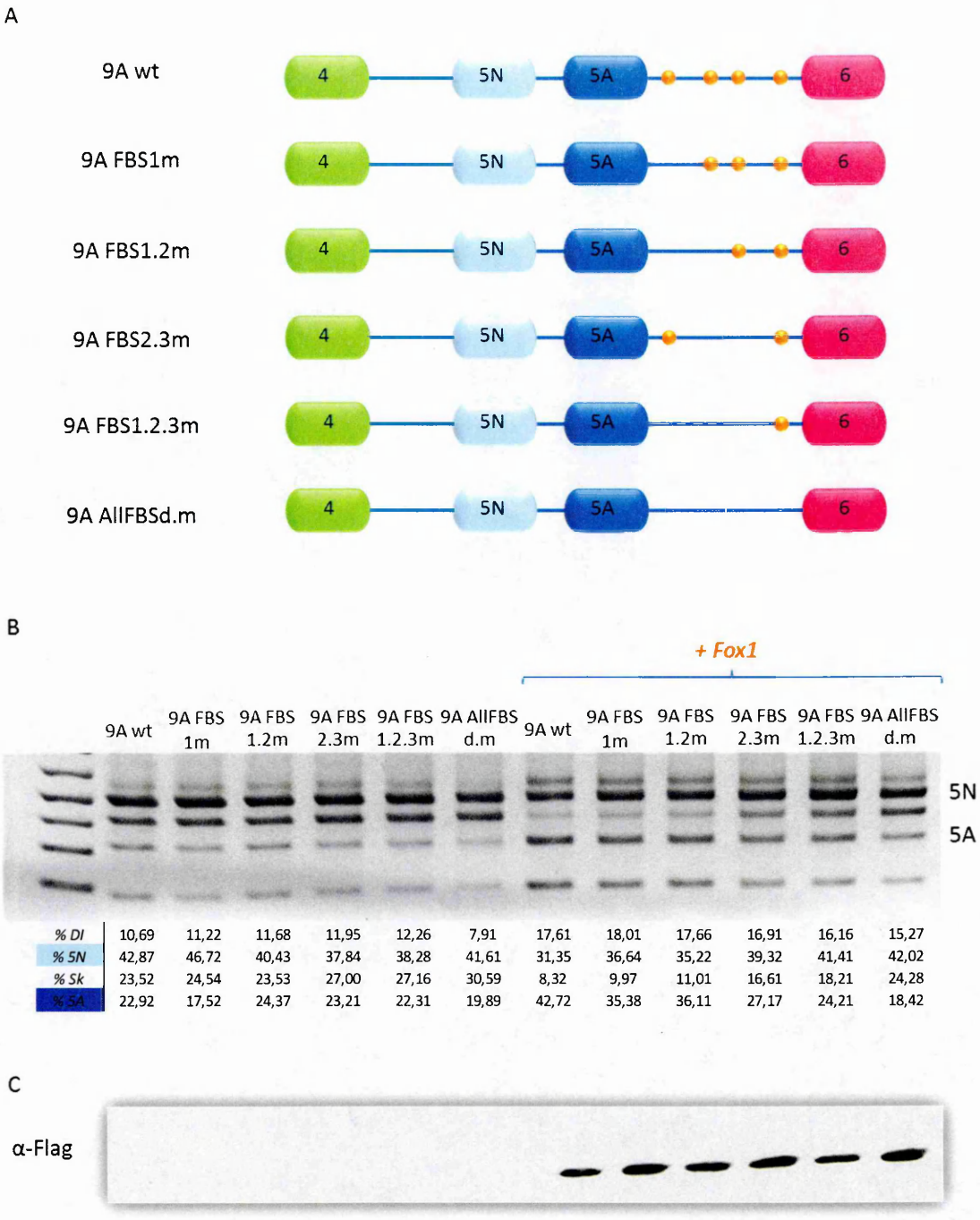

Figure 3.27. (A) Schematic representation of 9A wt minigene and all the minigenes in which each of the putative Fox binding elements (orange dots) downstream of exon 5A are mutated either singly or in combination. The absence of one particular orange dot means that this Fox binding site is mutated. (B) Agarose gel electrophoresis showing Nde I digested RT-PCR products after the transfection in HeLa cells of all the constructs, with the upper band representing a cDNA product including exon 5N and 5A, the second band representing 5N inclusion, the third one the skipping and the two lower bands derived from the digestion of the PCR product containing only 5A exon. Each product was quantified as a percentage of the total of double inclusion (DI), 5N inclusion, double skipping (Sk) and 5A inclusion. (C) Western blot using anti-flag to monitor the level of the overexpressed Fox1.

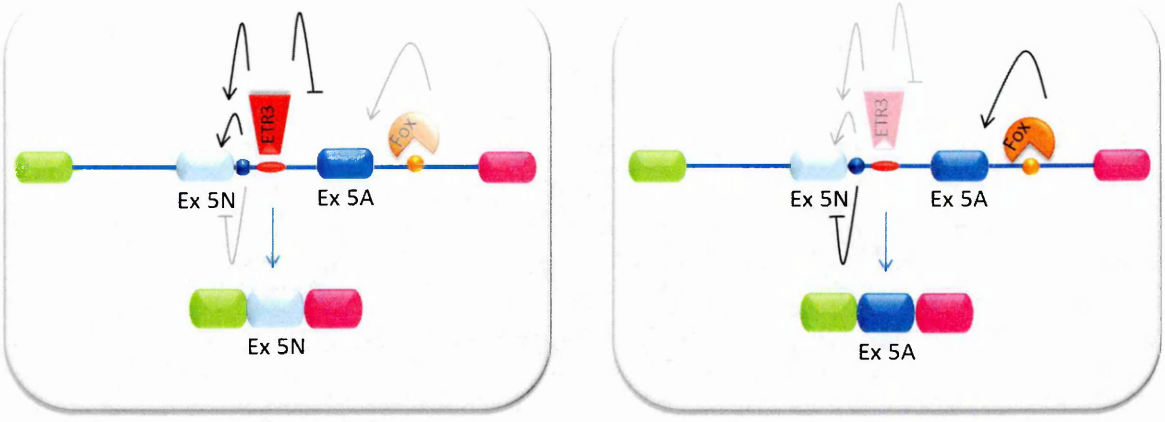

Figure 3.28. Building up the model for the mechanism of *SCN9A* exon 5 mutually exclusive splicing. The region of intron 5 comprised between +6 and +20 represents a composite regulatory element of splicing containing three regulatory elements: two of them favouring 5N inclusion (bound by ETR3 and TRA2β) and one exerting a negative effect (in blue). ETR3 promotes exon 5N inclusion and inhibits exon 5A inclusion by binding a broader TG-rich region within intron 5 (in red). Fox1 enhances exon 5A inclusion recognising four Fox binding sites downstream of exon 5A (in orange).

3.3.2. PTB protein binds in different exonic and intronic regions modulating the splicing pattern.

Several mutually exclusive events are regulated by a competition between CELF proteins and the polypyrimidine tract binding protein (PTB) (Southby et al., 1999; Llorian et al., 2010; Sureau et al., 2011; Tang et al., 2011).

Polypyrimidine tract binding protein is a well-characterized repressive regulatory element, that recognizes U-rich regions, with optimal binding sites UCUUC and CUCUCU (Perez et al., 1997). Mechanisms proposed to explain how PTB inhibits exon inclusion include competition with the binding of U2AF65, covering the polypyrimidine tract, multimerization on multiple PTB binding sites creating zone of silencing. Sometimes there are PTB sites in both the introns flanking one exon, looping it out. The protein can also

interact with ESS blocking exon definition or with ISS blocking intron definition (Spellman and Smith, 2006)(Spellman R., 2006). However a recent study based on high-density Affymetrix microarray revealed that among 263 alternative splicing events affected by the knockdown of PTB, 67 events were downregulated confirming also a positive role of this protein previously shown in few works. In particular it has been shown that positive-regulated exon were characterized by PTB binding sites only on the downstream region (Llorian et al., 2010).

Analysing the entire sequence from exon 4 to exon 6 through a splicing factors prediction program (http://193.206.120.249/splicing_tissue.html, SpliceAid 2), many optimal PTB binding sites were found in the intronic regions surrounding the ME exons and also one in exon 5N, so I decided to investigate the putative role of these multiple elements (scheme of the putative PTB binding sites in Fig. 3.33A, 9A wt).

3.3.2.1. Analysis of a putative PTB binding site in the middle of exon 5N.

The first putative PTB binding element that I investigated is located in the middle of exon 5N, interestingly in a region that is not conserved among the two ME exons (Fig. 3.29A). I disrupted this putative optimal PTB binding site by changing the 5N residues with the 5A ones, both singly and in combination, without introducing any modification in the amino acidic sequence (Fig. 3.29B).

Transfections of the three minigenes 9APTB5Nmut1, 9APTB5Nmut2 and 9APTB5Nmut3, RT-PCR and *NdeI* digestion showed an increase in 5N inclusion suggesting that the mutations disrupted an exonic negative regulatory element (Fig. 3.29C). The 9APTB5Nmut1 was observed to show stronger enhancement in 5N inclusion respect to 9APTB5Nmut3 minigene, in which I mutated all the three residues, possibly due to also a creation of a positive element (Fig. 3.29C).

This hypothesis was supported by data obtained from a bioinformatic program, that predicted the lacking of the PTB binding site in all the three mutants, but SRp30 binding only for 9APTB5Nmut1, suggesting that the greater enhancement of 5N inclusion might be not only due to the disruption of a silencer but also a creation of an enhancer element (SpliceAid 2, http://193.206.120.249/splicing_tissue.html).

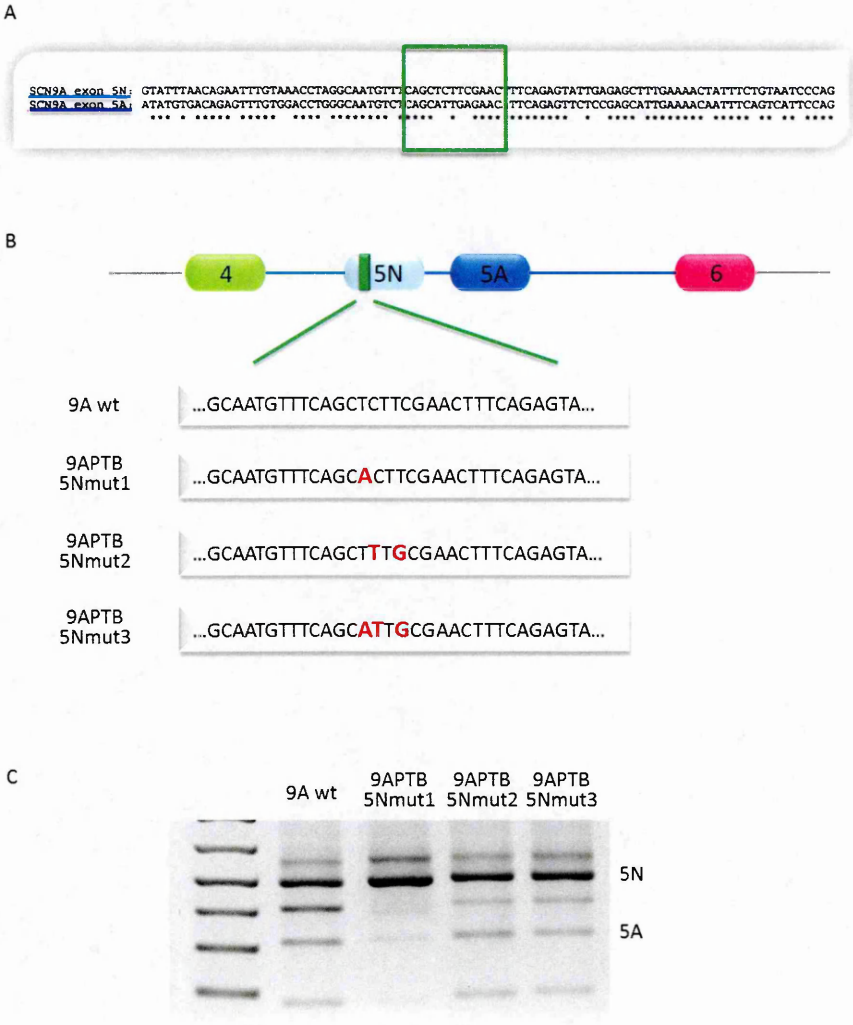

Figure 3.29. (A) Alignment of the two mutually exclusive exons. In the green box the region under investigation. (B) Schematic representation of respectively 9A wt, 9APTB5Nmut1, 9APTB5Nmut2 and 9APTB5Nmut3 minigenes (in red the mutated residues). (C) Agarose gel electrophoresis showing *NdeI* digested RT-PCR products after the transfection of the minigenes in HeLa cells with the upper band representing a cDNA product including exon 5N and 5A, the second band representing 5N inclusion, the third one the skipping and the two lower bands derived from the digestion of the PCR product containing only 5A exon.

To continue the investigation regarding this putative PTB binding site I performed a pull down analysis using two RNAs, one corresponding to the wild type sequence of exon 5N covering the region containing the putative PTB binding site, and the other one carrying the triple mutation on the PTB binding site. To evaluate the amount of RNA linked to beads I inserted in the primers four TG repeats, that will be bound by TDP-43, as an internal control (Fig. 3.30A).

The pull down analysis clearly showed that PTB could not bind the mutant RNA while it perfectly bound the wild type RNA sequence (Fig. 3.30B).

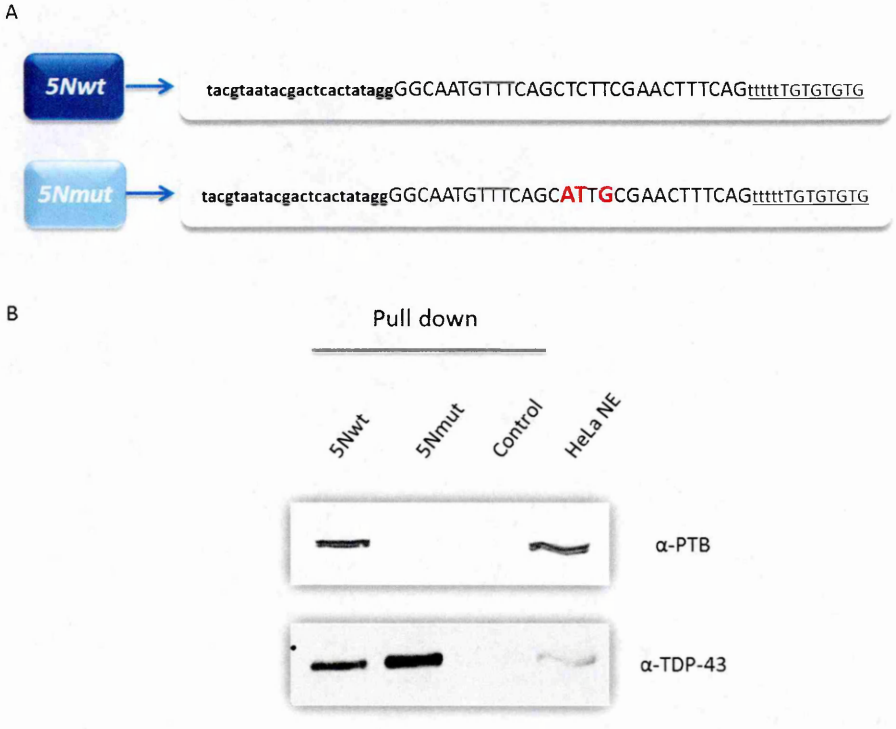

Figure 3.30. (A) DNA sequences used for the *in vitro* transcription of 5Nwt and 5Nmut RNAs. The underlined sequence represents a tag for the recruitment of TDP-43 to normalize the pull down results. (B) Western blot against PTB of the pull down assay performed using 5Nwt and 5Nmut RNAs incubated with HeLa NE. The control is derived from the beads without RNA, incubated with the nuclear extract.

I then tested the effect of PTB overexpression on the splicing outcome of the wild type and the three mutant constructs (Fig. 3.31A). The co-transfection with the 9A wt led to a decrease of 5N inclusion, together with an increase in 5A. The same effect was also observed with the 9APTB5Nmut2 and 9APTB5Nmut3 minigenes (Fig. 3.31B). These results suggested that PTB could bind other elements and play a positive regulatory role on 5A inclusion. The result after RT-PCR and *NdeI* digestion of the co-transfection experiment of 9APTB5Nmut1 and PTB overexpression plasmid showed a high increase in double inclusion that could be explained by the positive effect on 5A inclusion by PTB and the positive effect on 5N inclusion by a positive element probably introduced with the mutation (Fig. 3.31B).

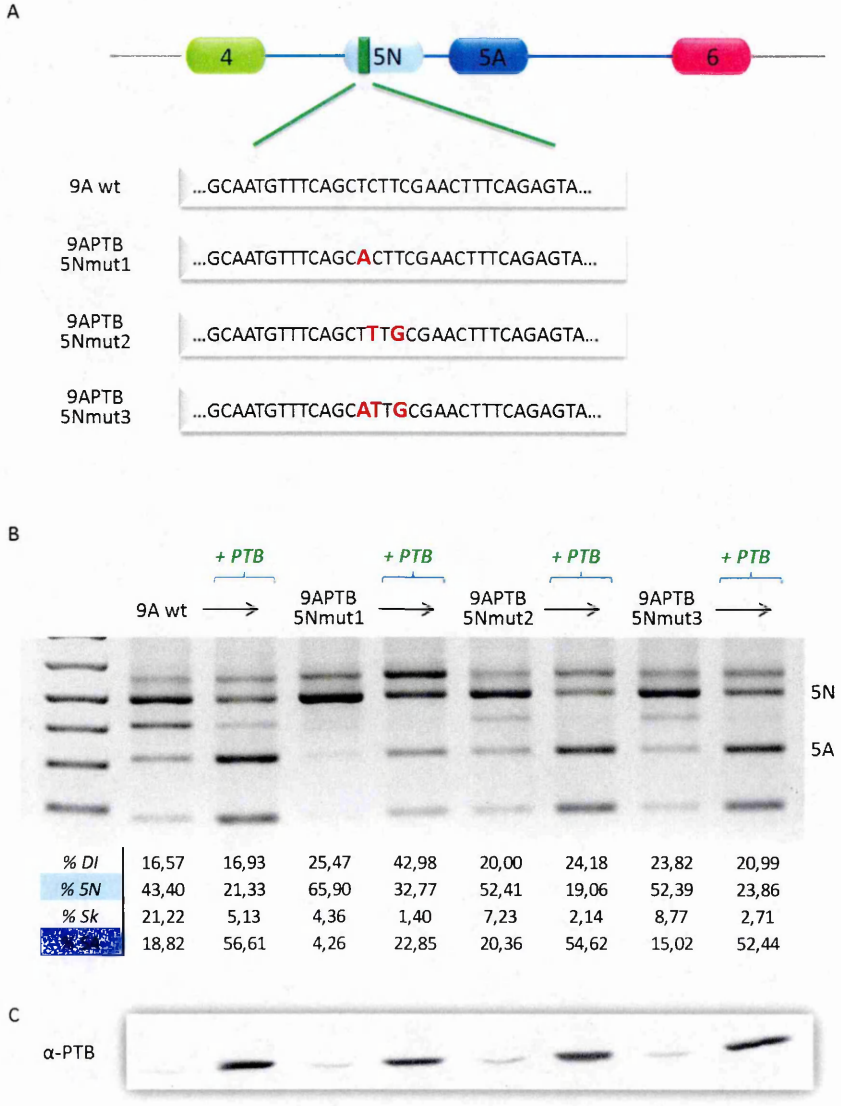

Figure 3.31. (A) Schematic representation of respectively 9A wt, 9APTB5Nmut1, 9APTB5Nmut2 and 9APTB5Nmut3 minigenes (in red the mutated residues). (B) Agarose gel electrophoresis showing *NdeI* digested RT-PCR products after the co-transfection of the minigenes with PTB overexpression plasmid in HeLa cells with the upper band representing a cDNA product including exon 5N and 5A, the second band representing 5N inclusion, the third one the skipping and the two lower bands derived from the digestion of the PCR product containing only 5A exon. Each product was quantified as a percentage of the total of double inclusion (DI), 5N inclusion, double skipping (Sk) and 5A inclusion. (C) Western blot using anti-PTB to monitor the level of the overexpressed protein.

I also performed the silencing of PTB together with neuronal PTB (nPTB), since the downregulation of PTB led to an increase in nPTB level, that could play a redundant effect on the splicing regulation (Fig. 3.32B). Although both the proteins were reduced significantly, I could not observe any effect on splicing pattern, probably because the remaining amount of protein was sufficient to maintain the normal splicing outcome (Fig. 3.32A).

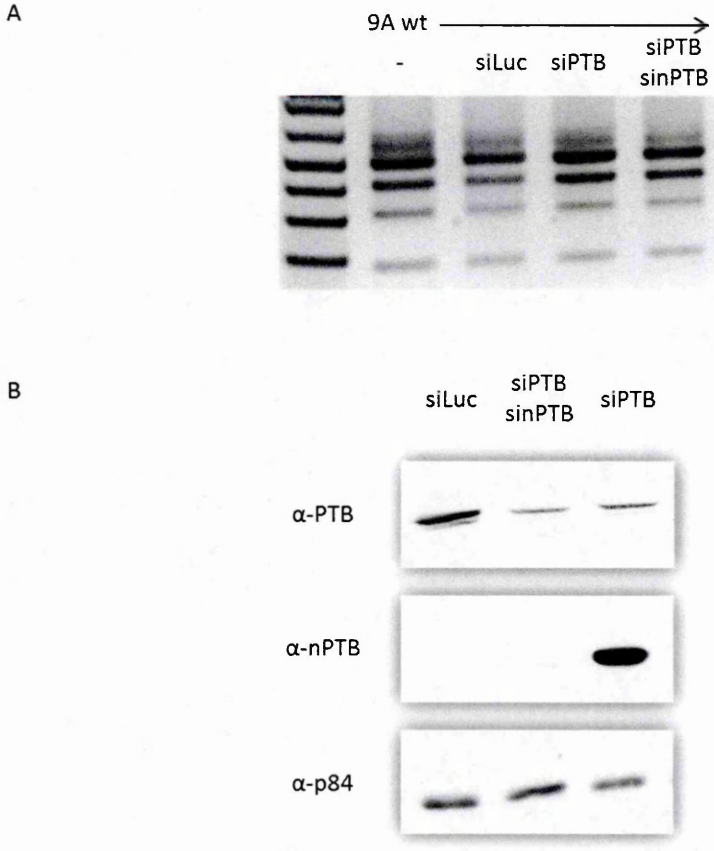

Figure 3.32. (A) Agarose gel electrophoresis showing *NdeI* digested RT-PCR products after transfection analysing the effect of PTB and PTB/nPTB knockdown experiments in HeLa cells with the upper band representing a cDNA product including exon 5N and 5A, the second band representing 5N inclusion, the third one the skipping and the two lower bands derived from the digestion of the PCR product containing only 5A exon. (B) Western blot analysis of siRNA experiments, depleting PTB and PTB/nPTB.

3.3.2.2. Evaluating the role of multiple intronic PTB binding sites.

In the intronic sequences surrounding the two ME exons there were other putative optimal PTB binding sites including one within intron 5 and several downstream of exon 5A. Different minigenes were created trying to assess the role of these elements. Firstly I mutated six putative strong PTB binding sites downstream of exon 5A in the wild type minigene, to investigate if the positive effect on 5A inclusion could be caused by these, creating the minigene 9APTBmut intdo5A (Fig. 3.33A). After transfection, RT-PCR and *NdeI* digestion, I detected a decrease in skipping with an increase in double inclusion. Moreover, after the overexpression of PTB, the splicing pattern obtained from this new minigene was almost the same observed for the wild type after PTB overexpression, suggesting that the positive effect on 5A was not due to these putative PTB binding sites *per se* (Fig. 3.33B). To further investigate the role of these multiple binding sites I mutated them in combination with the PTB binding site in intron 5N or in exon 5N, creating respectively the minigenes 9APTBmut intdo5N intdo5A and 9APTBmut ex5N intdo5A (Fig. 3.33A). After transfection, RT-PCR and *NdeI* digestion both the minigenes displayed the same splicing pattern characterized by an increase in 5A. Overexpressing PTB in presence of these two minigenes gave a strong increase in 5A inclusion, as observed for the 9A wt (Fig. 3.33B).

I also mutated in combination the PTB binding sites in exon 5N and in intron 5, obtaining the minigene 9APTBmut ex5N intdo5N (Fig. 3.33A). After transfection, RT-PCR and *NdeI* digestion I observed a strong increase in 5N inclusion, as previously seen in Fig. 3.29B, with the minigene 9APTB5Nmut3. PTB overexpression led to the same splicing outcome detected for all the other minigenes (Fig. 3.33B).

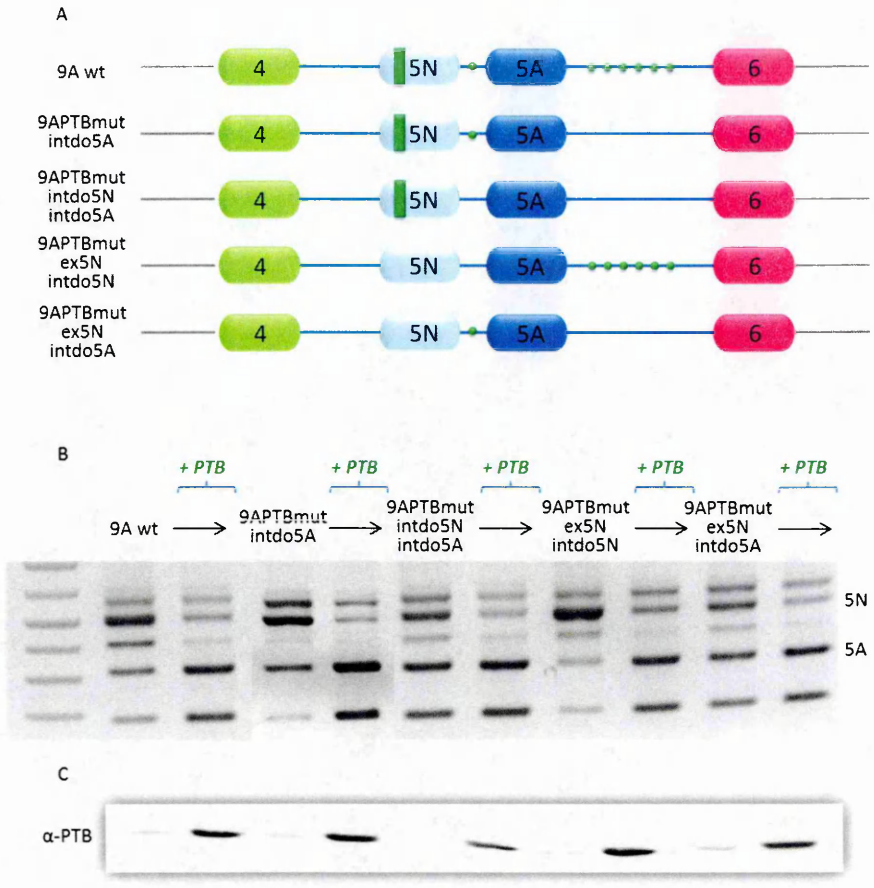

Figure 3.33. (A) Schematic representation of respectively 9A wt, 9APTBmut intdo5A, 9APTBmut intdo5N intdo5A, 9APTBmut ex5N intdo5N and 9APTBmut ex5N intdo5A minigenes (in green the PTB binding sites). The absence of one particular green dot or/and box means that the PTB binding site is mutated. (B) Agarose gel electrophoresis showing *NdeI* digested RT-PCR products after the co-transfection of the minigenes with PTB overexpression plasmid in HeLa cells with the upper band representing a cDNA product including exon 5N and 5A, the second band representing 5N inclusion, the third one the skipping and the two lower bands derived from the digestion of the PCR product containing only 5A exon. (C) Western blot using anti-PTB to monitor the level of the overexpressed protein.

In an attempt to understand the positive role of PTB, I tried also to overexpress PTB in the presence of the minigene 9AintGlo5'ss(+6), in which intron 5 had been substituted with a *globin* intron. This new minigene contained the PTB binding site in exon 5N and all the intronic PTB binding sites downstream of exon 5A (Fig. 3.34A). After RT-PCR and *NdeI* digestion I observed that there was an increase in 5A inclusion (Fig. 3.34B). This enhancement in 5A inclusion could be due to the inhibitory effect of the PTB on the

exonic element in exon 5N. To test this hypothesis I mutated the PTB binding site in exon 5N creating the minigene 9AintGlo5'ss(+6)PTBmutex5N (Fig. 3.34A). The co-transfection of this minigene with PTB overexpression plasmid, RT-PCR and *NdeI* digestion did not showed any increase in 5A inclusion (Fig. 3.34B). So the increase showed with the 9AintGlo5'ss(+6) after PTB overexpression was probably due to the inhibitory effect on exon 5N. Furthermore this result suggested that intron 5 could be necessary to achieve the positive effect on exon 5A (Fig. 3.35).

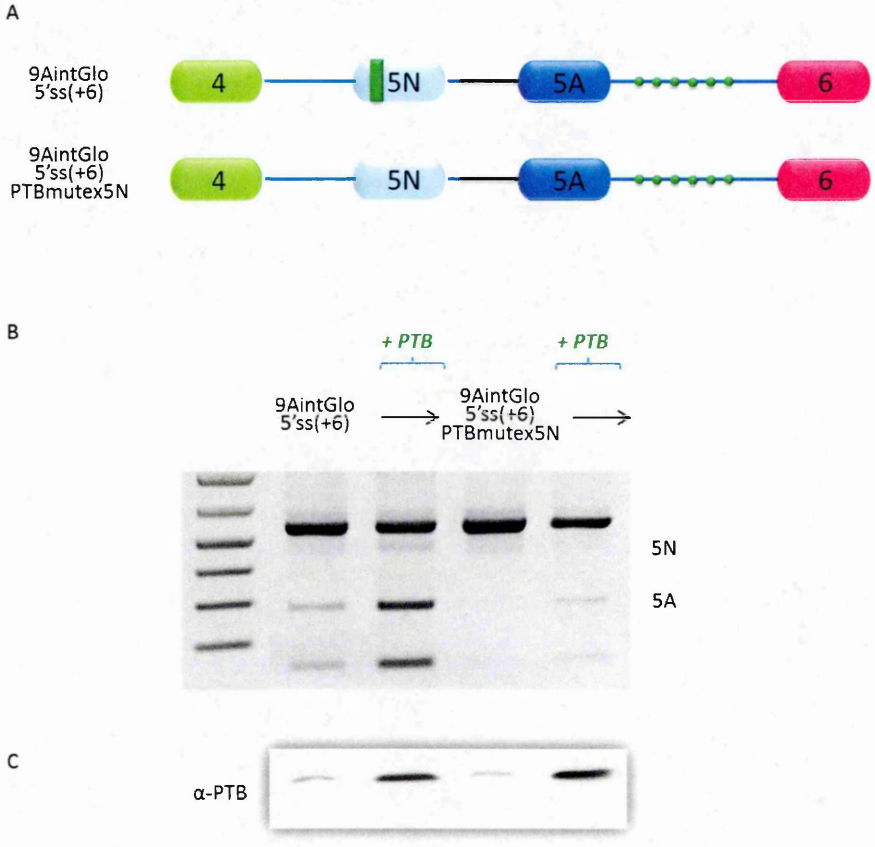

Figure 3.34. (A) Schematic representation of respectively 9AintGlo 5'ss(+6) and 9AintGlo 5'ss(+6) PTBmutex5N (in green the PTB binding sites). The absence of one particular red dot or/and box means that the PTB binding site is mutated. (B) Agarose gel electrophoresis showing *NdeI* digested RT-PCR products after the co-transfection of the minigenes with PTB overexpression plasmid in HeLa cells with the upper band representing a cDNA product including exon 5N and 5A, the second band representing 5N inclusion, the third one the skipping and the two lower bands derived from the digestion of the PCR product containing only 5A exon. (C) Western blot using anti-PTB to monitor the level of the overexpressed protein.

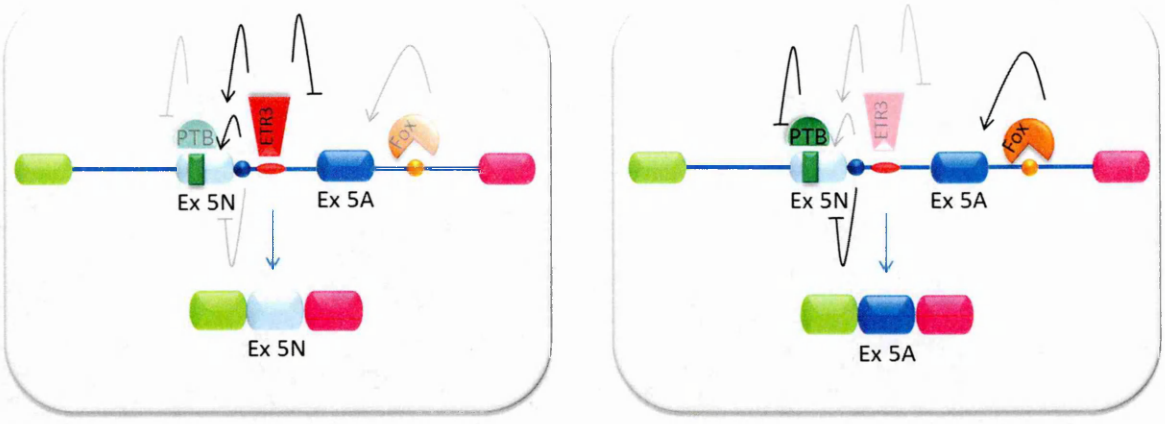

Figure 3.35. Building up the model for the mechanism of *SCN9A* exon 5 mutually exclusive splicing. The region of intron 5 comprised between +6 and +20 represents a composite regulatory element of splicing containing three regulatory elements: two of them favouring 5N inclusion (bound by ETR3 and TRA2β) and one exerting a negative effect (in blue). ETR3 promotes exon 5N inclusion and inhibits exon 5A inclusion by binding a broader TG-rich region within intron 5 (in red). Fox1 enhances exon 5A inclusion recognising four Fox binding sites downstream of exon 5A (in orange). PTB inhibits 5N inclusion through an exonic silencer (in green).

3.3.3. Assessing the strength of 5A 3' splice site and its polypyrimidine tract.

During the mapping of intron 5 I noticed that the 3' splice site of exon 5A was weaker than the one introduced by the *α-globin* intron (section 3.3.1.2.1). For this reason I decided to evaluate role of the strength of the 3' ss of 5A in the alternative splicing by mutating the first base of the exon from A to G in order to make it more conform to the consensus sequence; moreover the G is also present in 5N 3' splice site (Fig. 3.36A, 36B).

To study this region I generated a new minigene to be used as a backbone as some of the mutations, that I had planned to do, disrupted the *NdeI* site. For this reason I took advantage of a minigene largely used in the lab, a human hybrid three-exon α-globin/ fibronectin minigene, called pTB (Vibe-Pedersen et al., 1984). Firstly I modified this construct by changing the fibronectin cassette with one derived from *SCN9A* gene. This

cassette comprised exon 4 and part of the downstream intron and exon 6 with a section of its upstream intronic region. In the middle of the hybrid intronic region an *NdeI* site was introduced to allow the insertion of small sequences under investigation (Fig. 3.36C). Using this new backbone I cloned into the *NdeI* site the exon 5A with part of its flanking intronic regions (Fig. 3.36C). After transient transfection of this minigene pTB5Awt and RT-PCR I observed two PCR products, the upper amplicon representing exon 5A inclusion and the lower one representing exon 5A skipping. Notwithstanding exon 5N was absent, exon 5A remained only partially included, suggesting that exon 5N was not directly influencing 5A inclusion (Fig. 3.36D).

The 3'ss of exon 5A was mutated by changing the A with a G in this new construct pTB5Awt (Fig. 3.36C). After transfection of the pTB5Amut3'ss and RT-PCR I could observe clear increase in 5A inclusion (Fig. 3.36D), suggesting that 5A 3' splice site is weaker than the 5N one.

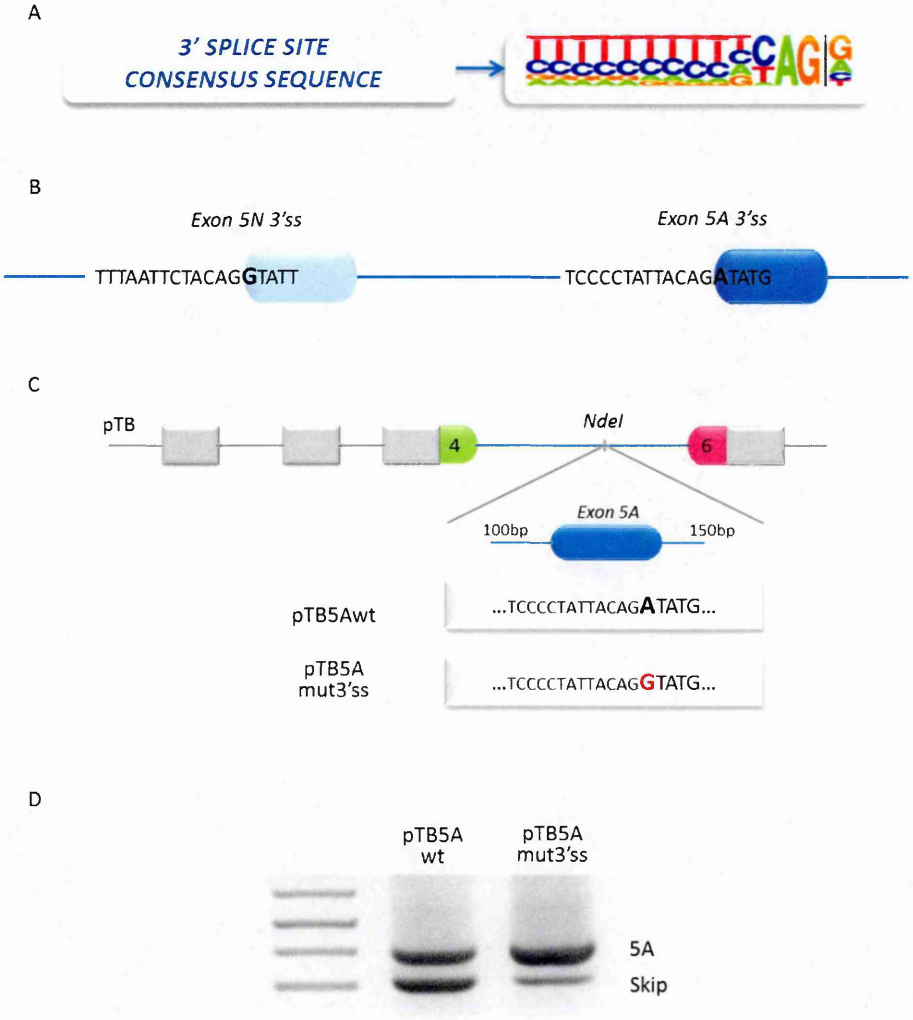

Figure 3.36. (A) 3' splice site consensus sequence. (B) Schematic representation of 3' splice sites of the two mutually exclusive exon. (C) Schematic representation of pTB5Awt and pTB5Amut3'ss minigenes. (D) Agarose gel electrophoresis showing RT-PCR products after the transfection in HeLa cells with the upper band representing a cDNA product including exon 5A and the lower band representing the skipping.

I also analysed the putative polypyrimidine tract of intron 5 (Fig. 3.37A). I mutated four A residues into T to extend the sequence of pyrimidines downstream the branch point already mapped (Fig. 3.37B). The transfection of the minigene 9Amut4A, the RT-PCR and *NdeI* digestion led to a complete inclusion of exon 5A, most likely because the mutations enforced the polypyrimidine tract (Fig. 3.37C).

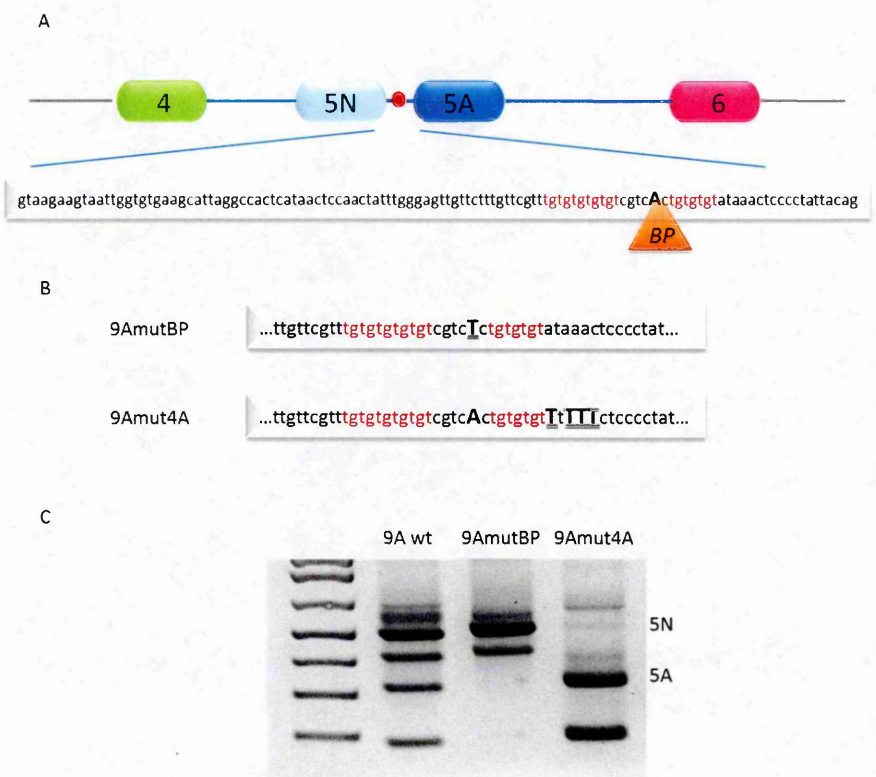

Figure 3.37. (A) Schematic representation of intron 5 of the 9A wt minigene. (B) Schematic representation of the minigenes containing respectively the branch point mutated (9AmutBP) and the polypyrimidine tract enforced (9Amut4A). (B) Agarose gel electrophoresis showing *NdeI* digested RT-PCR products after the transfection in HeLa cells with the upper band representing a cDNA product including exon 5N and 5A, the second band representing 5N inclusion, the third one the skipping and the two lower bands derived from the digestion of the PCR product containing only 5A exon.

3.3.3.1. An exonic splicing enhancer aids 5A inclusion.

Since both the 3' splice site and the polypyrimidine tract of exon 5A are quite weak, it was reasonable to hypothesize that other elements could help its definition, similar to the scenario demonstrated for its 5' splice site (section 3.3.1.3.1). Interestingly the two mutually exclusive exons 5N and 5A encode two peptidic fragments that differ by only two amino acids, that are located close to the 3' splice site (Fig. 3.38A) (Jarecki et al., 2009) (Chatelier et al., 2008). Since this feature is well conserved also in other genes of the same family (section 1.4.5.1, Tab. 1.5), I decided to investigate if this region could contain important splicing regulatory elements present in exon 5A and absent in exon 5N. The alignment of the two exons showed that differences in three nucleotidic differences were responsible for the aminoacidic changes (Fig. 3.38B). I started the analysis of the residues involved in the amino acidic changes by inserting the corresponding nucleotides present in exon 5N into exon 5A both singly or in combination, creating the minigenes pTB5AmutVD, pTB5AmutVD*NdeI*, pTBmutV and pTBmutD (Fig. 3.38C). As the mutation in fifth exonic base would disrupt the *NdeI* restriction site used to distinguish which of the two exons is included, this experiment was initially performed using the hybrid minigene pTB5Awt (section 3.3.3). After transfection and RT-PCR of the minigene pTB5AmutVD, that contained the three residues mutated into those present in exon 5N, I observed that 5A inclusion was almost completely abolished (Fig. 3.38C, 38D). An increase in skipping was detected also for all the other minigenes with a more pronounced effect observed using the minigene with a mutation on the residue encoding for the aspartic acid (pTB5AmutVD*NdeI* and pTB5AmutD)(Fig. 3.38C, 3.38D). These results suggested the presence of a putative exonic splicing enhancer (ESE) in the region that enhances the inclusion of the exon.

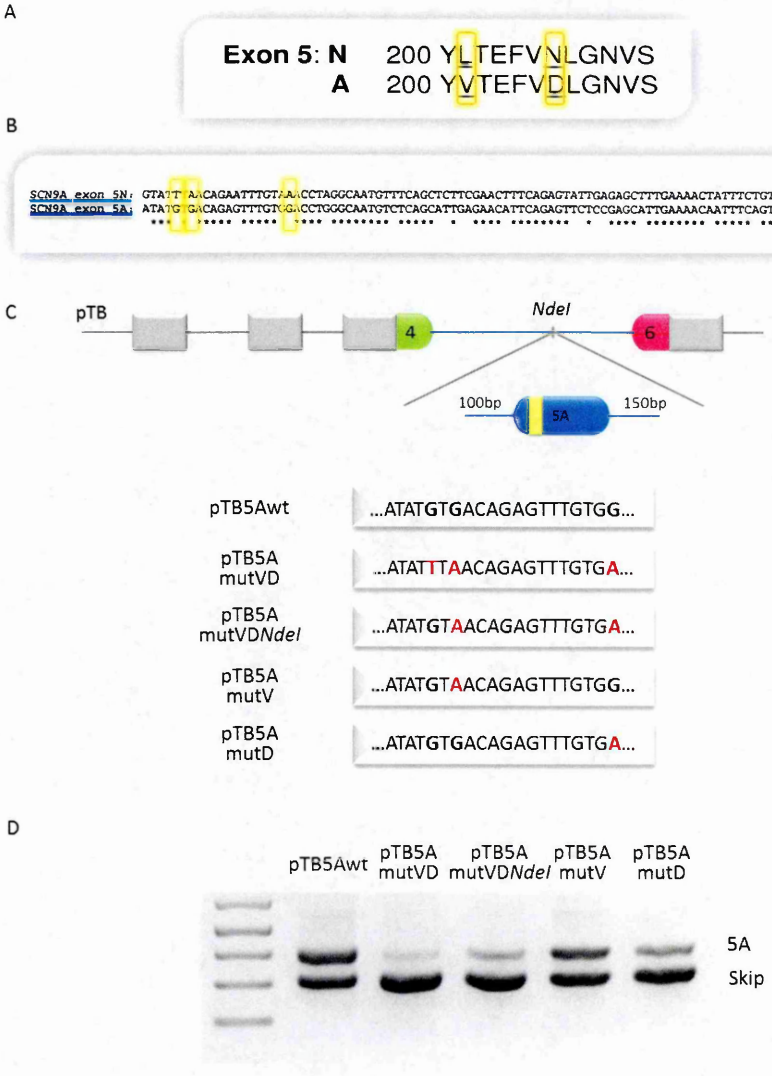

Figure 3.38. (A) Alignment of aminoacidic sequences encoded by exon 5N and exon 5A; the two aminoacidic differences are highlighted in yellow boxes. (B) Alignment of exon 5N and exon 5A DNA sequences; the three residues marked in yellow are important for the amino acidic changes. (C) Schematic representation of pTB5Awt, pTB5AmutVD, pTB5AmutVD*NdeI*, pTB5AmutV and pTB5AmutD minigenes. In red the residues mutated. (D) Agarose gel electrophoresis showing RT-PCR products after the transfection in HeLa cells with the upper band representing a cDNA product including exon 5A and the lower band representing the skipping.

At this point it was of interest to confirm if the lack of exon 5A definition would also occur upon disruption of the putative ESE in a context that contained both mutually exclusive exons. Using the minigene 9A wt as a backbone I introduced only the mutations that did not affect the formation of the *NdeI* site. The *NdeI* site is formed by the last residue of

exon 4 and the first five residues of exon 5A, precisely in the junction between exon 4 and 5A. For this reason the mutation in position +5 (G→T) in exon 5A can not be introduced in the 9A wt minigene without losing the restriction site used to discriminate the two ME exons (Fig. 3.39A).

As previously shown in the hybrid minigenes derived from pTB5A (Fig. 3.38), all three minigenes 9AmutVD*NdeI*, 9AmutV and 9AmutD, after RT-PCR and *NdeI* digestion, highlighted strong differences in the splicing pattern with respect to the wild type minigene, characterized by a strong decrease in 5A inclusion (Fig. 3.39B), confirming the presence of a positive splicing regulatory element in this region.

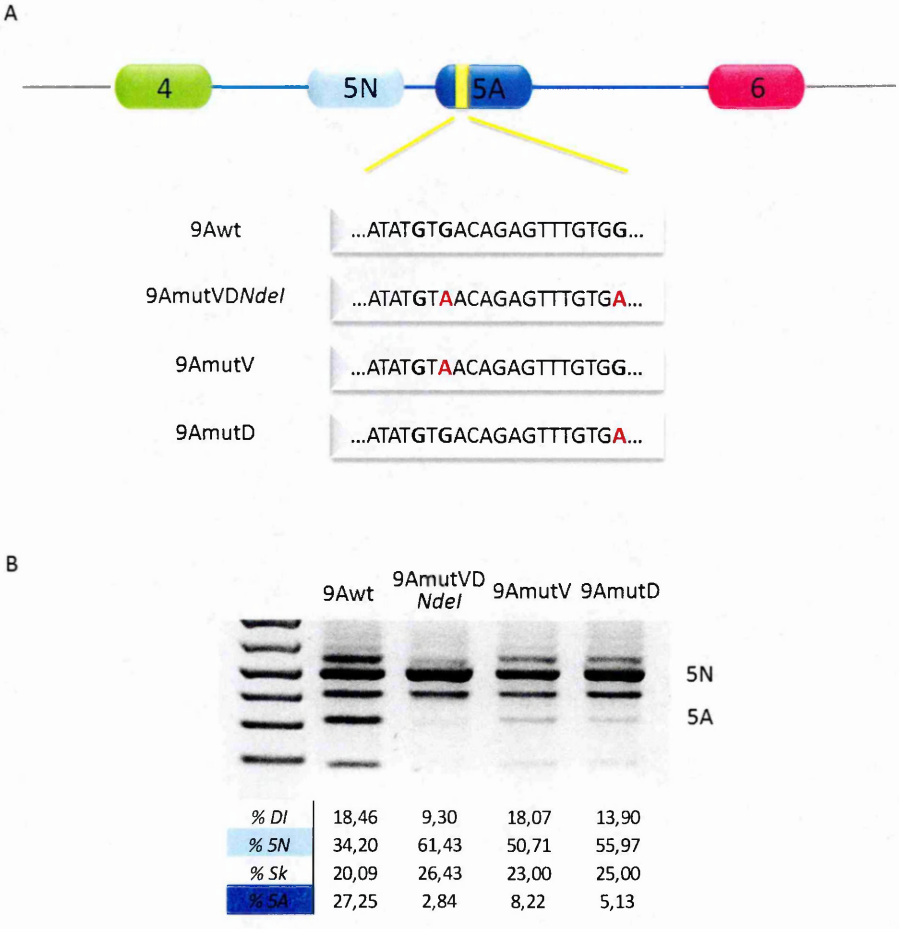

Figure 3.39. (A) Schematic representation of 9A wt, 9AmutVD*NdeI*, 9AmutV and 9AmutD minigenes. The yellow box marked the region of the ESE. (B) Agarose gel electrophoresis showing *NdeI* digested RT-PCR products after the transfection in HeLa cells with the upper band representing a cDNA product including exon 5N and 5A, the second band representing 5N inclusion, the third one the skipping and the two lower bands derived from the digestion of the PCR product containing only 5A exon. Each product was quantified as a percentage of the total of double inclusion (DI), 5N inclusion, double skipping (Sk) and 5A inclusion.

To further study the role of this putative enhancer I performed the reverse experiment inserting the residues of 5A into 5N, focusing my attention on the region encoding for the aspartic acid, that seemed to be the most critical one, creating two minigenes 9AintroESE5N and 9AintroESE5Nd.m. In the former, a point mutation, in position +20 of exon 5N changes the triplet encoding for the asparagine to aspartic as present in exon 5A. In the latter (9AintroESE5Nd.m.) two mutations +19 and +20 were introduced altering the region that was not conserved among the two ME exons (Fig. 3.40A, 3.40B). After transfection, RT-PCR and *NdeI* digestion, the minigene 9AintroESE5N displayed a splicing pattern similar to that observed for the wild type minigene, while the minigene with the double mutation (9AintroESE5Nd.m.) led to almost 100% of 5N inclusion, underlining the positive role of this *cis*-acting element, also when introduced into another context (Fig. 3.40C).

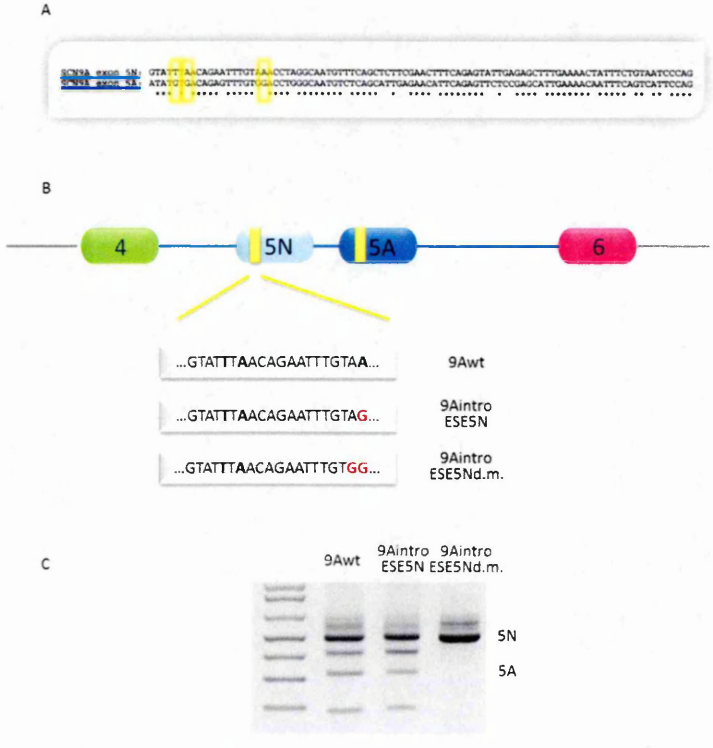

FIgure 3.40. (A) Alignment of exon 5N and exon 5A DNA sequences; the three residues marked in yellow are important for the aminoacidic changes. (B) Schematic representation of 9A wt, 9AintroESE5N and 9AintroESE5Nd.m minigenes. The yellow box marked the region of the ESE. (C) Agarose gel electrophoresis showing *NdeI* digested RT-PCR products after the transfection in HeLa cells with the upper band representing a cDNA product including exon 5N and 5A, the second band representing 5N inclusion, the third one the skipping and the two lower bands derived from the digestion of the PCR product containing only 5A exon.

3.3.3.2. SRSF6 and SRSF1 bind an exonic splicing enhancer in exon 5A.

To identify the *trans*-acting factor(s) binding the ESE region in exon 5A I performed a pull down analysis using two synthetic RNAs. The two RNAs covered the region encoding for the aspartic acid, that seemed to be the most relevant in splicing regulation. In particular, the two RNAs were composed of the wild type sequence of exon 5A from +14 to +26 and the second carried the nucleotide difference in position +20 that changed the amino acid from aspartic acid to asparagine. Both RNAs also carried in four UG repeats, that would be bound by TDP-43, allowing this to be used as a normalisation control (Fig. 3.41A).

Following the standard protocol (section 6.28), I divided the proteins bound to the RNAs in two different fractions. One fraction was visualized by coomassie blue staining after polyacrylamide electrophoresis, and with the other fraction I performed a western blot analysis using a battery of antibodies for the most common SR proteins.

The coomassie staining highlighted one protein band that was present only using the wild type RNA. This band was excised from the gel, together with the corresponding region from the mutated RNA, trypsin digested and analysed by mass-spectrometry (Fig. 3.41B). From this analysis I could not identify any proteins that could match exactly with the molecular weight respect to the size suggested by the marker.

Western blot analysis of the pull down experiments against the most common SR proteins was initially performed using the 1H4 antibody, that recognizes a series of different SR proteins: SRSF4 (SRp75), SRSF6 (SRp55), SRSF5 (SRp40), SRSF1 (ASF/SF2), SRSF2 (SC35) and SRSF3 (SRp20). Two SRs proteins, SRSF1 and SRSF6 were observed to bind the wt RNA but not the mutant RNA. The binding of SRSF1 was also confirmed using a specific antibody against SRSF1 (Fig. 3.41C).

These experiments highlighted the presence of an exonic splicing enhancer in the region of the aspartic acid in exon 5A, recognized by at least two SR proteins, SRSF1 and SRSF6.

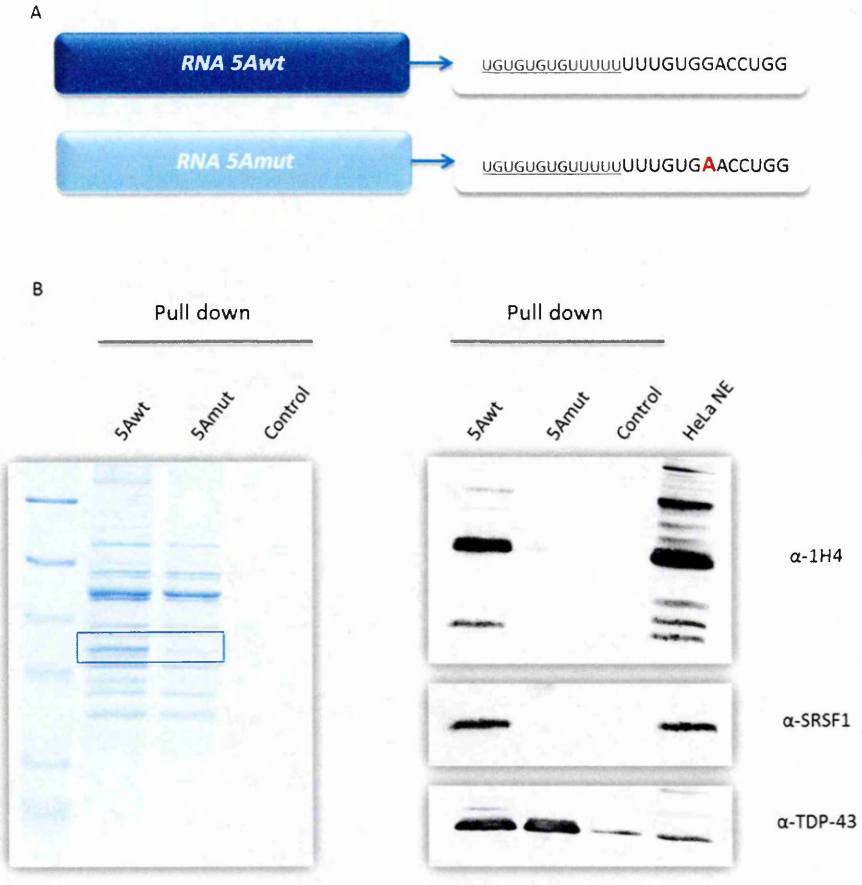

Figure 3.41. (A) Sequence of the synthetic 5Awt and 5Amut RNAs spanning the region of the ESE, used for the pull down assay. The underlined sequence represents a tag for the recruitment of TDP-43 to normalize the pull down results. (B) Coomassie stained gel (the analised region is marked with a blue box) and (C) western blot of the pull down assay performed using 5Awt and 5Amut RNAs incubated with HeLa NE. The control is derived from the beads without RNA, incubated with the nuclear extract.

3.3.3.3. SRs recruitment on the exonic splicing enhancer favours 5A inclusion.

To further assess the role of these *trans*-acting factors, I performed co-transfection experiments with plasmids that overexpressed either SRSF1 or SRSF6 with the 9A wt minigene. After RT-PCR and *NdeI* digestion, the co-transfection experiments of both SRSF1 or SRSF6 overexpression plasmids with the 9A wt minigene led to an increased

skipping, with also a reduction in 5A inclusion upon overexpression of SRSF6 (Fig. 3.42). These data are difficult to interpret. They most likely are due to the effects of the SRs overexpression in other areas of the minigene. For this reason I decided to selectively inhibit the binding of the two SRs to the ESE. This approach has been already used to modulate the mutually exclusive splicing pattern of pyruvate kinase M exon 9 and 10 (Wang et al., 2012)

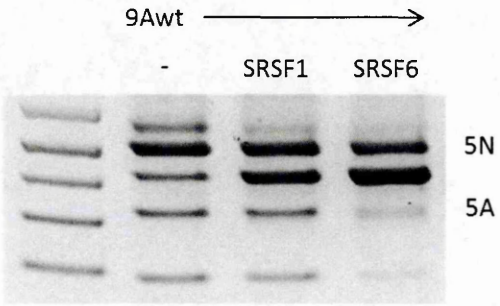

Figure 3.42. Agarose gel electrophoresis showing *NdeI* digested RT-PCR products after transfection analysing the effect of SRSF1 and SRSF6 overexpression. The upper band representing a cDNA product including exon 5N and 5A, the second band representing 5N inclusion, the third one the skipping and the two lower bands derived from the digestion of the PCR product containing only 5A exon.

I tested two different antisense techniques to block the access to the enhancer by the *trans*-acting factors, namely a modified U7 snRNA containing a sequence antisense to the ESE in exon 5A, from position +13 to +34, and a morpholino targeting the region from position +13 to +36. I decided to target a longer region in the case of the morpholino since a 24-mer sequence has been reported to have better activity (about 70%) and to reach a correct GC content.

To create the modified U7 snRNA I started from the original vector U7 SmOPT, that contains the murine U7 gene and the U7 Sm binding site optimized to increase the accumulation into the nucleus (Gorman et al., 1998). I substituted the histone antisense sequence with the antisense sequence for the exonic splicing enhancer on 5A exon (Fig. 3.43A). This modified construct was then co-transfected with the 9A wt minigene in HeLa

cells and 24 hours after transfection, I extracted the RNA and performed RT-PCR and *NdeI* digestion to analyse the splicing pattern. As control I co-transfected the 9A wt minigene and the empty vector or one containing an unrelated sequence (U7x8Asn). As shown in figure 3.43B I observed that the U7 (U7ese5A) directed against the region containing the ESE was able to completely block 5A inclusion.

The morpholino was synthesised to target the same region of the modified U7ese5A. I transfected the cells with the 9A wt and three different concentrations of morpholino. After 24 hours I collected the cells and the mRNA processing of the minigene was analysed by RT-PCR and *NdeI* digestion. Using the morpholino at the concentration of 10 µM 5A inclusion was completely abolished (Fig. 3.43C).

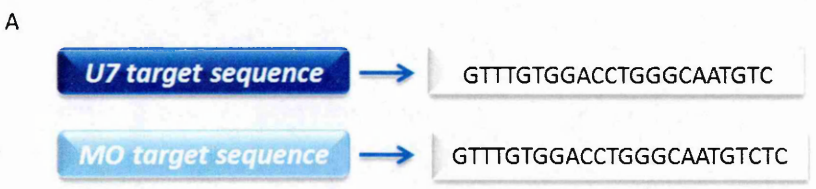

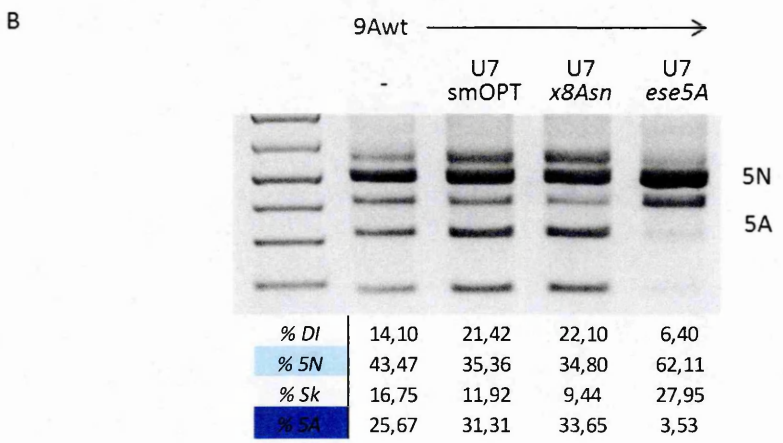

	-	U7 smOPT	U7 x8Asn	U7 ese5A
% DI	14,10	21,42	22,10	6,40
% 5N	43,47	35,36	34,80	62,11
% Sk	16,75	11,92	9,44	27,95
% 5A	25,67	31,31	33,65	3,53

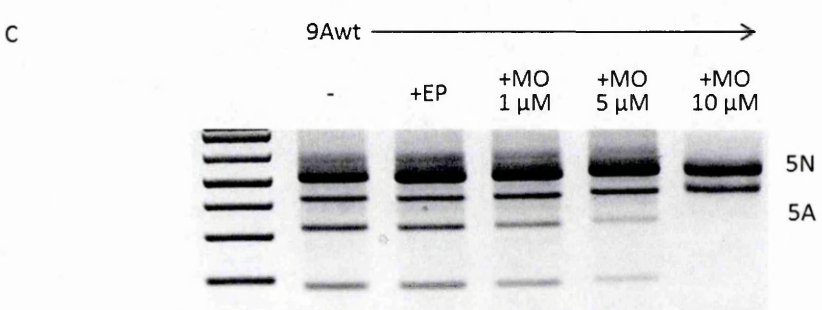

	-	+EP	+MO 1 µM	+MO 5 µM	+MO 10 µM
% DI	6,76	8,41	6,29	8,63	0,78
% 5N	47,94	53,55	55,88	55,14	61,59
% Sk	19,82	15,94	21,87	26,37	36,17
% 5A	25,48	22,09	15,96	9,86	1,46

Figure 3.43. (A) Target sequences of the U7ese5A and of the morpholino. (B) Agarose gel electrophoresis showing *NdeI* digested RT-PCR products after the co-transfection in HeLa cells of the 9A wt minigene with three different U7 vectors: the empty one, one containing one unrelated sequence and the third one with the antisense sequence. The upper band representing a cDNA product including exon 5N and 5A, the second band representing 5N inclusion, the third one the skipping and the two lower bands derived from the digestion of the PCR product containing only 5A exon. Each product was quantified as a percentage of the total of double inclusion (DI), 5N inclusion, double skipping (Sk) and 5A inclusion. (C) Agarose gel electrophoresis showing *NdeI* digested RT-PCR products after the transfection in HeLa cells of the 9A wt minigene followed by morpholino treatment, using three different concentrations. EP: endo porter, the reagent for the delivery system. The upper band representing a cDNA product including exon 5N and 5A, the second band representing 5N inclusion, the third one the skipping and the two lower bands derived from the digestion of the PCR product containing only 5A exon. Each product was quantified as a percentage of the total of double inclusion (DI), 5N inclusion, double skipping (Sk) and 5A inclusion.

In conclusion both approaches were able to block the binding of the SR proteins to the exonic splicing enhancer present in exon 5A; without the positive effect exerted by these *trans*-acting factors, 5A inclusion was strongly inhibited (Fig. 3.44).

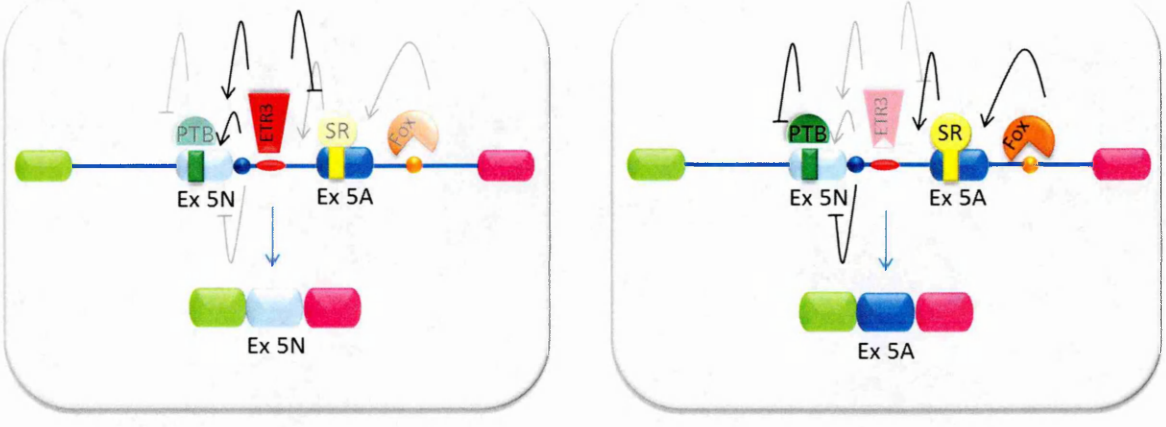

Figure 3.44. Building up the model for the mechanism of *SCN9A* exon 5 mutually exclusive splicing. The region of intron 5 comprised between +6 and +20 represents a composite regulatory element of splicing containing three regulatory elements: two of them favouring 5N inclusion (bound by ETR3 and TRA2β) and one exerting a negative effect (in blue). ETR3 promotes exon 5N inclusion and inhibits exon 5A inclusion by binding a broader TG-rich region within intron 5 (in red). Fox1 enhances exon 5A inclusion recognising four Fox binding sites downstream of exon 5A (in orange). The definition of exon 5A is also controlled by two SR proteins that bind the ESE in the adult exon (in yellow). PTB inhibits 5N inclusion through an exonic silencer (in green).

3.4. The exonic splicing enhancer in the adult exon is conserved in other voltage-gated sodium channels.

In higher vertebrates nine voltage-gated sodium channels have been described; the duplication of the exon encoding part of segment S3 and S4 in domain I is largely conserved among the family, in particular in six out of nine genes (Diss et al., 2004). Interestingly in all these channels the adult form contains an aspartic acid, negatively charged with respect to a positively or non-charged amino acid in the neonatal form (Tab. 3.2).

Channel	*Aminoacidic alignment*
SCN1A Na_v 1.1	ITFAFVTEFVNLGNFSALRTFRVLRALKTISVIPGLKTI ITFAYVTEFVDLGNVSALRTFRVLRALKTISVIPGLKTI **** ***** *** **********************
SCN2A Na_v 1.2	ITFAYVTEFVNLGNVSALRTFRVLRALKTISVIPGLKTI ITFAYVTEFVDLGNVSALRTFRVLRALKTISVIPGLKTI ********** **********************
SCN3A Na_v 1.3	IVMAYVTEFVSLGNVSALRTFRVLRALKTISVIPGLKTI IVMAYVTEFVDLGNVSALRTFRVLRALKTISVIPGLKTI ********** **********************
SCN5A Na_v 1.5	IIMAYVSENIKLGNLSALRTFRVLRALKTISVIPGLKTI IIMAYTTEFVDLGNVSALRTFRVLRALKTISVISGLKTI ***** * *** ****************** *****
SCN8A Na_v 1.6	IMMAYITEFVNLGNVSALRTFRVLRALKTISVIPGLKTI IMMAYVTEFVDLGNVSALRTFRVLRALKTISVIPGLKTI ***** **** **********************
SCN9A Na_v 1.7	IMMAYITEFVNLGNVSALRTFRVLRALKTISVIPGLKTI IMMAYVTEFVDLGNVSALRTFRVLRALKTISVIPGLKTI ***** **** **********************

Table 3.2. Aminoacidic alignment of the peptidic fragments encoded by the two mutually exclusive exons of all the six channels containing the exon duplication. The star marked the conservation of the amino acid.

As demonstrated in the previous section, the sequence encoding this residue is part of an exonic splicing enhancer that helps *SCN9A* exon 5A definition. Inspection of the alignment of the regions encoding the aspartic acid in the adult exon of all the VGSC genes

highlighted a high conservation in the nucleotidic sequences (Tab. 3.3), raising the possibility of the presence of a common ESE element important for the definition of the adult form in all these genes.

Channel	ESE sequence
SCN1A Na_v 1.1	GTTTGTGGACCTGGGCAATGTCTC **********
SCN2A Na_v 1.2	GTTTGTGGACCTGGGCAATGTCTC **********
SCN3A Na_v 1.3	GTTTGTGGACCTGGGCAATGTCTC **********
SCN5A Na_v 1.5	ATTTGTGGACCTGGGCAATGTCTC **********
SCN8A Na_v 1.6	GTTTGTGGACCTGGGCAATGTCTC **********
SCN9A Na_v 1.7	GTTTGTGGACCTGGGCAATGTCTC **********

Table 3.3. Alignment of the ESE region of all the six channels containing the exon duplication. The star marked the conservation of the residue.

Unlike *SCN9A* gene, in which the transcript containing exon 5A is expressed predominantly in dorsal root ganglia and in sympathetic ganglia neurons, the adult form of exon 5 (or 6) of other VGSCs are more broadly expressed. This fact allowed me to evaluate the presence of the ESE directly looking at the endogenous splicing pattern by using cell lines where channels are expressed.

After a screen of possible cell lines expressing the VGSCs of interest I chose two different type of cells to monitor directly the endogenous splicing pattern of three voltage-gated sodium channels: *SCN3A* and *SCN8A* transcripts were analysed in the neuroblastome cell line SH-SY5Y and *SCN5A* transcript in primary cardiomyocytes.

Both cell lines were treated with the higher dose of morpholino, following the same protocol and the same delivery system reagent used for HeLa cells. After RT-PCR and enzymatic digestion the splicing pattern of all the three channels reverted towards a major inclusion of the neonatal form upon morpholino treatment (Fig. 3.45). This data highlighted the conservation of the exonic splicing enhancer in the adult exon in at least three other members of the family.

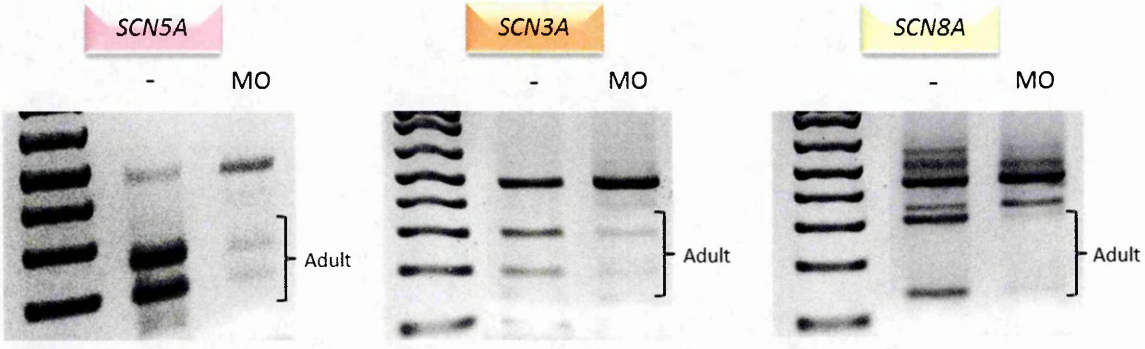

Figure 3.45. Agarose gel electrophoresis showing the changes in the endogenous splicing pattern due to morpholino treatment of three other voltage-gated sodium channels: *SCN5A* in adult cardiomyocytes (ex6-*ApaI* digested), *SCN3A* (ex5A-*AvaII*) and *SCN8A* (ex5A-*NdeI*) in SH-SY5Y cells. The upper band in all the lanes represents the neonatal form. The two lower bands derived from the digestion of the PCR product containing only adult exon.

3.4.1. Inhibition of *SCN5A* adult exon inclusion due to morpholino treatment *in vivo*.

The Na_v 1.5 channel, as discussed in the introduction, is the major channel expressed in heart and it plays an important role in the insurgence of the cardiac action potential both in cardiomyocytes and in Purkinje fibres (Tan, 2006). As described for the other channels, *SCN5A* contains an exon duplication (6a and 6) in the region encoding part of the voltage sensor of the channel and the two splice variants are characterized by different electrophysiological parameters with the neonatal form allowing an additional Na^+ entry which may be important for cardiac function, pH regulation, activity of enzymes and Ca^{2+} homeostasis (Onkal et al., 2008; Schroeter et al., 2010).

It was then of interest to use the ability of the morpholino to block the inclusion of the adult exon *in vivo*. In this way it would eventually be possible to study the difference of the two channels in a physiological setting. These experiments were performed in mice in collaboration with Serena Zacchigna from the Molecular Medicine Group taking advantage of the equipment present in the institute.

For the treatment of the mice a vivo-morpholino was used, that consists of the morpholino oligo, targeting the ESE, coupled with eight guanidinium groups on dendrimer scaffold. This modification increases the stability and also the delivery efficiency in a wide range of tissues. Two different delivery approaches were used: the first one through direct injection in the left ventricle of the heart and the second one through intrajugular injection, to achieve a systemic release.

The vivo-morpholino was first injected at 12 mg/Kg dose directly in the left ventricle of the heart of an adult mouse. The control mouse underwent the same operation with the injection of the same volume of PBS. After 48 hours the heart was collected and the RNA was extracted from three different parts (left ventricle, right ventricle and the rest of the heart) and then the splicing pattern was analysed through RT-PCR. The inhibition of exon 6 (the adult form)(Tab. 1.5) inclusion following the antisense treatment was clearly evident in the left ventricle of the treated mouse. However the compound did not spread properly to rest of the heart (Fig. 3.46A). From the literature, especially from the numerous studies on Duchenne muscular dystrophy, it is known that this organ is one of the most difficult to target (Moulton and Jiang, 2009).

Regarding the second approach the vivo-morpholino was injected in the jugular vein at 10 mg/Kg concentration for three days. The heart together with other organs were collected at day four. The control mouse was treated exactly as the treated mouse and injected with the same amount of PBS. After RNA extraction and RT-PCR I noticed that the

inhibitory effect on the adult form was still detectable in heart, although not as strong as obtained through direct injection. Interestingly *SCN5A* is expressed also in other organs and an effect on splicing due to the morpholino was also observed in muscle, spleen, diaphragm and kidney, but not for example in lung (Fig. 3.46B).

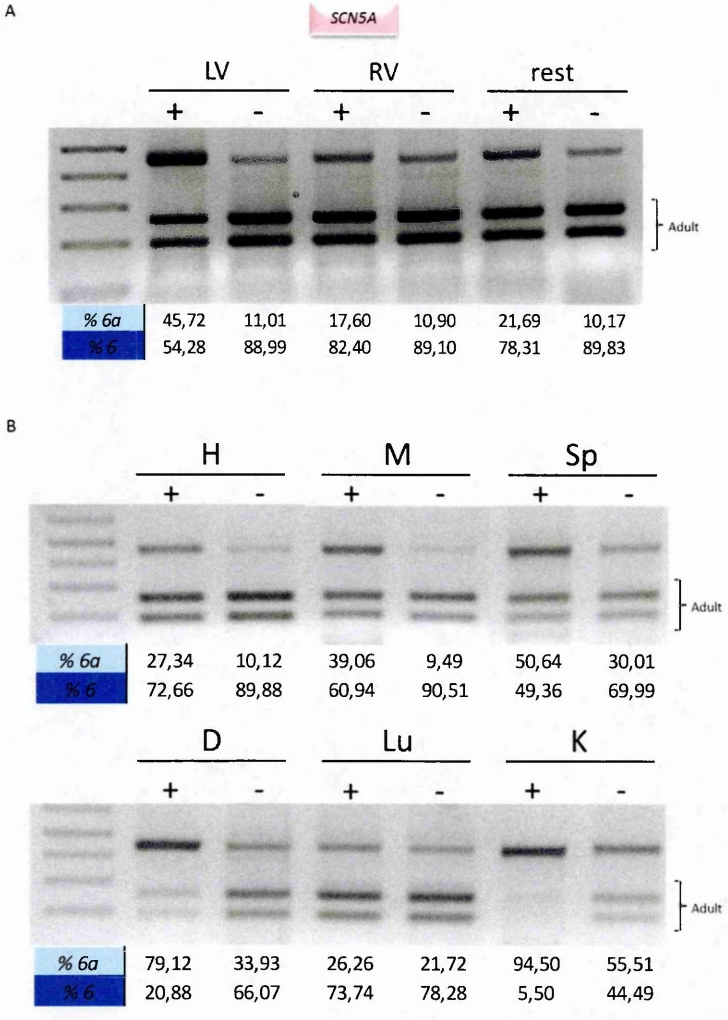

Figure 3.46. (A) Agarose gel electrophoresis showing the changes in *SCN5A* endogenous splicing pattern due to vivo-morpholino treatment (12 mg/Kg concentration) in mice through direct injection in heart (ex6-*ApaI* digested). The upper band in all the lanes represents the neonatal form. The two lower bands derived from the digestion of the PCR product containing only adult exon. LV: left ventricle, RV: right ventricle, rest: the rest of the heart. Each product was quantified as a percentage of the total of double inclusion (DI), 5N inclusion, double skipping (Sk) and 5A inclusion. (B) Agarose gel electrophoresis showing the changes in *SCN5A* endogenous splicing pattern due to vivo-morpholino treatment (3 x 10 mg/Kg) in mice through intrajugular injection (ex6-*ApaI* digested). The upper band in all the lanes represents the neonatal form. The two lower bands derived from the digestion of the PCR product containing only adult exon. H: heart, M: muscle, Sp: spleen, D: diaphragm, Lu: lung, K: kidney. Each product was quantified as a percentage of the total of double inclusion (DI), 5N inclusion, double skipping (Sk) and 5A inclusion.

Taking together these preliminary results obtained *in vivo*, further confirm the important role of the ESE present in *SCN5A* exon 6 for definition and inclusion of the adult form. From the literature it is known that the differences between the two isoforms result in differences in the electrophysiological parameters with the neonatal form allowing an additional Na^+ entry which may be important for pH regulation, activity of enzymes and Ca^{2+} homeostasis (Onkal et al., 2008; Schroeter et al., 2010). Other experiments were necessary to improve the efficiency of delivery of the antisense molecule in heart and to understand the impact of the splicing pattern change on heart activity.

3.5. Investigation of common splicing regulatory elements in *SCN9A, SCN3A* and *SCN8A* exon 5 mutually exclusive splicing.

The conservation of exon duplication together with the spatial and temporal control of their splicing in the family of voltage-gated sodium channels raised the intriguing possibility that some of the mapped elements, aside the splicing enhancer, may be common.

Alignment of intron 5 of *SCN9A*, *SCN3A* and *SCN8A* showed that the TG-rich regions displayed a high level of conservation (Tab. 3.4) I initially tested if this region may be important in other channels by performing the knockdown of ETR3 in SH-SY5Y cell. After RT-PCR and *NdeI* digestion in the case of *SCN3A* the silencing of ETR3 increased the level of the adult form in a significative way (Fig. 3.47A). The effect on *SCN8A* splicing outcome was not so strong, but there was a slight increase in 5A and in double inclusion (Fig. 3.47B). In both cases this *trans*-acting factor appeared to exert a positive effect on the neonatal inclusion, proposing it as a second common regulatory element.

```
SCN8A          CAGGTAAGATGGTCCGGGGTTGGTGTTAGGTGTTGGGATAGGGCCCTGACGTGACGTATT
SCN9A          CAGGTAAGA-----AGTAATTGGTGTGAAGCAT-----TAGGCCAC------------TC
SCN3A          CAGGTAAGA-----AGAAACTGGTGTAAGGTAG-----TAGGCCCC------------TT
               *********      *    ****** * *        **** * *            *

SCN8A          GTACTTTTTGTTTTGTTGTGGTTTTGTTTTTTCCTTTGGTGTTTGTGTTTGTGTCTGTGT
SCN9A          ATAACTCCAACTATTTGGGAGTTGTTCTTTGTT------CGTTTGTGTGTGTGTC-----
SCN3A          ATATCTCCAACTTTTCT----------------------TGTGTGTTATTGTGTT-----
                **  *     * *                          ** ***    *****

SCN8A          TTGTCACTTGTGTCTGTGTGTGACCTCCCTTACTACAGATATG
SCN9A          --GTCACTG-----TGTGTATAAACTCCCCTATTACAGATATG
SCN3A          -------------TGTGTGTGAACTCCCCTATTACAGATATG
                           ***** * * ***** ** **********
```

Table 3.4. Alignment of intron 5 of three VGSC genes: *SCN8A*, *SCN9A* and *SCN3A*. The star marked the conservation of the residue.

I then tested the effect of the double knockdown of PTB and nPTB and the changes in the splicing pattern differed in the two genes: *SCN3A* showed a decrease in 5N inclusion (Fig. 3.47A), whereas regarding *SCN8A* the double silencing induced an increase in skipping of both ME exons (Fig. 3.47B).

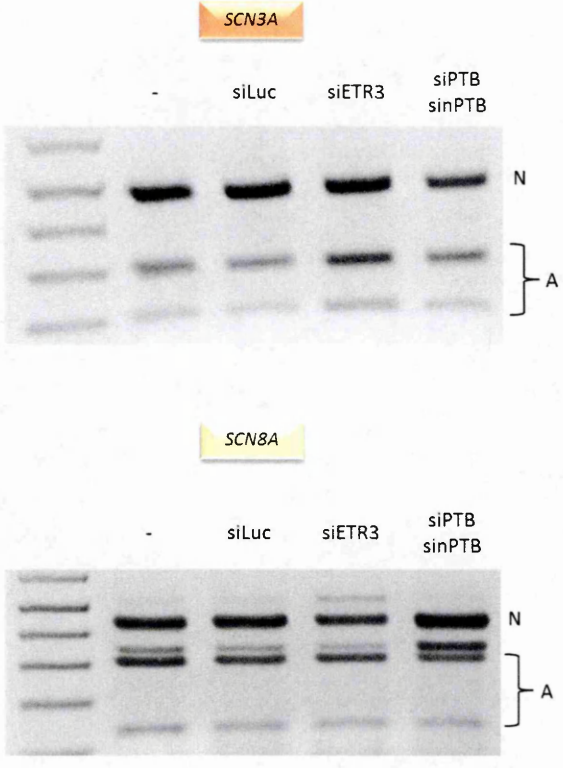

Figure 3.47. Agarose gel electrophoresis showing the changes in the endogenous splicing pattern due to ETR3 and PTB/nPTB knockdown of two voltage-gated sodium channels: *SCN3A* (ex5A-*AvaII*) and *SCN8A* (ex5A-*NdeI*) in SH-SY5Y cells. The upper band in all the lanes represents the neonatal form. The two lower bands derived from the digestion of the PCR product containing only adult exon.

Analysing the sequence of the two genes, I noticed that the putative exonic PTB binding site in exon 5N and the intronic one were absent in the *SCN8A* gene: this might expain the different impact of the knockdown of this *trans*-acting factor between the two genes. Other experiments are necessary to better investigate the role of these regulatory elements and also of the others as RbFox proteins. Regarding the role of the RbFox proteins it has already been published that they control the mutually exclusive splicing of *SCN8A* exon 5 confirmed by *in vivo* studies using Rbfox1$^{+/-}$Rbfox2$^{-/-}$ mice (Gehman et al., 2012).

3.6. Mutations mapped in *SCN9A* exon 5N causing Na_v 1.7-related pain disorders.

The Human Gene Mutation Database (http://www.hgmd.org) reported three mutations in exon 5N of *SCN9A* (631T>C S211P, 647T>C F216S and 684C>G I228M), two of them related to insurgence of inherited erythromelalgia (IEM) and one to idiopathic small fiber neuropathy. All affected residues, that are part of the voltage sensor of the channel, display a high rate of conservation among the members of the VGSCs family. Therefore the studies hypothesised that the mutations most probably introduce changes in amino acids essential for protein function (Drenth et al., 2005; Drenth and Waxman, 2007; Estacion et al., 2010; Dib-Hajj et al., 2013).

An alternative hypothesis considering their position is that these mutations may affect the inclusion of exon 5N normally expressed 50% in adults. Indeed analysing the position in exon 5N of the mutations S211P and F216S, I observed that they are exactly upstream and downstream of the exonic PTB site, the silencer element that inhibits 5N inclusion.

Taking advantage of the 9A wt construct I decided to check for a possible effect of the mutations on the splicing pattern, creating three minigenes each one carrying each one of these point mutations: 9AS211P, 9AF216S and 9AI228M (Fig. 3.48A).

I transfected the minigenes into HeLa cells and after RT-PCR and *NdeI* digestion I analysed the splicing outcome: interestingly, the mutations S211P and F216S markedly altered the pattern abolishing skipping and adult form, while the I228M did not introduce evident changes (Fig. 3.48B).

Since both S211P and F216S led to a strong increase in 5N inclusion, they could disrupt other silencer elements flanking the mapped one or interfere in some way with the negative effect exerted by this element.

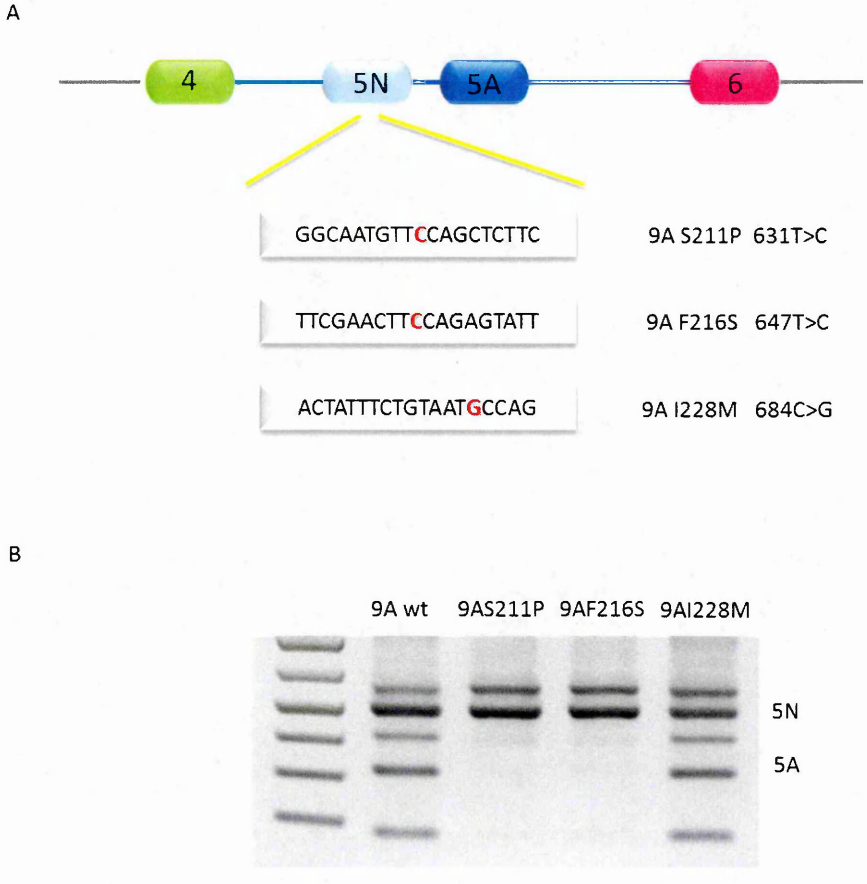

Figure 3.48. (A) Schematic representation of respectively 9A wt, 9AS211P, 9AF216S and 9AI228M minigenes (in red the mutated residues). (C) Agarose gel electrophoresis showing *NdeI* digested RT-PCR products after the transfection of the minigenes in HeLa cells with the upper band representing a cDNA product including exon 5N and 5A, the second band representing 5N inclusion, the third one the skipping and the two lower bands derived from the digestion of the PCR product containing only 5A exon.

To further investigate the effect of the mutations I performed a pull down analysis to identify the putative proteins involved in this alteration of splicing pattern. The RNA-interacting proteins collected were divided in two parts, one for coomassie staining and the other one for a screening of different antibodies through western blot. Comparison of wild type RNA with that one carrying the mutation (S211P) did not result in evident differences through the coomassie staining (Fig. 3.49B). However, western blot analysis showed that the mutant RNA was strongly bound by one SR protein recognized by 1H4 antibody, considering the size, probably SRSF2 (SC35). Moreover it also displayed a decrease in hnRNP A2/B1 binding (Fig. 3.49C).

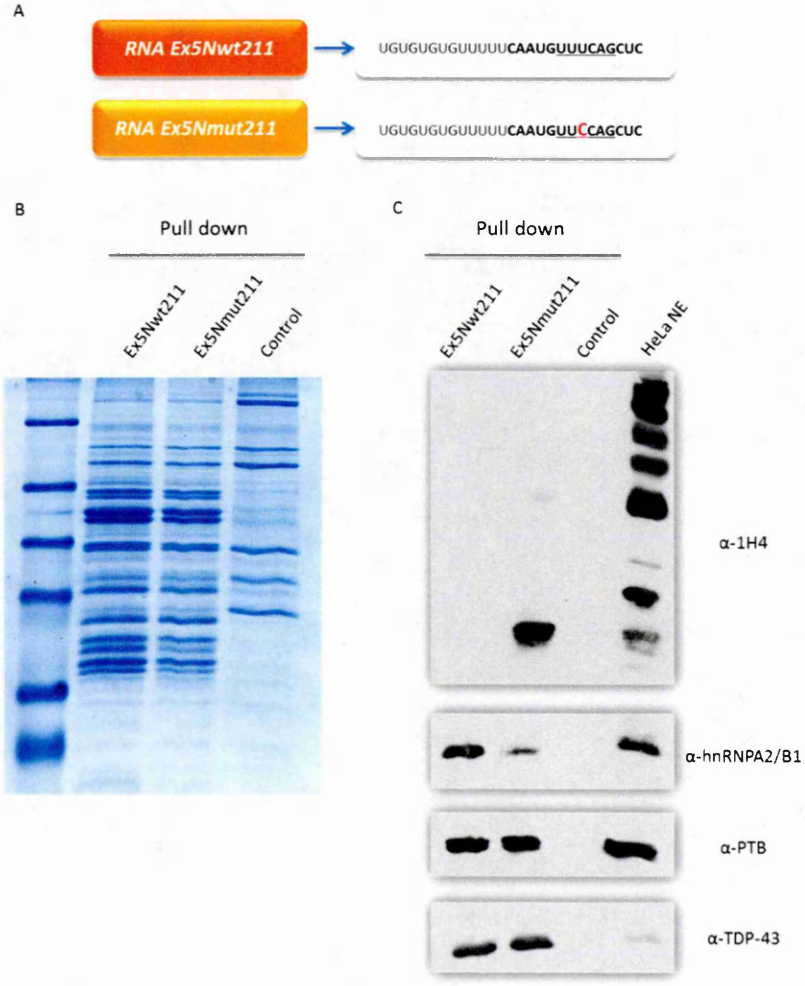

Figure 3.49. (A) Sequence of the synthetic Ex5Nwt211 and Ex5Nmut211 RNAs spanning the region of the mutation S211P (underlined), used for the pull down assay. Both the RNAs contain a tag for the recruitment of TDP-43 to normalize the pull down results. In red the mutated residue. (B) Coomassie stained gel and (C) western blot of the pull down assay performed using Ex5Nwt211 and Ex5Nmut211 RNAs incubated with HeLa NE. The control is derived from the beads without RNA, incubated with the nuclear extract.

The mutation F216S showed some differences at the coomassie stained gel when compared to the wild type RNA. Three bands both from the wild type and the mutant RNAs were analysed by mass-spectrometry by the Protein Networks group. The most interesting predictions obtained from this analysis were for band 1.mut that could be SRSF2 (SC35), and for band 2.mut and 3.mut that could represent SRSF3 (SRp20)(Fig. 3.50B). Through western blot I tried to confirm these results but using the 1H4 antibody neither the wild type nor the mutant RNA bound these SR proteins. However I detected both a decrease in PTB and hnRNPA2/B1 binding in the mutant RNA (Fig. 3.50C).

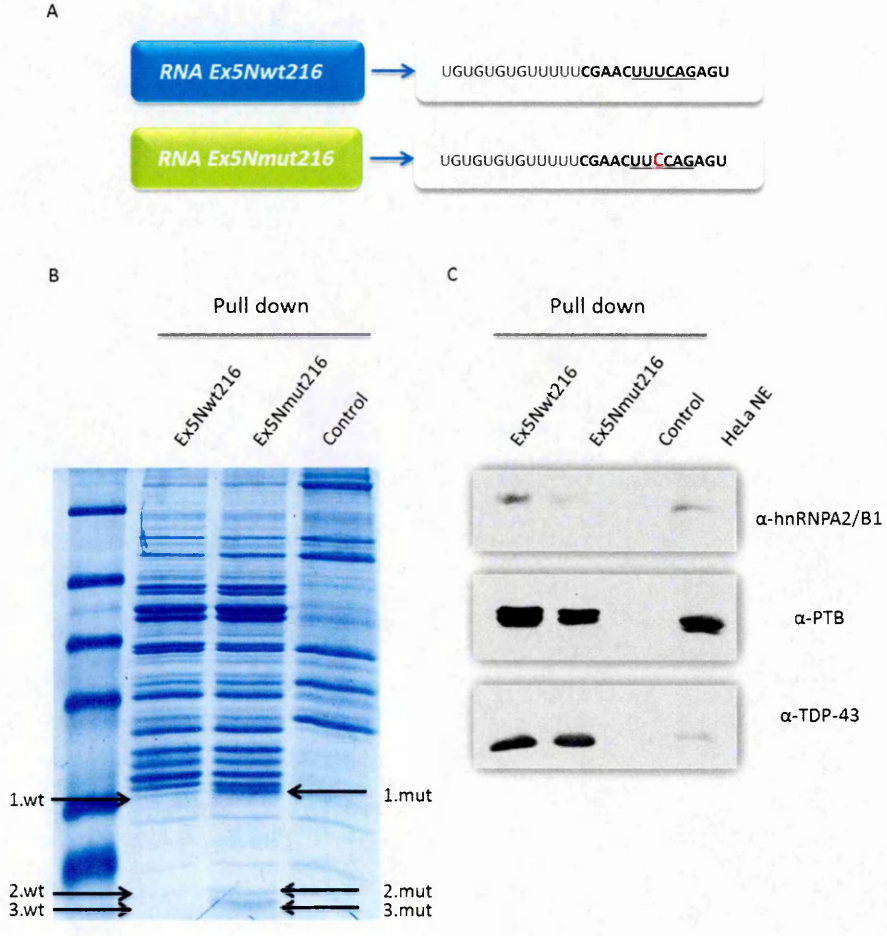

Figure 3.50. (A) Sequence of the synthetic Ex5Nwt216 and Ex5Nmut216 RNAs spanning the region of the mutation F216S (underlined), used for the pull down assay. Both the RNAs contain a tag for the recruitment of TDP-43 to normalize the pull down results. In red the mutated residue. (B) Coomassie stained gel and (C) western blot of the pull down assay performed using Ex5Nwt216 and Ex5Nmut216 RNAs incubated with HeLa NE. The control is derived from the beads without RNA, incubated with the nuclear extract. The bands of the coomassie gel analysed by mass-spectrometry are marked by arrows.

Since the two mutations are very close one to each other and also to the silencer previously mapped (section 3.3.2.1) I performed a pull down analysis using a longer RNA encompassing all the three elements (Fig. 3.51A). The RNA containing the mutation in position 211 was bound, also in this case, by an SR protein that did not recognize the wild type RNA. The other differences given by 1H4 antibody present in the picture were not reproducible. As shown before with the small RNAs, there was a decrease in hnRNP A2/B1 binding for both the mutations and also a slight decrease in the biding of PTB (Fig. 3.51B).

Summarizing, both mutations analysed led to a strong increase in 5N inclusion, most likely due to the fact that they mutate a region characterized by the presence of negative *cis*-acting elements. Regarding the mutation S211P it was also evident that it introduced an enhancer bound by an SR protein in exon 5N probably counteracting the other silencer elements.

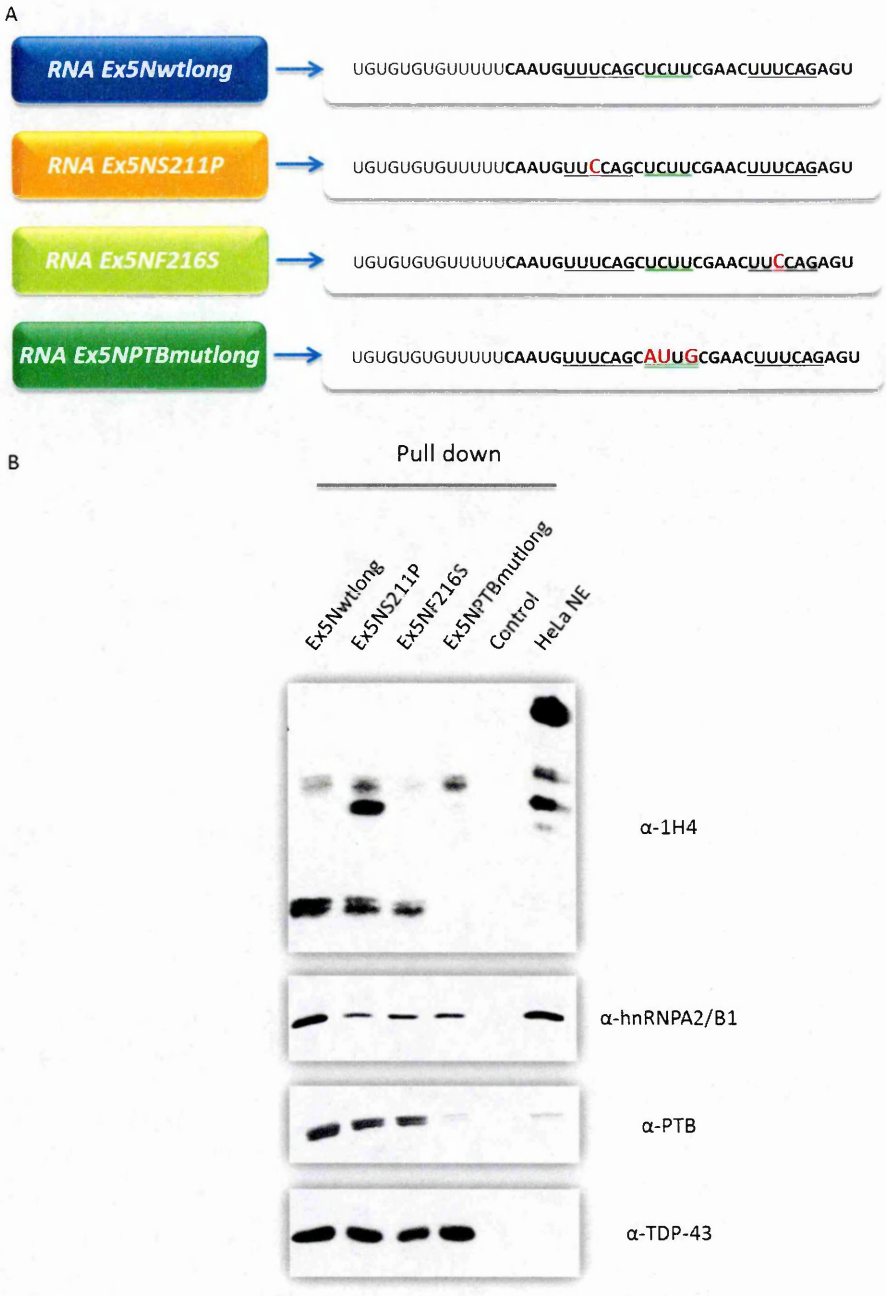

Figure 3.51. (A) Sequence of the synthetic Ex5Nwtlong, Ex5NS211P, Ex5NF216S and EX5NPTBmutlong RNAs spanning a larger exonic region of 5N, used for the pull down assay. The RNAs contain a tag for the recruitment of TDP-43 to normalize the pull down results. In red the mutated residue. The regions of disease-related mutations are underlined in black. The region of the PTB binding site is underlined in green. (B) Western blot of the pull down assay performed using Ex5Nwtlong, Ex5NS211P, Ex5NF216S and EX5NPTBmutlong RNAs incubated with HeLa NE. The control is derived from the beads without RNA, incubated with the nuclear extract.

4. Discussion

The excitability of mature neurons is dependent on the activity of voltage-gated ion channels. To increase neuronal plasticity, these channels are under the control of several forms of regulation, such as transcriptional control of gene expression, post-translational modifications and alternative splicing of transcripts. All these events can influence channel kinetics and properties (Schulz et al., 2008).

In particular, the voltage-gated sodium channels (VGSCs) are responsible for the depolarization and the insurgence of the action potential in many electrically active cells such as neurons, cardiac and skeletal muscle cells (Goldin, 1999). To date nine different channels have been described. These proteins, derived from gene duplication during the evolution (Widmark et al., 2011), are characterized by different tissue distribution and biophysical properties. Interestingly, the voltage-gated sodium channel family shares an aminoacidic homology of at least 75%, with some conserved regions also at the nucleotidic level (Yu and Catterall, 2003)(Tab. 3.3, Tab. 3.4). Six out of nine genes of the voltage-gated sodium channels family contain the duplication of an exon in the region of the domain I encoding part of the voltage sensor of the channel (exon 5 or 6 in the case of *SCN5A* gene) (Tab. 3.3). Alternative splicing is a largely exploited level of regulation in the nervous system, allowing the production of specialized proteins that increase the specific properties of the different neurons, producing different structurally and functionally protein isoforms from a single gene (Koopmann et al., 2006). In this specific case, mutually exclusive splicing of the duplicated exon 5, that encodes part of the voltage sensor of the channel, allows a fine-tuned regulation of the electrophysiological activity

(Chatelier et al., 2008; Onkal et al., 2008; Schroeter et al., 2010; Fletcher et al., 2011). Notably, it has been shown that some pathogenic mutations in genes encoding for these channels could have a different impact on the disease depending on the two backgrounds, the neonatal or adult splice variants (Jarecki et al., 2009; Choi et al., 2010). Moreover the two variants could also change the sensitivity to some compounds, such as antiepileptic drugs (Heinzen et al., 2007). The conservation of this feature across the VGSC genes and across species might have an adaptive significance, probably exerting an important role in the precise regulation of the gating characteristics of the channels (Copley, 2004). Despite the important role of this splicing event in modifying channel activity, to date it has been scarcely investigated.

The work performed in this thesis was focused on the characterization of the mechanism directing the mutually exclusive splicing of *SCN9A* exon 5. This gene is predominantly expressed in the dorsal root ganglia and encodes the Na_v 1.7 channel (Rush et al., 2007). Several studies have demonstrated that this channel is involved in the regulation of sensory neuron excitability, setting the gain of nociceptors, and mutations in the *SCN9A* gene are implicated in various human genetic pain disorders (Dib-Hajj et al., 2013; Waxman and Zamponi, 2014).

To date the literature describes four general mechanisms to control mutually exclusive patterns: spliceosomal incompatibility, steric hindrance, tissue-specific regulation by *trans*-acting factors and RNA secondary structure. In the case of *SCN9A* exon 5, spliceosomal incompatibility as the driving mechanism behind the mutually exclusive splicing was excluded, since the two *SCN9A* ME exons 5 are characterized by the presence of classical GU/AG signals, recognized by the major spliceosome. Furthermore I also excluded steric interference, that inhibits spliceosomal formation, by distancing the two exons (section 3.2). Moreover, the substitution of intron 5 with another intron of the

same size resulted in complete loss of mutually exclusivity feature, leading to a strong increase in double inclusion. This data underlined the relevant role of the intronic region among the two ME exons in the regulation of the mutually exclusive splicing event. Considering this and also that the swapping of the two ME exons dramatically changes the splicing pattern towards a total inclusion of exon 5A, the regulation of *SCN9A* exon 5 mutually exclusive splicing appeared to be principally directed by *trans*-acting factors. Indeed, subsequent work (section 3.3) showed that the mechanism involved in the mutually exclusive splicing of exons 5N and 5A of *SCN9A* gene is regulated by specific *cis*-acting elements and relative *trans*-acting factors, that bind to them. The precise selection of one isoform, highly regulated during development and also in a tissue-specific manner, is directed both by tissue-specific factors, that are characterized by a well-defined expression, and also by alteration of the abundance of constitutive splicing factors such as members of the SR or hnRNP proteins families.

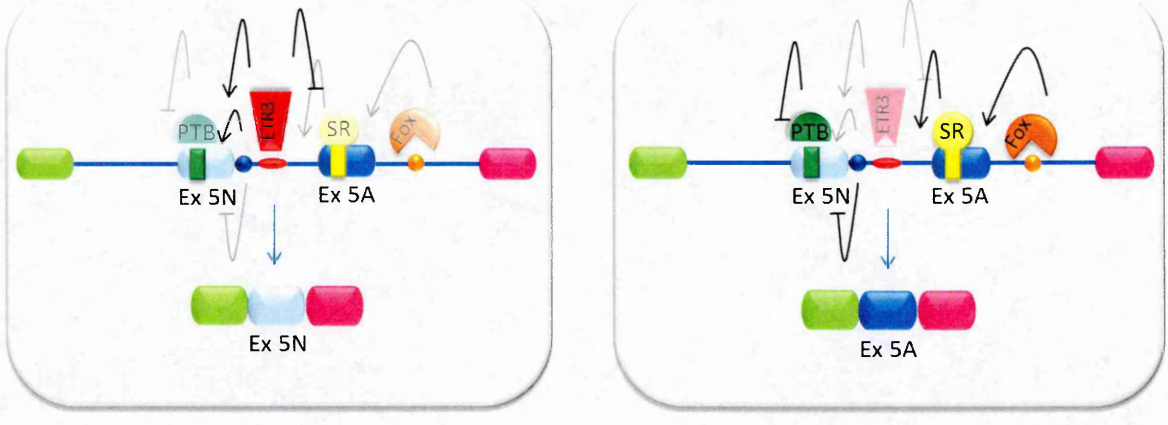

Fig. 4.1. Proposed model for the mechanism of *SCN9A* exon 5 mutually exclusive splicing. Left panel: exon 5N inclusion is directed by ETR3, that promotes exon 5N inclusion binding TG repeats surrounding the branch point (in red) and a region close to 5N 5' splice site (blue dot). At the same time, ETR3 inhibits exon 5A inclusion, masking the branch point, through the binding to the TG repeats (in red). Right panel: the definition of exon 5A is controlled by two SR proteins, that bind the ESE in the adult exon (in yellow) and by Fox1, that enhances 5A inclusion recognising Fox binding sites downstream of exon 5A (in orange). Neonatal inclusion is inhibited by an exonic silencer bound by PTB (in green) and a negative regulatory element in the region of intron 5 comprised between +6 and +20 (blue dot).

In the first stages of development the major form of *SCN9A* transcript contains the neonatal form of exon 5 (Raymond et al., 2004; Choi et al., 2010). My results have allowed a model to be postulated of how this occurs (Fig. 4.1, left panel). The experimental data in sections 3.3.1.1 and 3.3.1.2 indicate that the binding of ETR3 (CELF2) to a TG-rich region in intron 5 improves exon 5N definition. Furthermore, this protein recognizes an intronic region close to the 5' splice site of exon 5N and also in this case it enhances 5N inclusion (section 3.3.1.2.3.1). The expression of ETR3, is to a certain extent, in accordance with this hypothesis as the expression of this *trans*-acting factor is highly regulated during development in a tissue-specific manner. In many tissues, such as liver, thigh, stomach, lung and heart, ETR3 is down-regulated during development. In brain however, the amount of protein does not change (Ladd et al., 2005). Regarding the level of ETR3 in dorsal root ganglia, the tissue in which *SCN9A* is expressed, few data are available. However in mice high levels of its transcripts have been observed at embryonic stage, supporting the model previously described (Blech-Hermoni et al., 2013).

During development there is an increase in 5A inclusion in dorsal root ganglia, starting from a 35% at the neonatal stage, reaching approximately a 50% in adulthood (Raymond et al., 2004; Choi et al., 2010). In the first stages of development the adult exon is inhibited by ETR3 (section 3.3.1.1.3), that exerts a negative effect on 5A inclusion most likely is due to the masking of the branch point, directly antagonising U2AF65 or U2 snRNP recruitment (Dembowski and Grabowski, 2009). The higher percentage of inclusion of the adult exon during development is promoted by several auxiliary regulatory elements that enhance the usage of 3' and the 5' splice sites of exon 5A, which are weaker compared to the 5N ones, as shown in section 3.3.1.3 and 3.3.3. From my studies two principal *cis*-acting elements emerged that help exon 5A definition. The first

was a series of (T)GCATG motifs downstream of exon 5A that functioned through the binding of Fox1. Indeed, overexpression of the protein increased inclusion of exon 5A and this affect was abolished when the (T)GCATG motifs were mutated (section 3.3.1.3.1). RbFox proteins are known to be important players during neural development and differentiation in the regulation of many neuronal transcripts (Jin et al., 2003; Underwood et al., 2005). In mammals three main family members have been described Fox1, Fox2 and Fox3 (Kuroyanagi, 2009). To test the role of the four (T)GCATG motifs downstream of exon 5A, the wild type construct was co-transfected with Fox1 overexpression plasmid, since in HeLa cells this splicing factor is not detectable (Underwood et al., 2005). The choice of overexpressing Fox1 was determined taking into consideration that the role of this member in neuronal development has already largely been studied. Moreover in the knockout mice this protein was seen to increase the inclusion of the adult form of *SCN8A* exon 5, that encodes the Na_v 1.6 channel, widely expressed in the nervous system (Gehman et al., 2011; Fogel et al., 2012). This positive effect exerted by the binding of Fox1 to the downstream Fox binding sites agrees with the general mechanism described in literature (Kuroyanagi, 2009). Moreover, this family of proteins is characterized by tissue specificity and the expression of each isoform is highly regulated during development depending on the tissue in analysis (Kuroyanagi, 2009). For example Fox1 is known to be upregulated postnatally during adult heart development (Kalsotra et al., 2008). In the chick neural tube there is an increase in Fox3 level, that is necessary for the late spinal neuronal development (Kim et al., 2013). The Fox proteins are characterized by temporally different expression pattern also during cerebellar development, with an increased level of Fox1 in the later stages (Gehman et al., 2012). To date the levels of these *trans*-acting factors in DRGs have not yet been assessed, indeed further

experiments are needed to evaluate changes on the amount of these proteins during development in these particular neurons.

A second regulatory element responsible for the inclusion of the adult form was mapped in exon 5A, that favours the definition of its weak 3' splice site. This exonic splicing enhancer (ESE) is bound at least by two SR proteins: SRSF1 (ASF/SF2) and SRSF6 (SRp55) (section 3.3). It spans the region encoding the only two amino acids that differ between the neonatal and the adult isoforms. Despite this small difference, these changes affect the electrophysiological properties of the channel, in particular, the inclusion of the adult form increases neuron excitability (Chatelier et al., 2008).

Considering SR proteins can substitute each other (Zahler et al., 1992) , this element was further studied through two different antisense approaches U7smOPT vector, carrying the antisense target sequence, and a morpholino. Both the approaches completely abolished the inclusion of the adult form highlighting the important role of this *cis*-acting element in the definition of exon 5A (section 3.3.3.3).

The developmental switch towards a major inclusion of the adult form is controlled not only by the presence of positive elements acting on 5A, but also by negative elements inhibiting 5N inclusion. Indeed, I have identified an exonic splicing silencer (ESS) in exon 5N that is bound by PTB. Inserting point mutations on the binding site of this factor the splicing pattern shows drastic changes, characterized by almost total inclusion of exon 5N, confirming the presence of this inhibitory region. However, the result of PTB overexpression experiments suggests also a positive role on 5A inclusion probably due to the presence of other PTB binding sites located in the intronic regions surrounding the ME exons, but so far it has not been possible to understand in detail the role of this *trans*-acting factor in exerting a positive role on the adult form.

From the fine mapping of intron 5, another negative *cis*-acting element was identified close to the 5' splice site of exon 5N, from position +6 to position +20. The deletion of this intronic region led to an increase in 5N inclusion, suggesting the presence of another silencer element in this region. I identified *trans*-acting factors, such as hnRNP A1 and hnRNP H, that could bind this region. However, further experimentation, performed to study the effect of them through overexpression and silencing experiments, did not confirm these as the main players acting through this element.

The mutually exclusive splicing of exon 5 is a very well conserved event, being present in six out of nine genes of the family. This raised the possibility that the mechanism behind the mutually exclusive splicing described above for *SCN9A* exon 5 splicing could be common for the other voltage-gated sodium channels containing exon 5 (or 6 in *SCN5A* gene) duplication. Indeed, the ESE element in the adult exon, fundamental for its inclusion, is located in the region encoding the aspartic acid. This negatively charged residue in the adult exon is widely conserved in all the voltage-gated sodium channels containing the exon duplication, suggesting an essential role in the functionality of the channel (Diss et al., 2004). Furthermore, the nucleotidic alignment of this region showed a 100% conservation in all the VGSCs (Tab. 3.3). Taking into consideration the high level of conservation, the morpholino previously used to block this element in *SCN9A* was tested in *SCN3A*, *SCN8A* and *SCN5*A. The antisense treatment was able to inhibit the inclusion of the adult exon in all the three channels, confirming the functional importance of this ESE element. I also tested the possibility to modulate *in vivo* the splicing pattern of *SCN5A* transcript using mice. To do so, I used a vivo-morpholino that was either directly injected in heart or intra-jugularly administrated. The preliminary results obtained are promising since a decrease in the adult form is clearly detectable in heart, but also in other organs in

the case of the systemic delivery. Further experiments are required to better set up the antisense treatment in order to obtain a stronger inhibitory effect; at that point it will be also interesting to monitor the cardiac function after the splicing pattern alteration. Furthermore, to investigate the effect in the other channels expressed in the central nervous system, it will be necessary to study a different delivery approach to overcome the problem of the blood brain barrier.

The other elements that had a prominent role in the choice of exon included in the final transcript were the TG repeats functioning through ETR3, Fox1 binding to (T)GCATG motifs and PTB binding to TCTT site. Regarding the TG repetitions I observed that these were conserved, as shown for example in table 3.4 from *SCN3A* and *SCN8A* intron 5 alignment. The silencing of ETR3 resulted in a decrease in 5N inclusion with a consequent increase in 5A inclusion, highlighting this element and protein as another common element for mutually exclusive splicing of exon 5 in the voltage-gated sodium channels that contain this particular exon duplication. Analysing the intronic sequence downstream of the adult exon Fox binding sites have been found in the other family genes. To date I have not yet unravelled if Fox proteins play an active role in the definition of the adult exon in all the channels, but from the literature it is known that this protein family exerts an important role in promoting *SCN8A* 5A exon thanks to *in vivo* studies using Rbfox1$^{+/-}$ Rbfox2$^{-/-}$ mice (Gehman et al., 2012). The PTB binding sites are not so well conserved among the different family members so a more accurate study is necessary to assess the putative role of this regulatory element on the definition of the mutually exclusive splicing pattern.

The work performed in this thesis has revealed the existence of new splicing regulatory elements in the *SCN9A* gene. Over the last decades the presence of splicing elements has

being the study of many mutations, whose previous effect in disease pathology was often unknown or misdiagnosed. In fact, a mutation can affect the amino acid and result in disease, but this may also affect splicing. Indeed, possibly the most significant conceptual shift in recent years is that even translationally silent sequence variations should raise suspicion and be seriously considered as being responsible for the pathology observed in the patient. For this reason, I decided to analyse mutations identified in *SCN9A* exon 5N for their effect on splicing. To date three mutations have been reported in literature: c.631T>C (p.Ser211Pro) and c.647T>C (p.Phe216Ser), related to insurgence of inherited erythromelalgia (IEM), and c.684C>G (p.Ile228Met), generating idiopathic small-fibre neuropathy. These are gain of function mutations that produce an increase in neuron excitability. Patients suffer intermittent burning and redness in the extremities, such as feet and hands.

All the three mutations are located in the segment S4 of the domain I, that is characterized by the presence of positively charged amino acid at every third position (Catterall et al., 2005). S211P and F216S determine a change in the activation phase, making easier the opening of the mutant channel, due to the different feature of the amino acid substituted. The mutation I228M does not introduce a dramatic change, since both isoleucine and methionine are neutral, non polar amino acids. In theory, as reported in literature, this event might not introduce a functional effect, but I228M is known to produce hyperexcitability in neurons. The hypothesis is that the local structure of the helix could be affected by the diverse side chain of the amino acid, altering the slow inactivation of the channel (Drenth et al., 2005; Drenth and Waxman, 2007; Estacion et al., 2010; Dib-Hajj et al., 2013). However, in all three cases the 5N variant of the channel should decrease during development, diminishing the level of the affected protein, that, at least theoretically, should also decrease the severity of the disease.

To understand more about these disease-causing mutations I tested if they could have an impact on the splicing pattern of exon 5. The mutations at positions 211 and 216 drastically altered the splicing pattern, blocking 5A inclusion and leading to an high increase in 5N inclusion (section 3.6). These results can explain why the symptoms are not relieved in adulthood, since the developmental switch toward a major inclusion of the adult isoform seems to be abolished. The mutation I228M instead does not affect the splicing outcome, so other experiments are necessary to better understand what happens in patients.

It is of interest that the mutations at positions 211 and 216 are located exactly upstream and downstream of the exonic splicing silencer mapped in exon 5N bound by PTB, suggesting the possibility of a wider complex inhibitory region in the middle of the neonatal exon. Both the mutations impair the binding of hnRNP A2/B1 confirming the hypothesis of two other exonic silencer elements. Altogether these three negative elements form a wide region important for the inhibition of the neonatal exon. Furthermore the S211P introduces an exonic enhancer element recognized by an SR protein, probably SRSF2.

5. Conclusions

The duplication of exon 5 (or 6), encoding part of the voltage sensor of voltage gated sodium channels, is a feature conserved in six out of nine VGSCs. Although the two splice variants differentially affect the protein function, covering an important role in setting the exact activity of the channel, the mechanism behind the mutually exclusive splicing choice of only one of two ME exons has not yet been described in literature. In this project the mutually exclusive splicing of *SCN9A* exon 5 was characterised and a model has been proposed.

Although the two peptidic fragments derived from exon 5N and 5A differ by only two amino acids, the two splice variants differentially affect protein function. In particular, neurons containing the 5A variant of the channel are more excitable respect to neurons containing the 5N one. From studies performed on rat dorsal root ganglia, during development there is a change in the inclusion of the two exons, characterised by an increase in 5A inclusion, increasing neuron excitability. In particular at the neonatal stage 5A is included at 35%, reaching about a 50% of inclusion in adulthood (Raymond et al., 2004; Choi et al., 2010). Since the choice of one among the two ME exons has to be strictly regulated to ensure the proper functionality of the voltage-gated sodium channel, the precise selection of one isoform, highly regulated during development and also in a tissue-specific manner, is directed by a combinatorial control of different *trans*-acting factors. These are both tissue-specific factors, that are characterized by a well-defined expression, such as ETR3 and Fox1, and also by alteration of the abundance of constitutive splicing factors such as the SR proteins. During the early stage of

development the inclusion of the neonatal exon is controlled in particular by the positive effect exerted by ETR3 that at the same time represses exon 5A. To ensure the increase of the inclusion of the adult form later during development, the decrease of ETR3 levels may occur, eliminating its negative effect, combined with presence of several *trans*-acting factors, necessary to better define the weaker 3' and 5' splice sites of this exon: Fox1 enhancing 5' splice site usage and SRFS1 and SRSF6 helping the definition of the 3' splice site. Furthermore in the adult stage PTB exerts an inhibitory effect on 5N inclusion by binding an ESS, favouring even more high level of inclusion of the adult form.

From preliminary data, this mutually exclusive splicing mechanism regulated by tissue-specific and developmentally regulated *trans*-acting factors seems to be partially conserved also in other voltage gated sodium channels containing this exon duplication. Although further experiments are required to better understand the single role of each factor, for example the ESE region in the adult exon displays 100% conservation among all the six channels. This suggests an essential role of this element in adult definition, confirmed by my preliminary data in three channels (*SCN3A*, *SCN5A* and *SCN8A*). This splicing regulatory element appears to be an interesting target to revert the splicing pattern toward a neonatal background. For example in the case of SCN1A gene a decrease in 5N inclusion due to a polymorphism led to an higher risk of febrile seizures and also less sensitiveness to the antiepileptic drugs. In this case it could be interesting to study the effect of a reversion towards a major inclusion of the neonatal form (Heinzen et al., 2007; Thompson et al., 2011; Sterjev et al., 2012).

The last part of the project was focused on the characterization of the effect on the splicing outcome of three mutations occurring on *SCN9A* exon 5N, leading to gain of function of the channel. The mutations S211P and F216S affect the splicing pattern in a significant manner, strongly increasing 5N inclusion. The hypothesis, emerged from the

obtained data, is that the two mutations destroy two exonic splicing silencer bound by hnRNP A2/B1, flanking the other negative element present in exon 5N, the PTB binding site. Moreover the S211P, in addition to eliminate a silencer, introduces an exonic splicing enhancer bound by an SR protein, that might be SRSF2.

6. Materials and methods

6.1. Chemical reagents.

Chemical reagents were purchased from Sigma Chemical Co., Merek, Gibco BRL, Boehringer Mannheim, Carlo Erba and Serva.

6.2. Commonly used solutions.

- PBS: 137 mM NaCl, 2,7 mM KCl, 10 mM Na_2HPO_4, 1.8 mM KH_2PO_4, pH=7.4
- 10X TBE: 108 g/l TRIS, 55 g/l Boric Acid, 9.5 g/l EDTA
- 5X DNA sample buffer: 0.5 g/ml Sucrose, 0.24 g /ml Urea, 0.5 ml TBE 10X, 0.01 ml 1% bromophenol blue
- 5X SDS protein sample buffer: 250 mM Tris/HCl pH=6.8, 10% w/v SDS, 30% v/v Glycerol, 5% v/v β-mercaptoethanol, 0.002% v/v bromophenol blue
- 10X Transfer buffer: 30.3 g/l TRIS, 144 g/l Glycine
- 1X SDS-PAGE running buffer: 50mM TRIS, 0.38 Glycine, 0.1% w/v SDS

6.3. Synthetic oligonucleotides.

Synthetic DNA oligonucleotides were purchased from Sigma-Aldrich and Integrated DNA Technologies (IDT).

6.4. Bacterial culture.

The *E. coli* K12 strain DH5α was always used to perform transformation with the plasmid of interest and its amplification. Bacterial colonies were maintained at +4°C on agar plates

containing the proper antibiotic. When necessary, an overnight culture of bacteria was grown in Luria-Bertani medium (LB) made of 10 g/l Difco Bactotryptone, 5 g/l Oxoid yest extract, 10 g/l NaCl, pH=7.5. The appropriate antibiotic was added to LB medium to allow selected bacterial growth at a final concentration of 100 μg/ml.

6.5. Preparation of bacterial competent cells.

For bacterial competent cells preparation, *E. coli* strains were grown overnight at 37°C in 10 ml of LB. The day after, the pre-inoculum was transferred to 300 ml of fresh LB medium (kept at room temperature) and cells were grown at 37°C for about 4-5 hours until OD_{600} was 0.3-0.4.

Cell growth was then arrested by putting them on ice and then centrifuged at +4°C for 10 minutes at 1000 rpm dividing the 300 ml in 6 50 ml tubes. The pellet of each 50 ml tube was resuspended in 5 ml of cold TSS solution (10% w/v PEG, 5% v/v DMSO, 35mM $MgCl_2$, pH=6.5 in LB medium). Cells were aliquoted, rapidly frozen in liquid nitrogen and stored at -80°C. Competition was checked by transformation with 0.1 ng of pUC19 and it was considered satisfactory if more than 100 colonies grew.

6.6. Bacteria transformation.

Transformation of ligation was carried out using ½ of the reaction volume. Transformation of clones was performed using 20 ng of plasmid DNA. DNA was incubated with 60 μl of competent cells for 20 minutes on ice, then a heat shock at 42°C was performed for 1.5 minutes. After another 2 minutes of incubation on ice, 60 μl of LB were added and the bacteria allowed to recover for 20 minutes at 37°C. Cells were then spread on agar plates containing the appropriate antibiotic and the plates were incubated for about 12 hours at 37°C.

6.7. Small scale preparation of plasmid DNA from bacterial cultures.

Quick DNA extraction from bacteria was performed using the Wizard plus SV minipreps DNA purification system (Promega) according to the manufacturer's instructions. An inoculation of a single colony was grown in 4 ml of LB medium in the presence of the proper antibiotic, overnight at 37°C.

6.8. Large scale preparation of plasmid DNA from bacterial cultures.

After an overnight inoculation of a single colony in 50 ml LB medium at 37°C with the proper antibiotic, the JetStar purification kit (Genomed) was used for DNA extraction, according to manufacturer's instructions.

6.9. Quantification of nucleic acid concentration.

An optical density of 1.0 at 260 nm is usually considered equivalent to a concentration of 50 μg/ml for double stranded DNA and 40 μg/ml for single stranded DNA and RNA. The ratio of values measured at 260 nm and 280 nm indicates purity of the samples. A value of 1.8 for DNA and 2 for RNA is indicator of pureness.

6.10. Enzymatic DNA modifications.

6.10.1. Restriction enzymes.

Restriction enzymes were purchased from Promega or New England Biolabs, Inc., together with Klenow fragment of *E. coli* DNA polymerase I and T4 polynucleotide kinase. Taq polymerase and T4 DNA ligase were obtained from Roche Diagnostic. All enzymes were used according to the manufacturer's instructions.

6.10.2. Plasmidic DNA digestion.

DNA digestion was performed using the appropriate digestion buffer specifically created by the same company for each restriction enzyme. In general, analytical digestion was performed by digesting 100-500 ng of DNA in a final volume of 50 µl containing 5 units of the restriction enzyme of interest. A 2-3 hours incubation was performed at the optimal temperature indicated by the manufacturer. A preparative digestion was instead made using 3-5 µg of DNA in the previously mentioned condition, in a final reaction volume of 100 µl.

6.10.3. Large fragment of *E. Coli* polymerase I, T4 polynucleotide kinase and alkaline phosphatase, calf intestinal.

The large fragment of DNA polymerase I (Klenow) is a proteolytic product of *E. coli* DNA polymerase I. It is characterized by polymerization and 3'->5' exonuclease activities, but has lost 5'->3' exonuclease activity. This enzyme was used to generate compatible ends for blunt ligations thanks to its ability to digest specific residues added by Taq DNA polymerase at the 3' terminus. To perform Klenow reaction, 2.5U of enzyme were added to 30 µl of initial product, together with the appropriate buffer at the final concentration 1X and dNTPs 5mM. After 15 minutes incubation at 25°C, the reaction was blocked by adding EDTA to a final concentration of 10mM. Klenow heating inactivation was performed at 75°C for 15 minutes.

Phosphorylation of the 5'-hydroxyl terminus of polynucleotides was achieved by adding 10U of T4 polynucleotide kinase, ATP to a final concentration of 1mM and the proper quantity of kinase buffer. Following 30 minutes incubation at 37°C the samples were stored at -20°C for further use.

Alkaline Phosphatase, Calf Intestinal (CIP) catalyses in a non-specific manner the dephosphorylation of 5′ and 3′ ends of DNA and RNA phosphomonoesters. In cloning, dephosphorylation prevents religation of linearized plasmid DNA. The enzyme acts on 5′ protruding, 5′ recessed and blunt ends. The standard protocol used for the dephosphorylation of the 1 µg of vector (25 µl) consisted in adding 5X OPA (one for all) buffer, 4 µl of a dilution of the CIP 1:100 in final volume of 50 µl. Following 60 minutes incubation at 37°C, CIP heating inactivation was performed at 80°C for 15 minutes.

6.10.4. T4 DNA ligase.

T4 DNA ligase is the enzyme used to join double stranded DNA fragments having compatible sticky or blunt ends. To perform this reaction, 20 ng of digested vector were ligated with a 5-10 fold molar excess of digested insert in a total volume of 30 µl containing 1X ligase buffer and 1U of T4 DNA ligase. Reaction was carried out at room temperature for 4-12 hours.

6.11. Agarose gel electrophoresis of DNA.

Size fractionation of DNA samples was performed through electrophoresis in agarose gel having an agarose concentration ranging from 1% (large and medium size fragments) to 2% (small fragments) in TBE1X buffer. The gels containing ethidium bromide (0.5 µg/ml) were loaded with samples of interest in DNA loading buffer at a final concentration of 1X. Gels were electrophoresed at 80mA in 1X TBE running buffer. DNA was finally visualized by UV transillumination and the result recorded by digital photography.

6.12. Purification of DNA fragments from agarose gel.

After agarose gel electrophoresis, DNA bands were excised from the gel under UV light. DNA extraction was performed using the EuroGold gel extraction kit (Euroclone) according to the manufacturer's instructions.

6.13. Amplification of selected DNA fragments.

The Roche Diagnostic Taq DNA Polymerase protocol was exploited to perform the polymerase chain reaction (PCR). A final volume of 50 µl was used to obtain a mix of reaction constituted by 1X Taq buffer, dNTPs mix 5mM each, oligonucleotide primers 1 nM each, Taq DNA polymerase 2.5U. As template, 0.1 ng of plasmid or 100-500 ng of genomic DNA were used for amplification.

6.14. DNA sequencing.

Sequence analysis was performed by sending 2 µg of plasmid DNA preparation to Macrogen Inc. company. Own primers were sent at concentration of 5 pmol/µl in deionized water, 2 µl per each run.

6.15. Generation of minigenes.

In this thesis two different minigene backbones have been utilised to the analysis of the splicing regulation. The first one consists in an homologous minigene containing the whole region under investigation cloned into the commercial vector pcDNA3, that carries a CMV promoter and the appropriate stop signals of transcription. The second minigene used is a modified version of the hybrid construct containing exons from the α-globin and fibronectin, under the control of the α-globin promoter, called pTB. The intronic region

among the fibronectin exons contains a unique *NdeI* site in which an exon and its flanking regions can be inserted.

In this thesis the most largely used minigene, as starting point to introduce mutations, deletions or insertions, is the 9A wt minigene. To generate this construct the DNA comprising the entire region from SCN9A exon 4 and 6 was amplified from genomic DNA using oligonucleotides with two different restriction sites inserted in the extremities. The obtained DNA insert was digested with the *BamHI* and *XhoI* enzymes (New England Biolabs), gel extracted (section 6.12) and ligated with T4 DNA ligase (section 6.10) into the pcDNA3 plasmid using the *BamHI* and *XhoI* restriction sites.

Regarding the pTB vector, firstly it has been modified by substituting the fibronectin cassette containing the fibronectin exons and the intronic region with the unique *NdeI* site with a new cassette taking advantage of two *BstelI* restriction sites . The new cassette contains part of *SCN9A* exon 4 and *SCN9A* exon 6 within an hybrid intronic region composed of partial intronic region downstream and upstream respectively to exon 4 and 6; also in this case the intronic region is characterised by the presence of an unique *NdeI* site. In particular the pTB vector was digested with *BstelI* enzyme (New England Biolabs) and the CIP treatment was performed on both the two fragments obtained. Then the new cassette digested with the *BstelI* enzyme (New England Biolabs) was ligated with T4 DNA ligase into the digested and dephosphorylated vector (section 6.10). This new construct was called pTBmod4-6.

The DNA fragment containing exon 5A and part of its intronic regions was amplified and then cloned into the pTBmod4-6 using the unique *NdeI* restriction site. In the generation of the minigenes the orientation of the inserted fragment was checked through colony PCR using one of oligonucleotides used for the amplification of the insert and one universal primer that recognizes the vector: the amplification product could be detected

only in the case of correct orientation. The positive clones were then controlled through sequencing.

Minigene: **9A wt**

For9ABamHI	5' - CGGGATCCCGATTACACTTTTACTGGAATATATAC - 3'
Rev9AXhoI	5' - GGCGAGCTCGCCCTATTCTAAAGTCTTCTTCACTCTCA - 3'

Minigene: **pTBmod4-6**

For4PTB-*Bst*EII	5' - GCGGTGACCAAGAGGCTTCTGTGTAGGAGAATTC - 3'
Rev4PTB	5' - AGTGACACCCAGCAGGTAGCAGATGGAACTG - 3'
For6PTB	5' - ACCTGCTGGGTGTCACTATATGCTGTAATT - 3'
Rev6PTB-*Bst*EII	5' - GCGGTCACCATGAACAGCTGTAGTCCAATTAG - 3'

Minigene: **pTB5Awt**

For9ApTBA	5' - GGAATTCCATATGGAATATTTGGGAGTTGTTCTTTG - 3'
Rev9ApTBA	5' - TTCCATATGGAATTCCAGCCAAGTAGTCATCCTCAT - 3'

Universal primers

Up	5' - GTTTTCCCAGTCACGAC - 3'
Rp	5' - GGAAACAGCTATGACCATG - 3'
T7	5' - TAATACGACTCACTATAGGG - 3'
Sp6	5' - ATTTAGGTGACACTATAGAATA - 3'

6.15.1. QuickChange mutagenesis PCR method.

Mutagenesis, insertions and deletions were obtained using the QuickChange site-directed methodology. Oligonucleotide primers, each complementary to opposite strands of the area of interest and carrying the proper modifications, were designed and utilized during temperature cycling by *PfuTurbo* DNA polymerase (Promega). Incorporation of the oligonucleotide primers generated a mutated plasmid containing staggered nicks.

The mix of reaction was made in a final volume of 50 µl containing 1 µl of *PfuTurbo* DNA polymerase, *PfuTurbo* Buffer at 1X final concentration, 125 ng of each forward and reverse primers (detailed sequence of each primer used is described hereinafter), dNTP mix 5mM each and 50 ng of the desired template to be modified. The amplification conditions were the following:

- 95°C 30 seconds
- 95°C 30 seconds
- 55°C 1 minute
- 68°C 1 minute/Kb of vector used
- 72°C 7 minutes

Amplification reaction was repeated for 18 cycles.

Following QC PCR, the product was treated with 1 µl of *DpnI* enzyme, an endonuclease (target sequence: 5´-Gm6ATC-3´) specific for methylated and hemimethylated DNA used to digest the parental DNA template and to select for mutation-containing synthesized DNA. After at last one hour at 37°C of *DpnI* digestion, 10 µl of the nicked vector DNA containing the desired modifications were transformed into DH5α competent cells and the clones were then controlled through sequencing.

6.15.2. Complete list of constructs and primers used in section 3.

Minigenes section 3.2

QuickChange site directed mutagenesis PCR technique has been used for generating the 9AmutBP minigene using 9A wt construct as a template and these primers:

Minigene: **9AmutBP**

For 9Aint branch point	5' - GTTTGTGTGTGTCGTCTCTGTGTGTATAAACTCCCC - 3'
Rev 9Aint branch point	5' - GGGGAGTTTATACACACAGAGACGACACACACACAAAC - 3'

To create the minigene 9AintNF1, firstly an *Age I* site was introduced in intron 5 through QuickChange site directed mutagenesis PCR technique, using the 9A wt as a template, obtaining the 9A wt AgeI construct. Then the amplification of the fragment from one intron of NF1 gene has been done using oligonucleotides carrying *AgeI* restriction sites in order to direct clone the fragment into the 9A wt AgeI minigene (see section 6.15 for general protocol).

Minigene: **9A wt AgeI**

For AgeI	5' - GGTGTGAAGCATTAGACCGGTCATAACTCCAAC - 3'
Rev AgeI	5' - GTTGGAGTTATGACCGGTCTAATGCTTCACACC - 3'

Minigene: **9AintNF1**

For NF1 int31 AgeI	5' - TATATAACCGGTGAGATAGGGTTTTGCCATGTTGC - 3'
Rev NF1 int31 AgeI	5' - TATATAACCGGTTACAATTTATTATAAAATATC - 3'

Minigenes section 3.3.1

To create the minigene 9AExswap, firstly two *SacII* sites were introduced in the intronic regions upstream and downstream of the two ME exons through QuickChange site directed mutagenesis PCR technique, using the 9A wt as a template, obtaining the 9A wt SacUpDown construct. After *SacII* digestion the entire region containing the two ME among the two *SacII* sites was removed and substituted with a synthetic fragment (produced by GenScript) of the same region but with the two ME exons swapped, obtaining 9AExSwap minigene (see section 6.15 for general protocol).

Minigene: **9A wt SacUpDown**

For SacII up	5' - ACCTTGACTAAAGGCCGCGGTAAGTATCATAG - 3'
Rev SacII up	5' - CTATGATACTTACCGCGGCCTTTAGTCAAGGT - 3'
For SacII down	5' - GGGGTTAAACACCGCGGCTGACTTTGATC - 3'
Rev SacII down	5' - GATCAAAGTCAGCCGCGGTGTTTAACCCC - 3'

QuickChange site directed mutagenesis PCR technique has been used for generating the 9AExSw Del ex 5A and 9AExSw Del ex 5N minigenes using 9AExSwap construct as a template and these primers:

Minigene: **9AExSw Del ex 5A**

For del ex1	5' - TAATTCTGATTTAATTCTACAAGAAGTAATTGGTGTGAAG - 3'
Rev del ex1	5' - CTTCACACCAATTACTTCTTGTAGAATTAAATCAGAATTA - 3'

Minigene: **9AExSw Del ex 5N**

For del ex2	5' - GTGTATAAACTCCCCTATTACGAGAGTGGGGTTAAACACCAGG - 3'
Rev del ex2	5' - CCTGGTGTTTAACCCCACTCTCGTAATAGGGGAGTTTATACAC - 3'

Minigenes section 3.3.1.1

To create the minigene 9AintNF1TGup, I used the 9A wt AgeI construct previously described. Then the amplification of the fragment from one intron of NF1 gene has been done using oligonucleotides carrying the region containing the TG repeats to insert and *AgeI* restriction sites in order to direct clone the fragment into the 9A wt AgeI minigene (see section 6.15 for general protocol).

Minigene: **9AintNF1TGup**

For NF1 int31 TG AgeI	5' - TATATAACCGGTTTTGTGTGTGTCGTC ACTGTGTGTATGAGATAGGGTTTTGCCATG- 3'
Rev NF1 int31 AgeI	5' - TATATAACCGGTTACAATTTATTATAAAATATC - 3'

QuickChange site directed mutagenesis PCR technique has been used for generating the 9AintNF1TGup downmut and 9A TGmut minigenes using respectively 9AintNF1TGup and 9A wt construct as templates and these primers:

Minigene: **9AintNF1TGup downmut; 9A TGmut**

For 9A intronic tgmut	5' - GTTGTTCTTTGTTCGTTTATGTCTTCGACG TCACTCTTCGAATAAACTCCCCTATTACAG - 3'
Rev 9A intronic tgmut	5' - CTGTAATAGGGGAGTTTATTCGAAGAGTGA CGTCGAAGACATAAACGAACAAAGAACAAC - 3'

Minigene section 3.3.1.2

To create the minigene 9AintGlo 5'ss(+6), I used the 9A wt SacUpDown construct described previously. After *SacII* digestion the entire region containing the two ME among the two *SacII* sites was removed and substituted with a synthetic fragment (produced by GenScript) of the same region but with the intron 5 substituted by the α-globin intron (see section 6.15 for general protocol).

Minigenes section 3.3.1.2.1

QuickChange site directed mutagenesis PCR technique has been used for generating the 9AintGlo5'ss(+12), 9AintGlo5'ss(+20), 9AintGlo5'ss(+47) and 9AintGlo5'ss(+70) minigenes using respectively 9A wt, 9AintGlo5'ss(+12), 9AintGlo5'ss(+20), 9AintGlo5'ss(+47) constructs as a template and these primers:

Minigene: **9AintGlo5'ss(+12)**

For 5ssmut(+12) 9AintGlo	5' - CTATTTCTGTAATCCCAGGTAAGAAG TAATCCCCTGCTCCGACCCGGGCTCC - 3'
Rev 5ssmut(+12) 9AintGlo	5' - GGAGCCCGGGTCGGAGCAGGGGATT ACTTCTTACCTGGGATTACAGAAATAG - 3'

Minigene: **9AintGlo5'ss(+20)**

For 5ssmut 9AintGlo	5' - ATTTCTGTAATCCCAGGTAAGAAGTAATTG GTGTGACCGACCCGGGCTCCTCGCCCGCCC - 3'
Rev 5ssmut 9AintGlo	5' - GGGCGGGCGAGGAGCCCGGGTCGGTCACA CCAATTACTTCTTACCTGGGATTACAGAAAT - 3'

Minigene: **9AintGlo5'ss(+47)**

For 5ssmut(+47) 9AintGlo	5' - GTAAGAAGTAATTGGTGTGAAGCATTAGGCCAC TCATAACTCCAACTCCCACAGGCCACCCTCAACCG - 3'
Rev 5ssmut(+47) 9AintGlo	5' - CGGTTGAGGGTGGCCTGTGGGAGTTGGAGTTAT GAGTGGCCTAATGCTTCACACCAATTACTTCTTAC- 3'

Minigene: **9AintGlo5'ss(+72)**

For 5ssmut(+72) 9AintGlo	5' - GGCCACTCATAACTCCAACTATTTGGGAGTTGTT CTTTGTTCGTTGGCCCCGGACCCAAACCCCACCC - 3'
Rev 5ssmut(+72) 9AintGlo	5' - GGGTGGGGTTTGGGTCCGGGGCCAACGAACAAA GAACAACTCCCAAATAGTTGGAGTTATGAGTGGCC - 3'

QuickChange site directed mutagenesis PCR technique has been used for generating the 9A Del(+6/+20) minigene using 9A wt construct as a template and these primers:

Minigene: **9A Del(+6/+20)**

For 9A Del(+6/+20)	5' - CTATTTCTGTAATCCCAGGTAAG AAGCATTAGGCCACTCATAACTCC - 3'
Rev 9A Del(+6/20)	5' - GGAGTTATGAGTGGCCTAATGCT TCTTACCTGGGATTACAGAAATAG - 3'

Minigene section 3.3.1.2.2

QuickChange site directed mutagenesis PCR technique has been used for generating the 9A(TG)5'ssmut minigene using 9A wt construct as a template and these primers:

Minigene: **9A(TG)5'ssmut**

For TG mut at 5ss ex5N	5' - GTAATCCCAGGTAAGAAGTAATTA GTCTTAAGCATTAGGCCACTCATAAC - 3'
Rev TG mut at 5ss ex5N	5' - GTTATGAGTGGCCTAATGCTTAAG ACTAATTACTTCTTACCTGGGATTAC - 3'

Minigenes section 3.3.1.2.3

QuickChange site directed mutagenesis PCR technique has been used for generating the 9AintGlo5'ss(+6)3'ss(-15), 9AintGlo5'ss(+6)3'ss(-32), 9AintGlo5'ss(+6)3'ss(-43) and 9AintGlo5'ss(+6)3'ss(-70), 9AintGlo5'ss(+20)3'ss(-15), 9AintGlo5'ss(+20)3'ss(-32), 9AintGlo5'ss(+20)3'ss(-43) and 9AintGlo5'ss(+20)3'ss(-70) minigenes using respectively 9AintGlo5'ss(+6), 9AintGlo5'ss(+6)3'ss(-15), 9AintGlo5'ss(+6)3'ss(-32), 9AintGlo5'ss(+6)3'ss(-43), 9AintGlo5'ss(+20), 9AintGlo5'ss(+20)3'ss(-15), 9AintGlo5'ss(+20)3'ss(-32) and 9AintGlo5'ss(+20)3'ss(-43) constructs as a template and these primers:

Minigene: **9AintGlo5'ss(+6)3'ss(-15); 9AintGlo5'ss(+20)3'ss(-15)**

For 3ssmut 9AintGlo	5' - GGACCCAAACCCCACCCCTCACTCACTCC CCTATTACAGATATGTGACAGAGTTTGTGG - 3'
Rev 3ssmut 9AintGlo	5' - CCACAAACTCTGTCACATATCTGTAATAGG GGAGTGAGTGAGGGGTGGGGTTTGGGTCC - 3'

Minigene: **9AintGlo5'ss(+6)3'ss(-32); 9AintGlo5'ss(+20)3'ss(-32)**

For 3ssmut(-32) 9AintGlo	5' - CCGTCCTGGCCCCGGACCCACGTCACTGT GTGTATAAACTCCCCTATTACAGATATGTG - 3'
Rev 3ssmut(-32) 9AintGlo	5' - CACATATCTGTAATAGGGGAGTTTATACAC ACAGTGACGTGGGTCCGGGGCCAGGACGG - 3'

Minigene: **9AintGlo5'ss(+6)3'ss(-43); 9AintGlo5'ss(+20)3'ss(-43)**

For 3ssmut(-43) 9AintGlo	5' - GGCCACCCTCAACCGTCCTGGTGTGTGTGTGTCGT CACTGTGTGTATAAACTCCCCTATTACAGATATGTG - 3'
Rev 3ssmut(-43) 9AintGlo	5' - CACATATCTGTAATAGGGGAGTTTATACACACAGTG ACGACACACACACACCAGGACGGTTGAGGGTGGCC - 3'

Minigene: **9AintGlo5'ss(+6)3'ss(-70); 9AintGlo5'ss(+20)3'ss(-70)**

For 3ssmut(-70) 9AintGlo	5' - GGGCTCCTCGCCCGCCCGGACTATTTGGGAGT TGTTCTTTGTTCGTTTGTGTGTGTCGTCACTG- 3'
Rev 3ssmut(-70) 9AintGlo	5' - CAGTGACGACACACACACAAACGAACAAAGAAC AACTCCCAAATAGTCCGGGCGGGCGAGGAGCCC - 3'

QuickChange site directed mutagenesis PCR technique has been used for generating the 9A Del(-70/-43), 9A Del(-70/-54), 9A Del(-60/-48) and 9A Del(-55/-43) minigenes using 9A wt construct as a template and these primers:

Minigene: **9A Del(-70/-43)**

For 9A Del(-70/-43)	5' - CATTAGGCCACTCATAACTCCAAT GTGTGTGTGTCGTCACTGTGTGTAT - 3'
Rev 9A Del(-70/-43)	5' - ATACACACAGTGACGACACACACAC ATTGGAGTTATGAGTGGCCTAATG - 3'

Minigene: **9A Del(-70/-54)**

For 9A Del(-70/-54)	5' - GCATTAGGCCACTCATAACTCCA ACTTTGTTCGTTTGTGTGTGTCG- 3'
Rev 9A Del(-70/-54)	5' - CGACACACACACAAACGAACAAA GTTGGAGTTATGAGTGGCCTAATGC- 3'

Minigene: **9A Del(-60/-48)**

For 9A Del(-60/-48)	5' - CTCATAACTCCAACTATTTGGGA TCGTTTGTGTGTGTGTCGTCACTG - 3'
Rev 9A Del(-60/-48)	5' - CAGTGACGACACACACACAAACG ATCCCAAATAGTTGGAGTTATGAG - 3'

Minigene: **9A Del(-55/-43)**

For 9A Del(-55/-43)	5' - CATAACTCCAACTATTTGGGAGTT GTTGTGTGTGTGTCGTCACTGTGTG - 3'
Rev 9A Del(-55/-43)	5' - CACACAGTGACGACACACACACAA CAACTCCCAAATAGTTGGAGTTATG - 3'

Minigene section 3.3.1.2.3.1

QuickChange site directed mutagenesis PCR technique has been used for generating the 9AintNF1insertup minigene using 9AintNF1 construct as a template and these primers:

Minigene: **9AintNF1insertup**

For 9A Insert (-60)(-43) up spacer	5' - GGTGTGAAGCATTAGACCGGTGTTGTTCTT TGTTCGTTGAGATAGGGTTTTGCCATGTTG - 3'
Rev 9A Insert (-60)(-43) up spacer	5' - CAACATGGCAAAACCCTATCTCAACGAACA AAGAACAACACCGGTCTAATGCTTCACACC - 3'

Minigenes section 3.3.1.3

QuickChange site directed mutagenesis PCR technique has been used for generating the 9A ex5A 5'ss mut and 9A ex5N 5'ss mut minigenes using 9A wt construct as a template and these primers:

Minigene: **9A ex5A 5'ss mut**

For mod 5'ss 5A	5' - CAATTTCAGTCATTCCAGGTAAGAGTGGGGTTAAACACCAG - 3'
Rev mod 5'ss 5A	5' - CTGGTGTTTAACCCCACTCTTACCTGGAATGACTGAAATTG - 3'

Minigene: **9A ex5N 5'ss mut**

For mod 5'ss 5N	5' - CTGTAATCCCAGGTGAGAAGTAATTGGTG - 3'
Rev mod 5'ss 5N	5' - CACCAATTACTTCTCACCTGGGATTACAG - 3'

Minigenes section 3.3.1.3.1

QuickChange site directed mutagenesis PCR technique has been used for generating the all the mutants of the Fox binding sites using 9A wt construct as a template or one of the minigene obtained already carrying a mutation in some Fox binding sites to create different combinations, and these primers:

Minigene: **9A FBS1m; 9A FBS1.2m; 9A FBS2.3m; 9A FBS1.2.3m; 9A AllFBSd.m**

For 9DFM1	5' - TAATCAATTGCGTGGGTCTTTAGGATGAGGATGACTA - 3'
Rev 9DFM1	5' - CATCCTAAAGACCCACGCAATTGATTAAACTCAAAG- 3'
For 9DFM2	5' - GATCATAAATATCAGCGTGGGGATATTGCA - 3'
Rev 9DFM2	5' - TGCAATATCCCCACGCTGATATTTATGATC - 3'
For 9DM2.3	5' – TCATAAATATCAGCGTGGGGATATTG CGTGACATTGTTTTTTATTTTTTCTCAGC - 3'
Rev 9DM2.3	5' – TAAAAAACAATGTCACGCAATATCC CCACGCTGATATTTATGATCTCCTTTC - 3'
For IVFBS9A	5' - ATTGATTTGATATAATGCGTGACTTTCTAGGAAAGCTTGTG- 3'
Rev IVFBS9A	5' - GCTTTCCTAGAAAGTCACGCATTATATCAAATCAATGACCTTAAG- 3'

Minigenes section 3.3.2.1

QuickChange site directed mutagenesis PCR technique has been used for generating the 9APTB5Nmut1, 9APTB5Nmut2 and 9APTB5Nmut3 minigenes using 9A wt construct as a template and these primers:

Minigene: **9APTB5Nmut1**

For 9A PTBbs ex mut1 in 5N	5' - AACCTAGGCAATGTTTCAGCACTTCGAACTTTCAGAGTATTGA - 3'
Rev 9A PTBbs ex mut1 in 5N	5' - TCAATACTCTGAAAGTTCGAAGTGCTGAAACATTGCCTAGGTT - 3'

Minigene: **9APTB5Nmut2**

For 9A PTBbs ex mut2 in 5N	5' - AACCTAGGCAATGTTTCAGCTTTGCGAACTTTCAGAGTATTGA - 3'
Rev 9A PTBbs ex mut2 in 5N	5' - TCAATACTCTGAAAGTTCGCAAAGCTGAAACATTGCCTAGGTT - 3'

Minigene: **9APTB5Nmut3**

For 9A PTBbs ex mut3 in 5N	5' - AACCTAGGCAATGTTTCAGCATTGCGAACTTTCAGAGTATTGA - 3'
Rev 9A PTBbs ex mut3 in 5N	5' - TCAATACTCTGAAAGTTCGCAATGCTGAAACATTGCCTAGGTT - 3'

Minigenes section 3.3.2.2

To create the minigene 9APTBmut intdo5A, firstly two *SacII* sites were introduced in the intronic regions downstream of exon 5A through QuickChange site directed mutagenesis PCR technique, using the 9A wt as a template, obtaining the 9A wt SacDown construct. After *SacII* digestion the entire intronic region among the two *SacII* sites was removed and substituted with a synthetic fragment (produced by GenScript) of the same region but with six putative strong PTB binding sites mutated (from TCTT to TGTT), obtaining 9APTBmut intdo5A minigene (see section 6.15 for general protocol).

Minigene: **9A wt SacDown**

For SacII down	5' - GGGGTTAAACACCGCGGCTGACTTTGATC - 3'
Rev SacII down	5' - GATCAAAGTCAGCCGCGGTGTTTAACCCC - 3'
For SacII down2	5' - GTTCATTTTGACAACCGCGGTATTCTTTGAGAATATG - 3'
Rev SacII down2	5' - CATATTCTCAAAGAATACCGCGGTTGTCAAAATGAAC - 3'

QuickChange site directed mutagenesis PCR technique has been used for generating the 9APTBmut intdo5N intdo5A, 9APTBmut ex5N intdo5N, 9APTBmut ex5N intdo5A and 9AintGlo5'ss(+6)PTBmutex5N minigenes using respectively 9APTBmut intdo5A, 9APTB5Nmut3, 9APTBmut intdo5A and 9AintGlo5'ss(+6) constructs as a template and these primers:

Minigene: **9APTBmut intdo5N intdo5A**

For mod 5N int PTB bs	5' - TTTGGGAGTTGTTGTTTGTTCGTTTG - 3'
Rev mod 5N int PTB bs	5' - CAAACGAACAAACAACAACTCCCAAA - 3'

Minigene: **9APTBmut ex5N intdo5N**

For mod 5N int PTB bs	5' - TTTGGGAGTTGTTGTTTGTTCGTTTG - 3'
Rev mod 5N int PTB bs	5' - CAAACGAACAAACAACAACTCCCAAA - 3'

Minigene: **9APTBmut ex5N intdo5A**

For 9A PTBbs ex mut3 in 5N	5' - AACCTAGGCAATGTTTCAGCATTGCGAACTTTCAGAGTATTGA - 3'
Rev 9A PTBbs ex mut3 in 5N	5' - TCAATACTCTGAAAGTTCGCAATGCTGAAACATTGCCTAGGTT - 3'

Minigene: **9AintGlo(+6)PTBmutex5N**

For 9A PTBbs ex mut3 in 5N	5' - AACCTAGGCAATGTTTCAGCATTGCGAACTTTCAGAGTATTGA - 3'
Rev 9A PTBbs ex mut3 in 5N	5' - TCAATACTCTGAAAGTTCGCAATGCTGAAACATTGCCTAGGTT - 3'

Minigenes section 3.3.3

QuickChange site directed mutagenesis PCR technique has been used for generating the pTB5Amut3'ss minigene using pTB5Awt construct as a template and these primers:

Minigene: **pTB5Amut3'ss**

For Mut 3'ss 5A	5' - ACTCCCCTATTACAGGTATGTGACAGAGTTTGTGG - 3'
Rev Mut 3'ss 5A	5' - CCACAAACTCTGTCACATACCTGTAATAGGGGAGT - 3'

QuickChange site directed mutagenesis PCR technique has been used for generating the 9Amut4A minigene using 9A wt construct as a template and these primers:

Minigene: **9Amut4A**

For mut4A downTG	5' - TGTGTGTCGTCACTGTGTGTTTTTTCTCCCCTATTACAGATATG - 3'
Rev mut4A downTG	5' - CATATCTGTAATAGGGGAGAAAAAACACACAGTGACGACACACA - 3'

Minigenes section 3.3.3.1

QuickChange site directed mutagenesis PCR technique has been used for generating the pTB5AmutVD, pTB5AmutVD*NdeI*, pTB5AmutV and pTB5AmutD minigenes using pTB5Awt construct as a template and these primers:

Minigene: **pTB5AmutVD**

For mod VD 5A	5' - CTCCCCTATTACAGATATTTAACAGAGTTTGTGAACCTGGGC - 3'
Rev mod VD 5A	5' - GCCCAGGTTCACAAACTCTGTTAAATATCTGTAATAGGGGAG - 3'

Minigene: **pTB5AmutVD*NdeI***

For mod VD NdeI 5A	5' - CTCCCCTATTACAGATATGTAACAGAGTTTGTGAACCTGGGC - 3'
Rev mod VD NdeI 5A	5' - GCCCAGGTTCACAAACTCTGTTACATATCTGTAATAGGGGAG - 3'

Minigene: **pTB5AmutV**

For mod V NdeI5A	5' - CTCCCCTATTACAGATATGTAACAGAGTTTGTGGACCTGGGC - 3'
Rev mod V NdeI 5A	5' - GCCCAGGTCCACAAACTCTGTTACATATCTGTAATAGGGGAG - 3'

Minigene: **pTB5AmutD**

For mod D NdeI 5A	5' - CTCCCCTATTACAGATATGTGACAGAGTTTGTGAACCTGGGC - 3'
Rev mod D NdeI 5A	5' - GCCCAGGTTCACAAACTCTGTCACATATCTGTAATAGGGGAG - 3'

QuickChange site directed mutagenesis PCR technique has been used for generating the 9AmutVD*NdeI*, 9AmutV and 9AmutD minigenes using 9A wt construct as a template and these primers:

Minigene: **9AmutVD*NdeI***

For mod VD NdeI 5A	5' - CTCCCCTATTACAGATATGTAACAGAGTTTGTGAACCTGGGC - 3'
Rev mod VD NdeI 5A	5' - GCCCAGGTTCACAAACTCTGTTACATATCTGTAATAGGGGAG - 3'

Minigene: **9AmutV**

For mod V NdeI5A	5' - CTCCCCTATTACAGATATGTAACAGAGTTTGTGGACCTGGGC - 3'
Rev mod V NdeI 5A	5' - GCCCAGGTCCACAAACTCTGTTACATATCTGTAATAGGGGAG - 3'

Minigene: **9AmutD**

For mod D NdeI 5A	5' - CTCCCCTATTACAGATATGTGACAGAGTTTGTGAACCTGGGC - 3'
Rev mod D NdeI 5A	5' - GCCCAGGTTCACAAACTCTGTCACATATCTGTAATAGGGGAG - 3'

QuickChange site directed mutagenesis PCR technique has been used for generating the 9AintroESE5N and 9AintroESE5Nd.m. minigenes using 9A wt construct as a template and these primers:

Minigene: **9AintroESE5N**

For introESE 5N	5' - CTACAGGTATTTAACAGAATTTGTAGACCTAGGCAATGTT - 3'
Rev introESE 5N	5' - AACATTGCCTAGGTCTACAAATTCTGTTAAATACCTGTAG - 3'

Minigene: **9AintroESE5Nd.m.**

For introESE 5Ndoumut	5' - CTACAGGTATTTAACAGAATTTGTGGACCTAGGCAATGTT - 3'
Rev introESE 5Ndoumut	5' - AACATTGCCTAGGTCCACAAATTCTGTTAAATACCTGTAG - 3'

Minigenes section 3.6

QuickChange site directed mutagenesis PCR technique has been used for generating the 9AS211P, 9AF216S and 9AI228M minigenes using 9A wt construct as a template and these primers:

Minigene: **9AS211P**

For 9A mut S211P	5' - AAACCTAGGCAATGTTCCAGCTCTTCGAACTTTCAGAGTATTGA - 3'
Rev 9A mut S211P	5' - TCAATACTCTGAAAGTTCGAAGAGCTGGAACATTGCCTAGGTTT - 3'

Minigene: **9AF216S**

For 9A mut F216S	5' - TTCAGCTCTTCGAACTTCCAGAGTATTGAGAGCT - 3'
Rev 9A mut F216S	5' - AGCTCTCAATACTCTGGAAGTTCGAAGAGCTGAA - 3'

Minigene: **9AI228M**

For I228M 5N	5' - TATTGAGAGCTTTGAAAACTATTTCTGT AATGCCAGGTAAGAAGTAATTGGTGTG - 3'
Rev I228M 5N	5' - GAGTGGCCTAATGCTTCACACCAAT TACTTCTTACCTGGCATTACAGAAATA - 3'

6.16. Cell culture.

The cell lines used for the experiments were:

- HeLa cells, an immortal cell line derived from cervical cancer cells
- Hek293, transformed human embryonic kidney cells
- SH-SY5Y, a neuroblastome cell line
- primary rat dorsal root ganglia.

6.17. Maintenance and analysis of cells in culture.

Different cell lines were used during the entire project. HeLa, Hek293, SH-SY5Y and F11 cell lines used were cultured in Dulbecco's Mem with Glutamax I (Gibco) (Dulbecco's modified Eagle's medium with glutamine, sodium pyruvate, pyridoxine and 4.5 g/l glucose), supplemented with 10% foetal bovine serum (FBS) (Euroclone) and antibiotic/antimycotic (Sigma) according to the manufacturer's instructions.

For cell seeding, dishes containing a confluent monolayer of cells were washed with PBS solution, treated with 1-2 ml of PBS/EDTA/trypsin solution (PBS containing 0.04% w/v EDTA and 0.1% w/v trypsin) at 37°C for 30 seconds or until cells were dislodged. Then

cells were collected and trypsin was inactivated by adding DMEM in a volume corresponding to 3 times of trypsin volume used. Cells were pelleted by centrifugation for 5 minutes at 1000 rpm at room temperature and then cells were resuspended in 10 ml of DMEM and 1 ml was used to seed cells in a new dish together with 9 ml of medium. A gentle mixture was done before incubation.

6.18. Rat dorsal root ganglia preparation.

Preparation of matrigel coated coverslips

The coverslips were incubated in 1M hydrochloric acid for a minimum of 4 hours to overnight 50-60°C and then were rinsed properly in sterile water. The coverslips were rinsed in 70% ethanol transferred to dishes and let dry. Poly-D-Lysine (PDL, Sigma) stock 50 µL (stock 2 mg/mL) was diluted into 20-40 mL sterile water (final 5-10 µL/mL) and 0.5 ml was added per coverslip. Then after three washes with sterile water the dishes were dried under the hood. 0.5 ml of the diluted matrigel (BD biosciences) was added per coverslip and after incubation at 37°C for 2-3 hours and one wash with water, the dishes were dried before adding the DRGs.

DRGs dissection from E15/E16 pregnant SD rat

Four petri dishes with MEM and a 15 ml Falcon tube with 13 ml MEM were prepared and kept on ice as much as possible when not under the dissecting microscope. After the removal of the embryos from the adult rat, they were decapitated and the organs and tail were removed. After cutting through the vertebrae the spinal cord intact was taken out by pulling from the rostral (neck) end and transferred to a fresh dish with MEM. The ganglia were then plucked off and collected into a 15 ml tube with fresh MEM.

Dissociating DRG cultures

The papain digestion mix was prepared as follow: 1 ml MEM, 40 µl papain (Worthington), 25 µl L-cysteine solution (final 0.24 mg/ml, Sigma) and 25 µl DNaseI type IV (final 40 µg/ml, Sigma). In the meanwhile DRGs were centrifuged at 1000 rpm, 5 minutes and then the excess media were removed such that total volume was less than 2 ml. Papain solution was filtered through 0.22 µM syringe onto the 15 ml tube containing DRGs and, after an incubation of 50-70 minutes at 37°C in incubator, the media (DMEM (4.5 g/l glucose DMEM + 1% Pen/Strep+ 10% FBS) was added to tube to quench enzyme action. After a centrifugation at 1000 rpm for 5 minutes, medium was aspirated and the DRGs were resuspended and triturated with 1ml pipette tip or with 21 gauge needle to help break apart cells, that finally were counted and ready to seed.

Next morning- Flood wells & Culture for 21 days

The cells were kept in culture in DMEM + 10% FBS +1% Pen/Strep + NGF (Serotec) and the media was changed every 2-3 days and alternated with the addition of FdU (5-Fluoro-2'-deoxyuridine, Sigma) for a total of 3 FdU pulses.

6.19. Transfection and co-transfection.

Liposome-mediated transfections of 2.5 x 10^5 HeLa cells were performed using Effectene reagent (Qiagen). 0.5 µg of construct DNA was mixed with 4 µl of Enhancer for each transfection and the mixture was incubated at room temperature for 5 minutes to allow the condensation of the DNA. Then 5 µl of Effectene were added to the mixture and an incubation of 10 minutes has been performed. After the addition of 500 µl of complete culture medium the mixture was added to the cells in 1.5 ml of the same medium and

incubated at 37°C. After 12 hours later the cells were harvested. In co-transfection experiments, cells were transfected with 0.5 μg of the minigene of interest and 0.5 μg or 1 μg of the overexpression plasmids. Each transfection experiment has been repeated five times.

6.20. RNA extraction.

To perform RNA extraction, cultured cells were washed with PBS once and then collected with Trizol reagent purchased from Invitrogen Inc.. RNA extraction was performed by adding chloroform to each sample and after 5 minutes incubation at room temperature, samples were centrifuged for 15 minutes at 12000 rpm at +4°C. The upper phase, containing RNA was transferred in a new tube and RNA was precipitated by adding an equal volume of isopropanol. After 10 minutes incubation at room temperature, a 10 minutes centrifugation at 12000 rpm at +4°C was done. RNA pellet was therefore washed with 70% ethanol and then resuspended in ddH_2O.

6.21. mRNA analysis by RT-PCR.

6.21.1. cDNA synthesis.

For cDNA synthesis, 1 μg of total extracted RNA was mixed with random primers (Pharmacia) in a 20 μl final volume. RNA denaturation was carried out at 94°C for 5 minutes and therefore 1 hour incubation at 37°C was performed by adding to the reaction mix 1X first strand buffer (Invitrogen), 10mM DTT, 5mM dNTPs each and the Moloney murine leukemia virus reverse transcriptase 100U (Invitrogen). For PCR analysis 1 μl of cDNA was used.

6.21.2. cDNA analysis.

PCR analysis of cDNA was carried out for 35 cycles (95°C 5 minutes, 95°C 30 seconds, 56°C 1 minute, 72°C 1 minute, 72°C 7 minutes) in 50 µl of final volume using specific oligonucleotides described below case by case.

Oligonucleotides used for minigenes in pcDNA3 vector

T7	5' - TAATACGACTCACTATAGGG - 3'
Rev9AXhoI	5' - GGCGAGCTCGCCCTATTCTAAAGTCTTCTTCACTCTCA - 3'

Oligonucleotides used for minigene in pTB vector

Alfa2,3	5' - CAACTTCAACTCCTAAGCCACTGC - 3'
Rev9ApTBA	5' - TTCCATATGGAATTCCAGCCAAGTAGTCATCCTCAT - 3'

Oligonucleotides used for endogenous human *SCN3A* transcript

ForSCN3A	5' - CAACTTCAACTCCTAAGCCACTGC - 3'
RevSCN3A	5' - TTCCATATGGAATTCCAGCCAAGTAGTCATCCTCAT - 3'

Oligonucleotides used for endogenous rat/mouse *SCN5A* transcript

ForSCN5A	5' - CAACTTCAACTCCTAAGCCACTGC - 3'
RevSCN5A	5' - TTCCATATGGAATTCCAGCCAAGTAGTCATCCTCAT - 3'

Oligonucleotides used for endogenous human *SCN8A* transcript

ForSCN8A	5' - CAACTTCAACTCCTAAGCCACTGC - 3'
RevSCN8A	5' - TTCCATATGGAATTCCAGCCAAGTAGTCATCCTCAT - 3'

Oligonucleotides used for endogenous rat/mouse *SCN9A* transcript

ForSCN9A	5' - CAACTTCAACTCCTAAGCCACTGC - 3'
RevSCN9A	5' - TTTTCAATTCTTCTTCACTCTCA - 3'

The PCR products were digested 4 hours with *NdeI* and then separated by electrophoresis in 2% agarose gels in the presence of ethidium bromide. The quantification of band intensities was performed using the ImageJ64 software. Each product was quantified as a percentage of the total of double inclusion, 5N inclusion, double skipping and 5A inclusion. Alternatively, another approach could be used to quantify the splicing pattern, that consists in performing a radioactive PCR. The digested products should be analyzed on a 5% native polyacrylamide gel, visualized by autoradiography and then quantified via phosphorimager.

6.22. Small interfering RNA (siRNA) transfections.

The siRNA sequences used for depletion are:

Human hnRNPA1	5' - CAGCUGAGGAAGCUCUUCA - 3' (Sigma)
Human hnRNPH	5' - GGAAAUAGCUGAAAAGGCU - 3' (Sigma)
Human PTB P1	5' - AACUUCCAUCAUUCCAGAGAA - 3' (Sigma)
Human nPTB N1	5' - GAGAGGAUCUGACGAACUA - 3' (Sigma)
Human TDP-43	5' - GCAAAGCCAAGAUGAGCCU - 3' (Sigma)
Human/Mouse ETR3	5' - UCGGCAUGAAACGCUUGAA - 3' (Sigma)
Luciferase	5' - GCCAUUCUAUCCUCUAGAGGAUG - 3' (Darmacon)

<u>In HeLa cells:</u>

siRNA transfections were performed in cells using Oligofectamine Reagent (Invitrogen) according to the manufactures instructions. Briefly, 40-50% confluent 35 mm well plates were prepared. 3 µl of 40 µM siRNA were mixed with 175 µl of Opti-MEM medium and, separately, 5 µl Oligofectamine with 15 µl of Opti-MEM medium.

The samples were incubated for 7 min at room temperature. Then the Oligofectamine mix was added to precomplexed siRNA mix and incubated for 20 min at room temperature. Finally, the mix was dropped onto the cells maintained in 800µl of Opti-MEM without antibiotics and FBS. After 24h, a second siRNA transfection was performed as described above, followed by the transfection with the different minigenes.

The following day, cells were harvested for RNA extractions, RT-PCR analyses and Western blots. Particularly, western blot was performed in order to check the depletion of each protein.

In SH-SY5Y cells:

siRNA transfections were performed in cells using HiPerFect Reagent (Qiagen) according to the manufactures instructions. In the first day of silencing, 4 µl of 40 µM siRNA were mixed with 94 µl of Opti-MEM medium. After 5 min at room temperature, 6 µl HiPerFect were added and incubated for 10 min at room temperature. In the meanwhile about 500,000 cells were seeded in complete DMEM. Passed the 10 min of incubation, the mix was added drop by drop onto the cells. After the second day of rest, the third day the cells were washed once with PBS solution and then they were incubated with 500 µl of PBS/EDTA/trypsin solution (PBS containing 0.04% w/v EDTA and 0.1% w/v trypsin) at 37°C for 3 min or until cells were dislodged. In the meanwhile 4 µl of 40 µM siRNA were mixed with 94 µl of Opti-MEM medium and after 5 min at room temperature, 6 µl HiPerFect were added and incubated for 10 min at room temperature.Then cells were collected and trypsin was inactivated by adding DMEM in a volume corresponding to 3 times of trypsin volume used. Cells were pelleted by centrifugation for 5 minutes at 1000 rpm at room temperature and then cells were resuspended in 2 ml of DMEM and they were seeded. Finally the mix was added drop by drop onto the cells.

The following day, cells were harvested for RNA extractions, RT-PCR analyses and Western blots. Particularly, western blot was performed in order to check the depletion of each protein.

6.23. Antisense derivative of U7 small nuclear RNA.

The U7 snRNP is a ribonucleoprotein complex specialized in 3' end processing of histone pre-mRNA. It contains a sequence complementary to a conserved histone downstream element located 3' of the histone pre-mRNA cleavage site. The Sm binding sequence of U7 snRNA deviates from the consensus 5'-(A/G)AUUU(G/U)UG(G/A)-3' found in spliceosomal snRNAs. It associates with five Sm proteins also found in spliceosomal snRNPs and two U7-specific Sm-like proteins, termed Lsm10 and Lsm11, which are essential for histone RNA processing. The U7 Sm OPT plasmid is obtained converting the U7-specific Sm binding sequence to the consensus found in spliceosomal snRNAs, which binds all seven Sm proteins found in spliceosomal snRNAs. This particle can no longer induce the cleavage of the histone pre-mRNAs, but can still bind to them by RNA:RNA base pairing. Another consequence is that the U7 Sm OPT RNA accumulates as nuclear snRNP about three times more efficiently than its wild type counterpart. The natural sequence binding to histone pre-mRNA can be exchanged with one directed against the interested target, converting the U7 Sm OPT into a sequence-specific competitor for components of the splicing machinery or make it bind any RNA molecule found in the nucleoplasm.

To introduce the antisense sequence against the ESE present in exon 5A, QuickChange site directed mutagenesis PCR technique has been used for generating the U7ese5A plasmid (section 3.3.3.3) using U7 Sm OPT original plasmid as a template and these primers:

Oligonucleotides used for U7ese5A

FOR mutagenic Primer U7	5' – GCTCGCTACAGAGGCCTTTCCGCAAGACATTGCCC AGGTCCACAAACAATTTTTGGAGCAGGTTTTCTGAC - 3'
REV mutagenic Primer U7	5' - GTCAGAAAACCTGCTCCAAAAATTGTTTGTGGACCT GGGCAATGTCTTGCGGAAAGGCCTCTGTAGCGAGC - 3'

The co-transfection experiments with the 9A wt minigene are performed as described in section 6.18.

6.24. Morpholino and Vivo-Morpholino treatments.

The Morpholino and the Vivo-Morpholino were purchased from Gene Tool, LLC. The Morpholino was resuspended in sterile water to obtain a 500 µM oligo stock. The aliquots were stored at -20°C. The Vivo-Morpholino arrived in solution ready for the injections.

For best delivery of the Morpholino, cells should be 80% confluent. After replacing the medium with fresh complete DMEM, Morpholino stock solution was added in different amount to reach the final concentration of 1, 5 and 10 µM and swirl well to mix. Then 6 µl of Endo-Porter were added for every 1ml media and immediately swirl to mix. This provided a final Endo-Porter concentration of 6 µM. Cells can be collected and assayed as soon as 16 hours after treatment and Endo-Porter can be left in the medium up to 72 hours without damage to your cells.

For a typical 20 g mouse, the Vivo-Morpholino was directly injected at 12.5 mg/kg in the left ventricle of the heart. The organ was collected after 48 hours after treatment and RNA extraction was performed following the protocol used for the cells. Regarding the systemic injection protocols, the mice were treated via intrajugular three times with the Vivo-Morpholino at 10 mg/kg for three consecutive days. At the fourth day the organs were collected and analysed.

6.25. Protein extraction.

For cellular protein analysis, confluent cultured cells were harvested and lysed with lysis buffer (15mM Hepes pH=7.5, 250mM NaCl, 0.5% NP-40, 10% Glycerol), unless differently specified, supplemented with protease inhibitor (Roche cocktail) and phosphatases inhibitors (10mM NaF, 1mM β-glycerolphosphate, 1mM Na_3VO_4). Cells were sonicated with 10 pulses (30% of pulse) at 50% of power and then centrifuged at 700xg for 10 minutes at +4°C. Pellet was discarded and total cell lysate was quantified by Bradford analysis using Biorad reagent (Bio-Rad Laboratories GmbH). For protein analysis, 50 μg of lysate were used to run an acrylamide gel.

6.26. SDS-page gel electrophoresis.

Protein samples were mixed with protein sample buffer 5X at a final concentration of 1X. SDS-PAGE was performed in vertical gels with the appropriate percentage of polyacrylamide (37.5:1 acrylamide-bis-acrylamide, ProtoGel, National Diagnostic), depending on the case. The gels were run at 25-30 mA in 1X SDS running buffer. After running gels were stained with Fixing (10% EtOH, 7% Acetic Acid in H_2O for 1 hour at room temperature) and Coomassie Blue solution (Ammonium sulfate 100 g/l, Phosphoric acid 85% 70 ml/l, Coomassie G-250 (SERVA) 2.5 g/l, MetOH 200 ml, H_2O up to 1l) or western blot was performed.

6.27. Western blot and antibodies.

SDS-PAGE gels were blotted on standard nitrocellulose membrane (Whatman PROTRAN) and incubated in blocking solution (PBS, 0.1% Tween, 5% milk) over night. Primary antibodies were incubated with the membrane in PBS 0.1% Tween, 2% milk for 2 hours. Afterwards, the membrane was washed three times in washing solution (PBS, 0.1%

Tween), incubated with the proper HRP-secondary antibodies (anti-mouse or anti-rabbit, Dako) in PBS 0.1% Tween, 2% milk, for 1 hour, washed three times (PBS, 0.1% Tween) and stained with ECL reagent (Thermo Scientific). Finally, an autoradiography was taken on Kodak Biomax XAR films. I used Roche western blocking solution in the place of the milk containing blocking solution and also to prepare all the SR antibodies.

The primary antibodies used in this study are:

- α-hnRNPA1: donated by E. Buratti
- α-hnRNPA2/B1: donated by E. Buratti
- α-hnRNPH: donated by E. Buratti
- α-PTB: donated by C.W.J Smith
- α-nPTB: donated by A. Willis
- α-1H2 (ETR3): donated by T. Cooper
- α-ASF/SF2: Invitrogen
- α-1H4 (SRp75, SRp55, SRp40, SRp30a/b and SRp20): Invitrogen
- α-flag epitope: Sigma
- α-TDP-43: donated by E. Buratti
- α-Tra2β: Abcam
- α-p84: Abcam

6.28. RNA preparation for pull down analysis.

Starting from 1 µg of DNA (annealed oligos), it was transcribed using T7 RNA Polymerase (Stratagene). The mix contained 8 µl of transcription buffer 5X (Stratagene), 4 µl of NTPs 15mM, 4 µl of DTT 100mM and 1 µl of T7 Polymerase (Stratagene) and H_2O to reach the final volume of 40 µl. For the pull down I prepared three times mix of transcription (final

volume 120 µl). Following incubation for 2 h at 37 °C, DNase treatment was performed incubated the mix for 15 min at 37°C. Then RNA was purified. 380 µl of water were added to reach the final volume of 500 µl. 500 µl of acid phenol were added and the sample was mixed vigorously using vortex for 10 sec, followed by a centrifugation at 13000 rpm for 5 min at 4°C. After collecting the upper phase, added 500 µl of chloroform, vortex and a centrifugation at 13000 rpm, 5 min at 4°C was performed. Then the RNA was precipitated using 1 ml of EtOH 100% and 50 µl of NaOAc 3M pH 5.2, keeping the sample in dry ice for 20 min. After a centrifugation at 13000 rpm for 10 min at 4°C the supernatant was removed and one wash with EtOH 70% was performed. The RNA was finally resuspended in 40 µl of sterile water.

6.29. Pull down analysis.

To each sample, 360 µl of a 5 mM Sodium m-Periodate (Sigma) solution in 0.1 mM NaOAc pH=5.0 were added. This 400 µl reaction mix was incubated for 1 hour in the dark (each test tube wrapped in aluminium foil) at room temperature in a rotator wheel. Each RNA was then ethanol precipitated according to standard protocols, washed once with EtOH 70%, and resuspended in 100 µl of 0.1 M NaOAC, pH 5.0. In the meantime, 100 µl of adipic acid dehydrazide agarose bead 50% slurry (Sigma) for each RNA sample to be conjugated were taken and placed in a 15 ml tube. The beads was washed two times with 10 ml of 0.1 M NaOAc pH 5.0. Each time spinning down at 3000 rpm for 5 minutes in a clinical centrifuge. After the final wash, the beads pellet was resuspended calculated 300 µl of 0,1 M NaOAc pH= 5.0 for each RNA sample. After mixing well, 300 µl aliquots were added to the 100 µl of periodate-treated RNA. Then the mix was incubate overnight in the dark at 4°C on a rotator (each test tube wrapped in aluminium foil).

Pull down the beads incubated overnight were then centrifuged at 4000 rpm for 5 min. The supernatant was threw out and the RNA loaded beads were washed twice with NaCl 2M, then, spin down at 4000 rpm for 5 min. The beads were washed three times with 1.0 ml of SolD 1X (20 mM Hepes pH=7.9, 100 mM KCl, 0.2 mM EDTA pH=8.0, 100 mM DTT, 6% v/v Glycerol), spinning down at 4000 rpm for 5 min and discarding supernatant each time. During the last spin down, 500 µl mix for each RNA sample was prepared: 50 µl SolD 10X (200 mM Hepes pH=7.9, 2 mM EDTA pH=8.0, 1M DTT, 60% v/v Glycerol), 50 µl KCl 1M, 100 µl NE (approx. 10-15 µg/µl), 300 µl H_2O, Heparin (200 µg/µl stock) to desired final concentration (0.5-2.5-5.0 µg/µl of the final volume). 500 µl Nuclear Extract mix were added to the individual samples and mixed gently by manually shaking the tube. The samples were incubated on a rotor for 30 min at room temperature.

After a centrifugation at 4000 rpm the supernatant was removed as much as possible. The beads were washed 4 times with 1.5 ml of SolD 1X by incubating them each time for 5 min on a rotating wheel at room temperature, each time spinning them down with a centrifugation at 4000 rpm to remove the supernatant. Finally 50 µl of SDS loading buffer were added and after denaturation the samples can be loaded on a SDS-PAGE gel.

6.30. In gel digestion and peptide extraction.

In order to address protein identity from SDS-PAGE, bands were cut out from the gel and reduced into small pieces of about $1mm^3$. Gel pieces were washed with 500µl of 100mM filtered EDTA and then shaken for 15 minutes at room temperature. Gel pieces were therefore dehydrated by adding about 50µl of filtered 100% MetOH and mixed for 5 minutes at room temperature. After removal of 100% MetOH, gel was rehydrated by adding 90µl of 30% MetOH to cover all the pieces and left at room temperature for 5 minutes shaking. At this point, 30% MetOH was removed and gel washed twice with 1ml

of ultra pure water for 10 minutes on a mixer. In the next step gel pieces were washed 4-6 times for 20-30 minutes each with 1ml of 50% MetOH containing 20mM TEAB. Afterwards, a 10 minutes wash with 1ml ultra pure water was performed and gels were finally dried in a SpeedVac for 15-30 minutes at medium temperature. An overnight incubation at 37°C was then carried out by adding to the gel pieces a trypsin solution made up by diluting 2µl Trypsin 0,5µg/ml in 98µl 20mM TEAB. The day after, the supernatants were removed and put in a new tube. Then, a little amount of 5% formic acid was added just to cover gel pieces and perform sonication extraction. Both the supernatants were finally combined and completely dried in a SpeedVac. Protein extracted were identified in Myers' Laboratory through mass spectrometry analysis.

7. References

Amin AS, Asghari-Roodsari A, Tan HL. 2010. Cardiac sodium channelopathies. Pflugers Arch 460:223-237.

Ast G. 2004. How did alternative splicing evolve? Nat Rev Genet 5:773-782.

Auweter SD, Fasan R, Reymond L, Underwood JG, Black DL, Pitsch S, Allain FH. 2006. Molecular basis of RNA recognition by the human alternative splicing factor Fox-1. EMBO J 25:163-173.

Bennett DL, Woods CG. 2014. Painful and painless channelopathies. Lancet Neurol 13:587-599.

Bennett E, Urcan MS, Tinkle SS, Koszowski AG, Levinson SR. 1997. Contribution of sialic acid to the voltage dependence of sodium channel gating. A possible electrostatic mechanism. J Gen Physiol 109:327-343.

Berget SM. 1995. Exon recognition in vertebrate splicing. J Biol Chem 270:2411-2414.

Black DL. 1992. Activation of c-src neuron-specific splicing by an unusual RNA element in vivo and in vitro. Cell 69:795-807.

Black DL. 2003. Mechanisms of alternative pre-messenger RNA splicing. Annu Rev Biochem 72:291-336.

Black JA, Dib-Hajj S, McNabola K, Jeste S, Rizzo MA, Kocsis JD, Waxman SG. 1996. Spinal sensory neurons express multiple sodium channel alpha-subunit mRNAs. Brain Res Mol Brain Res 43:117-131.

Black JA, Langworthy K, Hinson AW, Dib-Hajj SD, Waxman SG. 1997. NGF has opposing effects on Na+ channel III and SNS gene expression in spinal sensory neurons. Neuroreport 8:2331-2335.

Black JA, Liu S, Tanaka M, Cummins TR, Waxman SG. 2004. Changes in the expression of tetrodotoxin-sensitive sodium channels within dorsal root ganglia neurons in inflammatory pain. Pain 108:237-247.

Blanchette M, Chabot B. 1999. Modulation of exon skipping by high-affinity hnRNP A1-binding sites and by intron elements that repress splice site utilization. EMBO J 18:1939-1952.

Blech-Hermoni Y, Stillwagon SJ, Ladd AN. 2013. Diversity and conservation of CELF1 and CELF2 RNA and protein expression patterns during embryonic development. Dev Dyn 242:767-777.

Blencowe BJ. 2000. Exonic splicing enhancers: mechanism of action, diversity and role in human genetic diseases. Trends Biochem Sci 25:106-110.

Boutz PL, Stoilov P, Li Q, Lin CH, Chawla G, Ostrow K, Shiue L, Ares M, Jr., Black DL. 2007. A post-transcriptional regulatory switch in polypyrimidine tract-binding proteins reprograms alternative splicing in developing neurons. Genes Dev 21:1636-1652.

Brow DA. 2002. Allosteric cascade of spliceosome activation. Annu Rev Genet 36:333-360.

Buratti E, Baralle FE. 2001. Characterization and functional implications of the RNA binding properties of nuclear factor TDP-43, a novel splicing regulator of CFTR exon 9. J Biol Chem 276:36337-36343.

Buratti E, Baralle FE. 2004. Influence of RNA secondary structure on the pre-mRNA splicing process. Mol Cell Biol 24:10505-10514.

Buratti E, Brindisi A, Giombi M, Tisminetzky S, Ayala YM, Baralle FE. 2005. TDP-43 binds heterogeneous nuclear ribonucleoprotein A/B through its C-terminal tail: an important region for the inhibition of cystic fibrosis transmembrane conductance regulator exon 9 splicing. J Biol Chem 280:37572-37584.

Burd CG, Dreyfuss G. 1994. Conserved structures and diversity of functions of RNA-binding proteins. Science 265:615-621.

Burge CB, Padgett RA, Sharp PA. 1998. Evolutionary fates and origins of U12-type introns. Mol Cell 2:773-785.

Caceres JF, Screaton GR, Krainer AR. 1998. A specific subset of SR proteins shuttles continuously between the nucleus and the cytoplasm. Genes Dev 12:55-66.

Cantrell AR, Catterall WA. 2001. Neuromodulation of Na+ channels: an unexpected form of cellular plasticity. Nat Rev Neurosci 2:397-407.

Carson JH, Cui H, Barbarese E. 2001. The balance of power in RNA trafficking. Curr Opin Neurobiol 11:558-563.

Cartegni L, Krainer AR. 2002. Disruption of an SF2/ASF-dependent exonic splicing enhancer in SMN2 causes spinal muscular atrophy in the absence of SMN1. Nat Genet 30:377-384.

Castiglioni AJ, Raingo J, Lipscombe D. 2006. Alternative splicing in the C-terminus of CaV2.2 controls expression and gating of N-type calcium channels. J Physiol 576:119-134.

Catterall WA. 1992. Cellular and molecular biology of voltage-gated sodium channels. Physiol Rev 72:S15-48.

Catterall WA. 2000a. From ionic currents to molecular mechanisms: the structure and function of voltage-gated sodium channels. Neuron 26:13-25.

Catterall WA. 2000b. Structure and regulation of voltage-gated Ca2+ channels. Annu Rev Cell Dev Biol 16:521-555.

Catterall WA, Goldin AL, Waxman SG. 2005. International Union of Pharmacology. XLVII. Nomenclature and structure-function relationships of voltage-gated sodium channels. Pharmacol Rev 57:397-409.

Catterall WA, Kalume F, Oakley JC. 2010. NaV1.1 channels and epilepsy. J Physiol 588:1849-1859.

Chan RC, Black DL. 1997. The polypyrimidine tract binding protein binds upstream of neural cell-specific c-src exon N1 to repress the splicing of the intron downstream. Mol Cell Biol 17:4667-4676.

Charlet BN, Logan P, Singh G, Cooper TA. 2002. Dynamic antagonism between ETR-3 and PTB regulates cell type-specific alternative splicing. Mol Cell 9:649-658.

Chatelier A, Dahllund L, Eriksson A, Krupp J, Chahine M. 2008. Biophysical properties of human Na v1.7 splice variants and their regulation by protein kinase A. J Neurophysiol 99:2241-2250.

Chaudhury A, Chander P, Howe PH. 2010. Heterogeneous nuclear ribonucleoproteins (hnRNPs) in cellular processes: Focus on hnRNP E1's multifunctional regulatory roles. RNA 16:1449-1462.

Chen M, Manley JL. 2009. Mechanisms of alternative splicing regulation: insights from molecular and genomics approaches. Nat Rev Mol Cell Biol 10:741-754.

Choi JS, Cheng X, Foster E, Leffler A, Tyrrell L, Te Morsche RH, Eastman EM, Jansen HJ, Huehne K, Nau C, Dib-Hajj SD, Drenth JP, Waxman SG. 2010. Alternative splicing may contribute to time-dependent manifestation of inherited erythromelalgia. Brain 133:1823-1835.

Chou MY, Rooke N, Turck CW, Black DL. 1999. hnRNP H is a component of a splicing enhancer complex that activates a c-src alternative exon in neuronal cells. Mol Cell Biol 19:69-77.

Chou MY, Underwood JG, Nikolic J, Luu MH, Black DL. 2000. Multisite RNA binding and release of polypyrimidine tract binding protein during the regulation of c-src neural-specific splicing. Mol Cell 5:949-957.

Cooper TA. 2005. Use of minigene systems to dissect alternative splicing elements. Methods 37:331-340.

Copley RR. 2004. Evolutionary convergence of alternative splicing in ion channels. Trends Genet 20:171-176.

Cox JJ, Reimann F, Nicholas AK, Thornton G, Roberts E, Springell K, Karbani G, Jafri H, Mannan J, Raashid Y, Al-Gazali L, Hamamy H, Valente EM, Gorman S, Williams R, McHale DP, Wood JN, Gribble FM, Woods CG. 2006. An SCN9A channelopathy causes congenital inability to experience pain. Nature 444:894-898.

Cox JJ, Sheynin J, Shorer Z, Reimann F, Nicholas AK, Zubovic L, Baralle M, Wraige E, Manor E, Levy J, Woods CG, Parvari R. 2010. Congenital insensitivity to pain: novel SCN9A missense and in-frame deletion mutations. Hum Mutat 31:E1670-1686.

Crawford JB, Patton JG. 2006. Activation of alpha-tropomyosin exon 2 is regulated by the SR protein 9G8 and heterogeneous nuclear ribonucleoproteins H and F. Mol Cell Biol 26:8791-8802.

Crooke ST. 1999. Molecular mechanisms of action of antisense drugs. Biochim Biophys Acta 1489:31-44.

Cummins TR, Howe JR, Waxman SG. 1998. Slow closed-state inactivation: a novel mechanism underlying ramp currents in cells expressing the hNE/PN1 sodium channel. J Neurosci 18:9607-9619.

Dabby R. 2012. Pain disorders and erythromelalgia caused by voltage-gated sodium channel mutations. Curr Neurol Neurosci Rep 12:76-83.

Damianov A, Black DL. 2010. Autoregulation of Fox protein expression to produce dominant negative splicing factors. RNA 16:405-416.

Dasgupta T, Ladd AN. 2012. The importance of CELF control: molecular and biological roles of the CUG-BP, Elav-like family of RNA-binding proteins. Wiley Interdiscip Rev RNA 3:104-121.

de la Mata M, Alonso CR, Kadener S, Fededa JP, Blaustein M, Pelisch F, Cramer P, Bentley D, Kornblihtt AR. 2003. A slow RNA polymerase II affects alternative splicing in vivo. Mol Cell 12:525-532.

Del Gatto-Konczak F, Bourgeois CF, Le Guiner C, Kister L, Gesnel MC, Stevenin J, Breathnach R. 2000. The RNA-binding protein TIA-1 is a novel mammalian splicing regulator acting through intron sequences adjacent to a 5' splice site. Mol Cell Biol 20:6287-6299.

Dembowski JA, Grabowski PJ. 2009. The CUGBP2 splicing factor regulates an ensemble of branchpoints from perimeter binding sites with implications for autoregulation. PLoS Genet 5:e1000595.

Dias N, Stein CA. 2002. Antisense oligonucleotides: basic concepts and mechanisms. Mol Cancer Ther 1:347-355.

Dib-Hajj SD, Cummins TR, Black JA, Waxman SG. 2010. Sodium channels in normal and pathological pain. Annu Rev Neurosci 33:325-347.

Dib-Hajj SD, Yang Y, Black JA, Waxman SG. 2013. The Na(V)1.7 sodium channel: from molecule to man. Nat Rev Neurosci 14:49-62.

Diss JK, Fraser SP, Djamgoz MB. 2004. Voltage-gated Na+ channels: multiplicity of expression, plasticity, functional implications and pathophysiological aspects. Eur Biophys J 33:180-193.

Dominski Z, Kole R. 1993. Restoration of correct splicing in thalassemic pre-mRNA by antisense oligonucleotides. Proc Natl Acad Sci U S A 90:8673-8677.

Douglas AG, Wood MJ. 2013. Splicing therapy for neuromuscular disease. Mol Cell Neurosci 56:169-185.

Drenth JP, Michiels JJ. 1992. Clinical characteristics and pathophysiology of erythromelalgia and erythermalgia. Am J Med 93:111-114.

Drenth JP, te Morsche RH, Guillet G, Taieb A, Kirby RL, Jansen JB. 2005. SCN9A mutations define primary erythermalgia as a neuropathic disorder of voltage gated sodium channels. J Invest Dermatol 124:1333-1338.

Drenth JP, Waxman SG. 2007. Mutations in sodium-channel gene SCN9A cause a spectrum of human genetic pain disorders. J Clin Invest 117:3603-3609.

Drews VL, Lieberman AP, Meisler MH. 2005. Multiple transcripts of sodium channel SCN8A (Na(V)1.6) with alternative 5'- and 3'-untranslated regions and initial characterization of the SCN8A promoter. Genomics 85:245-257.

Dreyfuss G, Kim VN, Kataoka N. 2002. Messenger-RNA-binding proteins and the messages they carry. Nat Rev Mol Cell Biol 3:195-205.

Dreyfuss G, Matunis MJ, Pinol-Roma S, Burd CG. 1993. hnRNP proteins and the biogenesis of mRNA. Annu Rev Biochem 62:289-321.

Dreyfuss G, Philipson L, Mattaj IW. 1988. Ribonucleoprotein particles in cellular processes. J Cell Biol 106:1419-1425.

Dujardin G, Buratti E, Charlet-Berguerand N, Martins de Araujo M, Mbopda A, Le Jossic-Corcos C, Pagani F, Ferec C, Corcos L. 2010. CELF proteins regulate CFTR pre-mRNA splicing: essential role of the divergent domain of ETR-3. Nucleic Acids Res 38:7273-7285.

Escayg A, MacDonald BT, Meisler MH, Baulac S, Huberfeld G, An-Gourfinkel I, Brice A, LeGuern E, Moulard B, Chaigne D, Buresi C, Malafosse A. 2000. Mutations of SCN1A, encoding a neuronal sodium channel, in two families with GEFS+2. Nat Genet 24:343-345.

Estacion M, Choi JS, Eastman EM, Lin Z, Li Y, Tyrrell L, Yang Y, Dib-Hajj SD, Waxman SG. 2010. Can robots patch-clamp as well as humans? Characterization of a novel sodium channel mutation. J Physiol 588:1915-1927.

Faber CG, Lauria G, Merkies IS, Cheng X, Han C, Ahn HS, Persson AK, Hoeijmakers JG, Gerrits MM, Pierro T, Lombardi R, Kapetis D, Dib-Hajj SD, Waxman SG. 2012. Gain-of-function Nav1.8 mutations in painful neuropathy. Proc Natl Acad Sci U S A 109:19444-19449.

Fairclough RJ, Wood MJ, Davies KE. 2013. Therapy for Duchenne muscular dystrophy: renewed optimism from genetic approaches. Nat Rev Genet 14:373-378.

Faustino NA, Cooper TA. 2005. Identification of putative new splicing targets for ETR-3 using sequences identified by systematic evolution of ligands by exponential enrichment. Mol Cell Biol 25:879-887.

Favre I, Moczydlowski E, Schild L. 1996. On the structural basis for ionic selectivity among Na+, K+, and Ca2+ in the voltage-gated sodium channel. Biophys J 71:3110-3125.

Fertleman CR, Baker MD, Parker KA, Moffatt S, Elmslie FV, Abrahamsen B, Ostman J, Klugbauer N, Wood JN, Gardiner RM, Rees M. 2006. SCN9A mutations in paroxysmal extreme pain disorder: allelic variants underlie distinct channel defects and phenotypes. Neuron 52:767-774.

Fiesel FC, Weber SS, Supper J, Zell A, Kahle PJ. 2012. TDP-43 regulates global translational yield by splicing of exon junction complex component SKAR. Nucleic Acids Res 40:2668-2682.

Fletcher EV, Kullmann DM, Schorge S. 2011. Alternative splicing modulates inactivation of type 1 voltage-gated sodium channels by toggling an amino acid in the first S3-S4 linker. J Biol Chem 286:36700-36708.

Fogel BL, Wexler E, Wahnich A, Friedrich T, Vijayendran C, Gao F, Parikshak N, Konopka G, Geschwind DH. 2012. RBFOX1 regulates both splicing and transcriptional networks in human neuronal development. Hum Mol Genet 21:4171-4186.

Ford LP, Wright WE, Shay JW. 2002. A model for heterogeneous nuclear ribonucleoproteins in telomere and telomerase regulation. Oncogene 21:580-583.

Fox-Walsh KL, Dou Y, Lam BJ, Hung SP, Baldi PF, Hertel KJ. 2005. The architecture of pre-mRNAs affects mechanisms of splice-site pairing. Proc Natl Acad Sci U S A 102:16176-16181.

Friedman KJ, Kole J, Cohn JA, Knowles MR, Silverman LM, Kole R. 1999. Correction of aberrant splicing of the cystic fibrosis transmembrane conductance regulator (CFTR) gene by antisense oligonucleotides. J Biol Chem 274:36193-36199.

Fu XD. 1995. The superfamily of arginine/serine-rich splicing factors. RNA 1:663-680.

Fukumura K, Kato A, Jin Y, Ideue T, Hirose T, Kataoka N, Fujiwara T, Sakamoto H, Inoue K. 2007. Tissue-specific splicing regulator Fox-1 induces exon skipping by interfering E complex

formation on the downstream intron of human F1gamma gene. Nucleic Acids Res 35:5303-5311.

Gazina EV, Richards KL, Mokhtar MB, Thomas EA, Reid CA, Petrou S. 2010. Differential expression of exon 5 splice variants of sodium channel alpha subunit mRNAs in the developing mouse brain. Neuroscience 166:195-200.

Gehman LT, Meera P, Stoilov P, Shiue L, O'Brien JE, Meisler MH, Ares M, Jr., Otis TS, Black DL. 2012. The splicing regulator Rbfox2 is required for both cerebellar development and mature motor function. Genes Dev 26:445-460.

Gehman LT, Stoilov P, Maguire J, Damianov A, Lin CH, Shiue L, Ares M, Jr., Mody I, Black DL. 2011. The splicing regulator Rbfox1 (A2BP1) controls neuronal excitation in the mammalian brain. Nat Genet 43:706-711.

Gennarelli M, Lucarelli M, Capon F, Pizzuti A, Merlini L, Angelini C, Novelli G, Dallapiccola B. 1995. Survival motor neuron gene transcript analysis in muscles from spinal muscular atrophy patients. Biochem Biophys Res Commun 213:342-348.

Gilbert W. 1978. Why genes in pieces? Nature 271:501.

Goldin AL. 1999. Diversity of mammalian voltage-gated sodium channels. Ann N Y Acad Sci 868:38-50.

Goldin AL, Barchi RL, Caldwell JH, Hofmann F, Howe JR, Hunter JC, Kallen RG, Mandel G, Meisler MH, Netter YB, Noda M, Tamkun MM, Waxman SG, Wood JN, Catterall WA. 2000. Nomenclature of voltage-gated sodium channels. Neuron 28:365-368.

Goo YH, Cooper TA. 2009. CUGBP2 directly interacts with U2 17S snRNP components and promotes U2 snRNA binding to cardiac troponin T pre-mRNA. Nucleic Acids Res 37:4275-4286.

Gorman L, Suter D, Emerick V, Schumperli D, Kole R. 1998. Stable alteration of pre-mRNA splicing patterns by modified U7 small nuclear RNAs. Proc Natl Acad Sci U S A 95:4929-4934.

Goyenvalle A, Vulin A, Fougerousse F, Leturcq F, Kaplan JC, Garcia L, Danos O. 2004. Rescue of dystrophic muscle through U7 snRNA-mediated exon skipping. Science 306:1796-1799.

Grabowski P. 2011. Alternative splicing takes shape during neuronal development. Curr Opin Genet Dev 21:388-394.

Graveley BR. 2000. Sorting out the complexity of SR protein functions. RNA 6:1197-1211.

Graveley BR. 2005. Mutually exclusive splicing of the insect Dscam pre-mRNA directed by competing intronic RNA secondary structures. Cell 123:65-73.

Grellscheid SN, Dalgliesh C, Rozanska A, Grellscheid D, Bourgeois CF, Stevenin J, Elliott DJ. 2011. Molecular design of a splicing switch responsive to the RNA binding protein Tra2beta. Nucleic Acids Res 39:8092-8104.

Gromak N, Matlin AJ, Cooper TA, Smith CW. 2003. Antagonistic regulation of alpha-actinin alternative splicing by CELF proteins and polypyrimidine tract binding protein. RNA 9:443-456.

Habelhah H, Shah K, Huang L, Ostareck-Lederer A, Burlingame AL, Shokat KM, Hentze MW, Ronai Z. 2001. ERK phosphorylation drives cytoplasmic accumulation of hnRNP-K and inhibition of mRNA translation. Nat Cell Biol 3:325-330.

Han SP, Tang YH, Smith R. 2010. Functional diversity of the hnRNPs: past, present and perspectives. Biochem J 430:379-392.

Hanamura A, Caceres JF, Mayeda A, Franza BR, Jr., Krainer AR. 1998. Regulated tissue-specific expression of antagonistic pre-mRNA splicing factors. RNA 4:430-444.

Heinemann SH, Terlau H, Stuhmer W, Imoto K, Numa S. 1992. Calcium channel characteristics conferred on the sodium channel by single mutations. Nature 356:441-443.

Heinzen EL, Yoon W, Tate SK, Sen A, Wood NW, Sisodiya SM, Goldstein DB. 2007. Nova2 interacts with a cis-acting polymorphism to influence the proportions of drug-responsive splice variants of SCN1A. Am J Hum Genet 80:876-883.

Hemani Y, Soller M. 2012. Mechanisms of Drosophila Dscam mutually exclusive splicing regulation. Biochem Soc Trans 40:804-809.

Heron SE, Crossland KM, Andermann E, Phillips HA, Hall AJ, Bleasel A, Shevell M, Mercho S, Seni MH, Guiot MC, Mulley JC, Berkovic SF, Scheffer IE. 2002. Sodium-channel defects in benign familial neonatal-infantile seizures. Lancet 360:851-852.

Herzog RI, Cummins TR, Ghassemi F, Dib-Hajj SD, Waxman SG. 2003. Distinct repriming and closed-state inactivation kinetics of Nav1.6 and Nav1.7 sodium channels in mouse spinal sensory neurons. J Physiol 551:741-750.

Hoeijmakers JG, Merkies IS, Gerrits MM, Waxman SG, Faber CG. 2012. Genetic aspects of sodium channelopathy in small fiber neuropathy. Clin Genet 82:351-358.

Holland KD, Kearney JA, Glauser TA, Buck G, Keddache M, Blankston JR, Glaaser IW, Kass RS, Meisler MH. 2008. Mutation of sodium channel SCN3A in a patient with cryptogenic pediatric partial epilepsy. Neurosci Lett 433:65-70.

Hua Y, Sahashi K, Hung G, Rigo F, Passini MA, Bennett CF, Krainer AR. 2010. Antisense correction of SMN2 splicing in the CNS rescues necrosis in a type III SMA mouse model. Genes Dev 24:1634-1644.

Hua Y, Vickers TA, Baker BF, Bennett CF, Krainer AR. 2007. Enhancement of SMN2 exon 7 inclusion by antisense oligonucleotides targeting the exon. PLoS Biol 5:e73.

Huang SC, Ou AC, Park J, Yu F, Yu B, Lee A, Yang G, Zhou A, Benz EJ, Jr. 2012. RBFOX2 promotes protein 4.1R exon 16 selection via U1 snRNP recruitment. Mol Cell Biol 32:513-526.

Hui J, Stangl K, Lane WS, Bindereif A. 2003. HnRNP L stimulates splicing of the eNOS gene by binding to variable-length CA repeats. Nat Struct Biol 10:33-37.

Isom LL. 2001. Sodium channel beta subunits: anything but auxiliary. Neuroscientist 7:42-54.

Izquierdo JM, Majos N, Bonnal S, Martinez C, Castelo R, Guigo R, Bilbao D, Valcarcel J. 2005. Regulation of Fas alternative splicing by antagonistic effects of TIA-1 and PTB on exon definition. Mol Cell 19:475-484.

Jarecki BW, Sheets PL, Xiao Y, Jackson JO, 2nd, Cummins TR. 2009. Alternative splicing of Na(V)1.7 exon 5 increases the impact of the painful PEPD mutant channel I1461T. Channels (Austin) 3:259-267.

Jimenez-Garcia LF, Spector DL. 1993. In vivo evidence that transcription and splicing are coordinated by a recruiting mechanism. Cell 73:47-59.

Jin Y, Suzuki H, Maegawa S, Endo H, Sugano S, Hashimoto K, Yasuda K, Inoue K. 2003. A vertebrate RNA-binding protein Fox-1 regulates tissue-specific splicing via the pentanucleotide GCAUG. EMBO J 22:905-912.

Jones RB, Wang F, Luo Y, Yu C, Jin C, Suzuki T, Kan M, McKeehan WL. 2001. The nonsense-mediated decay pathway and mutually exclusive expression of alternatively spliced FGFR2IIIb and -IIIc mRNAs. J Biol Chem 276:4158-4167.

Julius D, Basbaum AI. 2001. Molecular mechanisms of nociception. Nature 413:203-210.

Jurica MS, Moore MJ. 2003. Pre-mRNA splicing: awash in a sea of proteins. Mol Cell 12:5-14.

Kalsotra A, Cooper TA. 2011. Functional consequences of developmentally regulated alternative splicing. Nat Rev Genet 12:715-729.

Kalsotra A, Xiao X, Ward AJ, Castle JC, Johnson JM, Burge CB, Cooper TA. 2008. A postnatal switch of CELF and MBNL proteins reprograms alternative splicing in the developing heart. Proc Natl Acad Sci U S A 105:20333-20338.

Kashima T, Rao N, David CJ, Manley JL. 2007. hnRNP A1 functions with specificity in repression of SMN2 exon 7 splicing. Hum Mol Genet 16:3149-3159.

Keppetipola N, Sharma S, Li Q, Black DL. 2012. Neuronal regulation of pre-mRNA splicing by polypyrimidine tract binding proteins, PTBP1 and PTBP2. Crit Rev Biochem Mol Biol 47:360-378.

Keren H, Lev-Maor G, Ast G. 2010. Alternative splicing and evolution: diversification, exon definition and function. Nat Rev Genet 11:345-355.

Kessler MM, Henry MF, Shen E, Zhao J, Gross S, Silver PA, Moore CL. 1997. Hrp1, a sequence-specific RNA-binding protein that shuttles between the nucleus and the cytoplasm, is required for mRNA 3'-end formation in yeast. Genes Dev 11:2545-2556.

Kiledjian M, Dreyfuss G. 1992. Primary structure and binding activity of the hnRNP U protein: binding RNA through RGG box. EMBO J 11:2655-2664.

Kim KK, Adelstein RS, Kawamoto S. 2009. Identification of neuronal nuclei (NeuN) as Fox-3, a new member of the Fox-1 gene family of splicing factors. J Biol Chem 284:31052-31061.

Kim KK, Nam J, Mukouyama YS, Kawamoto S. 2013. Rbfox3-regulated alternative splicing of Numb promotes neuronal differentiation during development. J Cell Biol 200:443-458.

Kole R, Krainer AR, Altman S. 2012. RNA therapeutics: beyond RNA interference and antisense oligonucleotides. Nat Rev Drug Discov 11:125-140.

Konarska MM. 1998. Recognition of the 5' splice site by the spliceosome. Acta Biochim Pol 45:869-881.

Koopmann TT, Bezzina CR, Wilde AA. 2006. Voltage-gated sodium channels: action players with many faces. Ann Med 38:472-482.

Kornblihtt AR, de la Mata M, Fededa JP, Munoz MJ, Nogues G. 2004. Multiple links between transcription and splicing. RNA 10:1489-1498.

Kuroyanagi H. 2009. Fox-1 family of RNA-binding proteins. Cell Mol Life Sci 66:3895-3907.

Lacerra G, Sierakowska H, Carestia C, Fucharoen S, Summerton J, Weller D, Kole R. 2000. Restoration of hemoglobin A synthesis in erythroid cells from peripheral blood of thalassemic patients. Proc Natl Acad Sci U S A 97:9591-9596.

Ladd AN. 2013. CUG-BP, Elav-like family (CELF)-mediated alternative splicing regulation in the brain during health and disease. Mol Cell Neurosci 56:456-464.

Ladd AN, Charlet N, Cooper TA. 2001. The CELF family of RNA binding proteins is implicated in cell-specific and developmentally regulated alternative splicing. Mol Cell Biol 21:1285-1296.

Ladd AN, Nguyen NH, Malhotra K, Cooper TA. 2004. CELF6, a member of the CELF family of RNA-binding proteins, regulates muscle-specific splicing enhancer-dependent alternative splicing. J Biol Chem 279:17756-17764.

Ladd AN, Stenberg MG, Swanson MS, Cooper TA. 2005. Dynamic balance between activation and repression regulates pre-mRNA alternative splicing during heart development. Dev Dyn 233:783-793.

Lampert A, O'Reilly AO, Reeh P, Leffler A. 2010. Sodium channelopathies and pain. Pflugers Arch 460:249-263.

Lee BJ, Cansizoglu AE, Suel KE, Louis TH, Zhang Z, Chook YM. 2006. Rules for nuclear localization sequence recognition by karyopherin beta 2. Cell 126:543-558.

Lee MS, Henry M, Silver PA. 1996. A protein that shuttles between the nucleus and the cytoplasm is an important mediator of RNA export. Genes Dev 10:1233-1246.

Lefebvre S, Burglen L, Reboullet S, Clermont O, Burlet P, Viollet L, Benichou B, Cruaud C, Millasseau P, Zeviani M, et al. 1995. Identification and characterization of a spinal muscular atrophy-determining gene. Cell 80:155-165.

Lefebvre S, Burlet P, Liu Q, Bertrandy S, Clermont O, Munnich A, Dreyfuss G, Melki J. 1997. Correlation between severity and SMN protein level in spinal muscular atrophy. Nat Genet 16:265-269.

Letunic I, Copley RR, Bork P. 2002. Common exon duplication in animals and its role in alternative splicing. Hum Mol Genet 11:1561-1567.

Lin CH, Patton JG. 1995. Regulation of alternative 3' splice site selection by constitutive splicing factors. RNA 1:234-245.

Llorian M, Schwartz S, Clark TA, Hollander D, Tan LY, Spellman R, Gordon A, Schweitzer AC, de la Grange P, Ast G, Smith CW. 2010. Position-dependent alternative splicing activity revealed by global profiling of alternative splicing events regulated by PTB. Nat Struct Mol Biol 17:1114-1123.

Lorson CL, Androphy EJ. 2000. An exonic enhancer is required for inclusion of an essential exon in the SMA-determining gene SMN. Hum Mol Genet 9:259-265.

Lou H, Helfman DM, Gagel RF, Berget SM. 1999. Polypyrimidine tract-binding protein positively regulates inclusion of an alternative 3'-terminal exon. Mol Cell Biol 19:78-85.

Lu CM, Brown GB. 1998. Isolation of a human-brain sodium-channel gene encoding two isoforms of the subtype III alpha-subunit. J Mol Neurosci 10:67-70.

Lynch KW, Maniatis T. 1995. Synergistic interactions between two distinct elements of a regulated splicing enhancer. Genes Dev 9:284-293.

Makielski JC, Ye B, Valdivia CR, Pagel MD, Pu J, Tester DJ, Ackerman MJ. 2003. A ubiquitous splice variant and a common polymorphism affect heterologous expression of recombinant human SCN5A heart sodium channels. Circ Res 93:821-828.

Maniatis T, Tasic B. 2002. Alternative pre-mRNA splicing and proteome expansion in metazoans. Nature 418:236-243.

Manley JL, Krainer AR. 2010. A rational nomenclature for serine/arginine-rich protein splicing factors (SR proteins). Genes Dev 24:1073-1074.

Mardon HJ, Sebastio G, Baralle FE. 1987. A role for exon sequences in alternative splicing of the human fibronectin gene. Nucleic Acids Res 15:7725-7733.

Markovtsov V, Nikolic JM, Goldman JA, Turck CW, Chou MY, Black DL. 2000. Cooperative assembly of an hnRNP complex induced by a tissue-specific homolog of polypyrimidine tract binding protein. Mol Cell Biol 20:7463-7479.

Marquis J, Meyer K, Angehrn L, Kampfer SS, Rothen-Rutishauser B, Schumperli D. 2007. Spinal muscular atrophy: SMN2 pre-mRNA splicing corrected by a U7 snRNA derivative carrying a splicing enhancer sequence. Mol Ther 15:1479-1486.

Marquis J, Paillard L, Audic Y, Cosson B, Danos O, Le Bec C, Osborne HB. 2006. CUG-BP1/CELF1 requires UGU-rich sequences for high-affinity binding. Biochem J 400:291-301.

Matlin AJ, Clark F, Smith CW. 2005. Understanding alternative splicing: towards a cellular code. Nat Rev Mol Cell Biol 6:386-398.

May GE, Olson S, McManus CJ, Graveley BR. 2011. Competing RNA secondary structures are required for mutually exclusive splicing of the Dscam exon 6 cluster. RNA 17:222-229.

McKee AE, Minet E, Stern C, Riahi S, Stiles CD, Silver PA. 2005. A genome-wide in situ hybridization map of RNA-binding proteins reveals anatomically restricted expression in the developing mouse brain. BMC Dev Biol 5:14.

McManus CJ, Graveley BR. 2011. RNA structure and the mechanisms of alternative splicing. Curr Opin Genet Dev 21:373-379.

Mercado PA, Ayala YM, Romano M, Buratti E, Baralle FE. 2005. Depletion of TDP 43 overrides the need for exonic and intronic splicing enhancers in the human apoA-II gene. Nucleic Acids Res 33:6000-6010.

Miau LH, Chang CJ, Shen BJ, Tsai WH, Lee SC. 1998. Identification of heterogeneous nuclear ribonucleoprotein K (hnRNP K) as a repressor of C/EBPbeta-mediated gene activation. J Biol Chem 273:10784-10791.

Minovitsky S, Gee SL, Schokrpur S, Dubchak I, Conboy JG. 2005. The splicing regulatory element, UGCAUG, is phylogenetically and spatially conserved in introns that flank tissue-specific alternative exons. Nucleic Acids Res 33:714-724.

Monani UR, Lorson CL, Parsons DW, Prior TW, Androphy EJ, Burghes AH, McPherson JD. 1999. A single nucleotide difference that alters splicing patterns distinguishes the SMA gene SMN1 from the copy gene SMN2. Hum Mol Genet 8:1177-1183.

Montell C, Berk AJ. 1984. Elimination of mRNA splicing by a point mutation outside the conserved GU at 5' splice sites. Nucleic Acids Res 12:3821-3827.

Moore MJ, Proudfoot NJ. 2009. Pre-mRNA processing reaches back to transcription and ahead to translation. Cell 136:688-700.

Moroy T, Heyd F. 2007. The impact of alternative splicing in vivo: mouse models show the way. RNA 13:1155-1171.

Moulton JD, Jiang S. 2009. Gene knockdowns in adult animals: PPMOs and vivo-morpholinos. Molecules 14:1304-1323.

Mourelatos Z, Abel L, Yong J, Kataoka N, Dreyfuss G. 2001. SMN interacts with a novel family of hnRNP and spliceosomal proteins. EMBO J 20:5443-5452.

Muntoni F, Wood MJ. 2011. Targeting RNA to treat neuromuscular disease. Nat Rev Drug Discov 10:621-637.

Murphy LL, Moon-Grady AJ, Cuneo BF, Wakai RT, Yu S, Kunic JD, Benson DW, George AL, Jr. 2012. Developmentally regulated SCN5A splice variant potentiates dysfunction of a novel mutation associated with severe fetal arrhythmia. Heart Rhythm 9:590-597.

Nabbout R, Gennaro E, Dalla Bernardina B, Dulac O, Madia F, Bertini E, Capovilla G, Chiron C, Cristofori G, Elia M, Fontana E, Gaggero R, Granata T, Guerrini R, Loi M, La Selva L, Lispi ML, Matricardi A, Romeo A, Tzolas V, Valseriati D, Veggiotti P, Vigevano F, Vallee L, Dagna Bricarelli F, Bianchi A, Zara F. 2003. Spectrum of SCN1A mutations in severe myoclonic epilepsy of infancy. Neurology 60:1961-1967.

Nassar MA, Stirling LC, Forlani G, Baker MD, Matthews EA, Dickenson AH, Wood JN. 2004. Nociceptor-specific gene deletion reveals a major role for Nav1.7 (PN1) in acute and inflammatory pain. Proc Natl Acad Sci U S A 101:12706-12711.

O'Brien JE, Meisler MH. 2013. Sodium channel SCN8A (Nav1.6): properties and de novo mutations in epileptic encephalopathy and intellectual disability. Front Genet 4:213.

Oberstrass FC, Auweter SD, Erat M, Hargous Y, Henning A, Wenter P, Reymond L, Amir-Ahmady B, Pitsch S, Black DL, Allain FH. 2005. Structure of PTB bound to RNA: specific binding and implications for splicing regulation. Science 309:2054-2057.

Onkal R, Mattis JH, Fraser SP, Diss JK, Shao D, Okuse K, Djamgoz MB. 2008. Alternative splicing of Nav1.5: an electrophysiological comparison of 'neonatal' and 'adult' isoforms and critical involvement of a lysine residue. J Cell Physiol 216:716-726.

Patel AA, Steitz JA. 2003. Splicing double: insights from the second spliceosome. Nat Rev Mol Cell Biol 4:960-970.

Perez I, Lin CH, McAfee JG, Patton JG. 1997. Mutation of PTB binding sites causes misregulation of alternative 3' splice site selection in vivo. RNA 3:764-778.

Pinol-Roma S, Dreyfuss G. 1992. Shuttling of pre-mRNA binding proteins between nucleus and cytoplasm. Nature 355:730-732.

Plummer NW, Meisler MH. 1999. Evolution and diversity of mammalian sodium channel genes. Genomics 57:323-331.

Polydorides AD, Okano HJ, Yang YY, Stefani G, Darnell RB. 2000. A brain-enriched polypyrimidine tract-binding protein antagonizes the ability of Nova to regulate neuron-specific alternative splicing. Proc Natl Acad Sci U S A 97:6350-6355.

Ponthier JL, Schluepen C, Chen W, Lersch RA, Gee SL, Hou VC, Lo AJ, Short SA, Chasis JA, Winkelmann JC, Conboy JG. 2006. Fox-2 splicing factor binds to a conserved intron motif to promote inclusion of protein 4.1R alternative exon 16. J Biol Chem 281:12468-12474.

Query CC, Strobel SA, Sharp PA. 1996. Three recognition events at the branch-site adenine. EMBO J 15:1392-1402.

Ram O, Ast G. 2007. SR proteins: a foot on the exon before the transition from intron to exon definition. Trends Genet 23:5-7.

Raymond CK, Castle J, Garrett-Engele P, Armour CD, Kan Z, Tsinoremas N, Johnson JM. 2004. Expression of alternatively spliced sodium channel alpha-subunit genes. Unique splicing patterns are observed in dorsal root ganglia. J Biol Chem 279:46234-46241.

Reed R, Maniatis T. 1988. The role of the mammalian branchpoint sequence in pre-mRNA splicing. Genes Dev 2:1268-1276.

Renganathan M, Dib-Hajj S, Waxman SG. 2002. Na(v)1.5 underlies the 'third TTX-R sodium current' in rat small DRG neurons. Brain Res Mol Brain Res 106:70-82.

Rogart RB, Cribbs LL, Muglia LK, Kephart DD, Kaiser MW. 1989. Molecular cloning of a putative tetrodotoxin-resistant rat heart Na+ channel isoform. Proc Natl Acad Sci U S A 86:8170-8174.

Romanelli MG, Diani E, Lievens PM. 2013. New insights into functional roles of the polypyrimidine tract-binding protein. Int J Mol Sci 14:22906-22932.

Rush AM, Cummins TR, Waxman SG. 2007. Multiple sodium channels and their roles in electrogenesis within dorsal root ganglion neurons. J Physiol 579:1-14.

Sapra AK, Anko ML, Grishina I, Lorenz M, Pabis M, Poser I, Rollins J, Weiland EM, Neugebauer KM. 2009. SR protein family members display diverse activities in the formation of nascent and mature mRNPs in vivo. Mol Cell 34:179-190.

Schaal TD, Maniatis T. 1999. Multiple distinct splicing enhancers in the protein-coding sequences of a constitutively spliced pre-mRNA. Mol Cell Biol 19:261-273.

Schaller KL, Krzemien DM, McKenna NM, Caldwell JH. 1992. Alternatively spliced sodium channel transcripts in brain and muscle. J Neurosci 12:1370-1381.

Schmucker D, Clemens JC, Shu H, Worby CA, Xiao J, Muda M, Dixon JE, Zipursky SL. 2000. Drosophila Dscam is an axon guidance receptor exhibiting extraordinary molecular diversity. Cell 101:671-684.

Schroeter A, Walzik S, Blechschmidt S, Haufe V, Benndorf K, Zimmer T. 2010. Structure and function of splice variants of the cardiac voltage-gated sodium channel Na(v)1.5. J Mol Cell Cardiol 49:16-24.

Schulz DJ, Temporal S, Barry DM, Garcia ML. 2008. Mechanisms of voltage-gated ion channel regulation: from gene expression to localization. Cell Mol Life Sci 65:2215-2231.

Sharma S, Falick AM, Black DL. 2005. Polypyrimidine tract binding protein blocks the 5' splice site-dependent assembly of U2AF and the prespliceosomal E complex. Mol Cell 19:485-496.

Sharp PA, Burge CB. 1997. Classification of introns: U2-type or U12-type. Cell 91:875-879.

Shi X, Yasumoto S, Kurahashi H, Nakagawa E, Fukasawa T, Uchiya S, Hirose S. 2012. Clinical spectrum of SCN2A mutations. Brain Dev 34:541-545.

Skordis LA, Dunckley MG, Yue B, Eperon IC, Muntoni F. 2003. Bifunctional antisense oligonucleotides provide a trans-acting splicing enhancer that stimulates SMN2 gene expression in patient fibroblasts. Proc Natl Acad Sci U S A 100:4114-4119.

Smith CW. 2005. Alternative splicing--when two's a crowd. Cell 123:1-3.

Smith CW, Nadal-Ginard B. 1989. Mutually exclusive splicing of alpha-tropomyosin exons enforced by an unusual lariat branch point location: implications for constitutive splicing. Cell 56:749-758.

Smith KJ. 2007. Sodium channels and multiple sclerosis: roles in symptom production, damage and therapy. Brain Pathol 17:230-242.

Sorensen JB, Nagy G, Varoqueaux F, Nehring RB, Brose N, Wilson MC, Neher E. 2003. Differential control of the releasable vesicle pools by SNAP-25 splice variants and SNAP-23. Cell 114:75-86.

Southby J, Gooding C, Smith CW. 1999. Polypyrimidine tract binding protein functions as a repressor to regulate alternative splicing of alpha-actinin mutally exclusive exons. Mol Cell Biol 19:2699-2711.

Spellman R, Llorian M, Smith CW. 2007. Crossregulation and functional redundancy between the splicing regulator PTB and its paralogs nPTB and ROD1. Mol Cell 27:420-434.

Spellman R, Smith CW. 2006. Novel modes of splicing repression by PTB. Trends Biochem Sci 31:73-76.

Sterjev Z, Kiteva G, Cvetkovska E, Petrov I, Kuzmanovski I, Ribarska T, Nestorovska K, Matevska N, Trajkovik-Jolevska S, Dimovski A, Suturkova L. 2012. Influence of the SCN1A IVS5N + 5 G>A Polymorphism on Therapy with Carbamazepine for Epilepsy. Balkan J Med Genet 15:19-24.

Stoss O, Stoilov P, Hartmann AM, Nayler O, Stamm S. 1999. The in vivo minigene approach to analyze tissue-specific splicing. Brain Res Brain Res Protoc 4:383-394.

Stuhmer W, Conti F, Suzuki H, Wang XD, Noda M, Yahagi N, Kubo H, Numa S. 1989. Structural parts involved in activation and inactivation of the sodium channel. Nature 339:597-603.

Summerton JE. 2007. Morpholino, siRNA, and S-DNA compared: impact of structure and mechanism of action on off-target effects and sequence specificity. Curr Top Med Chem 7:651-660.

Sureau A, Sauliere J, Expert-Bezancon A, Marie J. 2011. CELF and PTB proteins modulate the inclusion of the beta-tropomyosin exon 6B during myogenic differentiation. Exp Cell Res 317:94-106.

Tabb JS, Fanger GR, Wilson EM, Maue RA, Henderson LP. 1994. Suppression of sodium channel function in differentiating C2 muscle cells stably overexpressing rat androgen receptors. J Neurosci 14:763-773.

Tacke R, Manley JL. 1999. Determinants of SR protein specificity. Curr Opin Cell Biol 11:358-362.

Tacke R, Tohyama M, Ogawa S, Manley JL. 1998. Human Tra2 proteins are sequence-specific activators of pre-mRNA splicing. Cell 93:139-148.

Tan HL. 2006. Sodium channel variants in heart disease: expanding horizons. J Cardiovasc Electrophysiol 17 Suppl 1:S151-S157.

Tang ZZ, Sharma S, Zheng S, Chawla G, Nikolic J, Black DL. 2011. Regulation of the mutually exclusive exons 8a and 8 in the CaV1.2 calcium channel transcript by polypyrimidine tract-binding protein. J Biol Chem 286:10007-10016.

Tange TO, Damgaard CK, Guth S, Valcarcel J, Kjems J. 2001. The hnRNP A1 protein regulates HIV-1 tat splicing via a novel intron silencer element. EMBO J 20:5748-5758.

Thimmapaya R, Neelands T, Niforatos W, Davis-Taber RA, Choi W, Putman CB, Kroeger PE, Packer J, Gopalakrishnan M, Faltynek CR, Surowy CS, Scott VE. 2005. Distribution and functional characterization of human Nav1.3 splice variants. Eur J Neurosci 22:1-9.

Thompson CH, Kahlig KM, George AL, Jr. 2011. SCN1A splice variants exhibit divergent sensitivity to commonly used antiepileptic drugs. Epilepsia 52:1000-1009.

Tian M, Maniatis T. 1994. A splicing enhancer exhibits both constitutive and regulated activities. Genes Dev 8:1703-1712.

Trimmer JS, Cooperman SS, Tomiko SA, Zhou JY, Crean SM, Boyle MB, Kallen RG, Sheng ZH, Barchi RL, Sigworth FJ, et al. 1989. Primary structure and functional expression of a mammalian skeletal muscle sodium channel. Neuron 3:33-49.

Trimmer JS, Rhodes KJ. 2004. Localization of voltage-gated ion channels in mammalian brain. Annu Rev Physiol 66:477-519.

Trudeau MM, Dalton JC, Day JW, Ranum LP, Meisler MH. 2006. Heterozygosity for a protein truncation mutation of sodium channel SCN8A in a patient with cerebellar atrophy, ataxia, and mental retardation. J Med Genet 43:527-530.

Twyffels L, Gueydan C, Kruys V. 2011. Shuttling SR proteins: more than splicing factors. FEBS J 278:3246-3255.

Ule J, Ule A, Spencer J, Williams A, Hu JS, Cline M, Wang H, Clark T, Fraser C, Ruggiu M, Zeeberg BR, Kane D, Weinstein JN, Blume J, Darnell RB. 2005. Nova regulates brain-specific splicing to shape the synapse. Nat Genet 37:844-852.

Underwood JG, Boutz PL, Dougherty JD, Stoilov P, Black DL. 2005. Homologues of the Caenorhabditis elegans Fox-1 protein are neuronal splicing regulators in mammals. Mol Cell Biol 25:10005-10016.

Vanoye CG, Gurnett CA, Holland KD, George AL, Jr., Kearney JA. 2014. Novel SCN3A variants associated with focal epilepsy in children. Neurobiol Dis 62:313-322.

Vibe-Pedersen K, Kornblihtt AR, Baralle FE. 1984. Expression of a human alpha-globin/fibronectin gene hybrid generates two mRNAs by alternative splicing. EMBO J 3:2511-2516.

Vulin A, Barthelemy I, Goyenvalle A, Thibaud JL, Beley C, Griffith G, Benchaouir R, le Hir M, Unterfinger Y, Lorain S, Dreyfus P, Voit T, Carlier P, Blot S, Garcia L. 2012. Muscle function recovery in golden retriever muscular dystrophy after AAV1-U7 exon skipping. Mol Ther 20:2120-2133.

Wagner EJ, Garcia-Blanco MA. 2001. Polypyrimidine tract binding protein antagonizes exon definition. Mol Cell Biol 21:3281-3288.

Wahbi K, Algalarrondo V, Becane HM, Fressart V, Beldjord C, Azibi K, Lazarus A, Berber N, Radvanyi-Hoffman H, Stojkovic T, Behin A, Laforet P, Eymard B, Hatem S, Duboc D. 2013. Brugada syndrome and abnormal splicing of SCN5A in myotonic dystrophy type 1. Arch Cardiovasc Dis 106:635-643.

Wahl MC, Will CL, Luhrmann R. 2009. The spliceosome: design principles of a dynamic RNP machine. Cell 136:701-718.

Wang ET, Sandberg R, Luo S, Khrebtukova I, Zhang L, Mayr C, Kingsmore SF, Schroth GP, Burge CB. 2008. Alternative isoform regulation in human tissue transcriptomes. Nature 456:470-476.

Wang Z, Jeon HY, Rigo F, Bennett CF, Krainer AR. 2012. Manipulation of PK-M mutually exclusive alternative splicing by antisense oligonucleotides. Open Biol 2:120133.

Waxman SG, Zamponi GW. 2014. Regulating excitability of peripheral afferents: emerging ion channel targets. Nat Neurosci 17:153-163.

Weighardt F, Biamonti G, Riva S. 1995. Nucleo-cytoplasmic distribution of human hnRNP proteins: a search for the targeting domains in hnRNP A1. J Cell Sci 108 (Pt 2):545-555.

Weiss J, Pyrski M, Jacobi E, Bufe B, Willnecker V, Schick B, Zizzari P, Gossage SJ, Greer CA, Leinders-Zufall T, Woods CG, Wood JN, Zufall F. 2011. Loss-of-function mutations in sodium channel Nav1.7 cause anosmia. Nature 472:186-190.

Widmark J, Sundstrom G, Ocampo Daza D, Larhammar D. 2011. Differential evolution of voltage-gated sodium channels in tetrapods and teleost fishes. Mol Biol Evol 28:859-871.

Will CL, Luhrmann R. 2011. Spliceosome structure and function. Cold Spring Harb Perspect Biol 3.

Wood M, Yin H, McClorey G. 2007. Modulating the expression of disease genes with RNA-based therapy. PLoS Genet 3:e109.

Xu N, Chen CY, Shyu AB. 2001. Versatile role for hnRNP D isoforms in the differential regulation of cytoplasmic mRNA turnover. Mol Cell Biol 21:6960-6971.

Xu R, Thomas EA, Jenkins M, Gazina EV, Chiu C, Heron SE, Mulley JC, Scheffer IE, Berkovic SF, Petrou S. 2007. A childhood epilepsy mutation reveals a role for developmentally regulated splicing of a sodium channel. Mol Cell Neurosci 35:292-301.

Yamamoto H, Tsukahara K, Kanaoka Y, Jinno S, Okayama H. 1999. Isolation of a mammalian homologue of a fission yeast differentiation regulator. Mol Cell Biol 19:3829-3841.

Yang N, Horn R. 1995. Evidence for voltage-dependent S4 movement in sodium channels. Neuron 15:213-218.

Yang X, Bani MR, Lu SJ, Rowan S, Ben-David Y, Chabot B. 1994. The A1 and A1B proteins of heterogeneous nuclear ribonucleoparticles modulate 5' splice site selection in vivo. Proc Natl Acad Sci U S A 91:6924-6928.

Yeo GW, Xu X, Liang TY, Muotri AR, Carson CT, Coufal NG, Gage FH. 2007. Alternative splicing events identified in human embryonic stem cells and neural progenitors. PLoS Comput Biol 3:1951-1967.

Yu FH, Catterall WA. 2003. Overview of the voltage-gated sodium channel family. Genome Biol 4:207.

Zahler AM, Lane WS, Stolk JA, Roth MB. 1992. SR proteins: a conserved family of pre-mRNA splicing factors. Genes Dev 6:837-847.

Zamecnik PC, Stephenson ML. 1978. Inhibition of Rous sarcoma virus replication and cell transformation by a specific oligodeoxynucleotide. Proc Natl Acad Sci U S A 75:280-284.

Zhang W, Liu H, Han K, Grabowski PJ. 2002. Region-specific alternative splicing in the nervous system: implications for regulation by the RNA-binding protein NAPOR. RNA 8:671-685.

Zhang XH, Heller KA, Hefter I, Leslie CS, Chasin LA. 2003. Sequence information for the splicing of human pre-mRNA identified by support vector machine classification. Genome Res 13:2637-2650.

Zheng S, Gray EE, Chawla G, Porse BT, O'Dell TJ, Black DL. 2012. PSD-95 is post-transcriptionally repressed during early neural development by PTBP1 and PTBP2. Nat Neurosci 15:381-388, S381.

Zhou HL, Lou H. 2008. Repression of prespliceosome complex formation at two distinct steps by Fox-1/Fox-2 proteins. Mol Cell Biol 28:5507-5516.

Zhu J, Mayeda A, Krainer AR. 2001. Exon identity established through differential antagonism between exonic splicing silencer-bound hnRNP A1 and enhancer-bound SR proteins. Mol Cell 8:1351-1361.

Zipursky SL, Wojtowicz WM, Hattori D. 2006. Got diversity? Wiring the fly brain with Dscam. Trends Biochem Sci 31:581-588.

Zubovic L, Baralle M, Baralle FE. 2012. Mutually exclusive splicing regulates the Nav 1.6 sodium channel function through a combinatorial mechanism that involves three distinct splicing regulatory elements and their ligands. Nucleic Acids Res.

Acknowledgements

I wish to thank, first and foremost, Professor Francisco E. Baralle that gave me the opportunity to join his Molecular Pathology Group. I express immense gratitude for his help and his continuous support during all the time of this research experience. During these years his enthusiasm and immense knowledge have guided me in the numerous and stimulating discussions about the project.

I am deeply grateful to Dr. Marco Baralle that has always been by my side with his scientific expertise, patience and constructive suggestions. This work would have not been the same without his kind help, the rich exchange of scientific opinion and the accurate review of my thesis.

A very warm acknowledgement is conveyed to Professor Charles ffrench-Constant for his intense encouragement and the always stimulating discussions. I would like to express my sincere appreciation to Professor Matthew Wood and Dr. Vittorio Venturi for accepting the role of examiners and for their critical reading of this thesis.

A very special thank to Lorena Zubovic, that introduced me in this project, for her enthusiastic guidance and discussions and Giulia Bortolussi for her technical and scientific support during the first year of my PhD. I would like to thank all the current and former members of the Molecular Pathology Group for their constant assistance and for sharing a lot of fun in the lab. In particular I want to express my gratitude to Laura, Simona and Elisabete that have offered their scientific support, their technical advices, but most importantly they have made these years unforgettable with their friendship and caring, enriching every single day spent together outside and inside the lab.

One person has always been by my side during these years and my deepest gratitude is for her. Every single moment spent with Valentina will remain forever in my heart. In the most difficult moments she was the pillar of the strength that I needed, her hug has been as a magic pill that brought smile and caring, her friendship puts sunshine in my life. We have shared such a lot of joy and happiness together! She is "my person". I also want to warmly thank my "magggic" friend Simone. During these years he brought out the best in me. I am really grateful to him for the perfect moments we spent together smiling and enjoying life.

A special thank also to my friends beyond the lab for their friendship and support during these years, particularly to my dear friend Martina, because she has encouraged me during this adventure and constantly supported me, taking care of me.

Thanks also to Rosi, Sandro, Ettore and Elia, one of the most lovely family I have ever met. They brought smile in my life and they make me feel part of the family.

To Matteo... your true love and your smiles gave me the strength to continue over these years. Thanks for being always by my side, hugging me, making amazing every single instant of my life and holding my hands during these years in the realization of my dream.

Finally I would like to thank my parents and my sister Serena, that always believe in me. Their endless love together with their shining joy have sustained and warmed me during my entire life. Thanks for being the best crazy family ever!